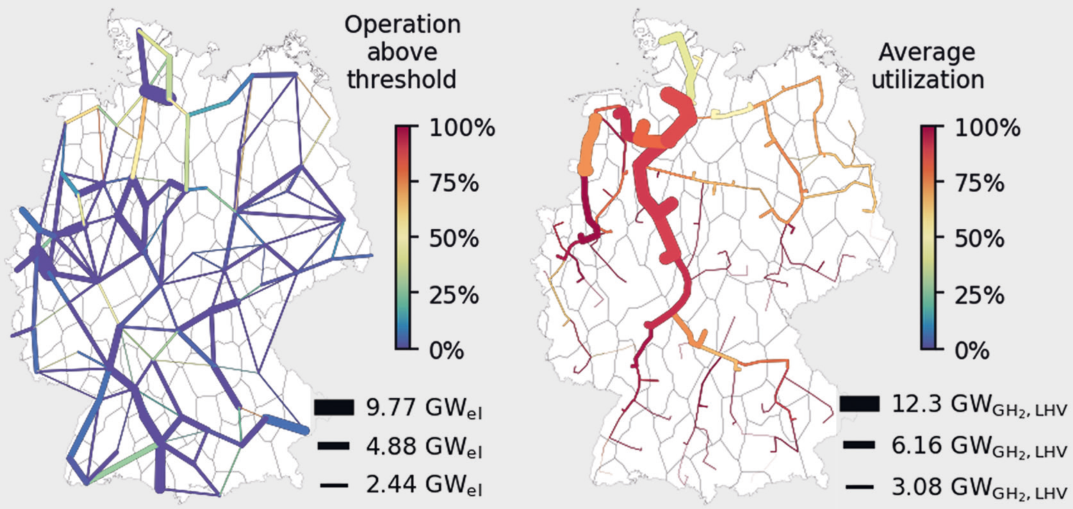

Optimizing Cross-linked Infrastructure for Future Energy Systems

Lara Welder

Energie & Umwelt / Energy & Environment
Band / Volume 591
ISBN 978-3-95806-659-5

JÜLICH
Forschungszentrum

Mitglied der Helmholtz-Gemeinschaft

Schriften des Forschungszentrums Jülich
Reihe Energie & Umwelt / Energy & Environment Band / Volume 591

Forschungszentrum Jülich GmbH
Institut für Energie- und Klimaforschung (IEK)
Techno-ökonomische Systemanalyse (IEK-3)

Optimizing Cross-linked Infrastructure for Future Energy Systems

Lara Welder

Schriften des Forschungszentrums Jülich
Reihe Energie & Umwelt / Energy & Environment Band / Volume 591

ISSN 1866-1793 ISBN 978-3-95806-659-5

Bibliografische Information der Deutschen Nationalbibliothek.
Die Deutsche Nationalbibliothek verzeichnet diese Publikation in der
Deutschen Nationalbibliografie; detaillierte Bibliografische Daten
sind im Internet über http://dnb.d-nb.de abrufbar.

Herausgeber und Vertrieb:	Forschungszentrum Jülich GmbH Zentralbibliothek, Verlag 52425 Jülich Tel.: +49 2461 61-5368 Fax: +49 2461 61-6103 zb-publikation@fz-juelich.de www.fz-juelich.de/zb
Umschlaggestaltung:	Grafische Medien, Forschungszentrum Jülich GmbH
Druck:	Grafische Medien, Forschungszentrum Jülich GmbH

Schriften des Forschungszentrums Jülich
Reihe Energie & Umwelt / Energy & Environment, Band / Volume 591

D 82 (Diss. RWTH Aachen University, 2022)

ISSN 1866-1793
ISBN 978-3-95806-659-5

Vollständig frei verfügbar über das Publikationsportal des Forschungszentrums Jülich (JuSER)
unter www.fz-juelich.de/zb/openaccess.

Abstract

Increasing shares of distributed, intermittent renewable electricity generation as well as the need to decarbonize all sectors in future energy systems require new infrastructure solutions. In these infrastructure solutions, energy transmission and storage technologies will serve as spatial and temporal balancing options. Technologies like electrolyzers will be deployed to create a renewable link between the power sector and other sectors. Together with technologies for power generation from renewably produced gases, electricity and gas infrastructure will be strongly cross-linked. The design of such cross-linked infrastructure is a computationally challenging undertaking and national cross-linked infrastructure analyses are scarce in literature.

In this thesis, a new approach which enables the modeling of spatially and temporally resolved energy supply systems is proposed. In this context, the generic, open-source available modeling framework *FINE* is developed from scratch. *FINE* enables the optimal design and operation of cross-linked infrastructure levels. With its generic character, it can also be applied to model households, districts, one-nodal energy systems or international energy supply pathways and it has already been adapted by other scientists for these applications.

By applying *FINE*, cross-linked infrastructure solutions for a German energy supply system in the year 2050 are investigated in this thesis. In the scenarios, onshore and offshore wind turbines, rooftop and open-field PV systems and renewable electricity imports are corner stones of renewable energy procurement. Pumped-hydro energy storage, batteries, geological storage of synthetic gases, electricity and hydrogen transmission networks as well as deferrable electricity demands of electrolyzers guarantee a temporally and spatially balanced energy supply. In general, the value of cross-linked infrastructure is demonstrated. Electrolyzers enable the cost-efficient integration of wind turbines. Hydrogen operated power plants are used as a flexible load balancing option. While for an 80% carbon dioxide reduction target, the hydrogen cost in the industry and transport sector are determined to be about 3.9 €/kg_{H_2} and 5.6 €/kg_{H_2}, these values decrease to 3.7 €/kg_{H_2} and 5.4 €/kg_{H_2} for a 100% reduction target as more intermittent low-cost electricity for electrolysis is available. For the electricity supply, costs of about 80 €/MWh_{el} (80%-target) and 120 €/MWh_{el} (100%-target) are determined. Based on the scenario results, the pursuit of an integrated cross-linked infrastructure development strategy is recommended for Germany, which diverges from previous German strategies which focus on single infrastructure layers only. Furthermore, when comparing these 2050 scenarios to the German energy supply system in 2017 / 2018, an urgent need for change is exposed which should be taken into consideration by respective decision makers.

Kurzfassung

Der steigende Anteil dezentraler, fluktuierender erneuerbarer Energien und das Bedürfnis alle Sektoren in zukünftigen Energiesystemen zu dekarbonisieren erfordert neue Infrastrukturlösungen. In diesen werden Energie-Transmission and Energie-Speicherung als räumliche und zeitliche Ausgleichsoptionen fungieren. Technologien wie Elektrolyseure werden eingesetzt werden, um eine erneuerbare Sektorenkopplung zwischen dem Stromsektor und anderen Sektoren zu ermöglichen. Zusammen mit Rückverstromungstechnologien, welche mittels synthetischer Gase Strom bereitstellen, werden Strom- und Gasinfrastrukturen eng miteinander gekoppelt sein. Die Auslegung solcher gekoppelten Infrastrukturszenarien ist rechentechnisch aufwendig und die Analyse dieser Szenarien ist bisher in der Literatur nicht ausreichend behandelt.

In dieser Doktorarbeit wird ein neuer Ansatz für die Modellierung von räumlich und zeitlich aufgelösten Energieversorgungsystemen vorgestellt. Hierfür wurde das generische, open-source verfügbare Modellierungsframework FINE in dieser Arbeit entwickelt. FINE ermöglicht die optimale Auslegung und den optimalen Betrieb von gekoppelten Energieinfrastrukturen. Durch seinen generischen Charakter kann FINE außerdem auch für die Optimierung von Haushalten, Stadtteilen, 1-Knoten Energiesystemen und internationalen Energieversorgungspfaden angewendet werden und wird bereits für diesen Zweck eingesetzt.

In dieser Doktorarbeit werden durch den Einsatz von FINE gekoppelte Infrastrukturlösungen für ein deutsches Energieversorgungssystem im Jahre 2050 analysiert. In diesen Szenarien sind Onshore- und Offshore-Windturbinen, Dach- und Freiflächenphotovoltaikanlagen sowie erneuerbare Energieimporte Eckpfeiler für eine erneuerbare Energieversorgung. Pumpspeicherkraftwerke, Batterien, geologische Speicher für synthetische Gase, Stromnetze und Wasserstoffnetze sowie flexible Stromnachfragen von Elektrolyseuren dienen als räumliche und zeitliche Ausgleichsoptionen. Die Kosten für den Einsatz von Wasserstoff im Industrie- und Transportsektor betragen 3.9 €/kg_{H_2} sowie 5.6 €/kg_{H_2} wenn Emissionen im Stromsektor im Vergleich zu 1990 um 80% reduziert werden. Für ein 100% Reduktionsziel reduzieren sich diese auf 3.7 €/kg_{H_2} beziehungsweise 5.4 €/kg_{H_2}. Für das 80% und 100% Reduktionsziel berechnen sich Stromkosten von jeweils 80 €/MWh_{el} und 120 €/MWh_{el}. Basierend auf den Szenario Ergebnissen wird für die Planung von zukünftigen deutschen Energieinfrastrukturen empfohlen eine Strategie zu nutzen, welche diese als gekoppelt und nicht wie bisher als eher separat betrachtet. Der Vergleich der erarbeiteten Szenarien zu dem in 2017 / 2018 bestehendem deutschen Energieversorgungsystem deckt einen dringenden Handlungsbedarf auf, welcher von Entscheidungsträgern berücksichtigt werden sollte.

Contents

List of Figures

List of Tables

Conventions

Throughout this thesis the following conventions are used.

Proper names are italic.

EXPLANATION:
Informal excurses of a model or definition.

Formula conventions:

- Functions are written in small, italic letters.
- Indices are written in small, roman letters.
- Parameters are written in roman letters.
- $\mathbb{S}$ is defined as the set of all strings.
- Sets are written in capital, calligraphic letters.
- Variables are written in small, italic letters.

This thesis is written in American English. Accordingly, commas are used as thousands delimiters.

All economic parameters are to be understood in reference to the year 2019, i.e. €$_{2019}$.

Nomenclature

Abbreviations

cf.	confer (Latin), compare to/ with
e.g.	exempli gratia (Latin), for example
e.V.	eingetragener Verein (registered association)
el	electrical
ex.	existing
i.e.	id est (Latin), that is
th	thermic
w/-	with
w/o	without

Acronyms

AC	Alternating Current
AEL	Anion Exchange Membranes
AGEB	Arbeitsgemeinschaft Energiebilanzen e.V.
BELS	Basic Electricity Supply Scenario
$BELS^{+}$	Basic Electricity Supply with Centralized H_2 Infrastructure Scenario
BLHYS	Basic Electricity and Hydrogen Supply Scenario
BMVI	Bundesministerium für Verkehr und digitale Infrastruktur
CCGT	Combined Cycle Gas Turbine
CHP	Combined Heat and Power
DC	Direct Current
DVGW	Deutscher Verein des Gas- und Wasserfaches
EEG	Erneuerbare Energien Gesetz

FINE	Framework for Integrated Energy System Assessment
FLH	Full Load Hours
GH_2	Gaseous Hydrogen
GHG	Greenhouse Gas
HDV	Heavy Duty Vehicle
H-gas	High-caloric Natural Gas
H-GH_2	High Hydrogen Demand Scenario
HHV	Higher Heating Value
HTEL	High Temperature Electrolysis
http	Hydrogen to Power
HVDC	High Voltage Direct Current
HyARC	Hydrogen Analysis Resource Center
JRC	Joint Research Center
LCOE	Levelized Cost of Electricity
L-gas	Low-caloric Natural Gas
L-GH_2	Low Hydrogen Demand Scenario
LH_2	Liquid Hydrogen
LHV	Lower Heating Value
LNG	Liquid Natural Gas
M-GH_2	Medium Hydrogen Demand Scenario
MHV	Material Handling Vehicle
MILP	Mixed Integer Linear Program
MRG	Methane Rich Gas

NEP	Netzentwicklungsplan
NG	Natural Gas
OCGT	Open Cycle Gas Turbine
OPEX	Operational Expenditure
PEM	Proton Exchange Membranes
PEMEL	Proton Exchange Membranes Electrolysis
PHES	Pumped Hydroelectric Energy Storage
PTC	PVUSA Test Condition
PtG	Power-to-Gas
PV	Photovoltaic
PVUSA	Photovoltaics for Utility Scale Applications
r-o-r	Run-of-river
TSO	Transmission System Operator
UGS	Underground Gas Storage
VSC	Voltage Source Converter
WACC	Weighted Average Cost of Capital
LRMC	Long-run Marginal Cost
TAC	Total Annual Cost
WT	Wind Turbines
RT	Rooftop
OF	Open-field

Chapter 1

Introduction

1.1 Motivation and Objective

Increasing the share of renewable electricity generation and implementing energy efficiency measures in energy systems are means to keep the global temperature rise well below 2 $^{\circ}$Celsius as stipulated in the *Paris agreement* of 2015 / 2016 [1]. However, the expansion of such renewable electricity generation capacities, specifically of wind and solar power, are accompanied by regionally distributed, intermittent generation profiles which are not necessarily correlated to regional demand profiles. Thus, with an increasing share of renewable electricity generation, mismatches between generation and demand, even after considering electricity transmission, occur more often, leading to positive and negative residual loads in the supply system.

As such, balancing options are required to facilitate the integration of intermittent renewable electricity generation capacities into the energy system. Here, the expansion of existing and the construction of new energy transmission infrastructure can function as spatial balancing options. Prominent infrastructure options are in this context electric cables or gas pipelines. Besides demand site management and the flexible operation of power plants, storage infrastructure can function as a temporal balancing option. For example, batteries can be operated as intraday storage and geological gas storage can function as a seasonal storage option [2, 3]. Moreover, stronger interactions between the sectors in the energy system by sector-coupling [4] will have to be considered to decarbonize all sectors. For this purpose, various *Power-to-X* technology pathways[1] can be considered, causing strong interdependencies between commodities and their respective infrastructure. In this context, the deferrable demands of the *Power-to-X* technology pathways can serve as additional temporal balancing options.

The correspondingly required structural transformation of the energy system sets the design of electricity and gas infrastructure in future energy systems into a new focus. Several reviews on energy and energy supply system modeling frameworks have been published in 2018 and 2019 [5–7]. The consideration of an adequate modeling representation of renewable energies is a topic in all of these studies. However, a critical reflection of the maturity of storage and transmission infrastructure modeling is only given by *Groissböck* [7]. Based on this study, it can be concluded that the available modeling frameworks become restrictive when infrastructure scenarios should be modeled in technical detail.

Also Germany has committed to reducing GHG emissions, with respect to the year 1990, by $80-95\%$ as specified in the *Climate Action Plan 2050* [8]. However, literature investigating German cross-linked infrastructure scenarios, including transmission technologies, is in general scarce. For Germany, a modeling approach in which first a regionally resolved electricity supply system is simulated, next electrolyzers are placed based on available surplus electricity and last a hydrogen transmission network is determined is proposed by *Robinius et al.* [9]. While providing high spatial detail, this modeling approach is not capable of determining an endogenous, optimal design and operation of the cross-linked electricity and hydrogen infrastructure.

In this setting, the objective of this thesis is twofold. On the one hand, a modeling framework which is suitable for cross-linked infrastructure investigations must be developed. On the other hand, comprehensive cross-linked infrastructure scenarios must be investigated for Germany, including a detailed representation of all relevant storage and transmission technologies. With this setup, the following research questions should be investigated:

- What is the optimal cross-linked infrastructure design and operation for a future German energy system scenario under varying carbon dioxide reduction targets?
- What is the role of individual technologies in such a scenario, i.e. when are specific technologies considered and how are they operated?
- Which opportunities and synergies but also challenges arise from such a cross-linked infrastructure design?

[1] I.e. pathways in which, preferably renewable, electricity is used to produce, for example, heat, hydrogen, methane, fuels or chemicals.

1.2 Structure

The objective of this thesis and the posed research questions are elaborated upon throughout the structure of this thesis. The structure is visualized in Figure 1.1.

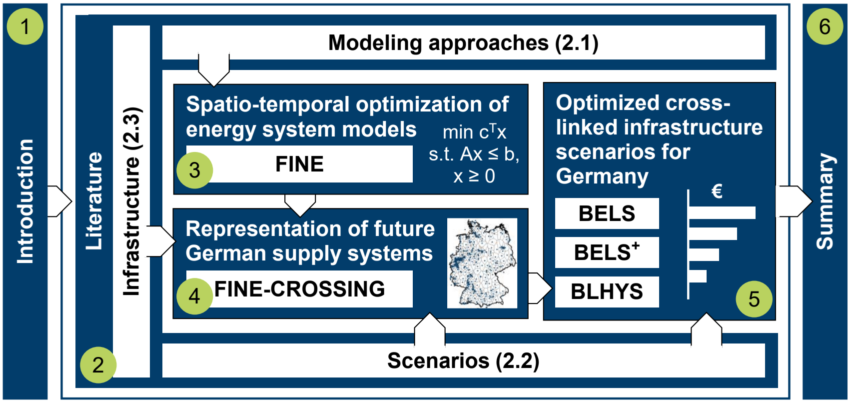

Figure 1.1: Structure of this thesis. Numbers highlighted in green refer to the respective chapters.

A review of energy and energy supply system modeling approaches is presented in chapter 2. The review is in this context threefold. First, general modeling approaches and existing modeling frameworks are identified. Second, scenarios from literature which investigate future German energy supply infrastructure are reviewed. Third, technologies which can be considered in a future German energy supply infrastructure are assessed. For these technologies, techno-economic parameters and geo-referenced modeling approaches are collected from literature.

The workflow / method to obtain an optimized, spatio-temporally resolved infrastructure scenario is presented in chapter 3. In this context, the spatial and temporal mathematical representation of an energy supply system model is discussed. Moreover, *FINE*, an energy system optimization Framework for INtegrated Energy system assessment is described which was developed and published open-source within the context of this thesis.

In chapter 4, the framework for the investigated German cross-linked infrastructure scenarios is set, named *FINE-CROSSING* (CROSS-linked INfrastructure scenarios for Germany). For this purpose, the input data identified in chapter 2 are modified with the in chapter 3 suggested modeling approach for spatial and temporal data and are in this context made compatible with *FINE*.

Optimized cross-linked infrastructure scenarios are investigated in chapter 5. The scenarios are subdivided into three scenario branches. In the first branch (*BELS*), Basic ELectricity Supply scenarios without a centralized hydrogen infrastructure are considered. In the second branch (*BELS*$^+$), basic electricity supply scenarios with a centralized hydrogen infrastructure are investigated. Here, the value of hydrogen reconversion for ambitious reduction targets is identified. In the third scenario branch (*BLHYS*), in addition to the Basic eLectricity supply, a HYdrogen Supply to mobility and industry is considered.

Finally, in chapter 6, a summary of the thesis and its key findings are presented.

Chapter 2

Energy Supply Systems Modeling in Literature

Infrastructure for future energy systems is assessed in different model types in literature. In Figure 2.1, the different model types are visualized together with the distribution of their computational budget in a simplified manner. In the figure, it is assumed that all model types have the same computational budget available, i.e. the same computational hardware and runtimes.

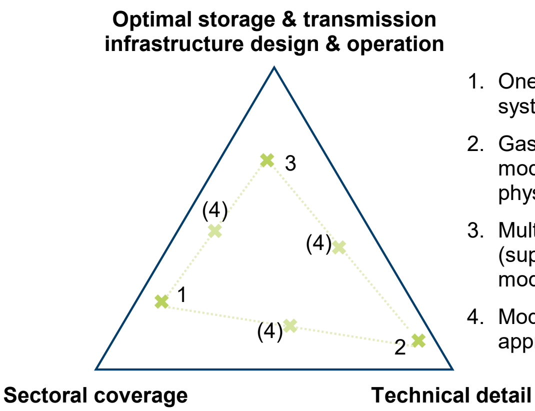

1. One-nodal energy system models
2. Gas/ electricity grid models (with physical details)
3. Multi-nodal energy (supply) system models
4. Model-coupling approaches

Figure 2.1: Computational budget distribution for different energy and energy supply system model types under the assumption of the identical computational hardware and runtimes.

While one-nodal energy system models spend the majority of their computational budget on a high sectoral coverage, comprehensive electricity and gas grid models spend their computational budget primarily on modeling technical details. Unlike one-nodal energy system models, multi-nodal energy supply system models can model transmission infrastructure in spatial detail; however, the increased spatial detail has to be traded in for a decreased sectoral coverage. Also, they cannot capture the high technical detail of dedicated electricity and gas grid models. The computational budget distribution of model-coupling approaches is located between the ones of the combined models. Inherently, the modeling detail of all approaches can be increased when the computational budget is increased.

Within this chapter, approaches to cross-linked infrastructure modeling existing in literature are reviewed. For this purpose, first general modeling approaches and existing modeling frameworks are reviewed in section 2.1. Then, German scenarios for energy supply infrastructure published in literature are assessed in section 2.2. The German scenarios are, on the one hand, reviewed to investigate the application of the modeling frameworks and, on the other hand, to investigate if cross-linked infrastructure scenarios have yet been investigated comprehensively in literature. Third, in section 2.3, potential infrastructure components which can be deployed in future energy systems are identified and their techno-economic data is collected.

2.1 Modeling Approaches and Frameworks

Reviews on frameworks and / or models[1] for energy system assessments are provided by *Lopion et al.* [5], *Ringkjøb et al.* [6] and *Groissböck* [7].

- *Lopion et al.* [5] evaluate national energy system models with respect to their (a) underlying modeling approach, (b) time horizon and transformation pathway analysis, (c) spatial and temporal resolution, (d) licensing and (e) modeling language.
- *Ringkjøb et al.* [6] investigate modeling tools for energy and electricity systems with large shares of variable renewable energies. In this context, they present, amongst other features, the (a) general logic, (b) spatio-temporal resolution as well as (c) the technological features of the models.
- The study of *Groissböck* [7] focuses on open source energy system optimization tools and checks the availability of 81 functionalities in the frameworks.

[1] Models in the sense of: being specifically tailored to represent one geographical context, i.e. without being generically adaptable.

In the following, the findings of these three studies are reflected upon. Modeling methods for energy and energy supply systems are presented in subsection 2.1.1. The spatial and temporal representation of the models is discussed in subsection 2.1.2. Functionalities which are of interest to being included in energy supply systems modeling frameworks are reflected upon in subsection 2.1.3. Finally, existing modeling frameworks and auxiliary software are listed in subsection 2.1.4. Alongside these discussions, additional literature of interest is added.

2.1.1 Modeling Methods

In general, *Lopion et al.* [5], *Ringkjøb et al.* [6] and *Groissböck* [7] differentiate between simulation and optimization approaches for energy systems modeling. *Ringkjøb et al.* [6] additionally add the category of equilibrium models.

A description of these approaches is given by *Ringkjøb et al.* [6]. They are summarized in the following.

- *Simulation models* are often applied to describe bottom-up energy system models with high technical detail. They enable the testing of given system topologies.
- *Optimization models* minimize or maximize a predefined objective function, e.g. the energy supply system's cost. The majority of energy system optimization models are formulated as Linear Programs (LPs) while only several are formulated as Mixed Integer Linear Programs (MILPs)[2]. Some are also formulated as nonlinear programs or with heuristic approaches[3].
- *Equilibrium models* are applied to model interactions between the energy sector and the economy of a region.

Ringkjøb et al. [6] also name different purposes of the models. These are again summarized in the following.

- *Power system analysis tools* are capable of modeling the electrical grid and its components in high technical detail. For an additional review on this topic, the study of *Syranidis et al.* [13] can be consulted.
- *Operation decision support tools* support the optimal / dispatch of an underlying energy supply system. These models normally operate on a short-term time horizon but can cover wide geographical scopes.

[2] Binary variables are in this context implemented via a so-called "big M" condition, cf. the work of *Bemporad and Morari* [10].

[3] Examples for heuristic optimization approaches applied to grid expansion planning are given by *Hagspiel et al.* [11] and *Neumann and Brown* [12].

- *Investment decision support tools* often consider a long-term time horizon and support optimal investment decision making.
- *Scenario tools* are deployed to investigate long-term scenarios in the energy sector.

Modeling tools which operate in the second or even milli-second regime are identified as power system analysis tools which are set up as simulation models by *Ringkjøb et al.* [6]. Models to support operation and investment decisions are on the other hand often LPs or MILPs.

To obtain additional detail, also "model-coupling" approaches are considered in literature. For example, *Robinius* and *Robinius et al.* [9, 14] first simulate a spatially resolved electricity supply system and determine positive and negative residual loads. Then, based on these residual loads, a hydrogen transmission network is designed. Another example is provided by *Reuß et al.* [15], in which a spatio-temporal resolved MILP is run first to determine the design and operation of cross-linked electricity and hydrogen infrastructure for a region in Germany. Then, the determined pipeline injection and withdrawal rates are post-processed and passed to another MILP which determines a robust, discrete pipeline design under the consideration of pressure losses.

2.1.2 Spatial and Temporal Representation

The considered spatial scope and temporal resolution varies for each application case. While the spatial scope ranges between single projects / technologies to global scopes, the temporal resolution ranges between subseconds to decades [6]. For the modeling of transformation pathways, different foresight approaches can be additionally applied, see *Lopion et al.* [5]. In these approaches, multi-annual time steps, for example for every 5 years, are introduced in addition to an intra-annual temporal representation. Thus, the temporal resolution is modeled on two different hierarchy levels. In "perfect foresight" approaches, only one optimization program is formulated. This optimization program considers the boundary conditions of both temporal hierarchy levels simultaneously. In "myopic foresight" approaches, multiple optimizations are performed consecutively. At each optimization step, only input data of the preceding inter-annual time steps is taken into account.

To be compatible with modeling frameworks based on LPs or MILPs, the input data of the models has to be discretized. The considered spatial and temporal resolution is dependent on the application case of a study. Energy system models with a comprehensive sectoral representation are often modeled as one node, cf. subsection 2.2.3. For the modeling of national and international energy supply systems, often either regions assigned to electric grid nodes [16–19] or administrative regions [20–24] are considered. For the modeling of districts, single houses can be considered [25]. Concerning the temporal resolution, the literature points to considering at least hourly time steps for the modeling of energy supply systems [6, 26].

To reduce the complexity of the discretized data further in the context of infrastructure modeling, clustering and aggregation methods are considered in literature. In the following, a short excursus on the application of spatial and temporal clustering approaches in the context of energy supply systems modeling is given.

Spatial Clustering Approaches for Energy Transmission Infrastructure

Several spatial clustering approaches, which consider a simultaneous transmission infrastructure reduction, exist in literature.

- *Sánchez-García et al.* [27] use a hierarchical, spectral clustering approach for electric grid clustering. They assign weights based on line admittances / average power flows to each transmission line. When using line admittances as a weight, the internal connectivity structure of the underlying network is revealed. The average power flow weight identifies islands that disrupt the power flow in the network as little as possible when separated.
- Another study which tests different methods for clustering the electric grid based on line admittances is provided by *Blumsack et al.* [28]. Even though the consideration of the line admittance as a weight gives insights into the connectivity of the network, it does not necessarily minimize the error of a copper plate assumption [13, 29]. An example is a line with a high admittance that is however heavily utilized. Spatial clustering based on the utilization of the line is not possible in the context of energy system design as the utilizations of the lines are not known beforehand.
- The E-Highway 2050 report [30] and the study by *Hörsch and Brown* [18] choose a different clustering approach that does not focus on the clustering of the electric grid but rather on the attributes of the regions assigned to the network busses. The weights, used in a *k-means* clustering approach, correlate in both cases with the electricity generation capacity and demand. Again, this approach does not necessarily minimize the error of a copper plate assumption as for example a badly connected bus to which a small electricity demand is assigned could still cause a bottleneck.

All of the above approaches can not necessarily be applied when infrastructure expansion and *Power-to-X* pathways are considered in the energy system as the model endogenously determines new electricity demands and generators and expands the commodity transmission infrastructure.

Temporal Clustering Approaches for Energy System Time Series

A comprehensive investigation of the impact of different time series clustering and aggregation methods on optimal energy system design is provided by *Kotzur et al.* [31]. The authors cluster time series data by averaging, *k-means*, *k-medoids* and *hierarchical* clustering. They recommend the usage of hierarchical data aggregation, based on the algorithms small computational load and its reproducibility. Furthermore, the authors conclude that using the medoids of the aggregated clusters to represent a typical period is more effective than using averaged periods. In the model formulation by *Kotzur et al.* [31] commodities cannot be exchanged between typical periods. An extended, interconnected typical period formulation, which enables the consideration of seasonal storage, is published in a later study of *Kotzur et al.* [32]. *Kannengießer et al.* [25] again build on the work of *Kotzur et al.* [32] and propose a two-step approach in which first aggregated MILP systems are optimized and then, in a second step, the systems are optimized with a full time series but fixed binary variables, i.e. in an LP formulation. Another approach to model interconnected typical periods is provided by *Samsatli et al.* [3, 33]. Here, the authors consider a week day and a weekend day for each season of the year which are interconnected in a storage formulation.

2.1.3 Features of Optimization Frameworks

While the optimization frameworks reviewed by *Groissböck* [7] are capable of formulating basic LPs for energy system models, they differ from each other with respect to additional modeling features and open-source availability. *Groissböck* [7] lists a total of 81 features to assess the maturity of the reviewed modeling frameworks. An aggregated list of the modeling features provided by *Groissböck* is given in the following.

- An exhaustive number of modeling features for power plants is given. Examples are constraints for unit commitment, part load behavior and ramping, see also *Palmintier and Webster* [34].
- The modeling of additional technical detail in electricity, gas, liquid and heat transmission networks is listed.
- Features to enable the modeling of transformation pathways are included.
- The consideration of an economy of scale is included as a feature.

- Storage and conversion modeling details are listed.
- Deferrable demand and curtailment are included into the list.
- With respect to robustness, features for reliability, risk and probability / uncertainty are included.
- With respect to applicability, open-source availability, geo-referenced plotting capabilities and available documentation are checked.

Based on these features, *Groissböck* [7] finds that none of the reviewed frameworks

- distinguishes between hot and cold start-ups or provide the option to model part load behavior,
- models technical detail for gas, liquid and heat transmission, e.g. pressure losses, temperature levels or fluid velocities,
- provides the option to model alternative objective functions,
- considers the impact of environmental conditions on technologies, e.g. for a more accurate modeling of heat pumps,
- models storage in technical details so that "health" considerations of the storage can be included into the modeling,
- includes maintenance planning in form of, for example, planned outages, and
- evaluates risk levels or reliability indicators.

Also, in the provided check list, none of the modeling frameworks is capable of modeling an economy of scale.

2.1.4 Optimization Frameworks and Auxiliary Software

Groissböck [7] investigates, amongst others, the *Python* based open-source modeling frameworks *calliope* [35, 36], *oemof* [37, 38], *OSeMOSYS* [39, 40], *pandapower* [41,42], *pypower* [43,44], *pypsa* [45,46], *Switch* [47] and *urbs* [48]. In the majority of in *Python* implemented frameworks, the open-source optimization modeling language *Pyomo* [49, 50] is applied to formulate the respective optimization problems. Optimization programs formulated with *Pyomo* can again be passed to several optimization solvers, among them are *Gurobi* [51][4] and the free solver *GLPK* [53]. In comparison to modeling frameworks which are implemented with the commercial software *GAMS*, as for examples *TIMES* [54,55] or *STeMES* by *Samsatli and Samsatli* [33], via *Pyomo* implemented modeling frameworks can be used exclusively with open-source software.

[4] *Gurobi* is a commercial software. However, free academic licenses are available. Additionally, a comprehensive documentation is available [51,52].

Based on the review of *Groissböck* [7] only *pandapower* [41, 42], *pypower* [43, 44] and *pypsa* [45, 46] of the *Python* based modeling frameworks consider additional technical constraints for electricity transmission. Also storage is often modeled with only basic assumptions and none of the frameworks consider an economy of scale in form of nonlinear cost-capacity correlations. Furthermore, a function to reduce temporal complexity while maintaining a seasonal storage formulation is only considered in the *GAMS* based modeling framework *STeMES* by *Samsatli and Samsatli* [33] and there, only eight typical days can be considered. All in all, the existing modeling framework landscape can be approved upon for the modeling of future cross-linked infrastructure scenarios which include seasonal storage and transmission technologies design.

In the following, utility *Python* packages which can be used in the context of energy supply systems modeling are shortly mentioned. The *pandas* package [56] provides the option to store, work with and analyze two-dimensional spatio-temporal system data in a computationally efficient manner. For geo-referenced operations and visualizations, the packages *GeoPandas* [57] or *GeoKit* [58] can be used. The package *tsam* [59] provides functionalities for times series aggregation. In addition to its core functionalities as a power systems analysis tool, the package *pypsa* [45, 46] provides additional functionalities for the spatial aggregation of electric grids.

2.2 German Scenarios for Energy Supply Infrastructure

The goal of the following literature review is to identify if future German energy supply scenarios considering cross-linked infrastructure exist in literature and, if so, with which detail they are modeled. For this purpose, studies from three research areas are consulted. The first and second research area investigate energy supply infrastructure in spatial detail. Here, studies investigating future German electricity and hydrogen infrastructure are reviewed. The third research area centers around energy system scenarios which are represented by only one node but are modeled with high sectoral detail.

In the following, scenarios from each of these three research areas are reviewed. For this purpose, the studies are categorized with respect to the chosen spatial and temporal resolution, modeling approach and considered technology portfolio. In chapter 5, the findings of the scenarios investigated within this thesis will be compared to this review.

2.2.1 Future German Electricity Infrastructure in Literature

The studies of *Leuthold et al.* [60], *Schroeder et al.* [61], *Schaber et al.* [62], *Bruninx et al.* [63], *Becker et al.* [20], *Ludig et al.* [64], *Gunkel and Möst* [21], *Koch et al.* [16], *Krüger et al.* [65], *Babrowski et al.* [22], *Egerer* [17], *Kemfert et al.* [66], *Heinemann et al.* [67], *Cebulla et al.* [68], *Gils et al.* [69], *Schlachtberger et al.* [23], *Buddeke et al.* [70], *Hörsch et al.* [19], *Neumann and Brown* [12], *Victoria et al.* [24] and *Kluschke and Neumann* [71] investigate electricity infrastructure for Germany or Europe in general.

Spatial Resolution

The geographical extent and the considered spatial resolution varies widely in the investigated scenarios. Their investigated spatial extent is focused on either Europe, Germany or a combination of both. Their spatial resolution varies between 5 and 3657 nodes.

Studies which investigate scenarios primarily focusing on Germany are provided by *Schroeder et al.* [61], *Schaber et al.* [62], *Bruninx et al.* [63], *Ludig et al.* [64], *Gunkel and Möst* [21], *Koch et al.* [16], *Babrowski et al.* [22], *Egerer* [17], *Kemfert et al.* [66], *Heinemann et al.* [67], *Cebulla et al.* [68], *Gils et al.* [69], *Neumann and Brown* [12] and *Kluschke and Neumann* [71]. The remaining studies have a more general focus on Europe.

Scenarios which are investigated with several thousand nodes are presented by *Leuthold et al.* [60] and *Hörsch et al.* [19]. The former study presents a large-scale spatial MINLP optimization model of the European electricity market with a detailed dispatch model. The latter study presents an open LP optimization model of the European transmission system. In general, these models can be applied to manifold temporal resolutions. However, for the mentioned scenarios which are modeled with this high spatial resolution, the investigated timeframe is set to 24 h and 1 h respectively and the considered technology portfolio is fixed.

Several studies also model Germany with more than 75 nodes / regions [12,17,21,22]. Here, *Gunkel and Möst* [21] consider 418 nodes, *Babrowski et al.* [22] consider 440 nodes, *Egerer* [17] considers 438 nodes, *Kluschke and Neumann* [71] consider 333 nodes and *Neumann and Brown* [12] vary their spatial resolution between 20, 40, 60, 80 and 100 nodes. For these studies, the temporal representation is again simplified. *Gunkel and Möst* [21] consider 27 weighted time sub groups to model a year and a simplistic storage formulation. *Babrowski et al.* [22] model a year with three days for each season. *Egerer* [17] considers weekly timeframes with storages being empty at the beginning and end of the week. *Kluschke and Neumann* [71] consider 4380 time steps for one year. *Neumann and Brown* [12] investigate 100 / 200 / 300 / 400 time steps with the omission of storage technologies.

Studies which model Germany with an hourly resolved, annual timeframe are provided by *Kemfert et al.* [66] and *Cebulla et al.* [68]. However, these scenarios consider only 21 / 20 regions for Germany, respectively.

Temporal Resolution

Also the considered temporal resolution varies widely between the studies in literature. The scope varies between 1 h / 2 h snapshots [12, 19, 71][5], to days and weeks [17, 21, 22, 60–62, 64, 72], to a rolling horizon formulation of a year [16, 17, 65, 67] to a full temporal resolution of the year [20, 23, 24, 66, 68, 73]. Some studies also model transformation pathways, as for example *Ludig et al.* [64].

All of the studies which consider an hourly resolved, annual temporal resolution model their scenarios with 30 regions or less. Four of these studies only consider one node for Germany. Only *Kemfert et al.* [66] and *Cebulla et al.* [68] model Germany with about 20 regions.

Chosen Modeling Approach

In addition to the spatial and temporal coverage, also the chosen modeling approach differentiates the scenarios. For *ELMOD*, a model of the European electricity market, *Leuthold et al.* [60] mention a MINLP (mixed integer nonlinear program) equation set. According to the authors, this set is however often simplified to obtain, for example, a MILP (mixed integer linear program) where the binary variables are required for unit commitment. Unit commitment is also considered by *Bruninx et al.* [63] and *Koch et al.* [16]. For the consideration of DC line expansions, *Neumann and Brown* [12] also present MINLP and MILP approaches. However, the authors conclude that for models with high spatial and temporal detail, a continuous relaxation of the investment cost, post-discretization and, if required (for AC line expansions), model iterations are beneficial. Models with higher spatial / temporal resolution and endogenous system design are often modeled as LPs (linear programs) [19, 24, 62, 64, 66, 71].

In general, the consideration of integer and binary variables provides additional valuable information on the energy supply system. However, they have to be traded

[5] Scenario with 3657 substations of the grid [19].

for increased computation times and thus come at the expense of smaller degrees of freedom for the spatial, temporal and technical representation of a scenario.

Technology Portfolio

Also the considered technology portfolio varies between the studies. Several studies focus on a detailed representation of a diverse thermal power plant fleet with some RES [17, 21, 66]. Other studies are designed to capture higher penetrations of RES and thus also consider, in addition to PHES, battery storage, cf. *Babrowski et al.* [22]. In some cases, also heat or hydrogen storage is considered [16, 23, 24, 62, 65, 67–70]. Studies which explicitly model hydrogen demands are provided by *Schaber et al.* [62], who consider hydrogen and heat demands in a German context, *Victoria et al.* [24], who supply electricity, heat and hydrogen for a 30-node European scenario and *Kluschke and Neumann* [71], who comprehensively investigate the interaction of a hydrogen fueling station network for heavy duty vehicles and the power system in Germany in 2050.

A hydrogen pipeline grid is not considered in any of the scenarios. However, electric grid expansion is considered in several scenarios, either as a sensitivity analysis [16, 67, 68] and / or an endogenous optimization output [12, 21, 23, 24, 66–68, 73]. In this context, DC power flow equations are often neglected. For this purpose, an approach to investigate DC and AC line expansions is proposed by *Neumann and Brown* [12]. The only study which models gas grid expansions on a basic level is proposed by *Schaber et al.* [62]. The authors model Germany with 20 regions and provide an option to transport synthetic methane via optimized gas grid capacities for spatial balancing.

A scenario which investigates a cross-linked infrastructure design including transmission technologies for Germany is only found by *Schaber et al.* [62]. However, the authors consider only a basic modeling approach for this purpose and hydrogen transmission is not considered.

2.2.2 Future German Hydrogen Infrastructure in Literature

Suggestions for a future German hydrogen infrastructure design are made by *Seydel* [74] / the *GermanHy* study [75], *Baufumé et al.* [76], *Almansoori and Betancourt-Torcat* [77] / *Bique and Zondervan* [78], *Robinius* [14] / *Robinius et al.* [9], *Weber and Papageorgiou* [79], *Welder et al.* [2], *Reuß et al.* [80], *Cerniauskas et al.* [81] and *Caglayan et al.* [82].

Spatial Resolution

Almansoori and Betancourt-Torcat [77] / *Bique and Zondervan* [78], *Weber and Papageorgiou* [79] and *Welder et al.* [2] consider hydrogen exchanges between the federal states of Germany and thus consider up to 16 regions. *Caglayan et al.* [82] model 16 regions in Europe with 4 being in Germany. *Seydel* [74] and the *GermanHy* study [75] further increase the spatial resolution by modeling hydrogen transmission between the administrative districts of Germany ($\approx$400). *Baufumé et al.* [76], *Robinius* [14] / *Robinius et al.* [9], *Reuß et al.* [80] and *Cerniauskas et al.* [81] model their hydrogen infrastructure scenarios by considering several thousand fueling stations and, for the study of *Cerniauskas et al.* [81], also consumers in the industry sector in their transmission infrastructure design.

Almansoori and Betancourt-Torcat [77] / *Bique and Zondervan* [78] add spatial technological detail by considering storage facilitates at each demand node. However, a specific, endogenous placement of storage sites is only considered by *Welder et al.* [2] and *Caglayan et al.* [82].

Temporal Resolution

In the study of *Baufumé et al.* [76], *Almansoori and Betancourt-Torcat* [77] / *Bique and Zondervan* [78] and *Weber and Papageorgiou* [79] hydrogen production rates are estimated based on a simple distribution logic. The transmission technologies considered in the respective studies are thus designed for one time step only. A similar approach is chosen by *Seydel* [74] / the *GermanHy* study [75], however a transformation pathway from 2015 to 2050 is considered as well. *Robinius* [14] / *Robinius et al.* [9] improve the approach from *Baufumé et al.* [76] by determining full load hours for electrolyzers based on a spatially and temporally resolved electricity supply scenario for Germany. Then, the authors design the pipelines for the resulting peak load of one time step in the pipeline grid. *Welder et al.* [2] consider a year with an hourly resolution, represented by 7 typical but interconnected days. Thus, the pipeline is designed based on 168 flow variations. *Reuß et al.* [80] improve the approach of *Robinius et al.* [9] once more by considering a robust selection of demand scenarios [14, 83], however neglect in this context the placement and operation of storage sites. *Cerniauskas et al.* [81] build on the approach of *Reuß et al.* [80] and add an additional temporal dimension by considering transformation pathways from 2023 to 2050.

An hourly resolution across the year, is, besides in the studies of *Welder et al.* [2] and *Caglayan et al.* [82], not considered for any of the studies.

Technology Portfolio

The considered hydrogen production, transmission, storage and distribution technologies vary between the studies from literature.

- Hydrogen production from fossil energy carriers, i.e. steam methane reforming or coal gasification, is considered in several scenarios [74–79, 81]. However, several of these studies also consider electrolyzers as an option for renewable hydrogen generation [74–76, 78, 81]. The remaining studies consider only electrolyzers for hydrogen production [2, 9, 80, 82].
- For transmission technologies, hydrogen pipelines [2,9,14,74–76,79–82] and trucks for gaseous and liquid hydrogen transport [74, 75, 77, 78, 80, 81] are most often considered. *Reuß et al.* [80] additionally consider trucks for the transmission of liquid organic hydrogen carriers (LOHC).
- For hydrogen storage, gas vessels [2,77,78,80–82], cryogenic tanks for liquid hydrogen storage [77, 78, 80, 81], LOHC tanks [80] and salt caverns [2, 9, 80–82] are considered in literature. *Seydel* [74] / the *GermanHy* study [75], *Baufumé et al.* [76] and *Weber and Papageorgiou* [79] do not model storage intrinsically.

An endogenous consideration of cross-linked infrastructure including electricity transmission is not considered in any of the listed scenarios.

Modeling Approach

The intended purposes and thus the chosen modeling approaches vary between the presented studies. The studies of *Seydel* [74] / the *GermanHy* study [75] and *Robinius et al.* [9] consider a workflow with coupled sub-modules, i.e. first they determine an electricity supply scenario and then, based on this scenario, they determine the required hydrogen infrastructure. *Reuß et al.* [80] build on the electricity supply scenario of *Robinius et al.* [9][6]. Several of the other studies just focus on the hydrogen infrastructure design [77–79, 81]. The only studies which approach an endogenous cross-linked infrastructure design are provided by *Welder et al.* [2] and *Caglayan et al.* [82].

The pipeline design is in all approaches at least partly based on linear or mixed integer linear programing. For the consideration of integer modeling decisions [77–80, 85], nonlinear cost functions [80, 81] or pressure losses [79, 80], some studies model the infrastructure design with a MILP.

[6] The authors build their demand scenario on the German electricity demand in 2013, cf. [84].

In the studies, storage design is either considered by a specified storage duration [9, 14, 77, 78, 80, 85], endogenously determined during optimization under the consideration of each time step [2, 82] or not considered at all [74, 75, 79].

2.2.3 Energy System 2050 Scenarios for Germany

In literature, several studies exist which present scenarios for a future German energy system under the consideration of greenhouse gas reduction targets. Within this review, scenarios which model the majority of the energy system sectors in the year 2050 are assessed. Furthermore, only scenarios are considered which provide sufficiently detailed data on electricity generation and consumption[7]. With their national focus, most of these studies are published in German.

In the following, the studies “Klimaschutz: Der Plan Energiekonzept für Deutschland” [86], “Was kostet die Energiewende? Wege zur Transformation des deutschen Energiesystems bis 2050” [87], “Erfolgreiche Energiewende nur mit verbesserter Energieeffizienz und einem klimagerechten Energiemarkt –Aktuelle Szenarien 2017 der deutschen Energieversorgung” [88], “Klimaschutzszenario 2050” [89], “Klimaschutzszenario 2050” [90], “Entwicklung der Energiemärkte - Energiereferenzprognose” [91], “Die Energiewende nach COP 21 - Aktuelle Szenarien der deutschen Energieversorgung” [92], “Langfristszenarien und Strategien für den Ausbau der erneuerbaren Energien in Deutschland bei Berücksichtigung der Entwicklung in Europa und global” [93], “Langfristszenarien für die Transformation des Energiesystems in Deutschland Modul 10.a: Reduktion der Treibhausgasemissionen Deutschlands um 95% bis 2050” [94], “Leitstudie Integrierte Energiewende” [95], “Energiesystem Deutschland 2050”, 80% reduction target [96], “Pathways to deep decarbonization in Germany” [97] and “Kosteneffiziente und klimagerechte Transformationsstrategien für das deutsche Energiesystem bis zum Jahr 2050” [98] are shortly assessed in an aggregated manner.

In principal, as the scenarios assessed in these studies model the majority of the German energy system, the studies have to describe and discuss a large amount of input parameters, general modeling assumptions and scenario results. This information is often spread across the voluminous studies and, in some cases, some of it is not provided. Identifying which spatial and temporal resolution, technology portfolio or modeling approach is considered is thus often challenging. Thus, instead of extracting this information from each study individually, general trends throughout the studies are identified in the following.

[7] The optimized scenario results presented in chapter 5 will be compared to this data.

Concerning spatial resolution, none of the scenarios are modeled with an explicit spatial resolution for Germany for which endogenous technology placements are considered. Only one study considers “pseudo-regions” in which selected technologies are regionalized [98]. However, several studies consider European electricity market / power flow models to account for electricity imports and exports [86, 89, 90, 93]. The more recent studies “Langfristszenarien für die Transformation des Energiesystems in Deutschland Modul 10.a: Reduktion der Treibhausgasemissionen Deutschlands um 95% bis 2050” [94], “Leitstudie Integrierte Energiewende” [95] and “Kosteneffiziente und klimagerechte Transformationsstrategien für das deutsche Energiesystem bis zum Jahr 2050” [98] couple comprehensive infrastructure models with their scenario results. The explicit consideration of transmission infrastructure is in the majority of the studies underrepresented, however most studies mention its importance. The majority of the studies models their scenarios with an hourly resolution and consider transformation pathways until the year 2050 [86, 87, 89, 90, 93–96, 98]. The explicit modeling of storage is mentioned in some studies but does in general not appear prominently in the results.

Concerning modeling approach and technology portfolio, it can be noted that many studies use hybrid approaches to model the different sectors of the German energy system. For example, (bottom-up) models for the household, industry, transport and / or agricultural sectors are run and their outputs subsequently provided to one or more models which determine the electricity, heat and / or fuel supply [89–91, 94, 95]. The electricity supply itself is in this context often optimized. Technologies for electricity and heat generation and, in some cases, the production of renewable fuels are considered but their techno-economic parameters are not always specified. In general, the modeling detail of the scenarios is, with respect to modeled consumers and considered technologies, high in comparison to the infrastructure studies presented in the two previous sections.

In general, it can be summarized that the sectors of the energy system and the consideration of transformation pathways are well captured in the studies. However, storage and transmission infrastructure is often not modeled in detail and explicit technology placement suggestions within the regions of Germany are not made. Comprehensive cross-linked infrastructure scenarios, including the design and operation of transmission technologies, leave a gap for future research to close.

2.3 Infrastructure of Future Energy Systems

This section gives an overview of cross-linked infrastructure components which are considered in literature in the context of future energy systems. The term "infrastructure" covers in this context all technologies that are required to supply final energy demands under given ecological boundary conditions. These technologies can procure, store, transmit or consume one or multiple commodities.

The assignment of technologies to a specific infrastructure level is not necessarily unambiguous and is dependent on how the system boundaries of a scenario are defined. In general, this thesis differentiates between electricity and hydrogen infrastructure as well as infrastructure for methane-containing gas, e.g. natural gas, biogas or synthesized methane. The considered infrastructure levels, which are coupled by technologies for commodity conversion, are visualized in Figure 2.2.

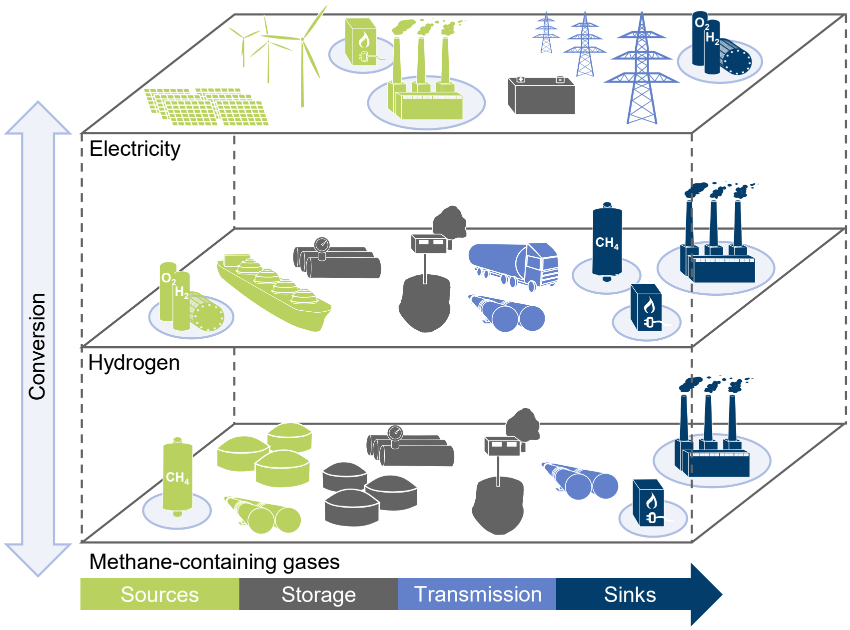

Figure 2.2: Principal modeling concept of coupled electricity and gas infrastructure levels. Prominent cross-linking conversion technologies are marked with a light blue circle.

- The upper level visualizes potential electricity infrastructure. This includes wind turbines, photovoltaic systems, power plants, batteries and hydroelectric energy storage, AC and DC lines and *Power-to-Hydrogen* technologies.
- The central level focuses on potential hydrogen infrastructure. Here, hydrogen generation from electrolysis, liquid hydrogen import, technical and geological

gas storage, pipelines and hydrogen-fueled power plants or methanation plants can be considered.

- The lower level visualizes infrastructure for methane-containing gases. Examples are technologies for biogas generation, methanation plants, natural gas imports, technical / geological gas storage, pipelines and power plants.

Naturally, this list cannot be exhaustive. For example, infrastructure related to heat supply or alternative *Power-to-X* pathways, e.g. for the production of fuels or chemicals, is not considered. Also, alternative renewable energy sources could be considered, as for example solar thermal energy. Moreover, with breakthroughs in research, additional technologies could become of interest. Nevertheless, the presented component list is adequate for the energy supply systems investigated within this thesis.

Within this section, a description for each considered infrastructure component is given. First, electricity related infrastructure is presented in subsection 2.3.1. In subsection 2.3.2, infrastructure for gaseous and liquid hydrogen is presented. Infrastructure for methane-containing gases, i.e. natural gas, biogas, purified biogas and synthetic methane, is presented in subsection 2.3.3. Technologies which convert commodities into each other are classified by their main output. For example, a gas power plant is listed under electricity infrastructure while an electrolyzer is listed under hydrogen infrastructure.

As the scenarios investigated within this thesis focus on the German energy supply system in the year 2050, special considerations for Germany are made in the descriptions. Alongside the descriptions, geo-referenced modeling approaches and techno-economic parameters assumptions, which are considered in the scenarios investigated within this thesis, are obtained from literature. These descriptions will serve as a basis for the spatial-temporal component modeling presented in chapter 4.

2.3.1 Electricity Infrastructure

For electricity generation, storage and transmission

- onshore wind turbines,
- offshore wind turbines,
- photovoltaic residential rooftop systems,
- photovoltaic open-field systems,
- run-of-river hydroelectric plants,

- decentralized electricity generation,
- centralized electricity generation,
- lithium-ion batteries,
- pumped hydroelectric energy storage,
- national AC and HVDC lines, and
- international cross-border AC and HVDC lines

are considered.

In addition to the techno-economic parameters required for the modeling of these components, capacity credits for electricity generating components are identified. The capacity credit captures the contribution of a component to a secure electricity supply, cf. [99]. The considered capacity credits are taken from a report of the German transmission system operators [100].

Onshore Wind Turbines

The installed capacity of onshore wind turbines which are financed by the *EEG (Erneuerbare-Energien-Gesetz; Renewable Energy Sources Act)* tripled from 2003 to 2017 in Germany [101]. While in 2003, about 17 GW_{el} were installed, this value reached 50 GW_{el} in 2017. In 2017, these turbines generated 86 TWh_{el} of electricity.

Considered geo-referenced modeling approach:

Approaches for the geo-referenced simulation of onshore wind turbines are provided in literature by, for example, *Ryberg et al.* [102] and *Staffell and Pfenninger* [103]. Within this thesis, future, geographically resolved onshore wind turbine potentials and their electricity generation profiles are determined by applying a workflow suggested in two publications by *Ryberg et al.* [102, 104]. In their first publication [104], *Ryberg et al.* conduct a land eligibility analysis for onshore wind turbines in Europe, considering social and political, physical, conservation and technical economic constraints. Within the remaining eligible land, wind turbines can be placed. In their second publication [102], *Ryberg et al.* describe a simulation workflow with which electricity generation profiles and required techno-economic parameters for these wind turbine locations can be efficiently computed. The generation profiles are computed from synthetic power curves. *Ryberg et al.* determine an onshore wind turbine capacity potential of in total 620 GW_{el} for Germany which have, when all placements are considered, full load hours of 1915 h.

Considered economic parameter assumptions:

The capacity specific investment of the turbines is an output of the simulation workflow by *Ryberg et al.* [102]. For the computation of the total annual cost during optimization, an economic lifetime of 20 years is assumed and the capacity specific OPEX is set to 2% of the capacity specific investment [102]. Additionally, a capacity credit of 1% on the secured electricity generation capacity is assumed [100].

Offshore Wind Turbines

According to the *Bundesnetzagentur* (*Federal Network Agency*) [101], in 2017, the installed capacity of offshore wind turbines which are financed by the *EEG* reached a value 5.4 GW_{el}. These turbines generated 17 TWh_{el} of electricity.

Considered geo-referenced modeling approach:

The workflow used within this thesis to determine future, geographically resolved offshore wind turbine potentials and their electricity generation profiles is presented by *Caglayan et al.* [105]. *Caglayan et al.* determine eligible turbine locations for Europe, factoring water depth, distance to shores and protected areas as well as shipping, pipeline and cable routes into their ocean eligibility analysis. The authors also provide technical information about the turbines' design as well as their techno-economic parameters for each location. The generation profiles of the turbines are obtained by applying the turbine simulation model of *Ryberg et al.* [102] for each offshore turbine. *Caglayan et al.* [105] determine an offshore wind turbine capacity potential of 82 GW_{el} in total.

Offshore cables which can connect the offshore wind turbines to the German mainland are considered by *Robinius et al.* [106]. Their data is based on the *Netzentwicklungsplan (NEP) Strom* (*network development plan - electricity*) from the year 2015, scenario *B2025* [107].

Considered economic parameter assumptions:

The economic parameter assumptions of the turbines are obtained from the study by *Caglayan et al.* [105]. For the computation of the total annual cost during optimization, an economic lifetime of 25 years is assumed and the capacity specific OPEX is set to 2% of the capacity specific investment. Additionally, a capacity credit of 1% on the secured electricity generation capacity is assumed [100].

Photovoltaic (PV) Residential Rooftop Systems

For the year 2017, the *Bundesnetzagentur (Federal Network Agency)* [101] determines 42 GW_p of installed solar capacities financed by the *EEG* in Germany. In 2017, these capacities generated 35 TWh_{el} of electricity. When assuming that from these 42 GW_p solar generation capacities 11 GW_p referred to PV open-field systems [108], a total of 31 GW_p of PV rooftop systems were installed.

Considered geo-referenced modeling approach:

Approaches for the geo-referenced simulation of PV rooftop systems are provided in literature by, for example, *Ryberg et al.* [102] and *Pfenninger and Staffell* [109]. To determine future capacity potentials and generation time series for PV residential rooftop systems, a workflow by *Ryberg* [110] is applied within this thesis. In the workflow, Europe is divided into equidistant grid cells and suitable rooftop areas are determined based on population density. Next, the capacity potentials within the cells are determined by considering a rooftop utilization factor of 50% and a module efficiency of 30% for the suitable area. Then, for each grid cell, electricity generation profiles can be simulated. In total, a capacity potential of 190 GW_p[8] is determined by *Ryberg* for Germany [110].

Considered economic parameter assumptions:

Within this thesis, the economic parameters of PV rooftop systems are taken from a report by the *Joint Research Center (JRC)* of the *European Commission* [111]. The capacity specific investment of the rooftop systems is set to 880 €/kW_p. Furthermore, an economic lifetime of 25 years is assumed and the capacity specific OPEX is set to 2% of the capacity specific investment [111]. Additionally, a capacity credit of 0% on the secured electricity generation capacity is assumed [100].

Photovoltaic (PV) Open-field Systems

In the year 2017, 11 GW_p of PV open-field systems were registered in Germany [108]. With a total of 42 GW_p of *EEG* financed solar capacities in 2017 [101], open-field systems provided a quarter of the installed solar capacities.

Considered geo-referenced modeling approach:

Ryberg [110] also provides a workflow to determine future capacity potentials and generation time series for PV open-field systems. In the workflow, first, a land

[8] Power generation at PTC (PVUSA Test Condition).

eligibility analysis is conducted that determines suitable land for open-field systems in Europe. Next, potential parks are assigned to the suitable land with a separation distance of 1 km. For each of the parks, a capacity potential is determined in the study by considering a ground coverage ratio of 3/7 and a module efficiency of 24%. Then, for each park, electricity generation profiles can be simulated. This simulation can be performed for systems with a fixed tilt or for systems with a tracking system used to manipulate the panel orientation. The latter are more expensive but utilize the available radiation more efficiently and thus have higher full load hours. A total, technology independent capacity potential of 54 GW_p is determined by *Ryberg* for Germany.

Considered economic parameter assumptions:

The economic parameters of the PV open-field systems are taken from a report by the *Joint Research Center (JRC)* of the *European Commission* [111].

1. The capacity specific investment of the PV open-field system with *Fixed-tilt* is set to 520 €/kW_p. Furthermore, an economic lifetime of 25 years is assumed and the capacity specific OPEX is set to 1.7% of the capacity specific investment.
2. The capacity specific investment of the PV open-field system with *Tracking* is set to 710 €/kW_p. Furthermore, an economic lifetime of 25 years is assumed and the capacity specific OPEX is set to 1.5% of the capacity specific investment.

Additionally, a capacity credit of 0% on the secured electricity generation capacity is assumed [100].

Run-of-river (r-o-r) Hydroelectricity Plants

Electricity generation from hydro-power can be categorized into run-of-river plants, reservoir plants and pumped hydro energy storage with natural water inflow. The annual peaks of electricity generation from hydro-power is naturally volatile. While the sum of installed hydro-power capacities stayed at 5.6 GW_{el} between 2011 and 2018, the annually generated electricity fluctuated between 16.5 and 23 TWh_{el}, cf. [112].

The in literature available German data for these three technologies is unfortunately often aggregated and might include data of plants stationed in Austria. Thus, technology specific information is difficult to extract from it. For maximum run-of-river generation capacities in Germany, values between 3 and 4 GW_{el} can be found in literature for Germany [101, 113].

Considered geo-referenced modeling approach:

Within this thesis, geo-referenced placements and electricity generation time series of run-of-river (r-o-r) hydroelectricity plants are obtained from the work of *Syranidis* [114]. In the work of the author, plant capacities with a total of 3.8 GW_{el} are considered. The electricity generation time series are scaled by *Syranidis* in such a way that they provide a capacity factor of 0.52 for each plant, i.e. FLHs of 4555 h/a, and so that their total annual sum equals 17.3 TWh_{el}.

Considered economic parameter assumptions:

The economic parameters of the run-of-river hydroelectricity plants are taken from a report by the *Joint Research Center (JRC)* of the *European Commission* [111]. Since it is assumed that the plants in the scenarios already exist and do not need to be built, the assumption is made that only operational cost occur. This cost is comprised of capacity and operation related cost contributions. The capacity related cost factor is set to 1.5% of the capacity specific investment (5,620 €/kW_{el}) and the operation related cost factor is set to 5 €/MWh_{el}. Additionally, a capacity credit of 25% on the secured electricity generation capacity is assumed [100].

Decentralized Electricity Generation

Combined heat and power (CHP) plants, fueled with biomass or hydrogen, provide an option to supply decentralized electricity and heat demands by renewable energy carriers. In 2017, decentralized, biomass-fueled combined heat and power (CHP) plants with electrical / thermal capacities of 0.45 GW_{el} / 1.9 GW_{th} were installed in Germany [101][9].

Forestry Biomass Potentials and Wood-fired CHP plants:

Solid biomass has the potential to significantly contribute to the electricity and heat supply in future energy systems. For example, the *Agentur für Erneuerbare Energien e.V.* (*Renewable Energies Agency*) identified in a meta-analysis [115] energetic uses of about 70-190 TWh_{heat} and 10-40 TWh_{el} in several future German energy scenarios.

A comprehensive study identifying spatial distributions of forestry potentials in Germany is provided by *Thrän et al.* [116]. In the study, a total forestry biomass potential of 142 $TWh_{wood,LHV}$ is identified for Germany.

[9] CHP plants with capacities larger than 10 MW.

Considered geo-referenced modeling approach:

Detailed, spatially resolved data are difficult to obtain from the study by *Thrän et al.* [116]. An option to distribute the identified potential across Germany in detail is a mapping by forest areas. The required data for such a mapping can be obtained by the Corine Land Cover data [117, 118]. The *Python* packages *geokit* [58] and *glaes* [119] can be used for the implementation of such a mapping workflow.

Considered economic parameter assumptions:

The techno-economic parameters of the wood-fired CHP plants are primarily based on a report of the *Danish Energy Agency* [120]. Thereby, the report's data for "*Medium Wood Chips CHP, 80 MW feed*" is used.

The capacity specific investment of a plant is set to 3300 €/kW$_{el}$ and an economic lifetime of 25 years is assumed. Furthermore, the capacity specific OPEX and the OPEX per operation are set to 4.3% of the capacity specific investment and 3.9 €/MWh$_{el}$, respectively. A commodity cost of 98 €/MWh$_{el}$ is considered for the *Source* component, as the plant is modeled with a conversion efficiency of 0.285 kW$_{el}$/kW$_{wood,LHV}$ and it is assumed that the forestry biomass can be purchased at a cost of 28 €/MWh$_{wood,LHV}$ [121]. Additionally, a capacity credit of 65% on the secured electricity generation capacity is assumed [100].

Biogas-/ Hydrogen-fueled CHP plants:

The combustion engine has been the dominating biogas operated co-generation technology in recent years, cf. [122]. Also, several CHP installations with hydrogen fueled combustion engines already exist in Germany [123, 124]. Alternative technologies for the co-generation of heat and power are for example turbines and fuel cells [122] but are not considered within the scope of this thesis.

Considered techno-economic parameters:

The techno-economic parameters of the CHP plants are, independent of the fuel type, based in thesis on data for a biogas operated spark ignition engine given in a report of the *Danish Energy Agency* [120]. Based on the experience made with a hydrogen operated CHP plant in 2018 [124], this assumption is suitable for the invest but might underestimate the efficiency of the hydrogen fueled CHP.

The capacity specific investment of the plant is set to 850 €/kW$_{el}$ and an economic lifetime of 25 years is assumed. Furthermore, the capacity specific OPEX and the OPEX per operation are set to 1% of the capacity specific investment and 6 €/MWh$_{el}$, respectively. The plant is modeled with a conversion efficiency of

$0.47\,kW_{el}/kW_{gas,LHV}$. Additionally, a capacity credit of 65% on the secured electricity generation capacity is assumed [100].

Centralized Electricity Generation from Thermal Power Plants

In 2017, 66% of the German net electricity generation came from conventional energy carriers [101]. Specifically, lignite and hard coal power plants had a share of 23% and 14% respectively on the net electricity generation while natural gas and nuclear power plants both had a share of 12%. The remaining 5% came from mineral oils and pump storage as well as non-renewable waste power plants and other energy carriers.

This electric power generation landscape will drastically change up until 2050 for several reasons:

1. According to the *Atomgesetz* (*Atomic Energy Act*) [125], the remaining German nuclear power plants are to be shut down until 2022.
2. Moreover, in the beginning of 2019, the German government formulated a report stating a coal fuel phase-out [126]. The phase-out should be completed latest in 2038, but preferably in 2035.
3. On top of that, the majority of today's natural gas power plants will be either decommissioned or will require significant refurbishment in 2050 when assuming average technical lifetimes of 30-33 years [127, 128]. Specifically, the natural gas power plant capacities given by the *Open-Power-System-Data* for 2018 would decrease from an original value of $26.1\,GW_{el}$ to a value of less than $2.4\,GW_{el}$ in 2050.

Thus, most of the power plants existing in 2018 are either decommissioned or assigned to the cold reserve in 2050. Power plants operating in 2050 will likely be newly built, gas-operated power plants with open cycle gas turbines (OCGT) or combined cycle gas turbines (CCGT). These can be fueled by methane-rich gas (MRG), e.g. natural gas, purified biogas or synthetically produced methane, but also with hydrogen. An example of a hydrogen-fueled CCGT plant can be found in *Fusina*, Italy, which started its operation in 2009 [129]. For a general overview of hydrogen reconversion technologies, see *Welder et al.* [99].

Considered geo-referenced modeling approach:

The *Open-Power-System-Data* for *Conventional power plants* [130] provides detailed data on these lignite, hard coal, natural gas and nuclear power plant capacities that contribute to the domestic net electricity generation in 2017. The data holds, amongst other information, the power plants' geo-referenced positions and technical information. The latter includes the plants' technology types and their capacities. Moreover, the data provides the plants' years of commission and, if applicable, the year of their retrofit.

Considered techno-economic parameters:

Within this thesis, the techno-economic parameters of the OCGT and CCGT plants are based on a report by the *Joint Research Center (JRC)* of the *European Commission* [111]. They are assumed to be the same for MRG and hydrogen. This assumption reflects to some extend the current literature, for example when the *JRC* report is compared to the study by *Welder et al.* [99]. However, future analyses could improve the reliability of this assumption with in-depth cost structure analyses of the plants. The chosen parameters are listed in Table 2.1.

Table 2.1: Techno-economic parameters of centralized thermal power plants.

Technology	Capacity specific invest [€/kW_{el}]	Capacity specific OPEX [€/($kW_{el}\cdot a$)]	OPEX per operation [€/MWh_{el}]	Economic lifetime [a]	Efficiency [kW_{el}/ $kW_{gas,LHV}$]
OCGT (GH_2) & *OCGT (MRG)*	550	$550 \cdot 3.0\%$	2	30	0.45
CCGT (GH_2) & *CCGT (MRG)*	850	$850 \cdot 2.5\%$	11	30	0.63

A capacity credit of 100% on the secured electricity generation capacity is assumed [100].

Lithium-ion Batteries

In recent years, the amount of installed electricity storage systems in Germany has continuously increased in the energy, household and transport sector, cf. the studies of *Stenzel et al.* [131, 132]. While only a few megawatt hours of large-scale electricity storage systems were installed in 2005, this number increased to about 550 MWh_{el} in 2018. Also, in households, the total number of installed battery storage systems in combination with photovoltaic panels has increased from 5,000 in 2014 to more than 120,000 (about 110 MWh_{el}) at the end of 2018. Moreover, while in 2013 the nominal capacity of newly approved electric cars amounted to a value of 158 MWh_{el} this value increased to 513 MWh_{el} in 2016. In all of these applications, lithium-ion batteries have been the prevalent technology.

With this prevalence of the lithium-ion battery and an expected further increase in its sales due to efforts of decarbonizing these sectors, the mass market could significantly improve the techno-economic parameters of the technology. The studies of *Elsner et al.* [133], *Fuchs et al.* [134] and *Pape et al.* [135] assess and review energy storage options in a future context and they predict these improvements for the lithium-ion battery.

A comparison between different storage options that serve as a daily storage can be made when comparing their round-trip efficiencies for a daily storage operation and their respective annual cost per usable storage capacity. In such a comparison with technology parameters from the study of *Elsner et al.* [133], it can be determined that the lithium-ion batteries are predicted to outperform most other storage options in the high efficiency storage segment, both in efficiency and in cost. An exception here can be pumped hydroelectric energy storage that might have smaller cost but however also lower round-trip efficiencies. However, it must be noted that this picture might shift with disruptive innovation breakthroughs of other storage technologies or if the sustainability of resources used for the manufacturing of the storage technologies is factored into the analysis.

Considered techno-economic parameters:

The techno-economic parameter assumptions of the lithium-ion batteries are based within this thesis on the study of *Elsner et al.* [133].

- Technical parameters: For the charge and discharge efficiency a value of 95% is considered and a self-discharge of 3% per month is assumed. The nominal capacity of the battery can be utilized to its full potential, meaning the permitted state of charge is between 0-100% of its nominal capacity. As already stated above, the battery can be fully charged / discharged within one hour. Moreover, a cyclic lifetime of 12,000 full cycle equivalents is assumed.
- Economic parameters: A capacity specific invest of 150 €/kWh$_{el}$ and a capacity specific OPEX of 1% of the invest are assumed. The economic lifetime of the battery is set to 22 years.

With their similarities to pumped hydroelectric energy storage, a capacity credit of 80% on the secured electricity generation capacity is assumed for the batteries [100].

Pumped Hydroelectric Energy Storage (PHES)

A detailed discussion of the German pumped hydroelectric energy storage (PHES) landscape is given in a study by *Stenzel et al.* [136]. In 2018, pumped hydroelectric generation capacities of 6.2 GW$_{el}$ and an attached electric storage capacity of

38.6 GWh_{el} were installed in Germany[10]. In addition to these capacities, several projects are in planning which will expand these capacities to values of 9.1 GW_{el} and 57.3 GWh_{el} respectively.

Considered geo-referenced modeling approach:

The database provided by *Stenzel et al.* [136] also enables a detailed geo-referenced modeling of PHES in Germany. For each plant, coordinates, installed capacities for turbines, pumps and basins are given. Based on these values, an average power-to-energy ratio of 1/7 can be determined. Moreover, the year of construction is also given in the database which can be used for retrofit strategies.

Considered techno-economic parameters:

Within this thesis, the techno-economic parameter assumptions of the PHES plants are primarily based on the study of *Elsner et al.* [133].

- Economic parameters: A capacity specific invest of 130 €/kWh_{el} and an economic lifetime of 40 years is assumed for refurbished *PHES*. For the *PHES* which does not require refurbishment, no investment is required. A capacity specific OPEX of 1.2% of the invest is however considered for both classes.
- Technical parameters: For the charge and discharge efficiency values of 88 / 89% are considered. The nominal capacity of the PHES plant can be utilized to its full potential, meaning its permitted state of charge is between 0-100% of its nominal capacity. As already stated above, the PHES plants can be fully charged / discharged within seven hours.

Additionally, a capacity credit of 80% on the secured electricity generation capacity is assumed [100]. This factor is applied to the maximum discharging capacity, i.e. the storage capacity multiplied by 1/7.

National AC and HVDC Lines

Quarterly reports on network and system security are published by the *Bundesnetzagentur* (*Federal Network Agency*) [137, 138]. In these, redispatching, deployment of reserve power plants, feed-in management and adjustment measures are documented. The biennial-published *Netzentwicklungsplan (NEP) Strom* (*network development plan - electricity*) gives a detailed account of the German electric grid and its future development in the next decades, cf. [107, 139, 140]. For the scenario year 2025 (scenario: *B*), the *NEP* version from 2015

[10] Capacities installed outside of Germany that are however partially associated to the German transmission system operator zones are not included in these numbers.

considers several AC (alternating current) expansions of new and in 2015 existing lines. Moreover, six HVDC (high-voltage direct current) connections are built. The HVDC lines are built with the intention to overcome a north-south division between electricity supply and demand. This division is, amongst other factors, rooted in high generation potentials from offshore and onshore wind turbines in the north and high electric load centers in the states of North Rhine-Westphalia in the west and Baden-Württemberg and Bavaria in the south. For the scenario year 2035 (scenario: *B*), the *NEP* version from 2019 already includes additional HVDC lines which enhance the connection between the North Sea and North Rhine-Westphalia and Baden-Württemberg even further. Moreover, the scenario also considers additional offshore cables that distribute the offshore electricity more effectively in the vicinity to shore. Thus, a trend towards an increased consideration of HVDC line connections can be observed.

Considered geo-referenced modeling approach:

For this thesis, geo-referenced data describing the lines considered in the *NEP-2015-B2025* is obtained from an infrastructure analysis study by *Robinius et al.* [106]. This data comprises information on capacities, lengths and reactances of the lines which can be used for the modeling of linearized power flow equations [13, 141]. The considered AC and HVDC lines are visualized in Figure 2.3. The regions around the electric grid busses are determined by a *Voronoi* tessellation[11].

Considered techno-economic parameters:

For the existing AC lines, no capital and operational expenditures are considered, and a lossless transmission is assumed. To mimic an N-1 security criterion, only 70% of the lines' nominal capacities can be used for electricity transmission [144]. The HVDC lines are generalized to being underground cables that have a voltage source converter (VSC) station at each end of the line. The losses and cost of the lines are aggregated with the ones of the converter stations.

- Technical parameters: Losses of 1.5% are assumed for each converter station [145]. In accordance with the study by *Boing et al.* [144], it is assumed that 100% of the HVDC lines' capacity can be used for electricity transmission.
- Economic parameters: Costs only arise for the additional HVDC line expansions, i.e. for *DC lines (new)*. The economic parameter assumptions of these additional connections are based on the cost specified in the *NEP* from 2019 [146]. Investments of 3,000 €/(km·MW_{el}) and 250,000 €/MW_{el} are assumed for the HVDC underground cables and each converter station respectively. For the computation of the annuities of the lines, an economic lifetime of 40 years is assumed for the aggregated system [147].

[11]The regions are determined via the *Python* package *SciPy* and its *Voronoi* class [142, 143].

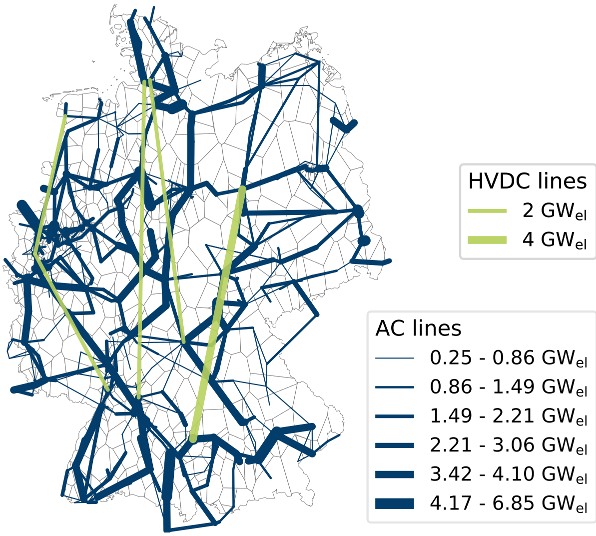

Figure 2.3: Considered electric lines in the scenarios. The lines are represented as point-to-point connections. A *Voronoi* region, indicated with gray lines, is assigned to each bus of the grid.

Cross-border AC and HVDC Lines

In 2017, Germany imported 26.7 TWh_{el} of electricity and exported 77.3 TWh_{el} of electricity[12]. The largest cross-national import flows were measured at the borders to France, the Czech Republic and Denmark. The largest cross-national export flows were located on the borders between Switzerland, Austria and the Netherlands.

Considered geo-referenced modeling approach:

The transformation from a fossil to a renewable energy supply will change the electricity generation landscape in Europe notably, cf. [114]. Correspondingly, typical import / export patterns between countries will change and thus have to be specifically modeled when assessing future energy systems.

The approach to model these future import and export potentials is based on the work of *Robinius et al.* [98]. *Robinius et al.* [98] set the electricity import and

[12] Actual, physical load flows.

export potentials for Germany equal to the negative / positive residual loads of the countries interconnected to Germany. Thus, only renewable electricity imports are considered. The residual loads are again determined by the subtraction of the renewable electricity generation from the *basic* electricity demands for each country and are given in an hourly resolution.

In this context, *Robinius et al.* consider a scenario from the work of *Syranidis* [114][13]. Figure 2.4 shows these potentials in form of the aggregated annual time series.

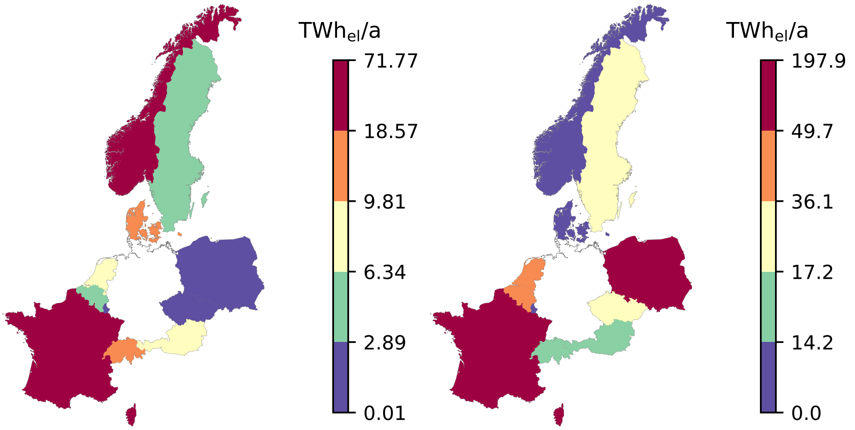

(a) Import potential (to Germany) **(b)** Export potential (from Germany)

Figure 2.4: Annual electricity import and export potentials from countries that are connected via AC / DC lines to Germany.

Norway displays high negative residual loads with its high hydroelectricity generation and small annual electricity consumption, in comparison to the other countries. France also is characterized by high negative residual loads, as large quantities of fluctuating renewable energy sources are installed in the country in the scenario. Even though France, the Netherlands and Poland have the highest installed wind turbine and photovoltaic (PV) capacities, they still display the largest positive residual loads due to their relatively high annual electricity consumptions.

The import and export time series are shown in appendix A.3 for all countries in form of heat maps. Electricity import potentials from hydroelectricity arise primarily during summer. Import potentials from PV cells are more dominant during the day

[13] *Syranidis* bases his work on the *E-Highway 2050* scenarios [148]. For the study, the *small & local* scenario with a weather year of 2013 from *Syranidis*' work is considered.

and are particularly strong in summer. Import potentials caused by wind turbines are more diffuse but are stronger during winter. Inherently, export potentials arise reversed to the import potentials.

Robinius et al. [98] provide the electricity imports and exports to a one-nodal energy system model of Germany. To translate their approach to a higher spatially resolved representation of Germany, grid data from *Robinius et al.* [106] is used within this thesis. The considered AC and DC lines are visualized in Figure 2.5.

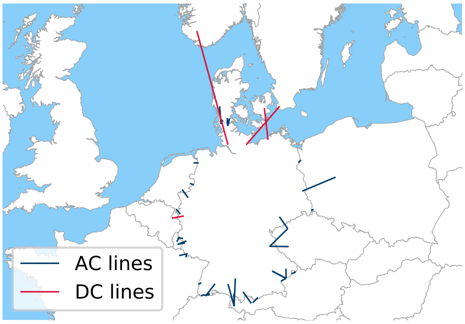

Figure 2.5: International AC lines (blue) and DC lines (red) in the scenarios.

Considered economic parameter assumptions:

The electricity import cost per MWh is set equal to the average levelized cost of electricity (LCOE) of the renewable electricity generators of each country. In the scenario of *Syranidis* [114], renewable electricity generators are onshore and offshore wind turbines, PV panels[14] as well as hydroelectricity and concentrated solar power plants. The cost parameters required for the computation of the LCOE are taken from a report by the *Joint Research Center (JRC)* of the European *Commission* [111]. Capacities and full load hours are taken from the study of *Syranidis*[15]. Table 2.2 presents these capacities and full load hours as well as the computed LCOE for each interconnected country.

For electricity export, a marginal revenue of 1 €/MWh_{el} is chosen. This value is below the LCOE of all electricity generators in the scenarios and is chosen for the sole reason to prevent unnecessary curtailment of domestic renewable electricity generators. Moreover, no electricity generators are built for the main purpose of

[14] It is assumed that half of the PV panels are open-field panels with a fixed-tilt angle and the other half are rooftop panels.

[15] Concentrated solar power plants are not listed as they only have minor installed capacities (Σ 0.5 GW_{el}) for these countries.

Table 2.2: Installed renewable electricity generators and their average full load hours (FLHs) and levelized cost of electricity (LCOE) in the interconnected countries.

	Onshore		Offshore		PV		Hydroelectricity		LCOE
	GW_{el}	FLHs	GW_{el}	FLHs	GW_{el}	FLHs	GW_{el}	FLHs	€/MWh_{el}
Austria	2.6	3314	-	-	2.8	984	13.7	3381	39
Belgium	10.9	1862	2.2	3423	21.1	919	1.4	1145	81
Czechia	3.1	2176	-	-	4.5	925	2.3	2059	69
Denmark	4.9	3532	1.7	3359	0.1	809	-	-	49
France	53.7	2713	-	-	76.6	1088	25.2	3108	58
Luxemburg	0.5	1219	-	-	0.9	941	-	-	94
Netherlands	14.5	3050	0.2	3026	31.6	894	-	-	74
Norway	3.5	4333	-	-	-	-	31.2	4140	26
Poland	14.8	2101	-	-	19.6	922	2.3	1366	76
Sweden	6.8	3308	0.2	3359	4.2	729	16.2	3724	44
Switzerland	1.4	3011	-	-	15	1020	13.7	3273	55

supplying electricity for export. As such, the optimization solver is motivated to sell unused surplus electricity to interconnected countries.

2.3.2 Hydrogen Infrastructure

The hydrogen infrastructure considered within this thesis is subdivided into infrastructure for liquid hydrogen (LH_2) and infrastructure for gaseous hydrogen (GH_2) at medium ($\sim$30 bar) and high ($\sim$100 bar) pressure levels.

For liquid hydrogen

- liquid hydrogen terminals for hydrogen imports,
- liquefaction plants (GH_2 at 30 bar $\rightarrow$ LH_2), and
- cryogenic storage tanks

are considered.

For gaseous hydrogen

- electrolyzers (p_{out}: 30 bar),
- regasification plants (LH_2 $\rightarrow$ GH_2 at 30 bar),
- compressors stations (30 bar $\rightarrow$ 100 bar),
- salt caverns ($p_{in/out}$: 100 bar),

- pipe storage systems ($p_{in/out}$: 30 bar),
- inter-regional transmission pipelines (p: 100 bar), and
- intra-regional distribution infrastructure (p: 100 bar)

are considered. Here, p is the respective pressure level of the gaseous hydrogen.

Shipping Terminals for Liquid Hydrogen (LH_2) Imports

A report by *King & Spalding* gives an overview of, in 2018, existing or planned liquid natural gas (LNG) terminals in Europe [149]. At these terminals, liquefied gas which arrives via ship can be stored and processed for further utilization. Traditionally, the terminals are used for regasification of LNG and its subsequent injection of the gas into national gas supply networks. However, also new terminal services are emerging as for example truck and rail loading of the liquefied gas.

In analogy to LNG terminals, LH_2 terminals can be designed and operated to consider hydrogen imports in an energy supply system. A description of such a LH_2 supply pathway by shipping, comprising renewable electricity generation and hydrogen production, storage and shipment, is given in a study by *Heuser et al.* [150].

Considered geo-referenced modeling approach:

As of 2018, no large-scale LNG terminals exist in Germany [149]. However several sites for future LNG terminals are under discussion [149, 151, 152] which can be used as potential future LH_2 terminals. These are located close to the cities of *Wilhelmshaven*, *Brunsbüttel* and *Stade* which are visualized in Figure 2.6.

Figure 2.6: Locations of potential liquid hydrogen terminals in the cities of *Wilhelmshaven*, *Brunsbüttel* and *Stade* in the north of Germany.

Considered economic parameter assumptions:

The cost per unit of imported hydrogen is dependent on the annual amount of imported LH_2. A cost curve as a function of the annually imported LH_2 is given in Figure 2.7. The cost curve is obtained from a study by *Forschungszentrum Jülich* [98]. In the study, the LH_2 selected for German import is produced in Iceland, Norway, Ireland and the United Kingdom.

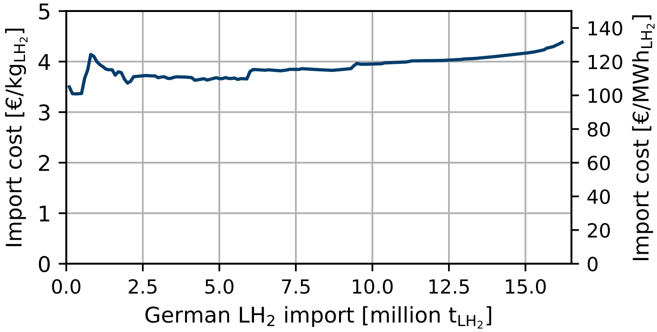

Figure 2.7: Underlying cost curve of the German liquid hydrogen import in the scenarios, data provided by [98].

The cost curve results from a trade-off between an *economy of scale* and the potential for renewable electricity generation in the respective countries. With an increasing amount of exported LH_2 in a country, the specific LH_2 cost first drops. Then, as less preferable renewable electricity generation locations have to be considered in this country, the cost increases again up until reaching the maximum eligible technical renewable potential. For small import amounts, the countries that produce and ship the LH_2 at least cost are selected first. With an increasing German import, countries that provide LH_2 at a higher cost are selected as well, leading to step-wise increases in the cost function.

Based on this data, a conservative value of 120 €/GWh$_{LH_2}$ (4 €/kg$_{LH_2}$) at German shipping terminals is a reasonable assumption if a constant expression of the cost is required.

Liquefaction Plants

Liquefaction plants enable the option to store hydrogen with a high energy density in cryogenic tanks at comparably low-cost. The liquefaction plants are discussed in technical detail and with respect to their economics by *Reuß* [153]. The author highlights the comparably high energy demand and required investment for the liquefaction plants.

Considered techno-economic parameters:

The techno-economic parameter assumptions made for the liquefaction units follow the set of assumptions made by *Reuß et al.* [154]. The invest is in this context determined for a unit of around 70 $MW_{LH_2,LHV}$, i.e. matching the capacity of one electrolyzer plant (100 MW_{el}). *Reuß et al.* again base a part of their assumptions on the *idealhy* report [155]. The assumptions are summarized in the following.

- Technical parameters: To convert 1.02/$kWh_{GH_2,LHV}$ of gaseous hydrogen at 30 bar into 1 $kWh_{LH_2,LHV}$ of liquid hydrogen, 0.2 kWh_{el} of electricity is required.
- Economic parameters: A capacity specific investment of 1500 €/$kW_{LH_2,LHV}$ and an economic lifetime of 20 years are assumed. The annual, capacity specific OPEX is set to 8% of the invest.

Cryogenic Tanks for Liquid Hydrogen (GH_2) Storage

Cryogenic tanks are considered for liquid hydrogen (LH_2) storage which are, for example, described by *Reuß et al.* [154] and *Reuß* [153]. In these isolated tanks, liquid hydrogen is stored at low temperature (< 21 K) and small overpressure (< 10 bar). Hydrogen boil-off losses have to be considered for these tanks as it is not possible to entirely prevent a heat transfer into the tank and the thus evaporated hydrogen needs to be vented with a pressure relief valve.

Considered techno-economic parameters:

The techno-economic parameter assumptions made for the LH_2 tanks follow the set of assumptions made by *Reuß et al.* [154]. These assumptions are summarized in the following.

- Technical parameters: A charge and discharge efficiency of 100% and a self-discharge of 0.03% per day are assumed. Furthermore, it is assumed that the tank can be fully charged and discharged within one hour.
- Economic parameters: A capacity specific investment of 0.75 €/$kWh_{LH_2,LHV}$ and an economic lifetime of 20 years are assumed. The annual, capacity specific OPEX is set to 2% of the invest.

Electrolyzers

For the years 2003 to 2018, 128 European *Power-to-Gas* (PtG) demonstration projects, in operation or in planning, are identified in a study by *Wulf et al.* [156]. Of these projects, 56 are located in Germany. A geo-referenced visualization of German PtG projects is given by the *Deutscher Verein des Gas- und Wasserfaches* (*DVGW*, *German association for gas and water*), cf. [157] (status: April 2019). *Wulf et al.* [156] show that from 2003 to 2014, electrolysis with anion exchange membranes, also known as alkaline electrolysis (AEL), is on average the predominant electrolysis type in these PtG projects. Since 2015, proton exchange membrane electrolysis (PEMEL) has become the more prominent technology type and is already incorporated in MW_{el}-scale projects. A few projects also consider high temperature electrolysis (HTEL) with solid oxide electrolysis cells. This trend between the electrolysis technology types is also identified by *Buttler and Spliethoff* [158] who in this context also identify a trend towards large-scale systems with electrolysis power in the MW_{el}-scale.

Buttler and Spliethoff [158] as well as *Schmidt et al.* [159] compare the different electrolysis technology types in their technical performance. They classify AEL as a mature technology, identify commercial applications for PEMEL and state that HTEL applications are on a pre-commercial level. Concerning load flexibility, PEMEL currently demonstrates the best performance characteristics. HTEL systems are on the other hand characterized by comparably long start-up times. Efficiency-wise, HTEL has the highest system efficiencies, followed by AEL and PEMEL which perform with similar efficiencies.

Smolinka et al. [160] also projects these performance characteristics into the future (2018, 2030 and 2050). In these projections, similar rankings between the technology types are identified concerning efficiency and start-up time. A deviation can however be identified in the start-up times of HTEL systems that are projected to significantly decrease up until 2050.

The studies of *Buttler and Spliethoff* [158], *Schmidt et al.* [159] and *Smolinka et al.* [160] as well as the studies from *Saba et al.* [161] and *Glenk and Reichelstein* [162] also project the cost of AEL and PEMEL into the next decades. The studies are consistent in stating an, on average, lower investment cost for AEL in comparison to PEMEL before 2030. The PEMEL does however display, on average, a higher cost decline in the studies. *Smolinka et al.* also give a cost projection for the year 2050 in which both technologies display similar values. *Schmidt et al.* [159] and *Smolinka et al.* [160] also give cost projects for HTEL and in this context identify a potential for large cost reductions. These cost reductions are however associated with large uncertainties and are moreover inherently dependent on the future market turn-over of the technology.

Considered techno-economic parameters:

Large-scale electrolysis plants with a plant size of 100 MW_{el} are considered. The techno-economic parameter assumptions made for the PEMEL sites follow the set of assumptions made by *Reuß et al.* [154]. These assumptions are summarized in the following.

- Technical parameters: A conversion efficiency of 0.7 $kW_{GH_2,LHV}/kW_{el}$ and an outlet pressure of 30 bar is assumed.
- Economic parameters: A capacity specific invest of 500 €/kW_{el} and an economic lifetime of 10 years are assumed. The annual, capacity specific OPEX is set to 3% of the invest.

Regasification Plants

For the regasification of liquid hydrogen (LH_2), the LH_2 is first pressurized with a pump and then turned to gaseous hydrogen in an evaporator. The principal concept of this process is described in a report by *Nexant et al.* on hydrogen delivery infrastructure [163].

Considered techno-economic parameters:

The techno-economic parameter assumptions made for the regasification plants follow the set of assumptions made by *Reuß et al.* for LH_2 pumps and evaporation units [154]. *Reuß et al.* again base a part of their assumptions on the mentioned report by *Nexant et al.* [163]. The assumptions are summarized in the following.

- Technical parameters: To convert 1 $kWh_{LH_2,LHV}$ of liquid hydrogen into 1 $kWh_{GH_2,LHV}$ of gaseous hydrogen at 100 bar, 0.02 kWh_{el} of electricity are required.
- Economic parameters: A capacity specific investment of 24 €/$kW_{GH_2,LHV}$ and an economic lifetime of 10 years are assumed. The capacity specific OPEX is set to 3% of the invest, i.e. 0.72 €/($kW_{GH_2,LHV}$·a).

Hydrogen Compressor Stations

Compressors must be considered at several steps of hydrogen supply systems. They are required to operate gas storage, to compress the gas for its transmission in pipelines or to reach a pressure level required by a final hydrogen demand. Different compressor types, varying in their structural shape and their power drive, are available for these tasks. In analogy to the assumptions made by *Reuß*, who discusses the deployment of hydrogen compressors in national supply systems [153], mechanical compressors with electric drives are considered within this thesis.

Considered techno-economic parameters:

The techno-economic parameter assumptions for the scenarios within this thesis are determined based on the methodology presented by *Reuß* [153]. The compressor is designed for a hydrogen flow of 70 $MW_{GH_2,LHV}$, i.e. matching the capacity of one electrolyzer plant (100 MW_{el}), that is compressed from 30 bar to 100 bar.

- Technical parameters: To convert 1 $kWh_{GH_2,LHV}$ of gaseous hydrogen at 30 bar into 1 $kWh_{GH_2,LHV}$ of gaseous hydrogen at 100 bar, 0.02 kWh_{el} of electricity is required.
- Economic parameters: A capacity specific invest of 42 €/$kW_{GH_2,LHV}$ and an economic lifetime of 15 years are assumed. The annual, capacity specific OPEX is set to 4% of the invest.

Salt Caverns for Gaseous Hydrogen (GH_2) Storage

A status quo of GH_2 storage in salt caverns is given in a study by *Welder et al.* [99] which was compiled within the context of this thesis and is portrayed in the following.

The storage of hydrogen or hydrogen-rich gas in salt caverns has been an interest of research since the 1970's [164]. Particularly the gas-tightness of salt caverns, even at high pressure, but also their inhibition of chemical reactions make them well-suited for the storage of gaseous hydrogen [165]. A general discussion of the feasibility of hydrogen storage in salt caverns is given by *Kruck et al.* [166]. Not only is hydrogen storage in salt caverns an interest of research but it has been put into practice for several decades, however mostly at petrochemical industry sites [166, 167].

Gas storage in salt caverns itself has been practiced in Germany for many decades, cf. the historical summary of underground gas storage (UGS) provided by *Sedlacek* [168]. This also includes the storage of the hydrogen-rich town gas, cf. [164, 168]. In 2017, 255 natural gas filled salt caverns were in use in Germany and 52 more were in planning [169, 170].

Considered geo-referenced modeling approach:

Within this thesis two classes of salt caverns for hydrogen storage are considered. On the one hand, the in 2017 existing salt caverns can be rededicated for hydrogen use [168]. On the other hand, new caverns can be built at eligible locations identified by *Welder et al.* [2].

Considered techno-economic parameters:

The techno-economic parameter assumptions of the hydrogen-filled salt caverns within this thesis are primarily based on the salt cavern parameters presented in a study of *Stolzenburg et al.* which was written on behalf of the *Bundesministerium für Verkehr und digitale Infrastruktur* (*BMVI*, *Federal Ministry of Transport and Digital Infrastructure*) [165]. The cost contribution of the compressor station at the salt caverns (6.2 million €) is calculated separately with a methodology presented by *Reuß* [153]. The electricity demand of the compressor, which is small in comparison to the other electricity demands in the scenarios, is neglected.

The following assumptions are made to differentiate between new and existing salt cavern locations. For a new salt cavern storage system (212 $GWh_{GH_2,LHV}$), investments for the solution-mining of the cavern (30 million €) and above-ground technical infrastructure (15 million €) are considered. An additional investment for streets and buildings (23 million €) is distributed over seven caverns and is in this context linearized to a capacity specific cost contribution. For existing salt cavern locations, the investments for the solution-mining and streets and buildings are omitted.

- Technical parameters: It is assumed that the gas injection into the cavern is lossless and that the self-discharge of the cavern is zero. The injection and withdrawal efficiencies are set to 100%. The allowed state of charge of the cavern ranges between 33-100% of its nominal capacity, i.e. the pressure of the cavern ranges between 58 and 175 bar. Furthermore, it is assumed that a maximum of 450 $MWh_{GH_2,LHV}$ can be injected into / withdrawn from a 212 $GWh_{GH_2,LHV}$ cavern within one hour.
- Economic parameters: Capacity specific invests of 0.07 €/$kWh_{GH_2,LHV}$ and 0.23 €/$kWh_{GH_2,LHV}$ are considered for existing and new salt cavern locations respectively. For all salt caverns, new and existing, an annual, capacity specific OPEX of 2% is assumed. The economic lifetime of the below and above-ground infrastructure is set to 30 years.

Pipe Systems for Gaseous Hydrogen (GH_2) Storage

The option to store hydrogen in near-surface pipe storage systems is suggested in a report of the *HyUnder* project published in 2013 [166]. In contrast to salt caverns, the pipe storage systems do not depend on specific geological structures but are rather dependent on local geology. In the report, several pipe storage systems in Europe are listed which are however operated with natural gas. However, the report suggests that pipe storage systems will soon also be an eligible option for hydrogen storage.

Considered techno-economic parameters:

Within this thesis, pipe storage systems are modeled based on techno-economic data for natural gas pipelines [171] and hydrogen compressors [153] as well as on information of existing pipe storage systems [166, 172]. The storage built in *Urdorf*, *Switzerland*, thereby serves as a reference case.

It is assumed that the pipes have a diameter of 1.4 m, pressure levels between 30 and 100 bar and a typical length of 4140 m. This results in a typical geometrical volume of 6373 m^3, a total working gas capacity of 1.18 $GWh_{GH_2,LHV}$ and a cushion gas content of 0.54 $GWh_{GH_2,LHV}$. Furthermore, it is assumed that the storage can be completely charged / discharged within 3.5 days, i.e. that it can serve as a weekly balancing option. This results in a total investment of 11.4 million € for the pipe storage[16] and of 1.1 million € for the compressor.

- Technical parameters: It is assumed that the gas injection and withdrawal into the pipe storage is lossless and that the self-discharge of the pipe storage is zero. The allowed state of charge of the pipe storage ranges between 31-100% of its nominal capacity, i.e. the pressure of the pipe storage ranges between 30 and 100 bar. Furthermore, as stated above, it is assumed that it takes a minimum of 3.5 days to fully charge / discharge the storage.
- Economic parameters: A capacity specific invest of 7 €/$kWh_{GH_2,LHV}$ and an annual, capacity specific OPEX 1% of the invest are assumed. The economic lifetime is set to 30 years.

Hydrogen Transmission Pipelines

In the work of *Reuß* [153], the cost of hydrogen supply is analyzed as a function of a daily hydrogen demand and an average hydrogen transport distance. Depending on the demand and the transport distance, the analysis identifies cost-effective storage and transport technologies that can be used for hydrogen supply, cf. Figure A.17 in the appendix A.6. The analysis finds that for hydrogen demands above 20 to 50 t/day, hydrogen transport by pipeline is the most cost-effective option on the transmission level. On the distribution level, either GH_2 trucks or pipelines achieve lowest supply cost. These results are confirmed in a corresponding, spatially resolved scenario analysis for Germany by *Reuß et al.*, cf. [80]. As the hydrogen demands considered within this thesis are of a similar or higher magnitude as the ones considered by *Reuß et al.* [80], hydrogen transmission pipelines are considered for the transport of hydrogen between regions.

[16] The investment includes a 5% surcharge for using the pipes for hydrogen instead of natural gas.

Hydrogen transmission pipelines are assessed in technical and economic detail by *Reuß* [153], who again refers in parts of his assessment to the work of the *Hydrogen Analysis Resource Center* (*HyARC*) [173], *Krieg* [174], *Yang and Ogden* [175], *Mischner et al.* [171] and *Robinius et al.* [83]. The assessment is summarized in the following with respect to pipeline network design, operation and cost.

- For the year 2016, the *HyARC* identified hydrogen pipeline networks with a total length of 4542 km on a global level [173]. These networks are often subclassified into transmission and distribution networks. The transfer point between the two levels has to be set a priori and can for example be based on administrative boundaries [174] or hydrogen demand centroids [175].

- A hydrogen flow within a network is enforced by the pressure differences between entry and exit points. The flows themselves are again associated with pressure losses. More information about the fundamentals of gas transport in pipeline networks is for example given by *Mischner et al.* [171]. If the pressure level at the entry points is not sufficient to guarantee a minimum pressure at the exit points, re-compressor stations within the pipeline network are required. However, re-compressor stations are not necessarily required as shown by *Robinius et al.* [83] and *Reuß et al.* [15].

- The investment required for a pipeline can be subclassified into installation and material cost [175]. For small pipeline diameters, the cost of installation is the dominant cost factor while for larger pipeline diameters, the material cost is predominant. Cost functions for hydrogen pipelines are provided from *Krieg* [174], which includes compressor stations, or can be deduced from cost functions of natural gas pipelines, as provided by *Mischner et al.* [171].

It can thus be concluded that hydrogen pipelines are an already well-established technology.

Considered geo-referenced modeling approach:

Potential routes for new pipelines are derived within this thesis from the study of *Baufumé et al.* [76]. In the study of *Baufumé et al.*, a linear approach to model fluid flows in pipelines is considered. In this approach an average fluid velocity of 15 m/s and an average fluid density of 5.7 kg_{GH_2}/m^3 (at 70 bar and 10 °C, cf. [176]) is assumed. With these values, the maximum energy flow / transport capacity can be determined for a given pipe diameter. Thus, pressure losses along the lines are not explicitly considered. In future work, an additional consideration of pressure losses can be applied with the methods proposed by *Robinius et al.* [83] and *Reuß et al.* [15].

Considered techno-economic parameters:

The cost contributions of the pipelines are modeled based on economic data for natural gas pipelines provided by *Mischner et al.* [171]. The data includes information about the invest and the operational expenditures for high pressure (100 bar) pipelines. The invest is again given as a function of the diameter which ranges between 100 mm and 1,400 mm. In addition to the investment specified by Mischner et al., a 5% surcharge on the investment is considered to operate the pipelines with hydrogen. The correlations between the resulting required investment of a pipeline and its diameter and estimated maximum transport capacity is visualized in Figure 2.8.

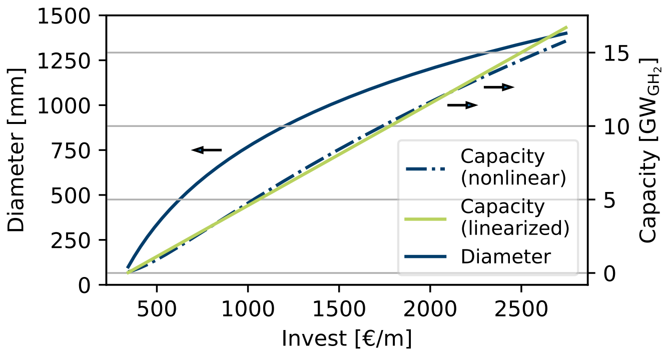

Figure 2.8: Correlation between GH_2 pipeline cost, diameter and estimated average transport capacity.

While the correlation between the diameter and the invest is evidently nonlinear, the correlation between the capacity and the invest can be approximated with minor deviations by a first-degree polynomial. This polynomial translates to a capacity specific invest of 144 €/(m·GW_{GH_2}) and a capacity independent invest contribution of 340 €/m.

- Technical parameters: If the supply system is modeled as with a MILP, binary design decision variables can be considered for the pipelines to model the nonlinear cost-capacity correlation and the pipelines can be modeled with a minimum capacity of 0.45 GW_{GH_2}, which correlates to a minimum pipeline diameter of 100 mm[17].
- Economic parameters: A capacity specific invest of 144 €/(m·GW_{GH_2}), a

[17] The supply systems in this thesis are modeled as linear programs and the binary cost contribution is assessed in the post-processing of the optimization results.

binary invest contribution of 340 €/m and a binary OPEX contribution of 5 €/(m·a) are assumed. The latter two parameters are only of relevance when the supply system is modeled a MILP. The economic lifetime is set to 40 years.

Hydrogen Distribution in Demand Regions

With transmission pipelines being considered for inter-regional hydrogen transmission, intra-regional hydrogen distribution must be considered to model the remaining distance between the pipeline transmission hubs and the end-consumers. Such an intra-regional supply chain comprises transmission technologies, e.g. trucks or pipelines, but also fueling stations, cf. [153].

Considered geo-referenced modeling approach:

The scenarios for hydrogen demands in the industry and transport sector are obtained from *Cerniauskas et al.* [81]. The hydrogen demand data provided by *Cerniauskas et al.* [81] is available as geo-referenced point data[18]. Figure A.2 in the appendix A presents this data in an aggregated form for each federal state of Germany for the *medium* market penetration scenario.

Table 2.3 gives respective hydrogen demands in the *low*, *medium* and *high* hydrogen demand scenario. The hydrogen demand increases from a total of 2.6 Million t_{H_2}/a in the *low* demand scenario to a value of 7.3 Million t_{H_2}/a in the *high* demand scenario.

Table 2.3: Penetration scenarios of the hydrogen market segments in the year 2050, based on *Cerniauskas et al.* [81] (HDVs: heavy duty vehicles, MHVs: material handling vehicles).

	Buses	Trains	Cars	Industry	HDVs	MHVs	$\Sigma\,\mathrm{Mt}_{H_2}$/a	$\Sigma\,\mathrm{TWh}_{H_2,LHV}$/a
Low	30%	50%	25%	30%	25%	30%	2.566	85.5
Medium	60%	75%	50%	60%	50%	60%	5.04	167.9
High	95%	95%	75%	95%	75%	95%	7.316	243.7

An estimate of the CO_2 emissions that can be prevented by providing renewably produced hydrogen to these sector can be made based on the German national inventory reports [177]. Table 2.4 provides such an estimate for the three different penetration scenarios.

[18] For the demand in the transport sector, a scenario from *Cerniauskas et al.* with a single fueling station type (maximum capacity: 1000 kg_{GH_2}/day, average utilization: 700 kg_{GH_2}/day) is considered.

Table 2.4: Estimate of avoided CO_2 emissions in the different penetration scenarios (in reference to the year 1990, estimated based on [177]).

	Cars	HDVs & buses	Railways	Ammonia production	$\Sigma Mt_{CO_2}/a$
Low	28	9.7	1.4	1.8	41
Medium	56	19.3	2.2	3.6	81
High	84	29	2.8	5.7	121

Emissions transport sector: HDVs and buses aggregated in the database $\rightarrow$ penetration rate of HDVs considered. Industry sector: only ammonia production; other process emissions, e.g. of methanol production, are either small or could not be identified and are thus neglected $\rightarrow$ emission budget underestimated.

Once Germany is disaggregated into regions, a comprehensive model provided by *Reuß* [153] is applied within this thesis to determine mass-specific, intra-regional hydrogen distribution cost for these demands. For the demands in the industry sector, gaseous hydrogen trucks or distribution pipelines are accounted for. For the demands in the transport sector, gaseous trucks and fueling stations are considered in the supply chain.

2.3.3 Infrastructure for Methane-containing Gases

The infrastructure considered within this thesis for methane-containing gases is subdivided into infrastructure for biogas, with a comparably low methane content, and methane-rich gas, referred to as MRG. MRG serves in this context as an umbrella term for natural gas, purified biogas and synthetic methane.

As infrastructure components for methane-containing gases,

- biogas plants,
- biogas purification and grid injection plants,
- methanation plants,
- salt caverns,
- pore storage,
- pipe storage systems,
- double membrane gas storage, and
- transmission pipelines

are considered.

Biogas Potentials and Plants

The deployment of gaseous biomass varies widely across scenarios available in literature. The *Agentur für Erneuerbare Energien e.V.* (*Renewable Energy Agency*) identified in a meta-analysis [115] annual energetic uses of about $0-38\,\text{TWh}_{el}$ (electricity generation), $0-31\,\text{TWh}_{heat}$ (heat generation) and $0-11$ TWh as a final energy demand in the transport sector in several future German energy scenarios.

Bio / green waste and liquid manure are residual material candidates for gaseous biomass production[19]. A detailed overview of their theoretical potentials in Germany is given in a study by the *Deutsches Biomasseforschungszentrum* (*German Biomass Research Center*) [116]. The study identifies a biogas potential of $6\,\text{TWh}_{biogas,LHV}$ from bio and green waste and a potential of $25\,\text{TWh}_{biogas,LHV}$ from liquid manure. These potentials are comparably moderate, cf. the meta-analysis by the *Agentur für Erneuerbare Energien e.V.* [115], and are considered in the following.

Considered geo-referenced modeling approach:

Biogas potentials are usually available in literature for each of the federal states of Germany, cf. [116, 180, 181]. A geological mapping is applied within this thesis to obtain a finer spatial resolution. For this mapping, the *Python* packages *geokit* [58] and *glaes* [119] are applied. Considered distribution keys are, for bio / green waste, the population density of Germany [182] and, for manure, pasture areas [118].

Considered techno-economic parameters:

The required infrastructure for the biogas production is not explicitly modeled but is assumed to be accounted for in the operational cost of the biogas plant. This operational cost is set to $70\,€/\text{MWh}_{biogas,LHV}$ which is, according to the *Fachagentur Nachwachsende Rohstoffe e.V.* (agency for renewable resources) [121], corresponding to a medium sized production plant.

Biogas Purification and Grid Injection Plants

A detailed account of biogas upgrading plants is given by the *Danish Energy Agency* in its in 2018 published report on *Technology Data for Renewable Fuels* [183]. These plants are usually composed of an upgrading plant, a compressors unit and a connection to the gas grid. The in 2017 most commonly

[19] An obligatory collection of bio / green waste has been introduced in Germany [178, 179]

used upgrading technologies are water scrubbing, chemical / amine scrubbing and pressure swing adsorption.

Considered techno-economic parameters:

The techno-economic parameter assumptions of the biogas purification and grid injection plants are derived from the data provided by the *Danish Energy Agency* [183]. The data includes the costs and auxiliary electricity demands of the purification and compressor units. A connection pipeline is not considered.

- Economic parameters: A capacity specific invest of 343 €/$kW_{MRG,LHV}$ and an economic lifetime of 15 years is assumed. The annual, capacity specific OPEX is set to 2.5% of the invest.
- Technical parameters: To generate 1 $MWh_{MRG,LHV}$ of methane-rich gas, 1 $MWh_{biogas,LHV}$ of biogas and 0.043 MWh_{el} of electricity are required.

Methanation Plants

According to *Wulf et al.* [156], in 2017, 12.6 MW_{el} of electrolyzers were installed in Germany to feed hydrogen to methanation plants. Of these, 8.6 MW_{el} fed into catalytic methanation plants and the remaining 4 MW_{el} into biological methanation plants.

Methanation plants are discussed and assessed in techno-economic detail in a study by *Agora Energiewende and Frontier Economics* [184]. The study assesses future *Power-to-Fuel* pathways and provides descriptions of the pathways' technologies as well as literature reviews on their cost parameters. Temperature swing adsorption is described as a technology which can be used for carbon dioxide capture from air and for which no locational eligibility constraints have to be considered. Subsequent to this process, the captured carbon dioxide can be converted together with hydrogen to methane. For this process, catalytic methanation is listed as a, in 2018, state-of-the-art methanation technology.

Considered techno-economic parameters:

The techno-economic parameter assumptions of the methanation plants are primarily derived from the study by *Agora Energiewende and Frontier Economics* [184]. The parameters for the temperature swing adsorption and the catalytic methanation are in this context aggregated. As an economic lifetime of the plant is not provided in the study, the economic lifetime is set based on a study by *Schmidt et al.* [185].

- Economic parameters: A capacity specific invest of 1800 €/$kW_{MRG,LHV}$ and an economic lifetime of 25 years is assumed. The capacity specific OPEX is set to 4% of the investment.
- Technical parameters: To generate 1 $MWh_{MRG,LHV}$ of methane-rich gas, 1.25 $MWh_{GH_2,LHV}$ of hydrogen, 201 kg_{CO_2} and 0.05 MWh_{el} of electricity are required.

Salt Caverns for Methane-rich Gas (MRG) Storage

Besides gas storage in salt caverns to ensure a supply security, future energy supply systems can use these salt caverns to buffer temporal fluctuations arising from injections and withdrawals of purified biogas or synthetic methane from and into the grid. The status quo of salt cavern gas storage in Germany is described in section 2.3.2. In general, it can be summarized that natural gas storage in salt caverns has been successfully practiced in Germany for many decades, cf. *Sedlacek* [168].

Considered geo-referenced modeling approach:

The same salt cavern locations which are considered for hydrogen storage are also considered for MRG storage. These are on the one hand the in 2017 existing salt caverns which are currently used for natural storage, but also new salt cavern locations are an option, cf. [2].

Considered techno-economic parameters:

A simplified approach, based on assuming ideal gas behavior, is chosen to adapt the techno-economic parameters of the MRG-filled salt caverns from the ones of the hydrogen-filled salt caverns: The parameters of interest are adapted by dividing them with the lower heating value of hydrogen (3 $kWh_{GH_2,LHV}/Nm^3$) and multiplying them with an average lower heating value of methane-rich gas (set to 10 $kWh_{MRG,LHV}/Nm^3$), respectively. Correspondingly, also the capacity specific invest and the operational expenditures are multiplied with a factor of 3/10. The techno-economic parameters with which the storage of methane-rich gases (MRG) in salt caverns is modeled are correspondingly set as follows.

- Technical parameters: It is assumed that the gas injection into the cavern is lossless and that the self-discharge of the cavern is zero. The injection and withdrawal efficiencies are set to 100%. The allowed state of charge of the cavern ranges between 29-100% of its nominal capacity, i.e. the pressure of the cavern ranges between 58 and 175 bar. Furthermore, it is assumed that a maximum of 1500 $MWh_{GH_2,LHV}$ can be injected into / withdrawn from a

707 $GWh_{GH_2,LHV}$ cavern within one hour.

- Economic parameters: Capacity specific invests of 0.02 €/$kWh_{MRG,LHV}$ and 0.07 €/$kWh_{GH_2,LHV}$ are considered for existing and new salt cavern locations respectively. For all salt caverns, new and existing, an annual, capacity specific OPEX of 2% of the original invest is assumed. The economic lifetime of the below and above-ground infrastructure is set to 30 years.

Geological Pore Storage for Methane-rich Gas (MRG)

Aquifers or former oil and gas fields, collectively named geological pore storage, are alternative options for the storage of MRG. In 2016, 18 pore storage sites were in operation in Germany to store natural gas [170]. At these sites, either aquifers or former oil and gas fields served as pore storage.

Considered geo-referenced modeling approach:

The locations of the existing pore storage sites are obtained from the study on underground gas storage (UGS) in Germany [170].

Considered techno-economic parameters:

The techno-economic parameters for pore storage represent an average pore storage site in Germany and are derived from a report on underground gas storage in Germany [170]. In general, and in comparison to other storage technologies, pore storage can be characterized by its slow operation but also by its low additional technical infrastructure requirements and correspondingly low associated cost.

- Technical parameters: It is assumed, as an average value, that it takes about 2,600 h to fully charge / discharge a pore storage. Furthermore, a minimum state of charge of 55% and a maximum state of charge of 100% is considered.
- Economic parameters: Cost contributions from existing pore storage are mainly dominated by operation and maintenance cost. An exchange of the above-ground infrastructure, as for example of the compressor station, could be additionally considered. However, overall, these cost contributions are so small when compared to the overall capacities of the storage sites that they cannot be sufficiently considered within the used optimality tolerance of the scenarios. Thus, only marginal operational charging cost of 1 €/$MWh_{MRG,LHV}$ are considered.

In principal, the available data allows for a more detailed regional representation of the pore storage. This modeling detail is however not the main focus of this thesis but might be considered in future work.

Pipe Systems for Methane-rich Gas (MRG) Storage

As established in 2.3.2, several pipe systems for natural gas storage existed in 2017. For the storage system built in *Urdorf*, *Switzerland*, ample information can be found in literature [166, 172]. The storage system in *Urdorf* was built with the intention to serve as a daily buffer storage [172].

Considered techno-economic parameters:

The MRG pipe storage systems are modeled analogously to the hydrogen pipe storage systems. However, no hydrogen surcharge for the pipelines is considered and the compressors are designed for methane-rich gas.

It is again assumed that the pipes have a diameter of 1.4 m, pressure levels between 30 and 100 bar and a typical length of 4140 m. This results in a typical geometrical volume of 6373 m^3, a total working gas capacity of 3.94 $GWh_{MRG,LHV}$ and a cushion gas capacity of 1.39 $GWh_{MRG,LHV}$. Furthermore, it is, again, assumed that the storage can be completely charged / discharged within 3.5 days, i.e. that it can serve as a weekly balancing option. This results in a total investment of 10.8 million € for the pipe storage and of 1.24 million € for the compressor.

- Technical parameters: It is assumed that the gas injection and withdrawal into the pipe storage is lossless and that the self-discharge of the pipe storage is zero. The allowed state of charge of the pipe storage ranges between 26-100% of its nominal capacity, i.e. the pressure of the pipe storage ranges between 30 and 100 bar. Furthermore, it is assumed that it takes a minimum of 3.5 days to fully (dis)charge the storage.
- Economic parameters: A capacity specific invest of 2.3 €/$kWh_{MRG,LHV}$ and an annual, capacity specific OPEX of 1% of the invest are assumed. The economic lifetime is set to 30 years.

Double Membrane Gas Storage for Raw Biogas

Several technology options are available for the storage of raw biogas. The *Deutsches Biomasseforschungszentrum* (*German Biomass Research Center*) differentiates in this context between low, medium and high pressure storage technologies [122]. Their report states that low-pressure storage, with overpressure levels of 0.5 until 30 mbar, are most commonly used. Medium- and high-pressure vessels are operation and cost extensive and are therefore practically not used in agricultural biogas plants in Germany. The report further differentiates between integrated and external low-pressure storage technologies. Integrated storage technologies are built above the biogas fermenter while external ones are built on a separate foundation. They usually operate under constant pressure and varying volume, i.e. with foil or membrane technologies.

Considered techno-economic parameters:

The techno-economic parameter assumptions for the double membrane gas storage are derived from a study by Barchmann et al. [186]. A geometrical volume of about 5,000 m^3 per storage unit is assumed which can function, for the assumed medium sized biogas plant sizes, as a daily storage. As the costs of internal and external double membrane gas storage are within similar range for these geometrical size [186], no differentiation between the two installations is made.

- Economic parameters: A capacity specific invest of 4 €/$kWh_{biogas,LHV}$ and an economic lifetime of 8 years is assumed.
- Technical parameters: The maximum, relative charging and discharging rates are set to (600 m^3/h) / 5,000 m^3. Furthermore, a minimum state of charge of 10% and a maximum state of charge of 90% are assumed.

It must be noted that the energy related, capacity specific invest is dependent on the lower heating value of the biogas. As the lower heating value can significantly vary with the production process (5 – 7.5 $kWh_{biogas,LHV}/Nm^3$ [121]), also the respective invest consequently varies. For the capacity specific invest stated above, a conservative value of 5 $kWh_{biogas,LHV}/Nm^3$ was assumed.

MRG Transmission and Natural Gas Imports

According to the *Bundesnetzagentur* (*Federal Network Agency*) [101], in 2017, Germany imported 1677 $TWh_{NG,LHV}$ of natural gas. Furthermore, 70 $TWh_{NG,LHV}$ of natural gas and 9 $TWh_{biogas,LHV}$ were produced domestically and 4 $TWh_{NG,LHV}$ were withdrawn from storage sites. Of these in total 1760 $TWh_{NG,LHV}$ of, mostly, natural gas, 744 $TWh_{NG,LHV}$ were again exported and 936 $TWh_{NG,LHV}$ domestically consumed.

The *Netzentwicklungsplan Gas 2018-2028* [152] (*Network Development Plan - Gas, 2018-2028*) and its corresponding online database give a detailed account of the current status quo of the German natural gas supply. Additionally, the development plan presents two methane-related gas demand and supply scenario pathways for Germany.

- In 2018, a MRG demand of 860 $TWh_{NG,HHV}$ is stated in the development plan. Less than 10% of this demand can be supplied by domestically produced natural gas (63 $TWh_{NG,HHV}$). The remaining demand needs to be supplied from natural gas imports or withdrawals from geological storage. The extensive German transmission pipeline grid enables the supply of this demand. Currently, the German pipeline grid is operated on two types of natural gas. It receives low caloric natural gas (L-gas) from its own wells as well as from Dutch gas imports. High caloric natural gas (H-gas) is delivered to Germany by pipeline from Denmark, Norway and the Russian Federation. The two gas types must be transported in separate systems. However, as the German L-gas production is decreasing and the Dutch L-gas imports are planned to be reduced, a shift from L-gas to H-gas is taking place. The shift is supposed to be completed up until 2030.

- In the two scenario pathways of the *Netzentwicklungsplan Gas 2018-2028*, a gas demand decrease from 2018 to 2028 of 9% and 19% is projected respectively. The final energy consumption of gas decreases in the industry, household and service sectors. Moreover, the gas demand of district heating plants is assumed to decrease. Increases in demand are seen in the transport sector and for gas-operated power plants. The demand for gas-operated power plants increases from 138 $\mathrm{TWh_{NG,HHV}/a}$ in 2015 to a maximum of 191 $\mathrm{TWh_{NG,HHV}/a}$. The report also suggests pipeline construction and deconstruction measures to ensure a secure gas supply for these scenario pathways.

In line with the scenario pathways suggested by the development plan, the study by *Hauser et al.* [187] identifies for a "Germany 2030" scenario an increasing natural gas demand in the power sector (2012: 61 $\mathrm{TWh_{el}/a} \rightarrow$ 2030: 91 $\mathrm{TWh_{el}/a}$). Only slight increases in load shedding due to pipeline congestion are identified by the authors. Thus, they conclude that the German natural gas system is robust against an increasing natural gas demand from power plants, however the extension of selected pipeline routes might be worthwhile to consider.

Considered geo-referenced modeling approach:

For the spatial resolved modeling of the natural gas grid in future energy supply systems, spatially resolved grid data from *Cerniauskas et al.* [85] is obtained. The linearized fluid flows can be estimated by considering an average fluid velocity of 10 m/s [171, 188], a fluid density of 55 $\mathrm{kg_{MRG,LHV}/m^3}$ (at 10 °C and 70 bar, cf. [176]) and a lower heating value of 10 $\mathrm{kWh_{MRG,LHV}/kg}$ for a pipeline connection. However, only 10% of the computed transmission capacities are used in the scenarios in order to provide additional transmission capacities to not modeled gas demands and fluid flows, e.g. heat demands or international gas imports and exports.

Considered economic parameter assumptions:

A commodity cost factor of 33 €/$\mathrm{MWh_{MRG,LHV}}$ is assumed for the imported natural gas [189]. In principal, this cost factor depends on the gas quality and the country of origin. As the cost factor is related to the lower heating value (LHV) of the gas, the effect of the gas quality is to some extend relativized. However, the price dependence on the country of origin is more challenging to consider and requires an intercontinental gas market model for the year 2050. As this is beyond the scope of this thesis, a uniform cost factor for the gas is assumed. The challenge of setting this value is reflected in literature, cf. [86, 89–91, 95, 190, 191]. In these studies of future German energy system scenarios, a wide range of cost values is given (30-69 €/$MWh_{MRG,LHV}$). Thus, the considered cost factor for natural gas is on the lower end of the spectrum.

Furthermore, it is assumed that burning 1 $MWh_{NG,LHV}$ of natural gas leads to 201 kg_{CO_2} of carbon dioxide [192]. Additionally, for the operation of the gas grid, a marginal cost factor of 1 €/($MWh_{MRG,LHV}$·100 km) is assumed which partially mimics operational expenditures for the grid but moreover leads to a cleaner optimization output.

2.4 Summary

In this chapter, cross-linked infrastructure modeling in literature was reviewed. For this purpose, first, general modeling approaches and frameworks were discussed. Next, German scenarios for energy supply infrastructure were reviewed. Last, technology candidates for a future German energy system infrastructure were assessed.

For the general modeling of energy supply systems, modeling methods, spatial and temporal data representation, features of optimization frameworks as well as specific optimization frameworks and auxiliary software were reflected upon.

- To determine optimal operation and investment planning of energy and energy supply systems, the literature points towards the application of linear or mixed integer linear programs.
- The spatial and temporal data has to be aggregated and discretized to be compatible with standard optimization modeling frameworks. For the temporal resolution of energy and energy supply systems with high shares of RES, at least hourly resolved time steps should be considered. For complexity reduction, spatial and temporal clustering approaches are considered in some studies.
- Modeling features which can / should be considered when modeling energy systems are identified based on a study in literature. In this study, these

features are reviewed for open-source energy system optimization tools.

- Available *Python*-based open-source optimization frameworks are shortly assessed. In the context of this thesis, the absence of power flow equations in several frameworks, the inability to model an economy of scale as well as the absence of temporal complexity reduction while maintaining the ability to model seasonal storage is of interest.

Three types of scenarios were reviewed for the German case study. The first type refers to studies which investigate future German electricity infrastructure. The second type of scenarios assesses future German hydrogen infrastructure. In the third scenario type, energy system 2050 scenarios for Germany with a high sectoral detail were reviewed. Each scenario type was investigated with respect to spatial and temporal detail, considered technology portfolio and chosen modeling approach. There, it becomes evident that while several modeling frameworks possess the theoretical ability to model energy supply systems with high technical detail, not all or even just a few of the available features are applied when modeling scenarios. Which of the features are considered is strongly scenario dependent. While systems with small spatial and temporal resolutions and / or small technology portfolios are modeled with integer variables, systems with high spatial and temporal resolutions are only modeled as linear programs. In some cases, additional heuristics or model-coupling approaches are applied to obtain additional modeling detail. In general, it can be noted that comprehensive German cross-linked infrastructure scenarios which model seasonal storage and investigate transmission infrastructure design are not found in literature at the point in time when this thesis was written.

Furthermore, technology options for a future German energy system infrastructure were assessed. For this purpose, the technologies were categorized into electricity infrastructure, hydrogen infrastructure and infrastructure for methane-containing gases (natural gas, biogas, synthetic methane). For each technology option, a short description was provided and, if applicable, the role of the technology in the German energy system of 2017 / 2018 mentioned. Alongside the descriptions, modeling approaches and input data for geo-referenced technology modeling were collected and techno-economic technology parameters identified.

Chapter 3

Spatio-temporal Energy System Optimization

Within this thesis, the assessment of infrastructure in future energy systems is based on the optimization of spatially and temporally resolved energy systems. The objective of this optimization is to design and operate the energy system's infrastructure in such a way that its total annual cost is minimized.

The first step to achieve such an optimal design and operation is the definition of a *model* of the energy system. For this, first the spatial and temporal scope of the energy system must be determined in such a way that they are suitable to model infrastructure design. Next, equations must be defined that model the behavior of all components of the energy system within this spatial and temporal scope. This results in the abstract model of the energy system. Thereby, the data, with which the general, abstract model is filled to obtain a specific expression of it, needs to be processed such that it is compatible with the model formulation. The considered data is based on a *scenario* which describes the framework of the future energy system.

The approach that is used within this thesis to determine the spatial and temporal representation of the investigated scenarios is described in section 3.1. In this context, also the methodology to aggregate the energy system's data, such that it is compatible with the chosen spatial and temporal representation, is presented. Section 3.2 introduces the framework that provides the abstract model formulation which was used to generate the scenarios. Based on these two sections, section 3.3 presents the overall workflow with which the investigated scenarios were generated. This chapter concludes with a discussion and a summary section, section 3.4 and section 3.5 respectively.

3.1 Spatial and Temporal Energy System Representation

The consideration of infrastructure in energy system models requires an adequate representation of the spatial and temporal dimension of the energy system in the model. To determine this representation, first the scope of the spatial and temporal dimension must be determined.

An energy system covers a wide geographical area with numerous primary energy sources, locations of secondary energy generation and final energy consumers that are interconnected with each other by transmission infrastructure. Thus, the chosen spatial representation must enable the modeling of the energy system's primary transmission infrastructure and, consequently, all data of the energy system must be geographically assigned.

The energy system must be designed and operated in such a way that it ensures the supply of final energy demands over a given timeframe. Thereby, dynamic system components, as for example storage components, necessitate the consideration of the timeframe as an interconnected entity. The chosen temporal representation must enable an adequate consideration of fluctuating generation and demand data as well as be suitable for storage infrastructure design. As seasonal energy storage is of interest in future energy systems, the timeframe should cover at least one year.

The consideration of a continuous space and time dimension would quickly become computationally intractable in this context. Therefore, the energy system must be modeled with a simplified spatial and temporal representation. Within this thesis, this representation is obtained in two steps that are visualized in Figure 3.1.

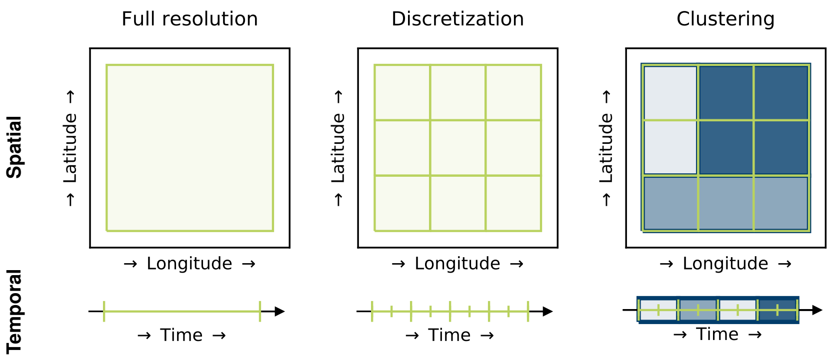

Figure 3.1: Discretization and clustering of the spatial and temporal dimension. The blue color shades indicate the cluster affiliations.

The principal concepts of these two steps are described in the following.

- First, the continuous spatial and temporal dimensions are discretized. The temporal discretization thereby considers two hierarchy levels, one coarse and one fine level. Within the time steps of the fine hierarchy level, non-dynamic components are modeled with a constant operating rate and dynamic components are modeled with a constant rate of change. A *copper plate* (see box below) is assumed within the discrete regions.
- Second, to reduce the complexity level even further, the spatial and temporal dimensions can be clustered respectively. In this context, the discrete regions are aggregated to interconnected clusters. Each period on the coarser temporal hierarchy level is assigned to a temporal cluster, called typical period.

In this context, the energy system's geo-referenced data is processed to match the spatial representation and, for all time series data, to match the temporal representation.

A detailed account of this procedure is given in the following two subsections, first for the spatial dimension and then for the temporal dimension.

COPPER PLATE ASSUMPTION:
The assumption of a perfect electric grid, i.e. electricity flows from generators to consumers are unrestricted, is known as the "copper plate" assumption in electric power systems research [13, 29]. A copper plate assumption is made when electric busses ("grid nodes") are spatially aggregated in an energy system model. Simple improvements of this assumption are possible, for example by assuming simple additional loss and / or cost factors without actually modeling the physical network itself simultaneously. The principal concept of the copper plate assumption can be transferred to gas networks, or in general commodity transportation networks, as well and gains relevance in energy system models focusing on gas infrastructure design and operation.

3.1.1 Spatial Discretization, Clustering and Data Aggregation

The regions of an energy system model should be chosen in such a way that the errors made with the *copper plate* assumption are as small as possible while keeping the computational effort to solve the model within a computational budget. With the focus on the integration of increasing distributed renewable electricity generation, the copper plate assumption becomes critical due to an increasing amount of congestion in the electric grid, cf. the German *Monitoring Report 2018* [101].

Choosing the regions with a focus on the electric grid is thus a reasonable approach and it is followed upon within this thesis. In theory, both the electric transmission and distribution networks could be considered in this context. However, as runtimes can already exceed reasonable computational budgets when solely the transmission grid is modeled, finer spatial resolution which incorporate distribution networks are not considered[1]. The highest possible spatial discretization level is thus given by the number of nodes, called busses, in the electric transmission network. Each area in the considered geographical scope of the energy system is assigned to the closest bus using the *Python* package *SciPy* and its *Voronoi* class [142, 143]. The resulting regions are called *Voronoi* regions. These regions can be aggregated again by a clustering method, cf. subsection 2.1.2.

In this thesis, the spatial clustering approach made in the *E-Highway 2050* report [30] and the study by *Hörsch and Brown* [18] is adapted. As the energy system scenarios that are modeled within this thesis consider on the one hand additional gas infrastructure and on the other hand allow the expansion of infrastructure in general, the weights in the *k-means* clustering approach are chosen differently. As an arbitrary choice of the weight parameter should be avoided, out of necessity, it is set to a uniform value of 1. Thus, the busses are clustered based on their *Euclidean* distance only. Furthermore, a hierarchical clustering algorithm is used to obtain deterministic clustering results. The clustering and subsequent network reduction is implemented with the *Python* package *PyPSA* [45, 46]. The exact number of clusters can be chosen in dependence of the investigated scenario. As an example, the spatial discretization of Germany by *Voronoi* regions and examples for regional aggregations are visualized in Figure 3.2.

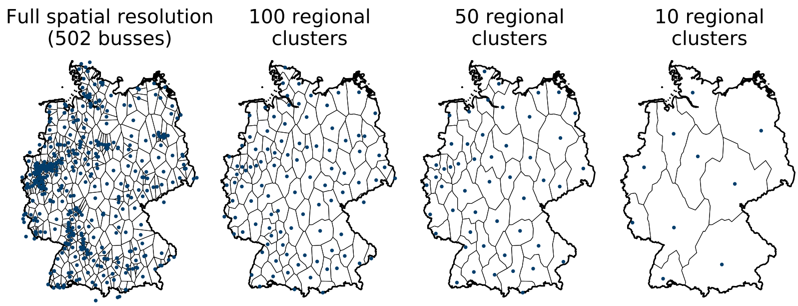

Figure 3.2: The spatial discretization of Germany by *Voronoi* regions and exemplary resulting regional clusters.

[1]Scenarios investigated within this thesis already exceeded reasonable computational budgets of more than several days when only the transmission grid was considered on workstations as Intel® Xeon® Platinum 8180 CPU @ 2.50GHz and Intel® Xeon® Gold 6154 CPU @ 3.00 GHz.

The busses that are outside of Germany and which *Voronoi* regions do not coincide with the administrative boundaries of Germany are assigned a small area containing only the electric bus.

The geo-referenced data which is associated with a scenario run is aggregated once the clustered regions are determined. Four geo-referenced data types are considered in the scenarios within this thesis. Their aggregation modes are visualized in Figure 3.3.

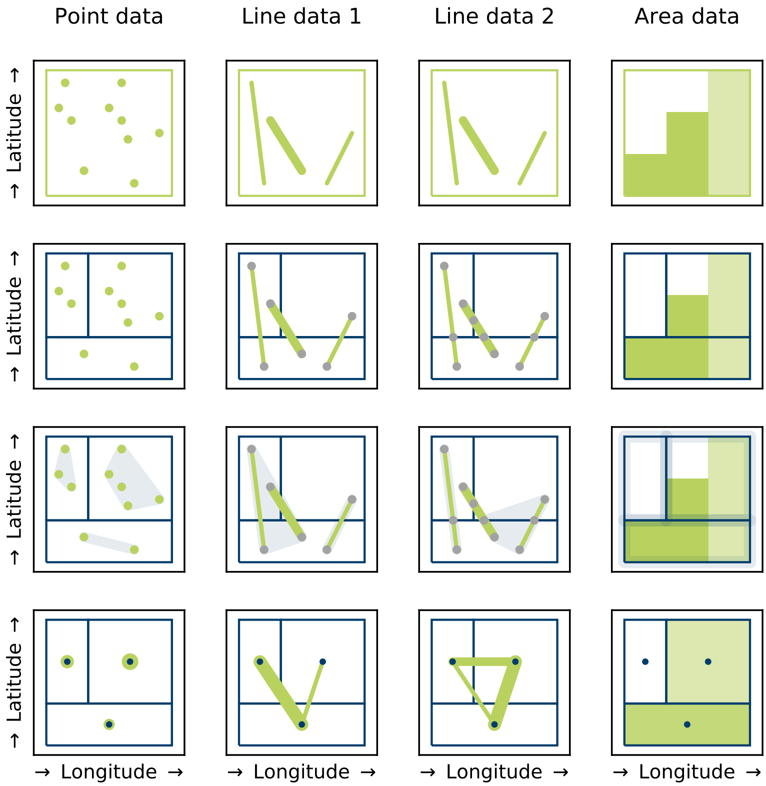

Figure 3.3: Spatial data aggregation modes.

Point data refers for example to potential locations of new wind turbines and their generation profiles. All point data is first categorized by its type and then summarized for each region and, if the data is a time series, for each time step. Two subcategories are considered for line data. The first one refers to line data that has only two entry/exit nodes, for example an electric line route. The second one refers to line data that can have multiple entry/exit nodes along its length, as for example pipeline route data. While the first one only connects the regions in which the entry/exit nodes are located in, the second one connects the regions which intersect with the line. If multiple lines connect two regions, their capacities are summarized. Area data refers, for example, to an electricity demand which is reported for a set of regions that does not coincide with the defined regions of the energy system. This data is distributed to the defined regions based on their regional overlap. After the area data is distributed, the resulting data shares within each region of the energy system are summarized.

3.1.2 Temporal Discretization, Clustering and Data Aggregation

The scenarios which are investigated within this thesis consider a snapshot of the year 2050 and focus, amongst other research questions, on the role of seasonal gas storage in energy systems. Therefore, the temporal representation of the investigated energy system models must cover at least one year and the chosen discrete time steps must be fully interconnected with each other. The selected time step length depends on three factors. These are required modeling detail, available computational budget and data availability. Several studies reviewed by *Ringkjøb et al.* [6] demonstrate how a temporal resolution with time steps larger than one hour can cause modeling errors in energy systems with large shares of variable renewable electricity sources. *Deane et al.* [26] even demonstrate how sub-hourly temporal resolutions, from 5 up to 60 minutes, affect the model output of an island system with a fixed generation portfolio. They find that while changes in the system cost and the total annual generation per technology remain relatively small, up to 1% and 4% respectively, the operation dynamic of the technologies and the runtime (3 h - 70 h) can change significantly. Thus, the literature points to having at least an hourly resolution to achieve an adequate modeling detail.

Within this thesis, a timeframe of one year with an hourly resolution was chosen. Even though sub-hourly resolutions would be of interest, they were not pursued within this thesis due to a very restricted availability of sub-hourly resolved generation and demand data. Moreover, higher temporal resolutions would have increased the already long runtimes of the models.

Time series clustering and aggregation is considered as an option to further reduce the complexity of the models. *Kotzur et al.* [31] investigate the impact of different time series aggregation methods on optimal energy system design. Their methodology was adopted within this thesis. In the modeling framework that was developed in the context of this thesis, the time series data can be disaggregated and clustered into typical periods. As daily patterns can be observed in a number of fundamental time series in the energy system, a typical period length of one day stands to reason. The exact number of typical days can be chosen in dependence of the investigated scenario. The algorithm is implemented with the *Python* package *tsam* [31, 59] which is again included in the *Python* package *FINE* [169] presented in section 3.2. The storage formulation in the *FINE* package thereby includes a storage formulation which interconnects the typical periods, thus making a seasonal storage investigation possible [2, 32, 169].

3.2 *FINE* - A Framework for INtegrated Energy System Assessment

With the spatial and the temporal representation of the energy system model being established, mathematical equations need to be formulated which represent the behavior of the energy system's components. These equations can then be used to determine the optimal design and operation of the energy system. As established in section 2.1 of the *Related Work* chapter, several models exist for this purpose in literature. However, they need to be adapted and expanded to generically model coupled infrastructure in technical detail. This new model formulation must not only provide an adequate modeling detail for storage and transmission infrastructure but also must deal with the corresponding increasing complexity of the models. In particular, it must consider an *economy of scale* with non-linear cost-capacity correlations for transmission infrastructure, but also a detailed storage infrastructure representation and the consideration of n-m conversion operations (n commodities in, m commodities out). In this context *FINE*, a framework for integrated energy system assessment, was developed by the author.

FINE is a generic, *Python*-based energy system optimization framework which is published open-source on GitHub[2]. The framework provides the capability to build user-defined mathematical abstractions of energy systems and to determine cost-optimal designs and operation strategies of them. Thereby, the energy systems are modeled with a discrete spatial and temporal resolution. The mathematical abstraction of the energy system is centered around balance equations and storage conservation for each specified commodity (e.g. electricity, natural gas, hydrogen, carbon dioxide, etc.). Additional equations and inequalities provide technical and ecological boundary conditions. Time series aggregation can be considered for complexity reduction. Variables, for example the capacity of a component or the amount of purchased natural gas, are associated with

[2] `https://github.com/FZJ-IEK3-VSA/FINE`, status: March, 2019

costs. The mathematical abstraction is used to build and optimize a mixed integer linear program (MILP). The objective of the program is to minimize the energy system's total annual cost. Balance equations and boundary conditions constitute the constraints.

The formulation of the MILP is described in detail in the next sections. Afterwards, the object-oriented *Python* implementation of *FINE* is presented.

3.2.1 Optimization Formulation

The optimization formulation of the mixed integer linear program comprises definitions of variables, constraints and an objective function that is to be minimized during optimization. The variable values that determine the smallest objective function value while fulfilling all constraints are determined during optimization. The optimization program provided by *FINE* is visualized in Figure 3.4. The modality in which the elements are aggregated and presented complies with the *Python* implementation of the program.

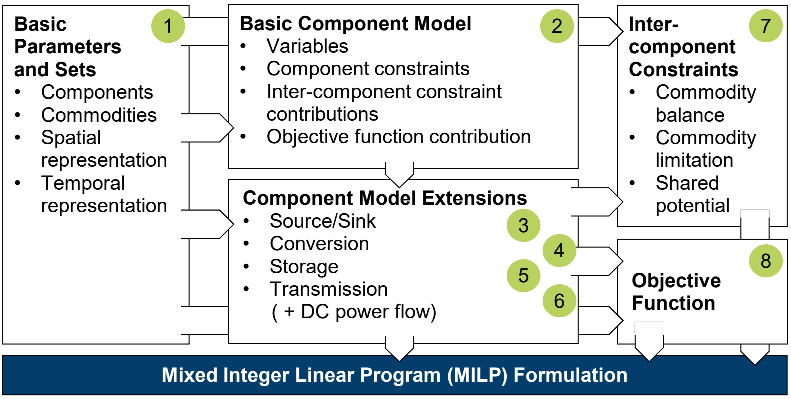

Figure 3.4: Structure of the optimization program provided by *FINE*. The numbers highlighted in green refer to the order in which the elements are presented in this subsection.

The optimization program is formulated with the following conventions:

- Functions and variables are written in italic letters.
- Parameters and indices are written in roman letters.
- Sets are written in calligraphic capital letters.
- $\mathbb{S}$ is defined as the set of all strings.

Basic Parameters and Sets

The energy system's basic framework is constituted by a number of parameters and sets that hold information about the components, commodities and the spatial and temporal resolution with which the energy system is modeled.

Component Set:

The set that contains the names of all $\bar{\mathrm{c}} \in \mathbb{Z}^{>0}$ components with which the energy system is modeled is given by

$$\mathcal{C} \ = \left\{\mathrm{comp}_0, \ldots, \mathrm{comp}_{\bar{\mathrm{c}}-1}\right\}, \text{ with } \mathrm{comp}_\mathrm{c} \in \mathbb{S} \ \ \forall \ \mathrm{c} \in \{0, \ldots, \bar{\mathrm{c}}-1\} \ . \tag{3.1}$$

Commodity Sets:

The set of all $\bar{\mathrm{m}} \in \mathbb{Z}^{>0}$ commodities that are considered in the energy system is given by

$$\mathcal{M} = \{\mathrm{comm}_0, \ldots, \mathrm{comm}_{\bar{\mathrm{m}}-1}\}, \text{ with } \mathrm{comm}_\mathrm{m} \in \mathbb{S} \ \ \forall \ \mathrm{m} \in \{0, \ldots, \bar{\mathrm{m}}-1\}. \tag{3.2}$$

The set $\mathcal{M}^{\mathrm{comp}} \subseteq \mathcal{M}$ associates each component with one or more commodities.

Location Sets:

The set of all $\bar{\mathrm{l}} \in \mathbb{Z}^{>0}$ locations that are considered in the energy system is given by

$$\mathcal{L} \ = \left\{\mathrm{loc}_0, \ldots, \mathrm{loc}_{\bar{\mathrm{l}}-1}\right\}, \ \text{ with } \mathrm{loc}_\mathrm{l} \in \mathbb{S} \ \ \forall \ \mathrm{l} \in \{0, \ldots, \bar{\mathrm{l}}-1\}. \tag{3.3}$$

A location is modeled as a *node* in the framework. A connection between two locations is modeled as an *edge*. Components in $\mathcal{C}$ can either be *node*- or *edge*-based.

If comp $\in \mathcal{C}$ is a *node*-based component, the set of locations at which the component is modeled is defined as

$$\mathcal{L}^{\mathrm{comp}} = \left\{\mathrm{loc} \mid \forall \ \mathrm{loc} \in \mathcal{L} : \mathrm{locEligibility}^{\mathrm{comp}}_{\mathrm{loc}} = 1\right\}. \tag{3.4}$$

If comp $\in \mathcal{C}$ is an *edge*-based component, the set of locations at which the component is modeled is defined as

$$\mathcal{L}^{\mathrm{comp}} = \left\{(\mathrm{loc}_{\mathrm{in}}, \mathrm{loc}_{\mathrm{out}}) \mid \forall \ (\mathrm{loc}_{\mathrm{in}}, \mathrm{loc}_{\mathrm{out}}) \in \mathcal{L} \times \mathcal{L} : \mathrm{locEligibility}^{\mathrm{comp}}_{(\mathrm{loc}_{\mathrm{in}}, \mathrm{loc}_{\mathrm{out}})} = 1\right\}. \tag{3.5}$$

The parameters $\mathrm{locEligibility}^{\mathrm{comp}}_{\mathrm{loc}}$ and $\mathrm{locEligibility}^{\mathrm{comp}}_{(\mathrm{loc}_{\mathrm{in}}, \mathrm{loc}_{\mathrm{out}})}$ state whether a component is eligible at that *node* / *edge* ($= 1$) or not ($= 0$). *Edge*-based components are modeled as being bidirectional. This implies that if a connection between loc_{l1} and loc_{l2} is eligible, also the connection between loc_{l2} and loc_{l1} is eligible.

Time Sets:

The parameter $t^{\text{total}} \in \mathbb{Z}^{>0}$, by default 8760 (i.e. 24 h/day $\cdot$ 365 day $=$ 8760 h), specifies the total number of time steps with which the energy system is modeled. The corresponding index set that encompasses all of these time steps is

$$\mathcal{T}^{\text{total}} = \left\{0, \ldots, t^{\text{total}} - 1\right\}. \tag{3.6}$$

The parameter $\tau^{\text{hours}} \in \mathbb{R}^{>0}$ defines the number of hours per time step, by default 1 h. The number of years τ^{years} which the energy system covers is determined by

$$\tau^{\text{years}} = \frac{t^{\text{total}} \cdot \tau^{\text{hours}}}{8760 \text{ h}} \text{ a}. \tag{3.7}$$

Thus, the default value represents one year (1 a). The parameter $t^{\text{per period}} \in \mathbb{Z}^{>0}$ specifies the number of time steps per period. Thereby, t^{total} must be a multiple of $t^{\text{per period}}$, i.e. $t^{\text{total}} \equiv 0 \pmod{t^{\text{per period}}}$. If the energy system is investigated with its full temporal resolution, $t^{\text{per period}}$ is set equal to t^{total}. If the energy system is modeled with typical periods, cf. subsection 3.1.2, $t^{\text{per period}}$ is set smaller or equal to t^{total}[3]. The corresponding set that contains all time steps within one period is given by

$$\mathcal{T}^{\text{per period}} = \left\{0, \ldots, t^{\text{per period}} - 1\right\}. \tag{3.8}$$

An additional time set is required to keep track of storage inventories. Storage inventories are defined right at the beginning and at the end of the regular time steps. The set

$$\mathcal{T}^{\text{per period}}_{\text{inter}} = \left\{0, \ldots, t^{\text{per period}}\right\} \tag{3.9}$$

gives these momentary points in time. Here, index 0 corresponds to the beginning of time step 0 and the index $t^{\text{per period}}$ corresponds to the end of time step $t^{\text{per period}} - 1$ within that period, respectively. The total number of periods p^{total} results from the total number of time steps and the time steps per period by

$$p^{\text{total}} = t^{\text{total}} \,/\, t^{\text{per period}}. \tag{3.10}$$

The corresponding set that encompasses all of these periods is

$$\mathcal{P}^{\text{total}} = \left\{0, \ldots, p^{\text{total}} - 1\right\}. \tag{3.11}$$

[3] Setting these two parameters equal to each other when typical periods are considered corresponds to modeling the full temporal resolution.

Thus, $|\mathcal{P}^{\text{total}}| = 1$ if the energy system is modeled with the full temporal resolution and $|\mathcal{P}^{\text{total}}| \geq 1$ if typical periods are considered. In analogy to the set $\mathcal{T}^{\text{per period}}_{\text{inter}}$, see equation (3.9), the momentary points at the beginning and at the end of a period are encompassed in the set

$$\mathcal{P}^{\text{total}}_{\text{inter}} = \left\{0, \ldots, \text{p}^{\text{total}}\right\}. \tag{3.12}$$

If typical periods are considered, each regular period is assigned one of $\text{p}^{\text{typical}} \in \mathbb{Z}^{>0}$ typical periods, cf. subsection 3.1.2. The set encompassing all typical periods is

$$\mathcal{P}^{\text{typical}} = \left\{0, \ldots, \text{p}^{\text{typical}} - 1\right\}, \quad \text{with } \mathcal{P}^{\text{typical}} \subseteq \mathcal{P}^{\text{total}}. \tag{3.13}$$

The function which maps the regular periods to a typical period is labeled

$$map : \mathcal{P}^{\text{total}} \rightarrow \mathcal{P}^{\text{typical}}. \tag{3.14}$$

The frequency with which each period occurs during the total investigated time is defined as

$$freq : \begin{cases} \{0\} \rightarrow \{1\} & \text{, with full temporal resolution, or} \\ \mathcal{P}^{\text{typical}} \rightarrow \mathbb{Z}^{>0} & \text{, with time series aggregation.} \end{cases} \tag{3.15}$$

In the following, all basic operation variables are declared for all periods or typical periods, depending on whether time series aggregation is considered, and all time steps within these periods. The cross-product of these sets is given by

$$\mathcal{P} \times \mathcal{T} = \begin{cases} \mathcal{P}^{\text{total}} \times \mathcal{T}^{\text{per period}} & \text{, for a full temporal resolution, or} \\ \mathcal{P}^{\text{typical}} \times \mathcal{T}^{\text{per period}} & \text{, with time series aggregation.} \end{cases} \tag{3.16}$$

Similarly, the cross-product for keeping track of storage inventories is defined by

$$\mathcal{P} \times \mathcal{T}_{\text{inter}} = \begin{cases} \mathcal{P}^{\text{total}} \times \mathcal{T}^{\text{per period}}_{\text{inter}} & \text{, for a full temporal resolution, and} \\ \mathcal{P}^{\text{typical}} \times \mathcal{T}^{\text{per period}}_{\text{inter}} & \text{, with time series aggregation.} \end{cases} \tag{3.17}$$

***Basic* Component Model**

The *Basic* component model comprises sets of variables, constraints, inter-component constraint-contributions and objective function contributions that apply to all components specified in $\mathcal{C}$. In this context, the variables and constraints can be divided into either being time-independent or time-dependent.

Basic time-independent variables and constraints:

The boolean parameter hasCapVars$^{\text{comp}}$ determines if a component is modeled with a physical capacity (True) or without one (False). A component which is modeled with physical capacity is for example a gas power plant while an electricity demand does not require one. The following variables and constraints refer to all components comp $\in \mathcal{C}$ that are modeled with a physical capacity.

A capacity variable $cap_{\text{loc}}^{\text{comp}} \in \mathbb{R}^{\geq 0}$ is declared for all locations loc $\in \mathcal{L}^{\text{comp}}$ in the energy system at which the component can appear. Implicitly, this capacity is modeled either as a continuous or discrete value by

$$cap_{\text{loc}}^{\text{comp}} = \begin{cases} \text{capPerUnit}^{\text{comp}} \cdot nbReal_{\text{loc}}^{\text{comp}} & \text{, if } cap_{\text{loc}}^{\text{comp}} \text{ is to be continuous, or} \\ \text{capPerUnit}^{\text{comp}} \cdot nbInt_{\text{loc}}^{\text{comp}} & \text{, if } cap_{\text{loc}}^{\text{comp}} \text{ is to be discrete.} \end{cases} \tag{3.18}$$

Here, capPerUnit$^{\text{comp}}$ is the capacity per plant unit and $nbReal_{\text{loc}}^{\text{comp}} \in \mathbb{R}^{\geq 0}$ and $nbInt_{\text{loc}}^{\text{comp}} \in \mathbb{Z}^{\geq 0}$ are the number of installed plant units.

Furthermore, the component can be modeled together with a binary design decision variable $bin_{\text{loc}}^{\text{comp}} \in \{0, 1\}$, for all locations loc $\in \mathcal{L}^{\text{comp}}$, if its boolean parameter hasDesignBinVars$^{\text{comp}}$ is set to true. The optimal value of this variable states whether a component is built ($= 1$) or not built ($= 0$). The consideration of the binary decision variables is enforced in the model for all $bin_{\text{loc}}^{\text{comp}}$ by the constraint

$$\text{M}^{\text{comp}} \cdot bin_{\text{loc}}^{\text{comp}} \geq cap_{\text{loc}}^{\text{comp}} , \tag{3.19}$$

where $\text{M}^{\text{comp}} \in \mathbb{R}^{\geq 0}$. The constraint enforces that $bin_{\text{loc}}^{\text{comp}}$ has to be set to 1 when $cap_{\text{loc}}^{\text{comp}}$ is greater than zero. The parameter M$^{\text{comp}}$ has to be chosen large enough such that it does not function as an upper limit on the capacity. It should however also not be chosen too large, as a large range of model coefficients can be numerically challenging for the optimization solver [52]. This modeling approach is based on the work of *Bemporad and Morari* [10] who give a general description and discussion of this approach in the context of linear integer programming.

Lower and upper boundaries can be specified for the capacity variables of the component. Lower bounds are enforced, if capMin$_{\text{loc}}^{\text{comp}} \in \mathbb{R}^{\geq 0}$ is defined for all loc $\in \mathcal{L}^{\text{comp}}$ of this component, by

$$cap_{\text{loc}}^{\text{comp}} \geq \begin{cases} \text{capMin}_{\text{loc}}^{\text{comp}} \cdot bin_{\text{loc}}^{\text{comp}} & \text{, if hasDesignBinVars}^{\text{comp}} = \text{True,} \\ \text{capMin}_{\text{loc}}^{\text{comp}} & \text{, else.} \end{cases} \tag{3.20}$$

Upper bounds are enforced, if capMax$_{\text{loc}}^{\text{comp}} \in \mathbb{R}^{\geq 0}$ is defined for all loc $\in \mathcal{L}^{\text{comp}}$, by

$$cap_{\text{loc}}^{\text{comp}} \leq \text{capMax}_{\text{loc}}^{\text{comp}} . \tag{3.21}$$

Moreover, for both the capacity and the binary decision variables, fixed values can be individually specified for a component by

$$cap_{\text{loc}}^{\text{comp}} = \text{capFix}_{\text{loc}}^{\text{comp}} \text{ and} \tag{3.22}$$
$$bin_{\text{loc}}^{\text{comp}} = \text{binFix}_{\text{loc}}^{\text{comp}} , \tag{3.23}$$

if $\text{capFix}_{\text{loc}}^{\text{comp}}$, $\text{binFix}_{\text{loc}}^{\text{comp}} \in \mathbb{R}^{\geq 0}$ are defined for all loc $\in \mathcal{L}^{\text{comp}}$, respectively.

Basic time-dependent variables and constraints:

Operational variables $op_{\text{loc,p,t}}^{\text{comp,opType}} \in \mathbb{R}^{\geq 0}$ are declared for all components in $\mathcal{C}$, for all operation types in the set $\mathcal{O}^{\text{comp}}$, for all locations loc $\in \mathcal{L}^{\text{comp}}$ and for all periods and time steps $(\text{p, t}) \in \mathcal{P} \times \mathcal{T}$. The set $\mathcal{O}^{\text{comp}}$ is individually defined in the respective component extension.

Each operation variable of a component that is modeled with a physical capacity is limited in one of three ways. First, the operation variable is limited by

$$op_{\text{loc,p,t}}^{\text{comp,opType}} \leq \tau^{\text{hours}} \cdot \text{opFactor}^{\text{comp,opType}} \cdot cap_{\text{loc}}^{\text{comp}} \tag{3.24}$$

if the operation of the component is merely limited by its capacity and a time-independent factor $\text{opFactor}^{\text{comp,opType}} \in \mathbb{R}^{\geq 0}$ (default: 1). This constraint can apply, for example, to the model of an electrolyzer. Second, the operation variable is fixed to

$$op_{\text{loc,p,t}}^{\text{comp,opType}} = \tau^{\text{hours}} \cdot \text{opRateFix}_{\text{loc,p,t}}^{\text{comp,opType}} \cdot cap_{\text{loc}}^{\text{comp}} \tag{3.25}$$

if a fixed, relative operation rate $\text{opRateFix}_{\text{loc,p,t}}^{\text{comp,opType}}$ is specified for all locations loc $\in \mathcal{L}^{\text{comp}}$ and for all periods and time steps $(\text{p, t}) \in \mathcal{P} \times \mathcal{T}$. This constraint can apply, for example, to the model of a run-of-river power plant. Lastly, the operation rate is limited by

$$op_{\text{loc,p,t}}^{\text{comp,opType}} \leq \tau^{\text{hours}} \cdot \text{opRateMax}_{\text{loc,p,t}}^{\text{comp,opType}} \cdot cap_{\text{loc}}^{\text{comp}} \tag{3.26}$$

if a maximum, relative operation rate $\text{opRateMax}_{\text{loc,p,t}}^{\text{comp,opType}}$ is specified for all locations loc $\in \mathcal{L}^{\text{comp}}$ and for all periods and time steps $(\text{p, t}) \in \mathcal{P} \times \mathcal{T}$. This constraint can apply, for example, to the model of a wind turbine.

Each operation variable of a component which is modeled without a physical capacity is limited in one of two ways. The operation variable is limited by

$$op_{\text{loc,p,t}}^{\text{comp,opType}} = \text{opRateFix}_{\text{loc,p,t}}^{\text{comp,opType}} \tag{3.27}$$

if a fixed, absolute operation rate $\text{opRateFix}_{\text{loc,p,t}}^{\text{comp,opType}}$ is specified for all locations loc $\in \mathcal{L}^{\text{comp}}$ and for all periods and time steps $(\text{p, t}) \in \mathcal{P} \times \mathcal{T}$. This constraint can apply, for example, to the model of an electricity demand. The operation variable is fixed to

$$op_{\text{loc,p,t}}^{\text{comp,opType}} \leq \text{opRateMax}_{\text{loc,p,t}}^{\text{comp,opType}} \tag{3.28}$$

if a maximum, absolute operation rate $\text{opRateMax}_{\text{loc,p,t}}^{\text{comp,opType}}$ is specified for all locations $\text{loc} \in \mathcal{L}^{\text{comp}}$ and for all periods and time steps $(\text{p}, \text{t}) \in \mathcal{P} \times \mathcal{T}$. This constraint can apply, for example, to the model of an optional commodity import.

Basic inter-component constraint contributions:

Inter-component constraint contributions are defined to model constraints which do not only affect one but multiple components. As such, the contributions are specified for each component individually and are afterwards aggregated to comprehensive constraints.

The constraints which model the basic structure of the energy system are thereby the commodity balance constraints. They have to be defined for all commodities $\text{comm} \in \mathcal{M}$, at all locations in $\text{loc} \in \mathcal{L}$ at which the commodity appears and there for all periods and time steps $(\text{p}, \text{t}) \in \mathcal{P} \times \mathcal{T}$. The contribution of a component to a balance equation is labeled $C_{\text{loc,p,t}}^{\text{comp,comm}}$ and has to be defined for each component which is added to the model. This takes place in the individual component model extensions.

Moreover, two or more components can compete for a limited capacity potential in an energy system. For example, existing salt caverns can be dedicated to be used for either hydrogen or methane storage. Components which share a potential in *FINE* are provided with an identifier ($\text{sharedPotentialID}^{\text{comp}} = \text{sharedPotentialID}, \text{sharedPotentialID} \in \mathbb{S}$, default: $\emptyset$). If an identifier is defined for a component, the share of that component on the maximum potential is at all locations $\text{loc} \in \mathcal{L}^{\text{comp}}$ defined by $cap_{\text{loc}}^{\text{comp}}/\text{capMax}_{\text{loc}}^{\text{comp}}$.

Basic objective function contribution:

The objective function in the framework is defined as the total annual costs TAC of all components in $\mathcal{C}$ and is minimized during optimization. As for the inter-component constraint contributions, the objective function contributions TAC^{comp} [costUnit/a] are specified for each component individually by

$$TAC^{\text{comp}} = \sum_{\text{loc} \in \mathcal{L}^{\text{comp}}} \left(TAC_{\text{loc}}^{\text{comp,cap}} + TAC_{\text{loc}}^{\text{comp,bin}} + TAC_{\text{loc}}^{\text{comp,op}} \right) \tag{3.29}$$

and are aggregated to one comprehensive objective function afterwards. The capacity related total annual cost contributions are determined by

$$TAC_{\text{loc}}^{\text{comp,cap}} = \text{F}_{\text{loc}}^{\text{comp,cap}} \cdot \left(\frac{\text{investPerCap}_{\text{loc}}^{\text{comp}}}{\text{CCF}_{\text{loc}}^{\text{comp}}} + \text{opexPerCap}_{\text{loc}}^{\text{comp}} \right) \cdot cap_{\text{loc}}^{\text{comp}} \quad (3.30)$$

if the component is modeled with a physical capacity. Otherwise, $TAC_{\text{loc}}^{\text{comp,cap}}$ is set to 0. The parameters $\text{investPerCap}_{\text{loc}}^{\text{comp}}$ [costUnit/nominalCapacity$^{\text{comp}}$] and $\text{opexPerCap}_{\text{loc}}^{\text{comp}} \in \mathbb{R}^{\geq 0}$ [costUnit/(nominalCapacity$^{\text{comp}}$·a)] describe the capital and annual operational expenditures in relation to the capacity. The parameter $\text{F}_{\text{loc}}^{\text{comp,cap}}$ can be defined individually for a component (default: 1). The total annual cost contributions related to the binary decision variables are determined by

$$TAC_{\text{loc}}^{\text{comp,bin}} = \text{F}_{\text{loc}}^{\text{comp,bin}} \cdot \left(\frac{\text{investIfBuilt}_{\text{loc}}^{\text{comp}}}{\text{CCF}_{\text{loc}}^{\text{comp}}} + \text{opexIfBuilt}_{\text{loc}}^{\text{comp}} \right) \cdot bin_{\text{loc}}^{\text{comp}} \quad (3.31)$$

if the component is modeled with binary decision variables. Otherwise $TAC_{\text{loc}}^{\text{comp,bin}}$ is set to 0. The parameters $\text{investIfBuilt}_{\text{loc}}^{\text{comp}}$ [costUnit] and $\text{opexIfBuilt}_{\text{loc}}^{\text{comp}} \in \mathbb{R}^{\geq 0}$ [costUnit/a] describe the capital and annual operational expenditures which arise if the component is built. The parameter $\text{F}_{\text{loc}}^{\text{comp,bin}}$ can be defined individually for a component (default: 1). The factor

$$\text{CCF}_{\text{loc}}^{\text{comp}}/\text{a} = \frac{1}{\text{WACC}_{\text{loc}}^{\text{comp}}} - \frac{1}{\left(1 + \text{WACC}_{\text{loc}}^{\text{comp}}\right)^{\tau_{\text{loc}}^{\text{comp,economic lifetime}}/\text{a}} \cdot \text{WACC}_{\text{loc}}^{\text{comp}}} \quad (3.32)$$

is applied to determine the annuity of the respective invest for one calender year. Thus, $\text{WACC}_{\text{loc}}^{\text{comp}} \in (0, 1]$ is the weighted average cost of capital and $\tau_{\text{loc}}^{\text{comp,economic lifetime}} \in \mathbb{Z}^{>0}$ [a] is the economic lifetime of the component in years. With the combination of a capacity-dependent and a capacity-independent cost factor, a simplified nonlinear *economy-of-scale* approach is realized. The operation related total annual cost contributions are determined by

$$TAC_{\text{loc}}^{\text{comp,op}} = \sum_{\substack{\text{(p,t)} \\ \in \mathcal{P} \times \mathcal{T}}} \sum_{\substack{\text{opType} \\ \in \mathcal{O}^{\text{comp}}}} \text{factorPerOp}_{\text{loc}}^{\text{comp,opType}} \cdot op_{\text{loc,p,t}}^{\text{comp,opType}} \cdot \frac{freq\,(p)}{\tau^{\text{years}}} \quad (3.33)$$

where $\text{factorPerOp}_{\text{loc}}^{\text{comp,opType}}$ [costUnit/(nominalCapacity$^{\text{comp}}$·h)] is defined in the individual component model extensions.

Source/Sink **Component Model Extension**

Components which generate or consume commodities across the energy system's boundary are modeled as so-called *Source* / *Sink* components. Examples for

Source components are wind turbines or natural gas imports. Examples for *Sink* components are electricity demands or electricity exports. The *Source* / *Sink* component model extends the *Basic* component model. In the following, the set of all *Source* and *Sink* components is labeled $\mathcal{C}^{\text{srcSnk}} \subseteq \mathcal{C}$.

Specification of operation variables and associated commodities:

A *Source* / *Sink* component comp $\in \mathcal{C}^{\text{srcSnk}}$ only has one type of basic operation variables $\mathcal{O}^{\text{comp}} = \{\text{op}\}$. It is associated with one commodity $\mathcal{M}^{\text{comp}} = \{\text{comm}\}$, comm $\in \mathcal{M}$, which is the commodity that the component generates / consumes. If a capacity is defined for this component, it is related to this commodity. For example, the capacity of a wind turbine is related to the electric power which it generates at full load, e.g. in MW_{el}.

Specification of commodity balance contributions:

Contributions to the commodity balance equations are modeled for a comp $\in \mathcal{C}^{\text{srcSnk}}$, for comm $\in \mathcal{M}^{\text{comp}}$, for all loc $\in \mathcal{L}^{\text{comp}}$ and for all $(\text{p}, \text{t}) \in \mathcal{P} \times \mathcal{T}$ as

$$\begin{aligned} C^{\text{comp, comm}}_{\text{loc,p,t}} &= \text{sign}^{\text{comp}} \cdot op^{\text{comp,op}}_{\text{loc,p,t}}, \quad \text{where} \\ \text{sign}^{\text{comp}} &= \begin{cases} +1 & \text{, if comp is a } \textit{Source} \text{ component, and} \\ -1 & \text{, if comp is a } \textit{Sink} \text{ component .} \end{cases} \end{aligned} \tag{3.34}$$

Specification of objective function contributions:

The cost factor factorPerOp$^{\text{comp,op}}_{\text{loc}}$, cf. equation (3.33), is for a *Source* / *Sink* component comp $\in \mathcal{C}^{\text{srcSnk}}$ given as

$$\begin{aligned} \text{factorPerOp}^{\text{comp,op}}_{\text{loc}} = \big(&\text{opexPerOperation}^{\text{comp,op}}_{\text{loc}} + \text{commodityCost}^{\text{comp,op}}_{\text{loc}} + \\ &\text{commodityRevenue}^{\text{comp,op}}_{\text{loc}}\ \big)\ . \end{aligned} \tag{3.35}$$

Thus, operational cost as well as a cost and revenue for the associated generated or consumed commodity can be considered with the parameters opexPerOperation$^{\text{comp,op}}_{\text{loc}} \in \mathbb{R}^{\geq 0}$, commodityCost$^{\text{comp,op}}_{\text{loc}} \in \mathbb{R}^{\geq 0}$ and commodityRevenue$^{\text{comp,op}}_{\text{loc}} \in \mathbb{R}^{\leq 0}$ respectively.

***Conversion* Component Model Extension**

A component which converts one set of commodities into another set of commodities, as for example a power plant is modeled to convert natural gas into electricity and carbon dioxide, is modeled in *FINE* as a so-called *Conversion* component. The *Conversion* component model thereby extends the *Basic* component model. In the following, the set of all *Conversion* components is labeled $\mathcal{C}^{\text{conv}} \subset \mathcal{C}$.

Specification of operation variables and associated commodities:

A *Conversion* component comp $\in \mathcal{C}^{\text{conv}}$ only has one type of basic operation variables $\mathcal{O}^{\text{comp}} = \{\text{op}\}$. It can however be associated with multiple ($\text{m}^{\text{comp}} \in \mathbb{Z}^{\geq 2}$) commodities $\mathcal{M}^{\text{comp}} = \{\text{comm}_0, \dots, \text{comm}_{\text{m}^{\text{comp}}-1}\}$, with $\text{comm}_m \in \mathcal{M}$ for all $m \in \{0, \dots, \text{m}^{\text{comp}} - 1\}$, as it converts commodities into each other. The nominal capacity of a *Conversion* component is related to one of these commodities labeled $\text{comm}^{\text{nominal}}$. For example, the capacity of an electrolyzer can be related to either the consumed electricity, e.g. in MW_{el}, or the lower heating value (LHV) of the generated hydrogen, e.g. in $\text{MW}_{\text{H}_2\text{,LHV}}$.

Specification of commodity balance contributions:

Inherently, a *Conversion* component contributes to the balance equations of multiple (m^{comp}) commodities. These contributions are modeled for a comp $\in \mathcal{C}^{\text{conv}}$, for all comm $\in \mathcal{M}^{\text{comp}}$, for all loc $\in \mathcal{L}^{\text{comp}}$ and for all (p, t) $\in \mathcal{P} \times \mathcal{T}$ as

$$C^{\text{comp, comm}}_{\text{loc,p,t}} = \text{conversionFactor}^{\text{comp}}_{\text{comm}} \cdot op^{\text{comp,op}}_{\text{loc,p,t}} . \tag{3.36}$$

The $\text{conversionFactor}^{\text{comp}}_{\text{comm}} \in \mathbb{R}$ is by convention negative if a commodity is consumed and positive if a commodity is generated. The nominal conversion factor $\left|\text{conversionFactor}^{\text{comp}}_{\text{comm}^{\text{nominal}}}\right|$ is set to 1.

Specification of objective function contributions:

The cost factor $\text{factorPerOp}^{\text{comp,op}}_{\text{loc}}$, cf. equation (3.33), is for a *Conversion* component comp $\in \mathcal{C}^{\text{conv}}$ given as

$$\text{factorPerOp}^{\text{comp,op}}_{\text{loc}} = \text{opexPerOperation}^{\text{comp,op}}_{\text{loc}} . \tag{3.37}$$

***Storage* Component Model Extension**

Components which store a commodity are modeled in *FINE* as so-called *Storage* components. Examples for *Storage* components are batteries or underground gas storage facilities. The *Storage* component model thereby extends the *Basic* component model. In addition to the *Basic* component model functionalities, the model requires sets of variables and constraints which can model storage inventories. This includes a set of variables and constraints enabling to transfer the information on storage inventories between typical periods. This storage formulation makes computationally efficient seasonal storage investigations possible. The *Storage* component model formulation extends the formulations given by *Welder et al.* [2] and *Kotzur et al.* [32]. In the following, the set of all *Storage* components is labeled $\mathcal{C}^{\text{stor}} \subset \mathcal{C}$.

Specification of basic operational parameters and associated commodities:

A *Storage* component comp $\in \mathcal{C}^{\text{stor}}$ has two types of basic operation variables $\mathcal{O}^{\text{comp}} = \{\text{charge, discharge}\}$. It is associated with one commodity $\mathcal{M}^{\text{comp}} = \{\text{comm}\}$, with comm $\in \mathcal{M}$, which is stored by the component. If a capacity is defined for this component, it is related to this commodity. For example, the capacity of a battery is related to the nominal electric energy it can store, e.g. in kWh_{el}. The rate at which a storage can be charged / discharged is generally limited. The parameter $\text{opFactor}^{\text{comp,opType}}$ in equation (3.24) is in this context used to define the relative charging / discharging rate per hour. For example, if it takes six hours to fully charge a storage, with respect to its nominal capacity, $\text{opFactor}^{\text{comp,charge}}$ is equal to $1/6$.

Specification of additional variables and constraints:

An additional set of variables is required to track how much commodity remains in the *Storage* component in between time steps. These variables are in the following referred to as SoC (state of charge) variables.

The variable $SoC^{\text{comp}}_{\text{loc,p,t}} \in \mathbb{R}^{\geq 0}$ defines for all comp $\in \mathcal{C}^{\text{stor}}$ and for all loc $\in \mathcal{L}^{\text{comp}}$ the state of charge within a period p at the beginning of time step t, with $(\text{p, t}) \in \mathcal{P} \times \mathcal{T}_{\text{inter}}$.

If typical periods are considered, an additional set of state of charge variables is declared that accounts for the state of charge in between periods. In this case, $SoC^{\text{comp,inter}}_{\text{loc,p}} \in \mathbb{R}^{\geq 0}$ describes the actual, real state of charge in between periods and is defined for all comp $\in \mathcal{C}^{\text{stor}}$, for all loc $\in \mathcal{L}^{\text{comp}}$ and for all p $\in \mathcal{P}^{\text{total}}_{\text{inter}}$. $SoC^{\text{comp}}_{\text{loc,p,t}}$, now in $\mathbb{R}$, functions as a virtual state of charge. The superposition of the two variables gives, with the consideration of a self-discharge factor, the real state of charge at period p at the beginning of time step t.

Linkage of SoC variables across the investigated timeframe:

The state of charge within a period p at the beginning of time step $\text{t}+1$ results from the state of charge at the beginning of time step t and the charge and discharge rate during time step t within that period with

$$SoC^{\text{comp}}_{\text{loc,p,t+1}} = SoC^{\text{comp}}_{\text{loc,p,t}} \cdot \left(1 - \eta^{\text{comp,self-discharge}}\right)^{\tau^{\text{hours}}/\text{h}} + op^{\text{comp,charge}}_{\text{loc,p,t}} \cdot \eta^{\text{comp,charge}} - op^{\text{comp,discharge}}_{\text{loc,p,t}} / \eta^{\text{comp,discharge}} \tag{3.38}$$

for all comp $\in \mathcal{C}^{\text{stor}}$, for all loc $\in \mathcal{L}^{\text{comp}}$ and for all $(\text{p, t}) \in \mathcal{P} \times \mathcal{T}$. The parameters $\eta^{\text{comp,self-discharge}}, \eta^{\text{comp,charge}}, \eta^{\text{comp,discharge}} \in (0,1]$ describe the self-discharge during one hour and the charging and discharging efficiency respectively.

If typical periods are considered, the virtual state of charge at the beginning of each typical period p $\in \mathcal{P}^{\text{typical}}$ has to satisfy the condition

$$SoC^{\text{comp,inter}}_{\text{loc,p}} + SoC^{\text{comp}}_{\text{loc,p,0}} = SoC^{\text{comp,inter}}_{\text{loc,p}} \quad \rightarrow \quad SoC^{\text{comp}}_{\text{loc,p,0}} = 0 \tag{3.39}$$

for all comp $\in \mathcal{C}^{\text{stor}}$ and for all loc $\in \mathcal{L}^{\text{comp}}$. The state of charge at the beginning of period p $+ 1$ results from the superposition of the state of charge at the beginning of period p and the state of charge at the end of the period by

$$SoC^{\text{comp,inter}}_{\text{loc,p+1}} = SoC^{\text{comp,inter}}_{\text{loc,p}} \cdot \left(1 - \eta^{\text{self-discharge}}\right)^{\text{t}^{\text{per period}} \cdot \tau^{\text{hours}}/\text{h}} + SoC^{\text{comp}}_{\text{loc},map(\text{p}),\text{t}^{\text{per period}}} \tag{3.40}$$

for all comp $\in \mathcal{C}^{\text{stor}}$, for all loc $\in \mathcal{L}^{\text{comp}}$ and for all $p \in \mathcal{P}^{\text{total}}$. The function map maps a period to a typical period, cf. equation (3.14).

The *Storage* component model imposes a constraint which sets the state of charge at the beginning and the end of the investigated timeframe equal to each other. The energy system is thus modeled as being self-repetitive. This constraint is given as

$$\begin{aligned} SoC^{\text{comp}}_{\text{loc,0,0}} &= SoC^{\text{comp}}_{\text{loc,0,t}^{\text{total}}}, \quad \text{with full temporal resolution } \left(\mathcal{P}^{\text{total}} = \{0\}\right), \text{ or} \\ SoC^{\text{comp,inter}}_{\text{loc,0}} &= SoC^{\text{comp,inter}}_{\text{loc,p}^{\text{total}}}, \quad \text{with time series aggregation,} \end{aligned} \tag{3.41}$$

for all comp $\in \mathcal{C}^{\text{stor}}$ and for all loc $\in \mathcal{L}^{\text{comp}}$.

Consideration of operating limits of SoC variables:

It must be ensured that the state of charge is within the operating limits of the installed storage capacity for all comp $\in \mathcal{C}^{\text{stor}}$ if they are modeled with a physical capacity. Here, three modeling approaches have to be distinguished from one another.

The first modeling approach applies to an energy system which is modeled with a full temporal resolution, i.e. no typical periods are considered. In this case, the upper and lower operating limits are given by

$$\text{SoC}^{\text{comp,min}} \cdot cap^{\text{comp}}_{\text{loc}} \;\leq\; SoC^{\text{comp}}_{\text{loc,0,t}} \;\leq\; \text{SoC}^{\text{comp,max}} \cdot cap^{\text{comp}}_{\text{loc}} \tag{3.42}$$

for all loc $\in \mathcal{L}^{\text{comp}}$ and for all t $\in \mathcal{T}^{\text{total}}$. Here, the parameters $0 \leq \text{SoC}^{\text{comp,min}} < \text{SoC}^{\text{comp,max}} \leq 1$ model relative lower and upper limits on the state of charge.

The second modeling approach applies when typical periods are considered, and the *Storage* component should be modeled with *precise* operating boundaries (doPreciseTSAmodeling$^{\text{comp}}$ $=$ True). In this case, the lower and upper operating limits are given by

$$\begin{aligned} &\text{SoC}^{\text{comp,min}} \cdot cap^{\text{comp}}_{\text{loc}} \leq SoC^{\text{comp,sup}}_{\text{loc,p,t}} \leq \text{SoC}^{\text{comp,max}} \cdot cap^{\text{comp}}_{\text{loc}}, \quad \text{with} \\ &SoC^{\text{comp,sup}}_{\text{loc,p,t}} = SoC^{\text{comp,inter}}_{\text{loc,p}} \cdot \left(1 - \eta^{\text{self-discharge}}\right)^{\text{t} \,\cdot\, \tau^{\text{hours}}/\text{h}} + SoC^{\text{comp}}_{\text{loc},map(\text{p}),\text{t}}\,, \end{aligned} \tag{3.43}$$

for all loc $\in \mathcal{L}^{\text{comp}}$ and for all p $\in \mathcal{P}^{\text{total}}$ and for all t $\in \mathcal{T}^{\text{per period}}$.

The third modeling approach applies when typical periods are considered, and the *Storage* component should be modeled with *simplified* operating boundaries (doPreciseTSAmodeling$^{\text{comp}}$ $=$ False). This approach reduces the computational load in comparison to the second approach even further and is a good estimate when the self-discharge of the *Storage* component is small. In this case, the lower and upper operating limits are given by

$$\begin{aligned} &\text{SoC}^{\text{comp,min}} \cdot cap^{\text{comp}}_{\text{loc}} \leq \underline{SoC}^{\text{comp,sup}}_{\text{loc,p,t}} \quad \wedge \quad \overline{SoC}^{\text{comp,sup}}_{\text{loc,p,t}} \leq \text{SoC}^{\text{comp,max}} \cdot cap^{\text{comp}}_{\text{loc}}, \\ &\text{with} \;\; \underline{SoC}^{\text{comp,sup}}_{\text{loc,p,t}} = SoC^{\text{comp,inter}}_{\text{loc,p}} \cdot \left(1 - \eta^{\text{self-discharge}}\right)^{\text{t}^{\text{per period}} \cdot\, \tau^{\text{hours}}/\text{h}} + SoC^{\text{comp,min}}_{\text{loc},map(\text{p})} \\ &\text{and} \;\; \overline{SoC}^{\text{comp,sup}}_{\text{loc,p,t}} = SoC^{\text{comp,inter}}_{\text{loc,p}} + SoC^{\text{comp,max}}_{\text{loc},map(\text{p})}\,, \end{aligned} \tag{3.44}$$

for all loc $\in \mathcal{L}^{\text{comp}}$ and for all p $\in \mathcal{P}^{\text{total}}$. The two variables $SoC^{\text{comp,min}}_{\text{loc},map(\text{p})} \in \mathbb{R}^{\leq 0}$ and $SoC^{\text{comp,max}}_{\text{loc},map(\text{p})} \in \mathbb{R}^{\geq 0}$ are auxiliary variables that describe the virtual minimum and maximum state of charge within the typical period $\bar{\text{p}}$ obtained by *map*(p). They are bounded from above / below by all $SoC^{\text{comp}}_{\text{loc},\bar{\text{p}},\text{t}}$ of the respective component comp within the typical period $\bar{\text{p}}$ by

$$SoC^{\text{comp,min}}_{\text{loc},\bar{\text{p}}} \leq SoC^{\text{comp}}_{\text{loc},\bar{\text{p}},\text{t}} \leq SoC^{\text{comp,max}}_{\text{loc},\bar{\text{p}}} \tag{3.45}$$

for all comp $\in \mathcal{C}^{\text{stor}}$, for all loc $\in \mathcal{L}^{\text{comp}}$ and for all $(\bar{\text{p}}, \text{t}) \in \mathcal{P} \times \mathcal{T}$. Thus, equation (3.44) over- and underestimates the minimum and maximum real SoC and therefore always gives feasible operating limits.

Additional constraints:

Additionally, a cyclic lifetime $\mathrm{t}^{\text{comp,cyclic lifetime}} \in \mathbb{Z}^{>0}$ can be considered for a storage component comp $\in \mathcal{C}^{\text{stor}}$. The cyclic lifetime limits the number of full cycle equivalents for all loc $\in \mathcal{L}^{\text{comp}}$ by

$$op^{\text{comp,charge}}_{\text{loc,annual}} \leq \left(\text{SoC}^{\text{comp,max}} - \text{SoC}^{\text{comp,min}}\right) \cdot cap^{\text{comp}}_{\text{loc}} \cdot \frac{\mathrm{t}^{\text{comp,cyclic lifetime}}}{\tau^{\text{comp,economic lifetime}}_{\text{loc}}},$$
$$\text{with } op^{\text{comp,charge}}_{\text{loc,annual}} = \sum_{(\text{p,t}) \in \mathcal{P}\times\mathcal{T}} op^{\text{comp,charge}}_{\text{loc,p,t}} \cdot freq\,(\text{p}) / \tau^{\text{years}}\,, \tag{3.46}$$

where $freq$ is the frequency of the period p within the investigated timeframe, cf. equation (3.15). This means that the commodity amount with which the storage is charged during its economic lifetime divided by the usable storage capacity ($\widehat{=}$ full cycle equivalents) has to be smaller than the cyclic lifetime, e.g. 10,000 cycles. It has to be noted that a storage can also be associated with a calendric lifetime. This calendric lifetime can be implicitly enforced in *FINE* by setting the economic lifetime to a value smaller than this calendric lifetime.

Specification of commodity balance contributions:

Contributions to the commodity balance equations are modeled for a comp $\in \mathcal{C}^{\text{stor}}$, for comm $\in \mathcal{M}^{\text{comp}}$, for all loc $\in \mathcal{L}^{\text{comp}}$ and for all $(\text{p, t}) \in \mathcal{P} \times \mathcal{T}$ as

$$C^{\text{comp, comm}}_{\text{loc,p,t}} = op^{\text{comp,discharge}}_{\text{loc,p,t}} - op^{\text{comp,charge}}_{\text{loc,p,t}}\,. \tag{3.47}$$

The term thus represents the amount of commodity comm which is at location loc, period p and time step p injected ($C^{\text{comp, comm}}_{\text{loc,p,t}} < 0$) or withdrawn ($C^{\text{comp, comm}}_{\text{loc,p,t}} \geq 0$) from the *Storage* component.

Specification of objective function contributions:

The cost factor $\text{factorPerOp}^{\text{comp,op}}_{\text{loc}}$, cf. equation (3.33), is for a *Storage* component comp $\in \mathcal{C}^{\text{stor}}$ given as

$$\text{factorPerOp}^{\text{comp,charge}}_{\text{loc}} = \text{opexPerChargeOperation}^{\text{comp,charge}}_{\text{loc}}$$
$$\text{factorPerOp}^{\text{comp,discharge}}_{\text{loc}} = \text{opexPerDischargeOperation}^{\text{comp,discharge}}_{\text{loc}}\,. \tag{3.48}$$

Transmission **Component Model Extension**

Components which transmit commodities between locations in $\mathcal{L}$ and along routes $(\text{loc}_{\text{in}}, \text{loc}_{\text{out}}) \in \mathcal{L} \times \mathcal{L}$ are modeled as bidirectional *Transmission* components.

Examples of *Transmission* components are electric lines or bidirectional gas pipelines. The *Transmission* component model extends the *Basic* component model. In the following, the set of all *Transmission* components is labeled $\mathcal{C}^{\text{trans}} \subset \mathcal{C}$.

Specification of operation variables and associated commodities:

A *Transmission* component comp $\in \mathcal{C}^{\text{trans}}$ only has one type of basic operation variables $\mathcal{O}^{\text{comp}} = \{\text{op}\}$. It is associated with one commodity $\mathcal{M}^{\text{comp}} = \{\text{comm}\}$, with comm $\in \mathcal{M}$, which is the commodity that the component transmits. If a capacity is defined for this component, it is related to this commodity. For example, the capacity of an electric line is related to the nominal electric power it can transmit, e.g. in MW_{el}.

Specification of additional constraints:

A *Transmission* component can be operated bidirectionally. This means that the flow from $\text{loc}_1 \in \mathcal{L}$ to $\text{loc}_2 \in \mathcal{L}$ has to use the same route and infrastructure as a flow from loc_2 to loc_1. To enforce this behavior in the context of equations (3.24)-(3.26), the constraint

$$cap^{\text{comp}}_{(\text{loc}_1,\text{loc}_2)} = cap^{\text{comp}}_{(\text{loc}_2,\text{loc}_1)} \tag{3.49}$$

is stated for all comp $\in \mathcal{C}^{\text{trans}}$ and all $(\text{loc}_1, \text{loc}_2) \in \mathcal{L}^{\text{comp}}$. Note that $\mathcal{L}^{\text{comp}}$ states for *edge*-based components a cross-product, cf. equation (3.5). Furthermore, equation (3.24) is supplemented with the equation

$$op^{\text{comp,op}}_{(\text{loc}_1,\text{loc}_2),\text{p,t}} + op^{\text{comp,op}}_{(\text{loc}_2,\text{loc}_1),\text{p,t}} \leq \tau^{\text{hours}} \cdot cap^{\text{comp}}_{(\text{loc}_{\text{in}},\text{loc}_{\text{out}})} \tag{3.50}$$

for all comp $\in \mathcal{C}^{\text{trans}}$ and all $(\text{loc}_1, \text{loc}_2) \in \mathcal{L}^{\text{comp}}$. This set of equations increases the tendency that, for basic optimization solutions, one of the commodity flows $op^{\text{comp,op}}_{(\text{loc}_1,\text{loc}_2),\text{p,t}}$ or $op^{\text{comp,op}}_{(\text{loc}_2,\text{loc}_1),\text{p,t}}$ is set to zero.

Specification of commodity balance contributions:

Contributions to the commodity balance equations are modeled for a comp $\in \mathcal{C}^{\text{trans}}$, for comm $\in \mathcal{M}^{\text{comp}}$, for all loc $\in \mathcal{L}$, with $(\text{loc}, \text{loc}_{\text{out}}) \in \mathcal{L}^{\text{comp}}$ or $(\text{loc}_{\text{in}}, \text{loc}) \in \mathcal{L}^{\text{comp}}$, and for all (p, t) $\in \mathcal{P} \times \mathcal{T}$ as

$$\begin{aligned} C^{\text{comp, comm}}_{\text{loc,p,t}} = & \sum_{\substack{(\text{loc}_{\text{in}},\text{loc}_{\text{out}}) \in \mathcal{L}^{\text{comp}}: \\ \text{loc}_{\text{in}}=\text{loc}}} \left(1 - \eta_{(\text{loc}_{\text{in}},\text{loc}_{\text{out}})} \cdot \text{l}_{(\text{loc}_{\text{in}},\text{loc}_{\text{out}})}\right) \cdot op^{\text{comp,op}}_{(\text{loc}_{\text{in}},\text{loc}_{\text{out}}),\text{p,t}} \\ & - \sum_{\substack{(\text{loc}_{\text{in}},\text{loc}_{\text{out}}) \in \mathcal{L}^{\text{comp}}: \\ \text{loc}_{\text{out}}=\text{loc}}} op^{\text{comp,op}}_{(\text{loc}_{\text{in}},\text{loc}_{\text{out}}),\text{p,t}} \; . \end{aligned} \tag{3.51}$$

Here, $\eta_{(\text{loc}_\text{in},\text{loc}_\text{out})}$ is a linear loss factor per length and capacity. $\text{l}_{(\text{loc}_\text{in},\text{loc}_\text{out})}$ is the length between loc_in and loc_out. The term thus represents incoming and outgoing flows of a commodity comm at the location loc at period p and time step p.

Specification of objective function contributions:

The parameters $\text{F}^{\text{comp,cap}}_{(\text{loc}_\text{in},\text{loc}_\text{out})}$ and $\text{F}^{\text{comp,bin}}_{(\text{loc}_\text{in},\text{loc}_\text{out})}$ in equations (3.30) and (3.31) are set equal to $1/2 \cdot \text{l}_{(\text{loc}_\text{in},\text{loc}_\text{out})}$ for *Transmission* components. The factor $1/2$ compensates that each connection is taken into account twice in the objective function. The length of the connection is included so that the capital and operational cost factors can be given as not only capacity but also length related.

The cost factor $\text{factorPerOp}^{\text{comp,op}}_{\text{loc}}$, cf. equation (3.33), is given as

$$\text{factorPerOp}^{\text{comp,op}}_{(\text{loc}_\text{in},\text{loc}_\text{out})} = \text{opexPerOperation}^{\text{comp,op}}_{(\text{loc}_\text{in},\text{loc}_\text{out})} \,. \tag{3.52}$$

DC power flow extension:

A basic *Transmission* component is modeled with a simple commodity exchange based on balance equations and a linear loss factor. However, the transmission of a commodity is generally subject to far more complex physics. The incorporation of a higher modeling detail of these physics into the optimization program has to be seen in the context of increasing computation times. With respect to this topic, *Syranidis et al.* [13] reviewed the modeling of electrical power flow across transmission networks. They discuss the general formulation of an AC power flow with a set of non-linear equations for which direct, analytical solutions are rarely obtainable and which are therefore often solved with iterative methods. Based on the premise that the optimization program provided by *FINE* should stay a mixed integer linear program, these equations cannot be incorporated in the framework. A linearization of these equations, as provided by the DC power flow method[4], is however suitable for incorporation. The linearized equations result in an acceptable increase in computation time while increasing the electrical power flow modeling detail to a more sophisticated level.

In the following, the constraints constituting the DC power flow are presented, based on the detailed description by Van den Bergh et al. [141]. The constraints thereby extend the *Transmission* component model. In the following, let $\mathcal{C}^{\text{trans,LPF}} \subseteq \mathcal{C}^{\text{trans}} \subset \mathcal{C}$ be the set of *Transmission* components that are modeled with a DC power flow.

The constraints that enforce the linear power flow are implemented for each

[4]The DC power flow method is applied to AC lines only.

component comp $\in \mathcal{C}^{\text{trans,LPF}}$, for all loc $\in \mathcal{L}^{\text{comp}}$, and for all $(\text{p}, \text{t}) \in \mathcal{P} \times \mathcal{T}$ as

$$op^{\text{comp,op}}_{(\text{loc}_{\text{in}},\text{loc}_{\text{out}}),\text{p},\text{t}} - op^{\text{comp,op}}_{(\text{loc}_{\text{out}},\text{loc}_{\text{in}}),\text{p},\text{t}} = \left(\theta^{\text{comp}}_{\text{loc}_{\text{in}},\text{p},\text{t}} - \theta^{\text{comp}}_{\text{loc}_{\text{out}},\text{p},\text{t}}\right) / \text{x}^{\text{comp}}_{(\text{loc}_{\text{in}},\text{loc}_{\text{out}})} \,. \tag{3.53}$$

Here, $\theta^{\text{comp}}_{\text{loc,p,t}} \in \mathbb{R}$ is the variable which models the phase angle. $\text{x}^{\text{comp}}_{(\text{loc}_{\text{in}},\text{loc}_{\text{out}})}$ represents the electric reactance of the line between locations loc_{in} and loc_{out}. These equations leave one degree of freedom for the phase angle variables at each time step. To obtain a unique solution, an additional set of constraints is given by

$$\theta^{\text{comp}}_{\text{loc}_{\text{ref}},\text{p},\text{t}} = 0 \tag{3.54}$$

for each component comp $\in \mathcal{C}^{\text{trans,LPF}}$ and for all $(\text{p}, \text{t}) \in \mathcal{P} \times \mathcal{T}$ which sets the phase angle for one location loc_{ref} to zero.

At this point, it should be remarked that the reactance parameter is in practice a function of the capacity of the line. The *PyPSA* documentation mentions two approaches to remedy this effect when AC line capacities are not assumed to be fixed but can be expanded [46]. The first one is an iterative approach suggested by Hagspiel et al. [11] and the second is a MILP approach published in a *PyPSA* branch. However, they are not considered in the context of this thesis, as only DC line expansions are considered in the scenarios, which are modeled as a regular *Transmission* component. AC line capacities, which are modeled with a *DC power flow*, are kept at a fixed value in the scenarios and thus their reactance parameters remain constant.

Inter-component Constraints

Inter-component constraints are constraints that involve variables and parameters from multiple components in $\mathcal{C}$. The inter-component constraints which are modeled within the framework are commodity balances, annual commodity inflow / outflow limits and so-called shared potential constraints.

Commodity balances:

The constraints that provide the basic structure of the energy system are the commodity balances. They are defined for all commodities comm $\in \mathcal{M}$, at all locations in loc $\in \mathcal{L}$, if the commodity appears at that location in the model, and, there, for all periods and time steps $(\text{p}, \text{t}) \in \mathcal{P} \times \mathcal{T}$. The commodity appears at a location when the set

$$\begin{aligned} \mathcal{C}^{\text{comm}}_{\text{loc}} = \{ &\text{comp} \mid \forall\, \text{comp} \in \mathcal{C} : \text{comm} \in \mathcal{M}^{\text{comp}} \,\wedge\, (\text{loc} \in \mathcal{L}^{\text{comp}} \,\vee \\ &(\exists\, \text{loc}^* \in \mathcal{L} : (\text{loc}, \text{loc}^*) \in \mathcal{L}^{\text{comp}} \,\vee\, (\text{loc}^*, \text{loc}) \in \mathcal{L}^{\text{comp}}))\} \end{aligned} \tag{3.55}$$

is not empty. In this case the commodity balance equation is given for all as

$$\sum_{\text{comp} \,\in\, \mathcal{C}_{\text{loc}}^{\text{comm}}} C_{\text{loc,p,t}}^{\text{comp,comm}} \;=\; 0\;. \tag{3.56}$$

The definition of $C_{\text{loc,p,t}}^{\text{comp,comm}}$ is given in the component model extensions, cf. equations (3.34), (3.36), (3.47) and (3.51).

Annual commodity inflow/outflow limit:

The annual commodity limitation constraints implemented in the framework enable the modeling of, for example, annual greenhouse gas emission limits. A commodity limitation is modeled with an identifier (commLimitID $\in \mathbb{S}$) and a limit (commLimit$^{\text{commLimitID}} \in \mathbb{R}$). Each component in $\mathcal{C}^{\text{srcSnk}}$ that generates or consumes the commodity of interest can be associated with this ID by setting the parameter commLimitID$^{\text{comp}}$ $=$ commLimitID (default: $\emptyset$).

Let $\mathcal{I}^{\text{commLimitIDs}}$ be the set containing all specified annual commodity limitation IDs. Then, the constraints limiting the total annual commodity inflow (commLimit$^{\text{commLimitID}} \leq 0$) or outflow (commLimit$^{\text{commLimitID}} \geq 0$) across the energy system's virtual boundary are given for all ID $\in \mathcal{I}^{\text{commLimitIDs}}$ by

$$\begin{aligned}
&\sum_{\text{comp} \,\in\, \mathcal{C}^{\text{ID}}} -1 \cdot op_{\text{annual}}^{\text{comp,op}} \cdot \text{sign}^{\text{ID}} \leq \text{commLimit}^{\text{ID}} \cdot \text{sign}^{\text{ID}}, \quad \text{with} \\
&\mathcal{C}^{\text{ID}} \quad = \left\{ \text{comp} \mid \forall \text{ comp} \in \mathcal{C}^{\text{srcSnk}} : \text{commLimitID}^{\text{comp}} = \text{ID} \right\}, \\
&op_{\text{annual}}^{\text{comp,op}} = \sum_{\text{loc} \,\in\, \mathcal{L}^{\text{comp}}} \; \sum_{(\text{p,t}) \,\in\, \mathcal{P}\times\mathcal{T}} \text{sign}^{\text{comp}} \cdot op_{\text{loc,p,t}}^{\text{comp,op}} \cdot freq\,(\text{p})\,/\tau^{\text{years}} \quad \text{and} \\
&\text{sign}^{\text{ID}} \quad = \frac{\text{commLimit}^{\text{ID}}}{\left|\text{commLimit}^{\text{ID}}\right|}\;.
\end{aligned} \tag{3.57}$$

Shared potential constraints:

As already explained in the *Basic* component model, two or more components can share a potential in an energy system. The framework ensures that for each location / connection where a shared potential is specified the share on the maximum capacity of all components with the same identifier (sharedPotentialID $\in \mathbb{S}$) does not exceed 100%. Each component for which a maximum capacity is defined can be associated with the shared potential by setting the parameter sharedPotentialID$^{\text{comp}}$ $=$ sharedPotentialID (default: $\emptyset$). Let $\mathcal{I}^{\text{sharedPotentialIDs}}$ be the set containing all shared potential IDs and let $\mathcal{L}^{\text{sharedPotentialID}}$ be the set of locations or connections at which components compete for a maximum potential, respectively. The shared potential constraints are then given for all $\text{ID} \in \mathcal{I}^{\text{sharedPotentialIDs}}$ and all $\text{loc} \in \mathcal{L}^{\text{ID}}$ by

$$\sum_{\text{comp} \in \mathcal{C}^{\text{ID}}} cap_{\text{loc}}^{\text{comp}} / \text{capMax}_{\text{loc}}^{\text{comp}} \leq 1,$$
$$\text{with } \mathcal{C}^{\text{ID}} = \left\{\text{comp} \mid \forall \text{ comp} \in \mathcal{C} : \text{sharedPotentialID}^{\text{comp}} = \text{ID}\right\} . \tag{3.58}$$

Objective Function

In the framework, the objective of the optimization is to minimize the total annual cost of the specified energy system. The objective function is defined as

$$TAC = \sum_{\text{comp} \in \mathcal{C}} TAC^{\text{comp}}. \tag{3.59}$$

The general definition of the TAC^{comp} is given in the *Basic* component model, cf. equations (3.29)-(3.33). Specifications of the objective functions in the model extensions are given in the paragraphs referring to the equations (3.35), (3.37), (3.48) and (3.52).

3.2.2 Python Implementation

The code, with which the energy system models are created, solved and assessed, is implemented in a *Python* package called *FINE* and is based on object-oriented programming. The package is open-source available on *GitHub*, a software development platform, and *PyPI*, a software repository for *Python* (status: March, 2019). It is licensed with an *MIT* license. The mathematical formulation of the optimization program provided by *FINE* is implemented with the *PYOMO* package by Hart et al. [49, 50] which provides an optimization modeling language. The data management of the package is primarily based on the *pandas* package by McKinney [56]. Figure 3.5 visualizes the class diagram of the object-oriented code of *FINE* and thus presents the conceptual structure of the code underlying the energy system model. In accordance with the *Unified Modeling Language (UML)* notation, the boxes in the figure represent *classes* and the blue and green connections indicate *compositions* and *inheritances*.

The *EnergySystemModel* class is the main container in the framework and is initialized once when an energy system is modeled. The class contains all basic parameters and sets and stores the component models. Furthermore, it provides

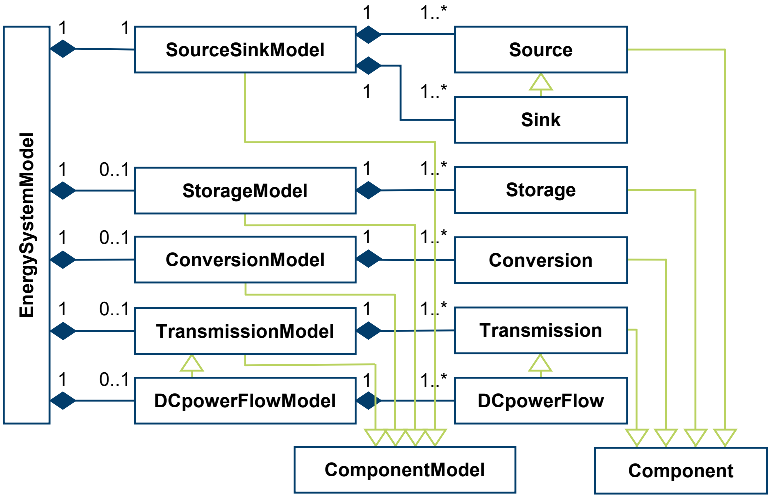

Figure 3.5: Simplified class diagram showing the conceptual structure of the energy system model provided by the *FINE Python* package.

functions for adding components, initializing and optimizing the energy system model and saving the optimization output.

All components and component modeling classes inherit from the *ComponentModel* and the *Component* class, respectively. The former provides the functions which model the basic component functionality while the latter stores the basic parameters of each individual component.

The component modeling classes *SourceSinkModel*, *StorageModel*, *ConversionModel* and *TransmissionModel* store the parameters of components and provide, in addition to the basic component model, the respective model extensions. Furthermore, they provide a function for post-processing the components' optimization output. The *DCpowerFlowModel* class inherits from the *TransmissionModel* class and extends it by declaring the additional variables and constraints required for the DC power flow modeling.

The component classes *Source*, *Storage*, *Conversion* and *Transmission* store, in addition to the basic parameters, the component data which is required in the component model extensions. The *Sink* class inherits from the *Source* class, as the respective components only differ from one another in the sign^{comp} parameter. The *DCpowerFlow* class inherits from the *Transmission* class by adding the reactance parameters to the component's data set.

3.3 Scenario Generation Workflow

The overall scenario generation workflow that encapsulates the methodology presented before is visualized in the flowchart in Figure 3.6.

The *Scenario database* holds all energy system related input data. This input data can be divided into geo-referenced time series data, geo-referenced capacity-related data and techno-economic component data which can again be geo-referenced.

All geo-referenced data is pre-processed before the optimization in the *Spatial aggregation* process which is implemented with the methodology presented in subsection 3.1.1. In this step, the discrete regions of the energy system are aggregated to a predefined number of clusters and the geo-referenced input data is assigned to these clusters.

Once the data is regionally aggregated, the *Energy system model class initialization* is executed with the *Python* package *FINE* and the component data and their abstract model formulations are added to this class, cf. section 3.2. If the time series should be aggregated, the *Python* package *tsam* is called next in the *Time series aggregation* sub-process. This is implemented with the methodology presented in subsection 3.1.2.

Next, in the *Energy system model formulation and optimization* process, the abstract component models are filled with the specific component data and the resulting scenario is optimized with an external solver considering the user-defined solver specifications.

Lastly, the optimization output data is post-processed and written into output files where it can be used for the analysis of the scenario's results.

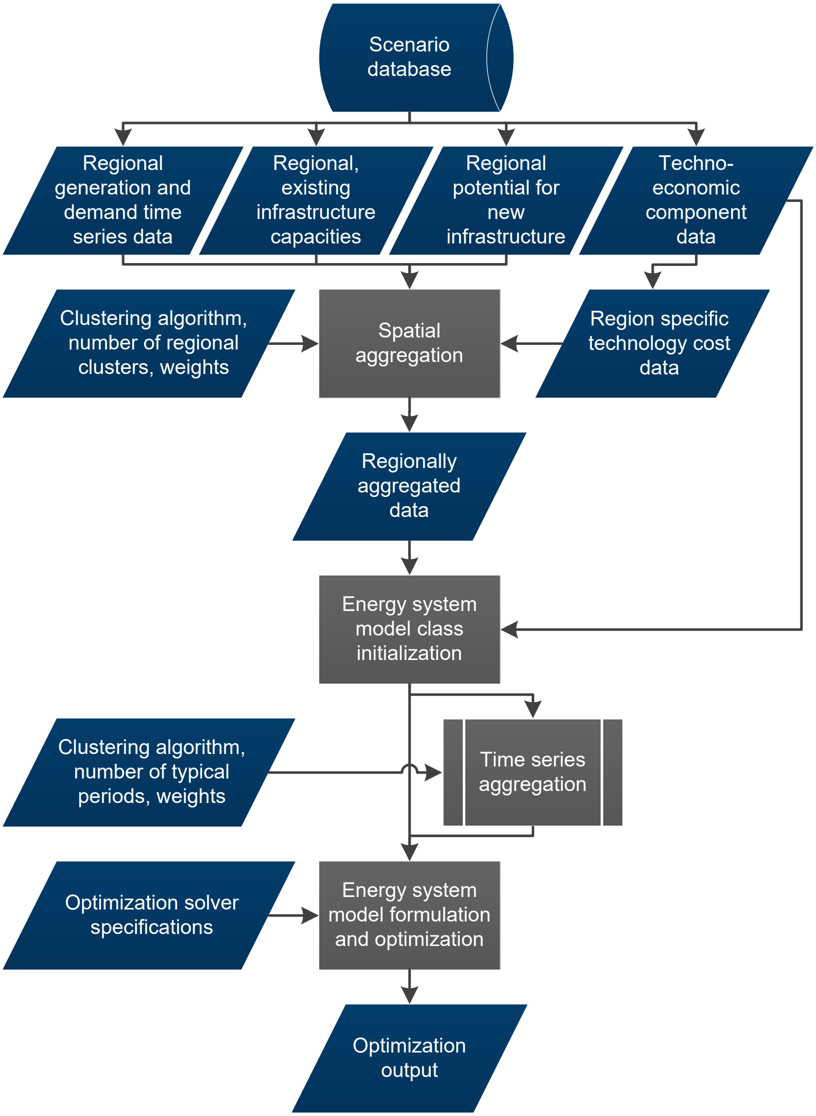

Figure 3.6: Spatio-temporal energy system optimization workflow. The cylinder refers to a database, rhomboids to data structures, rectangles to processes and the rectangle with additional vertical white lines to a subprocess.

3.4 Discussion

This section discusses the strengths and weaknesses of the presented modeling workflow. First, the spatial and temporal scope that can be chosen during modeling is critically reflected. Next, the developed optimization framework is discussed with a focus on its representation of transmission infrastructure and dynamic system components. Lastly, the open-source publishing of the *FINE* framework is discussed and, along with that, a perspective on further applications of the generic framework is given.

The presented workflow enables a flexible, spatially resolved modeling of energy systems based on geo-referenced data. For example, the regions can be chosen with a technology focus and are not restricted to administrative boundaries or transmission system operator (TSO) zones. With this flexible region definition, transmission infrastructure can be designed with the desired level of regional accuracy. If the region definition is then accompanied with high model runtimes, the spatial or temporal granularity can be coarsened with clustering algorithms and thus the complexity level of the model can be reduced. The clustering algorithms therefore provide a tool to find a balance between the runtime of a model and its regional and temporal accuracy level.

While this workflow provides the potential to model energy systems and their infrastructure with an arbitrarily high regional resolution, a critical examination of the actually available geo-referenced data must be given. The workflow works particularly well with frameworks that provide energy system data on a high spatial resolution. Examples of renewable electricity generation frameworks with a fine spatial and temporal granularity are presented by *Ryberg et al.* [104], *Caglayan et al.* [82], and by *Staffell and Pfenninger* [103, 109]. Moreover, geo-referenced databases for several already existing energy system components, as for example conventional power plants [130], are available. However, some data types are difficult to obtain with a sufficient regional granularity. This holds to be particularly true for any type of demand data. In this context, open-data initiatives can promote regionally accurate energy system modeling. Data which is available with an insufficient granularity level can be assigned to regions with distribution keys. These keys must be well justified or, even better, validated to a large extend. If they are not well justified but are used anyhow, the model might suggest a spurious accuracy.

The presented workflow also enables a flexible definition of the temporal scope of the energy system model. The chosen time step length depends on the temporal resolution of the available data. Although sub-hourly temporal resolutions are important for future energy system design and operation, cf. *Deane et al.* [26], data availability on this granularity level is often scarce. For example, the finest granularity of prominent wind energy modeling frameworks listed by *Ryberg et al.* [104] is one hour. In theory, the timeframe which can be considered in the workflow has no upper bound. In practice, as capacity variables must have the same value for all time steps in the presented version of the framework (March 2019), only a small number of years should be modeled. If transformation pathways should be considered, a myopic or perfect-foresight approach would have to be added to the framework, cf. *Lopion et al.* [5].

The presented mixed integer linear program (MILP) allows to consider a simplified *economy of scale* approach with non-linear cost-capacity correlations for the design of the energy system's components. The consideration of such an *economy of scale* is for some models a requirement for a reasonable design, cf. section 2.1. The longer model runtimes that accompany the consideration of binary variables are a necessity in this context. With the modeling of an *economy of scale* approach, the open-source available modeling framework *FINE*, which was developed in the context of this thesis, closes a gap in the literature with respect to the open-source energy system optimization tools listed by *Groissböck* [7].

An increase in modeling detail is obtained for AC lines with the integration of linearized expressions of the general power flow equations in *FINE*. Transmission components that are modeled with these additional constraints must have a fixed capacity as otherwise the optimization program would become non-linear. Approaches exist to remedy this non-linearity [11,46], they are however not pursued in the context of this thesis, as only DC line expansions were considered in the investigated scenarios. No further modeling detail, as for example the consideration of pressure losses, is currently considered for gas pipeline operation. However, the approach presented by *Robinius et al.* and *Reuß et al.* [15, 83], to which contributions were made within the scope of this thesis, allows to ensure a robust pipeline design under the consideration of pressure losses in the post-processing of the optimization.

The seasonal storage formulation, originally proposed by *Kotzur et al.* [32], of the MILP gives another option for complexity reduction during the overall workflow and is another unique characteristic of *FINE* with respect to the models listed by *Groissböck* [7]. Other uncommon but important features for storage infrastructure design are the consideration of shared potentials and cyclic lifetimes in the framework. The former is important to take the competition of gas commodities for existing geological storage facilities into account. The latter is important for an adequate modeling of batteries.

Apart from the storage components, no other component class in the framework is currently modeled with dynamic operation constraints[5]. The studies of *Palmintier and Webster* [34] and *NOW GmbH* [160] highlight the significance of dynamic operation constraints for power plants and electrolyzers, respectively. Inherently, this significance decreases with technology advancements towards highly flexible operation units. These units are assumed for the scenarios within this thesis. The consideration of additional dynamic constraints would again increase the model complexity and lead to higher model runtimes. Moreover, the implementation of these constraints would require ensuring that they are compatible with the typical period formulation of the model. In summary, additional dynamic constraints are not considered for the assumed, highly flexible operation units in this thesis. However, they are of interest for a wide range of other scenarios and should be included in future work.

With its flexible, generic model formulation regarding the spatial and temporal scope and the commodity and component selection, *FINE* is not only applicable to model national energy systems but can also be applied to a much broader scope in energy systems research. This is supported by the open-source availability of the framework on *GitHub* for which also an extensive documentation is given. For example, *Kannengießer et al.* use the framework to optimize urban districts [25] and *Caglayan et al.* use it to optimize a hydrogen supply system for Europe [82]. The option for cooperative code development on *GitHub* increases its usability to the scientific community. Moreover, the object-oriented programing scheme of the code allows an easy integration of future model extensions.

Concluding, it can be highlighted that:

- The presented overall workflow provides a novel, generic approach to model energy systems and their infrastructure based on geo-referenced data.
- The framework *FINE* used in the workflow was developed with the focus to design energy systems under the consideration of coupled transmission and storage infrastructure, a task which it is suitable for. The required consideration of a high spatial and temporal resolution always comes with a trade-off with respect to high model runtimes and other modeling detail. The presented workflow is therefore supplemented with two options to reduce the spatial and temporal complexity level.
- *FINE* is open-source available on a cooperative code development platform and is thus a contribution to the energy systems research community.
- *FINE* compares well with other open-source energy system optimization tools and provides unique features beyond existing models.

[5]Dynamic in this context means that the operation of the component during a time step is connected to its operation before and after that time step.

3.5 Summary

In this chapter, the workflow that was used to model the scenarios investigated within this thesis was described. The centerpiece of this workflow is a framework for modeling and optimizing energy systems under the consideration of a spatial and temporal resolution. Thus, the models generated with the framework are eligible to determine the optimal design and operation of transmission and storage infrastructure.

In section 3.1, the spatial and temporal representation that is considered in these models was presented. This representation is obtained in two steps. First, the spatial and temporal dimension is discretized. The second step is optional and allows to cluster the discrete regions and time steps to reduce the modeling complexity. Subsection 3.1.1 presented a regional discretization option that is based on *Voronoi* regions of electric grid busses. A clustering algorithm is selected out of regional clustering approaches for energy systems available in literature. Subsection 3.1.2 arrived at the conclusion that an annual timeframe with an hourly discretization level is a reasonable temporal representation of the investigated scenarios within this work, under the consideration of a limited computational budget. Scenario time series data can be clustered with a *Python* package for time series aggregation.

In section 3.2, the framework *FINE* for integrated energy system assessment was presented. The framework provides an optimization program which finds the cost-optimal design and operation of an energy system and its infrastructure under the consideration of technical and ecological boundary conditions. In subsection 3.2.1, the mathematical description of this optimization program was given. For this, basic parameters, sets, variables, constraints and the objective function are defined. Thereby, the variables and constraints are grouped to a basic component model and *Source/Sink*, *Conversion*, *Storage* and *Transmission* model extensions. The *Transmission* model is augmented with an optional *DC power flow* module. In subsection 3.2.2, the implementation and open-source publication of the program in the *Python* package *FINE* was presented.

In section 3.3, the overall scenario generation workflow was presented in a flowchart and discussed in detail.

In section 3.4, it was discussed how the overall workflow is both capable and well suitable for transmission and storage infrastructure design in energy system models. Also the data availability for such models was examined which is sparse for some data types. Furthermore, the section discussed strengths and benefits of potential model extensions and points to future work. Overall, this section concluded that *FINE* compares well with other open-source energy system optimization tools. Moreover, *FINE* provides unique features that are not covered by these existing tools.

Chapter 4

Setup of a Future German Energy Supply Systems Model

Within this thesis, scenarios for future German energy supply systems in the year 2050 are investigated. Depending on the scenario investigated, exogenously given energy demands in the electricity sector as well as parts of the mobility and industry sector are considered. The focus of these investigations is on the role of cross-linked infrastructure in such scenarios. To model such cross-linked infrastructure, including transmission and storage technologies, spatio-temporal representations of the considered energy supply systems are derived within this chapter. The spatio-temporal representations are thereby compatible with the modeling mimic presented in section 3.2, i.e. with the energy system modeling framework *FINE*.

A basic overview of the within this thesis considered components and their cross-links are, for an unrestricted scenario, visualized in Figure 2.2 and are categorized into *Source*, *Conversion*, *Storage*, *Transmission* and *Sink* components.

The scenarios are modeled with six basic commodities which interconnect the considered components, cf. Figure 4.1. These are electricity, methane-rich gas (MRG), biogas, liquid hydrogen (LH_2) and gaseous hydrogen (GH_2) at low and high pressure levels. Carbon dioxide reduction targets are enforced by a restriction of the annual natural gas import. The infrastructure for gaseous hydrogen is modeled with two pressure levels to explicitly consider compressor stations and their electricity demands. The low pressure level is intended to model a decentral hydrogen infrastructure while the high pressure level is intended to model a centralized hydrogen infrastructure. While biogas applications are considered on a decentral, low pressure level, the methane-rich gas infrastructure operates on a centralized,

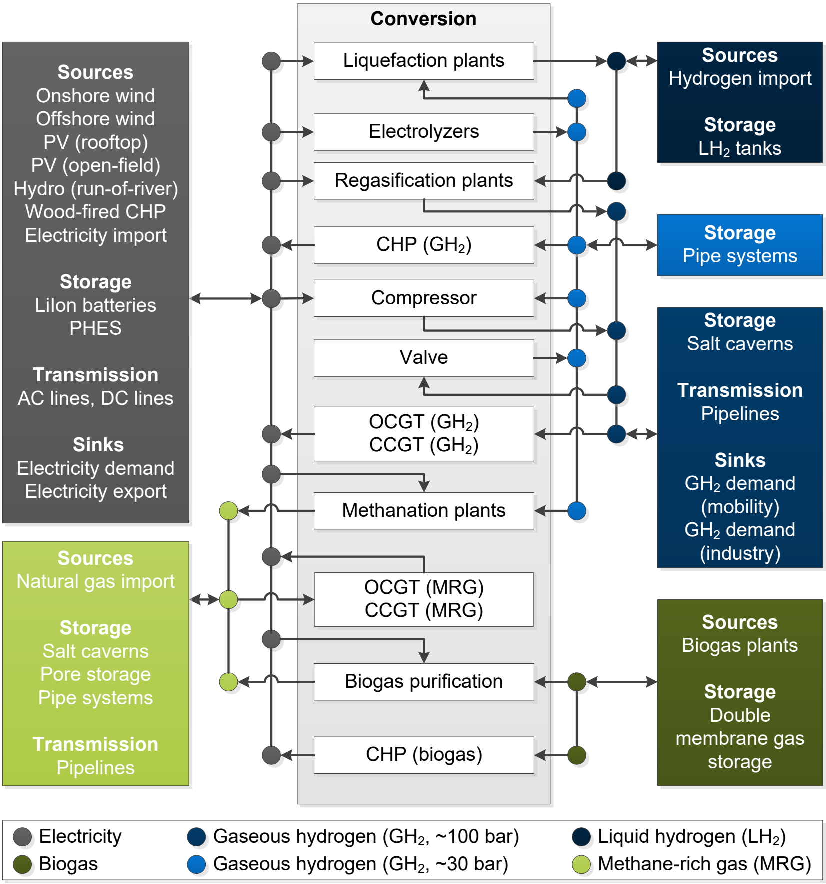

Figure 4.1: Basic component structure in an unrestricted scenario (CHP: Combined Heat and Power, OCGT: open cycle gas turbine, CCGT: combined cycle gas turbine, PHES: pumped hydroelectric energy storage, PV: photovoltaic).

high pressure transmission level. Methane-rich gas is in this context a collective term for natural gas, purified biogas and synthesized methane.

The general model setup is referred to as *FINE-CROSSING* (CROSS-linked INfrastructure scenarios for Germany; modeled with *FINE*) within this thesis. By turning components on and off and by varying their techno-economic data, different scenario settings can be investigated with the model setup.

A detailed description of the spatio-temporal representation of these components is given in the following. For this, first the spatial and temporal context of the scenarios is specified in section 4.1. Next, the basic energy and mass flows, namely final energy demands, energy imports and exports, and carbon dioxide restrictions, are described in section 4.2. A detailed description of the scenarios' cross-linked infrastructure is given in section 4.3.

4.1 Spatial and Temporal Context

The scenario scope presented in the following investigates German electricity and gas supply systems in the scenario year 2050. Thus, the considered spatial context is Germany, however international energy imports and exports are modeled as well. The temporal context is the year 2050. Consequently, the considered techno-economic parameters are projected into this year, taking potential cost reductions and efficiency gains into account.

Germany's regional scope is represented by discrete *Voronoi* regions of the electric grid busses, cf. subsection 3.1.1. For all scenarios, a spatial aggregation based on hierarchical clustering of the regions' centroids can be considered. The number of regions is chosen based on the specific scenario.

The scenarios are modeled with an hourly discretization level for one year, cf. subsection 3.1.2. If time series aggregation is applied, typical periods of 24 hours are considered and again a hierarchical clustering algorithm is applied. The number of typical periods is chosen based on the specific scenario. Even though typical periods are considered, the scenario year is still modeled as an interconnected entity with the seasonal storage formulation of the framework.

4.2 Basic Energy and Mass Flows

Basic energy demands and mass flows include final energy demands, energy imports and exports to and from Germany, as well as carbon dioxide emitted into the environment. From a modeling perspective, all these flows cross the virtual model boundary and are thus modeled as *Source* and *Sink* components.

In the following, first the final energy demands are presented in subsection 4.2.1. Next, the considered imports and exports are discussed in subsection 4.2.2. Finally, the assumptions made on the carbon dioxide restrictions are described in subsection 4.2.3.

4.2.1 Final Energy Demands

The design of the energy supply system is centered around a final electricity demand which covers all sectors and is based on Germany's electricity demand in the year 2013. In addition to this demand, hydrogen demands for applications in the transport and industry sector are considered.

Final Electricity Demand

The considered final electricity demand is obtained from the work of *Robinius et al.* [9]. The demand matches the annual net electricity consumption of 528 TWh_{el} reported by the *Arbeitsgemeinschaft Energiebilanzen e.V. (AGEB)* [84]. Consequently, the exogenously set consumption data covers all of 2013's net electricity demands. Additional electricity demands, for example for electrolysis, can endogenously arise during optimization. However, these are counted as additional electricity demands and are not accounted for in the final electricity demand.

The selected demand time series is distributed to the *Voronoi* regions. The total annual final electricity demand per square kilometer for these regions is visualized in Figure 4.2.

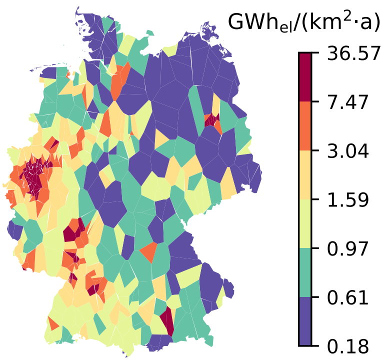

Figure 4.2: Annual final electricity demand of the scenarios (Σ 528 TWh_{el}).

High area-specific electricity demands occur in regions encompassing larger cities such as *Berlin*, *Hamburg*, *Munich*, *Frankfurt am Main* or *Stuttgart* and the *Ruhr* area. In general, it can be noted that particularly high annual electricity demands occurred in the west and south-west of Germany. An additional figure visualizing snapshots of the minimum and maximum electricity load for the *Voronoi* regions is given in the appendix, cf. Figure A.1.

Normalized profiles of the annual electricity demands within each of the four transmission system operator (TSO) zones are visualized in Figure 4.3.

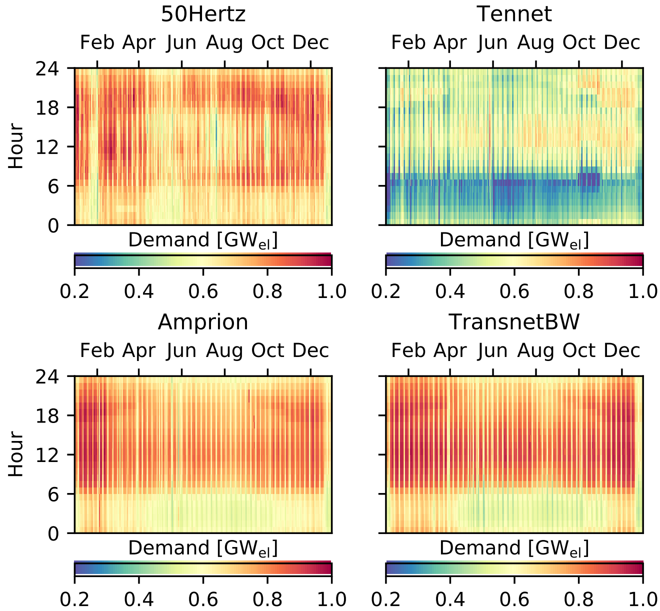

Figure 4.3: Electricity demand patterns in the four transmission system operator zones (normalized).

In general, the demand is most prominent during daytime. It is of a higher magnitude on weekdays and of a smaller one on weekends. Moreover, a seasonal pattern can be observed, in particular for the time series in the *50Hertz* and *Amprion* zone.

Figure 4.4 visualizes the results of *Fast Fourier Transformations* of the demand time series. High amplitudes are located at frequencies of 1/12 h^{-1}, 1/24 h^{-1}, 1/(7·24) h^{-1} and 1/8760 h^{-1} and thus emphasize daily, weekly and annual patterns in the demand data.

The final electricity demand is modeled as a *Sink* component in *FINE*.

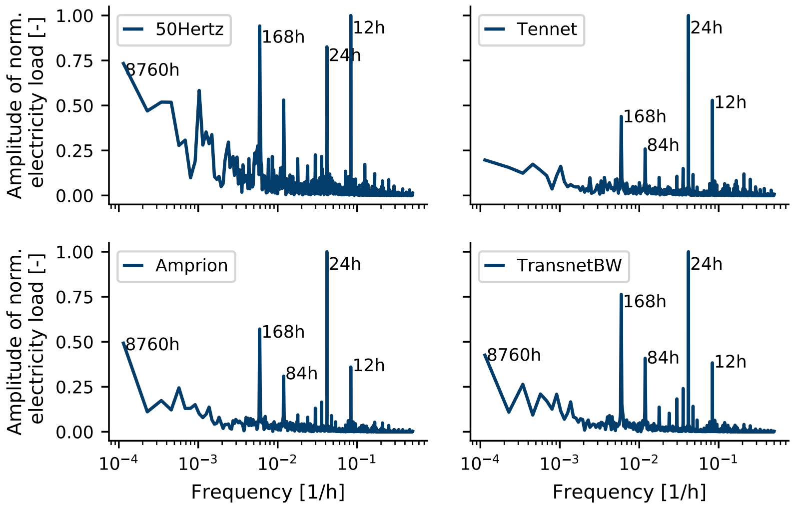

Figure 4.4: *Fast Fourier Transformation* of the electricity demand time series in the four transmission system operator zones (normalized).

Final Hydrogen Demand

The final hydrogen demands in the scenarios are modeled based on a study of *Cerniauskas et al.* [81], cf. section 2.3.2. In the study, *Cerniauskas et al.* investigate three exploratory market penetration scenarios (*low*, *medium*, *high*) for hydrogen utilization in the transport and industry sector. In the transport sector, fuel cell powered material handling vehicles (MHVs, i.e. forklifts), busses, trains, passenger cars and heavy-duty vehicles (HDVs) are considered. In the industry sector, processes for methanol and ammonia production from hydrogen, as well as hydrogen deployment in refineries are considered. Additionally, hydrogen sales from autonomous steam methane reformers are accounted for.

Figure 4.5 visualizes the annual hydrogen demand for the transport and the industry sector in the three scenarios. Demand centers are clustered around larger cities with high population densities and mobility demands as well as industrial regions with high hydrogen demands.

The final hydrogen demand is modeled as a *Sink* component in *FINE*. As all fueling stations are equipped with a daily buffer storage and it is assumed that the industrial processes have a constant operation rate, flat hydrogen demand profiles are assumed within this thesis for these demands.

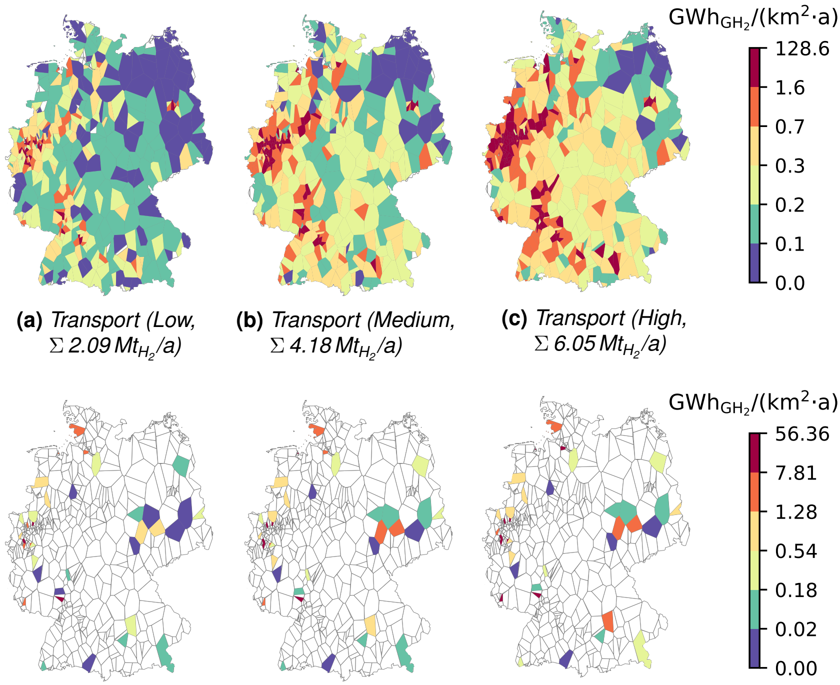

(a) *Transport (Low, Σ 2.09 Mt_{H_2}/a)*
(b) *Transport (Medium, Σ 4.18 Mt_{H_2}/a)*
(c) *Transport (High, Σ 6.05 Mt_{H_2}/a)*
(d) *Industry (Low, Σ 0.47 Mt_{H_2}/a)*
(e) *Industry (Medium, Σ 0.86 Mt_{H_2}/a)*
(f) *Industry (High, Σ 1.25 Mt_{H_2}/a)*

Figure 4.5: Annual hydrogen demands in the three market penetration scenarios, aggregated to the *Voronoi* regions.

Additional hydrogen demands can appear in the scenarios, for example to provide electricity. This demand is endogenously determined during optimization and is not accounted for in the final hydrogen demand.

4.2.2 Imports and Exports

In the scenarios, Germany is not modeled as an “island” but is modeled as being commodity-wise interconnected to other countries. Electricity imports and exports to countries that are connected to Germany via AC / DC lines are considered. Furthermore, hydrogen import by liquid hydrogen (LH_2) shipping and natural gas imports by gas pipeline are considered.

Electricity Imports and Exports

Electricity imports and exports are considered from and to countries that are connected to Germany via AC / DC lines. In the following, these countries are referred to as interconnected countries.

The electricity import and export are modeled as *Source* and *Sink* components in *FINE* with physical capacities equal to the restricting line capacities. Electricity imports and exports are considered for each line that crosses the German border and are obtained from a scenario of *Syranidis* [114], cf. section 2.3.1. If only the bus of the line which is inside of Germany is considered in the *Voronoi* regions, the imports / exports are assigned to this bus and the restricting line capacity is set equal to the crossing line's capacity. If both line's electric busses are considered in the *Voronoi* regions, the components are assigned to the bus outside of Germany and the restricting line capacity is set equal to the sum of all lines connecting this region to other regions. Moreover, an additional constraint is introduced that ensures that, at a given time step, the sum of all electricity imports / exports from the different busses that connect Germany to another country does not exceed the total available import / export potential from this country at that time step. This again means that the imports and exports are optional.

This simplified approach of import / export modeling could be enhanced in future work with a holistic European energy system model.

Hydrogen Import

In analogy to an LNG imports at LNG terminals, liquid hydrogen (LH_2) imports at LH_2 terminals, cf. section 2.3.2, are considered in the scenarios within this thesis. It is assumed that the ports which are currently under consideration for LNG terminals are also eligible locations for LH_2 terminals.

Furthermore, it is assumed that the ships that land at these ports have to deliver the imported LH_2 at a constant rate. Thus, the *Source* component that models the LH_2 import in *FINE* is modeled for all time steps of the year with a fixed, relative operation rate of 1. The absolute capacity, in terms of imported LH_2 per hour, is endogenously determined during optimization. As the cost of a commodity can only be modeled with a constant cost factor in the version of *FINE* used within this thesis, the cost of the imported LH_2 is set to a rather conservative value of 120 €/GWh$_{LH_2}$ (4 €/kg$_{LH_2}$). However, scenario variations are made which set the value to 105 €/GWh$_{LH_2}$ (3.5 €/kg$_{LH_2}$).

In analogy to traditional LNG terminals, liquid hydrogen can be stored in tanks at the LH_2 terminals and regasified for pipeline transmission. Other forms of hydrogen distribution are not considered but could be of interest in future work. The principal concept of such a terminal is described by *Nexant et al.* in a study on hydrogen delivery infrastructure [163]. Further descriptions of the LH_2 tanks and the regasification units are given in subsection 4.3.2.

Natural Gas Import

With the information provided in section 2.3.3, it can at first be assumed that bottlenecks in the gas grid will be unlikely, particularly for high greenhouse gas reduction targets. However, this assumption is dependent on several factors. For example, additional demands for carbon-neutral, methane-rich gases, as synthetic methane or purified biogas, could arise in the household, service and industry sector. Moreover, pipeline routes could be reassigned to transport other forms of gas, as for example hydrogen, and not be available for natural gas transport anymore.

Within this thesis, the only sinks for methane rich gases are gas-operated power plants. The purchase of imported natural gas for their operation is assumed to be a priority and consequently available in all regions.

The natural gas import is modeled as a *Source* component in *FINE*.

4.2.3 Carbon Dioxide Restriction

As the scenarios in this thesis only consider parts of the future German energy system, the scenarios' carbon dioxide restrictions must be tailored in such a way that they fit the modeled parts of the energy system. The assumed carbon dioxide restriction aims to fullfil the targets of the German government for the year 2050. These are to reduce the greenhouse gas (GHG) emissions, with respect to the year 1990, by 80 – 95%, cf. the *Klimaschutzplan 2050 (Climate Action Plan 2050)* by the *Bundesministerium für Umwelt, Naturschutz und nukleare Sicherheit* (*Federal Ministry for the Environment, Nature Conservation and Nuclear Safety*) [8].

By the design of the scenarios, GHG emissions can only occur during electricity generation in the form of carbon dioxide. These emissions are assumed to be solely constrained in relation to the 1990's emissions caused by electricity generation. The *Umweltbundesamt* (*Federal Environment Agency*) reports this value as 366 Mt_{CO_2}/a [192]. As already indicated in the *Klimaschutzplan 2050*, the energy sector must contribute above average, in comparison to the other sectors, to the overall GHG reduction goal. This stems from the difficulty of decarbonizing other sectors, particularly the agricultural sector [8]. Thus, electricity generation might have to be 100% renewable. To consider the bandwidth of the possible carbon dioxide restrictions on electricity generation, carbon dioxide restrictions from 80% up to 100% (73.2 – 0 Mt_{CO_2}/a) are investigated within this thesis. The lower and upper bound of this bandwidth are investigated in detail and a sensitivity analysis of intermediate emission targets is conducted.

The restriction is modeled by providing an annual limit to the import of natural gas. Here, it is assumed that 1 $MWh_{NG,LHV}$ of natural gas leads to 201 kg_{CO_2} of carbon dioxide [192].

4.3 Infrastructure Modeling

The modeling of the infrastructure components is described in the following three subsections. Modeling approaches which exist in literature and can be applied for this purpose were presented in section 2.3. There, also the considered techno-economic parameters were identified. Tables A.1-A.21 in the appendix A summarize the parameters of the components.

First, the electricity infrastructure is described in subsection 4.3.1. Next, infrastructure for gaseous and liquid hydrogen is presented in subsection 4.3.2. In subsection 4.3.3, infrastructure for methane-containing gases, i.e. natural gas, (purified) biogas and synthetic methane, is discussed.

Conversion components that convert multiple commodities into each other are in this context classified by their main output. For example, a gas fueled power plant is listed under electricity infrastructure and an electrolyzer under hydrogen infrastructure.

All techno-economic parameters are given in reference to the year 2019 and they are assumed to model the scenario year 2050. Inflation is not considered. Techno-economic parameters are preferably chosen from literature sources published in recent years. A weighted average cost of capital (WACC) of 8% is assumed for all technical components in the computation of the components' annuities.

4.3.1 Electricity Infrastructure

The technical components associated to the electricity infrastructure of the scenarios are presented in the following.

- First, *Source* components which produce electricity across the system's boundary are presented. These are onshore wind turbines, offshore wind turbines, photovoltaic residential rooftop systems, photovoltaic open-field systems, run-of-river hydroelectricity plants and decentralized, wood-fired combined heat and power plants.
- Next, *Conversion* components which convert other commodities into electricity are described. Here, decentralized, biogas-/hydrogen-fueled combined heat and power plants as well as centralized electricity generation from thermal power plants are considered.
- As *Storage* components, lithium-ion batteries and pumped hydroelectric energy storage are modeled and presented.
- Lastly, AC and HVDC lines are considered and introduced as *Transmission* components.

For additional descriptions of electricity infrastructure technologies and their respective literature references, see subsection 2.3.1.

Onshore Wind Turbines

The capacity potential and the generation time series of onshore wind turbines with a future turbine design are modeled and simulated based on the work of *Ryberg et al.* [102, 104]. The applied workflow is described in the following.

1. First, eligible wind turbine locations are determined for Germany. These are obtained from *Ryberg et al.* [104].
2. Second, these eligible wind turbines are categorized into two classes based on their levelized cost of electricity (LCOE) for a long-run average[1]. *Class I* holds the least expensive third of the turbine locations, i.e. all turbines with LCOE in the range of 27 – 65 €/MWh$_{el}$. *Class II* holds the remaining, more expensive two thirds, i.e. all turbines with LCOE in the range of 65 – 174 €/MWh$_{el}$[2]. While *Class I* adds up to a capacity potential of 219 GW$_{el}$, *Class II* adds up to a capacity potential of 401 GW$_{el}$.

[1] These LCOE were determined by *Ryberg et al.* [102], are based on multiple decades of weather years and are computed under the assumption that all of the generated electricity can be sold.

[2] This range refers to all turbines that are above the 1st tercile and below the 99.9th percentile of the LCOE distribution.

3. Third, aggregated capacity potentials, electricity generation profiles and turbine investments are determined for the two classes for each *Voronoi* region $\tilde{r}$.
    (a) First, turbine locations within $\tilde{r}$ are identified.
    (b) Then, for each of the turbine locations within $\tilde{r}$, an electricity generation profile is computed with a simulation module described by *Ryberg et al.* [102].
    (c) Finally, the aggregated capacity potential as well as the capacity specific electricity generation profiles and turbine investments within $\tilde{r}$ are determined for the two classes respectively. In this context, the capacities are summarized, and the electricity generation profiles and the turbines' investments are averaged to capacity specific values.

With the categorization of the turbines into two classes, the capacity specific generation profiles and investment factors of the least and the more expensive wind turbine locations do not have to be averaged. Rather, the optimizer has the chance to first select the most promising turbine locations and only then the less promising ones. A finer classification could refine this procedure even further but would increase the computational load of the model at the same time.

The determined capacity potential and average full load hours (FLHs) are visualized in Figure 4.6.

Figures 4.6a and 4.6b present the data for all turbine locations (*Class I* & *Class II*) for each *Voronoi* region. It can be noted that the capacity potential is smaller in urban and larger in rural areas. The full load hours are characterized by their proximity to the *North* and *Baltic Sea* and their vicinity to mountainous terrain.

Figures 4.6c – 4.6f visualize the simulation results for *Class I* and *Class II* respectively. Wind turbines of *Class I* are predominantly located in the north of Germany. A larger density of cost lucrative locations can also be found in *Lower* and *Upper Bavaria* as well as in the *Chemnitz* and *Leipzig* area. A comparably small density of *Class I* turbines can be found in the middle west of Germany. However, the ones that are located there are positioned at very favorable wind locations. Complementary, wind turbines of *Class II* are predominantly located in the middle and south of Germany. With a value of 2428 h/a, wind turbines of *Class I* have significant higher average full load hours then turbines of *Class II*, which have an average value of 1636 h/a.

A profile of a representative, capacity specific generation time series is visualized in Figure 4.7. Specific patterns are not straightforward to identify, however an annual pattern and a slight daily pattern can be observed.

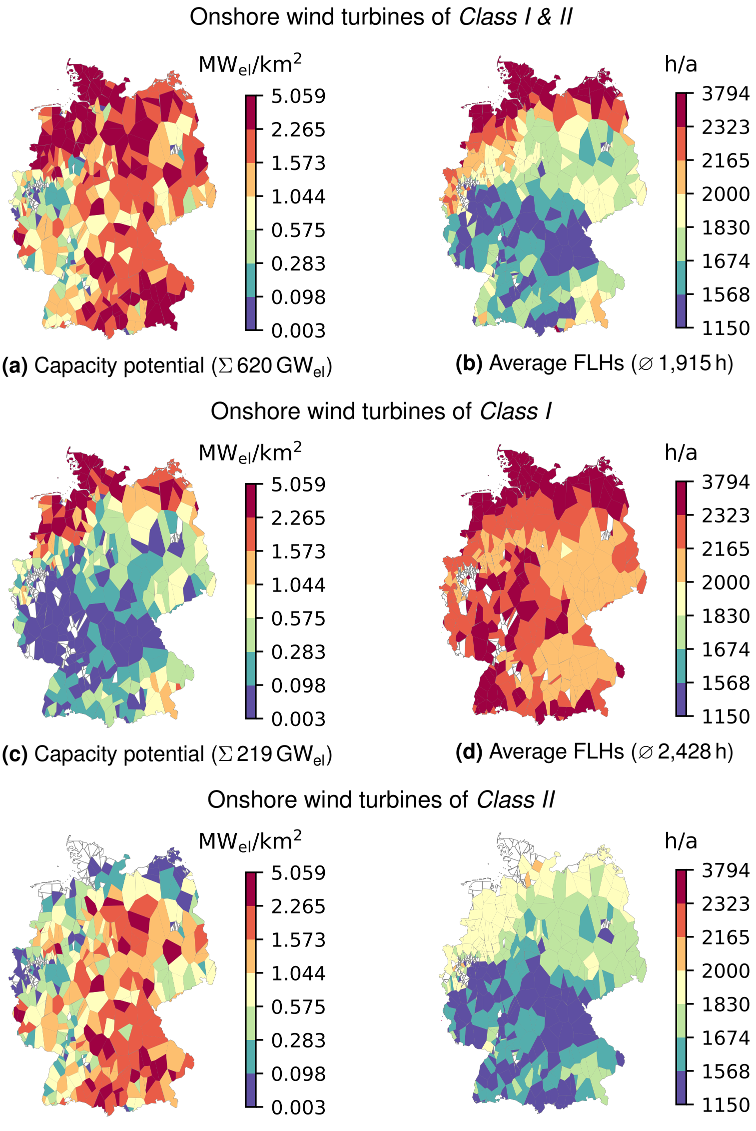

(a) Capacity potential (Σ 620 GW$_{el}$)
(b) Average FLHs ($\varnothing$ 1,915 h)
(c) Capacity potential (Σ 219 GW$_{el}$)
(d) Average FLHs ($\varnothing$ 2,428 h)
(e) Capacity potential (Σ 401 GW$_{el}$)
(f) Average FLHs ($\varnothing$ 1,636 h)

Figure 4.6: Capacity potentials and average full load hours (FLHs) of the onshore wind turbines in the scenarios (weather year 2013). Regions marked in white do not contain the respective turbine class(es).

The daily pattern is caused by irradiance surface heating and its effects on air temperature. The markedness of this pattern is related to the non-uniformity of the land cover for which the regional profile is generated.

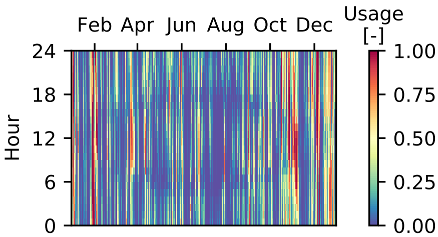

Figure 4.7: Electricity generation pattern from onshore wind turbines (weather year 2013).

A *Fast Fourier Transformation* is used to investigate the time series in further detail, cf. Figure 4.8.

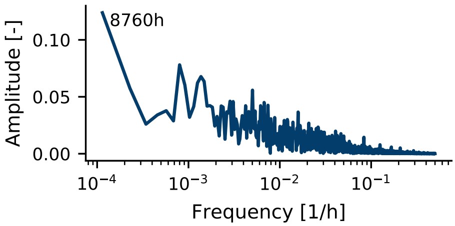

Figure 4.8: *Fast Fourier Transformation* of an electricity generation pattern from onshore wind turbines (weather year 2013).

An annual pattern can be observed, resulting from strong winds in winter which decline during spring, reach their base level in summer and then increase again during autumn. A prominent daily pattern cannot be identified.

The capacity specific investment of the turbines is an output of the simulation workflow by *Ryberg et al.* [102]. A histogram of the investments of the turbines is presented in Figure 4.9. The arithmetic means of the distributions are 1121 €/kW$_{el}$ and 1179 €/kW$_{el}$ for *Class I* and *Class II* respectively.

The two onshore wind turbine classes are modeled as *Source* components in *FINE* with a maximum capacity potential. The simulated regional electricity generation time series serve as an upper bound on the electricity generation of the turbines.

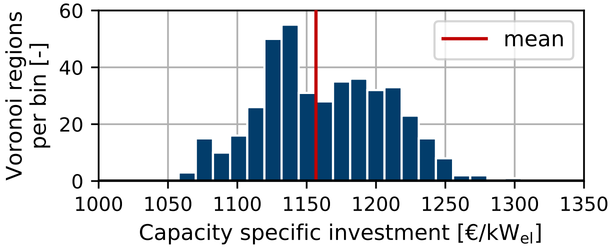

Figure 4.9: Histogram of the average, capacity specific investment of the considered onshore wind turbines.

Offshore Wind Turbines

The capacity potential and the generation time series of offshore wind turbines are modeled based on studies by *Caglayan et al.* [105] and *Ryberg et al.* [102]. Eligible turbine locations and their techno-economic parameters are obtained from the study of *Caglayan et al.* [105]. The generation profiles of the turbines are obtained by applying the turbine simulation model of *Ryberg et al.* [102].

As for the onshore wind turbines, the eligible offshore wind turbines are categorized into two classes so that turbine classes that show an inherently different system behavior do not have to be aggregated. For the offshore turbines, the turbine locations are categorized based on their foundation, i.e. a *floating* or a *fixed* foundation. This is again motivated by finding a split between less and more expensive turbines. In the data of *Caglayan et al.* [105], turbines with *fixed* foundation are located close to shore while *floating* foundations are considered in deeper water. Turbines with *floating* foundations have, on average, a higher capacity specific investment but also higher full load hours, cf. Figures A.14 and A.15 in the appendix A. These result, on a long-run average, in the levelized cost of electricity[3] (LCOE) visualized in Figure 4.10. Figure 4.10 also visualizes routes of existing and potential new offshore cables, obtained from an infrastructure analysis study by *Robinius et al.* [106], that can be used to transport the generated electricity to shore. Additionally, the electric busses that can be used for the feed-in of this electricity into the main grid are shown. In this context, also a bus close to the city of *Rendsburg* is considered, as it provides transport-capacity-wise a good feed-in location for the offshore turbines located outside of the city of *Kiel*. These cable routes and busses are used to assign the offshore turbines to the *Voronoi* regions.

[3] As for the onshore wind turbines, these LCOE were determined by *Caglayan et al.* [105], are based on multiple decades of weather years and are computed under the assumption that all of the generated electricity can be sold.

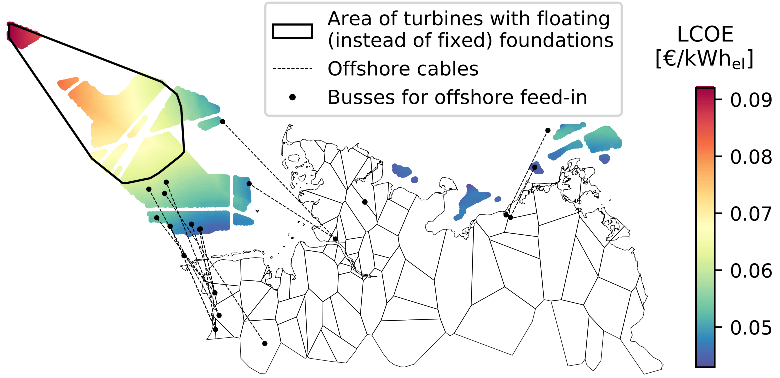

Figure 4.10: Locations and levelized cost of electricity (LCOE) of the considered offshore wind turbines.

For this, each turbine is assigned to the closest bus. If the bus is an offshore bus, its counterpart onshore is chosen. The corresponding assignment of the turbines to the *Voronoi* regions is visualized color-coded in Figure 4.11.

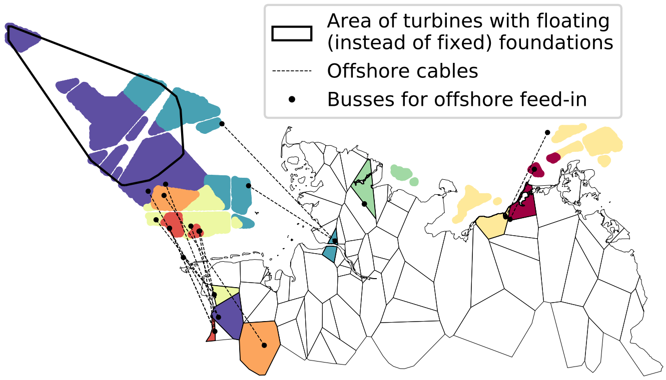

Figure 4.11: Color-coded assignment of offshore turbines to the *Voronoi* regions.

The resulting total capacities in the *Voronoi* regions are visualized in Figure 4.12. They add up to a capacity potential of 82 GW_{el}. Turbines with *fixed* foundations contribute with 46 GW_{el} to this value. The electricity feed-in from turbines with *floating* foundations is concentrated in only two regions. Thus, under high carbon dioxide reduction targets, these regions are likely candidates for electrolyzer placement and / or an expansion of the DC lines connected to these regions during

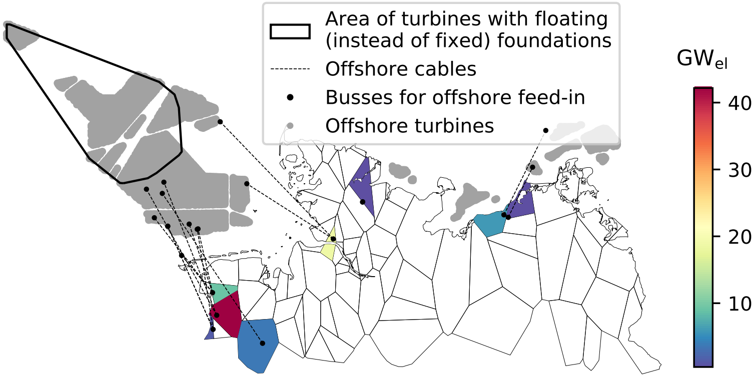

Figure 4.12: Capacity potential of the offshore wind turbines considered in the scenarios.

optimization as they can provide renewable electricity with high full load hours in magnitudes that are challenging to transport with the existing electric grid.

The generation profiles of the offshore wind turbines resemble the ones of the onshore turbines, only with, in general, higher full load hours.

Histograms of the capacity specific invest, resulting from applying the workflow of *Caglayan et al.* [105], are presented for the two offshore turbine classes in Figure 4.13. The arithmetic means of the distributions are 2372 €/kW$_{el}$ and 3398 €/kW$_{el}$ respectively.

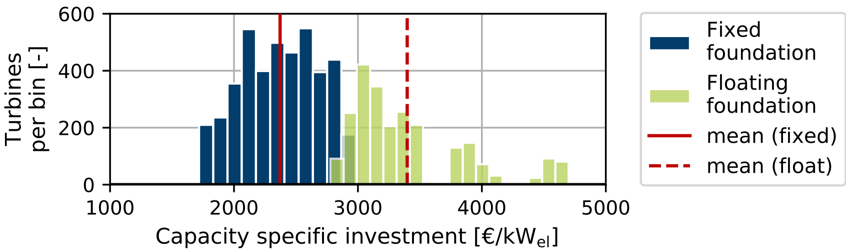

Figure 4.13: Histogram of the capacity specific investment of the considered offshore wind turbines.

The two offshore wind turbine classes are modeled as *Source* components in *FINE* with a maximum capacity potential. The simulated regional electricity generation series serve as an upper bound on the electricity generation of the turbines.

Photovoltaic (PV) Residential Rooftop Systems

Photovoltaic (PV) residential rooftop systems with a total capacity potential of 190 GW_p[4] are considered in the scenarios. This potential as well as the corresponding electricity generation time series are determined based on the work of *Ryberg* [110]. The workflow used to determine the capacity potential and electricity generation time series is described in the following.

1. First, the total available capacity potential for Germany is determined based on a workflow from the study of *Ryberg* [110]. For this, an equidistant grid with a 10 km separation distance is defined for Germany. The determined capacity potentials within these cells are assigned to the cells' centroids.
2. Second, aggregated capacity potentials and electricity generation profiles are determined for each *Voronoi* region $\tilde{r}$.
   (a) First, the grid centroids that overlap with $\tilde{r}$ are determined.
   (b) For each of the centroids within $\tilde{r}$, the electricity generation time series is simulated with a module from *Ryberg* [110]. For this simulation, a *Gaussian* distribution (mean: 35°, standard deviation: 15°) is assumed for the roof tilt angles. Differing from *Ryberg* [110], the rooftop azimuths (90 – 270°) are broken down into three classes of equal size, separating them into *eastwards* (90 – 150°), *southwards* (150 – 210°) and *westwards* (210 – 270°) facing rooftops.
   (c) Finally, the aggregated capacity potential and electricity generation profiles are determined for each of the three classes within $\tilde{r}$. In this context, the capacities are summarized, and the electricity generation profiles are averaged to capacity specific values.

The resulting total capacity potentials of all three classes are visualized in Figure 4.14. As the capacity potential is correlated to the population density in Germany, particularly high capacity potential densities can be observed in urban areas.

The geo-referenced full load hours are given, for the three classes respectively, in Figure 4.15.

Naturally, the south of the country is characterized by higher full load hours. However, due to maritime weather conditions, an increase in full load hours can also be observed towards the *North* and *Baltic Sea*.

[4] Power generation at PTC (PVUSA Test Condition).

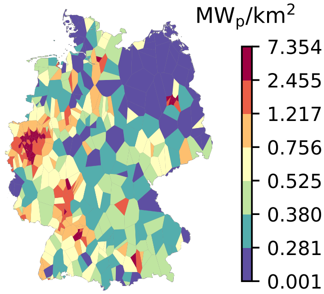

Figure 4.14: Capacity potential of the PV rooftop systems for the scenarios (Σ 190 GW_p).

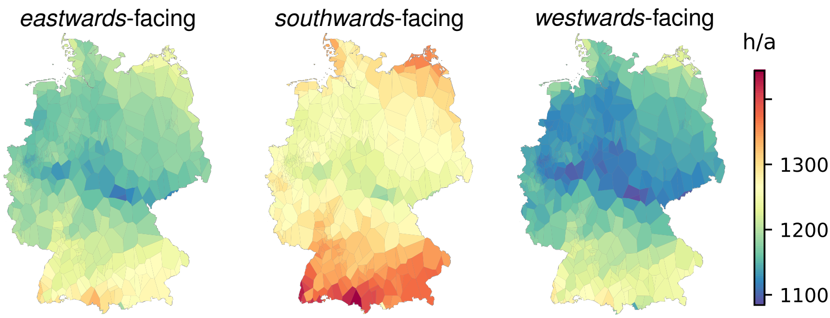

(a) ∅ FLHs: 1,093 **(b)** ∅ FLHs: 1,183 **(c)** ∅ FLHs: 1,062

Figure 4.15: Average full load hours of the PV rooftop systems for the scenarios (weather year 2013).

Representative profiles of capacity specific generation time series are visualized for the three classes in Figure 4.16. *Eastwards*-facing panels generate most of their electricity in the morning while *southwards*-facing and *westwards*-facing panels generate most of their electricity around noon and in the afternoon respectively. The highest full load hours during the day occur during summer. A *Fast Fourier Transformation* of the first of the three time series is visualized in Figure 4.17. An annual as well as a daily pattern can be identified.

The three PV rooftop systems are modeled as *Source* components in *FINE* with a maximum capacity potential. The simulated regional electricity generation series serve as upper bounds on the electricity generation of the systems.

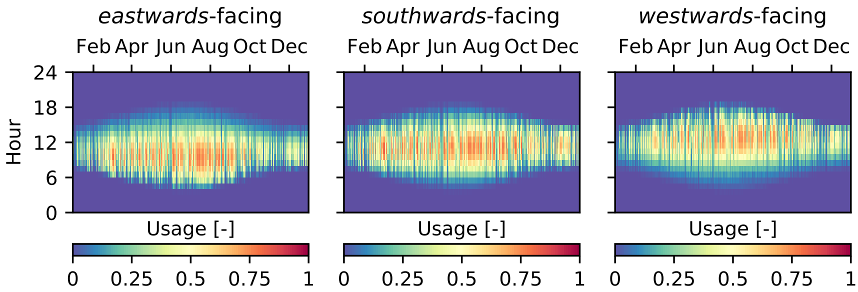

Figure 4.16: Electricity generation pattern from PV rooftop systems (weather year 2013).

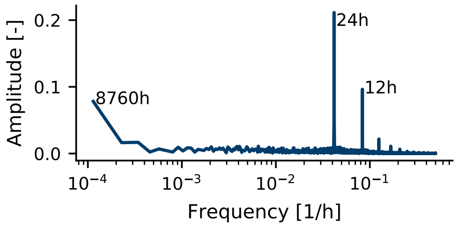

Figure 4.17: *Fast Fourier Transformation* of an electricity generation pattern from PV rooftop systems.

Photovoltaic (PV) Open-field Systems

Photovoltaic (PV) open-field systems with a total capacity potential of 54 GW_p are considered in the scenarios. As for PV rooftop systems, this potential and the corresponding electricity generation time series are determined based on the work of *Ryberg* [110]. The workflow used to determine capacity potential and electricity generation time series is described in the following.

1. First, the total available capacity potential for Germany is determined on a geo-referenced level. This information is obtained from the study of *Ryberg* [110].
2. Second, aggregated capacity potentials and electricity generation profiles are determined for each *Voronoi* region $\tilde{r}$.
   (a) First, the regional potentials that overlap with $\tilde{r}$ are determined.

(b) Next, the electricity generation time series is simulated twice for each of regional potential within $\tilde{r}$ with a module presented by *Ryberg* [110], once for a *Tracking* system and once for a system with a *Fixed-tilt*. These two system classes are modeled as competing technologies, meaning they share a maximum capacity potential.

(c) Lastly, the aggregated capacity potential and electricity generation profiles are determined for each of the two classes within $\tilde{r}$. In this context, the capacities are summarized, and the electricity generation profiles are averaged to capacity specific values.

The capacity potential that the two competing open-field systems share is visualized in Figure 4.18. Higher capacity potential densities can be observed in the north-east, the south-west and the south of Germany.

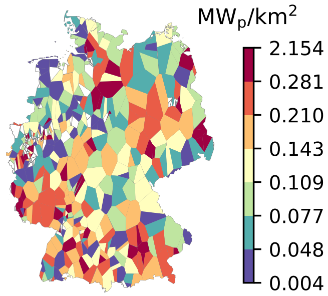

Figure 4.18: Capacity potential of the two competing open-field PV systems (*Fixed-tilt & Tracking*) in the scenarios (Σ 54 GW_{el}). Regions marked in white do not hold any capacities.

The full load hours of the two systems are visualized in Figure 4.19. Naturally, the geo-referenced distribution of the open-field systems' full load hours resembles the one of the residential rooftop systems. Moreover, and as expected, the open-field systems with a *Tracking* system to manipulate the panel orientation have in general higher full load hours than the one with a *Fixed-tilt*.

This can also be observed in Figure 4.20 which representatively visualizes capacity specific electricity generation time series of the two technologies. As for the PV rooftop systems, electricity is generated during the day, reaching its peak at midday. The highest full load hours during the day occur during summer. Furthermore, it can be observed that the *Tracking* systems utilize the available solar radiation to a higher potential. Thus, in comparison to the systems with a *Fixed-tilt*, they lead to more flattened generation potential curves.

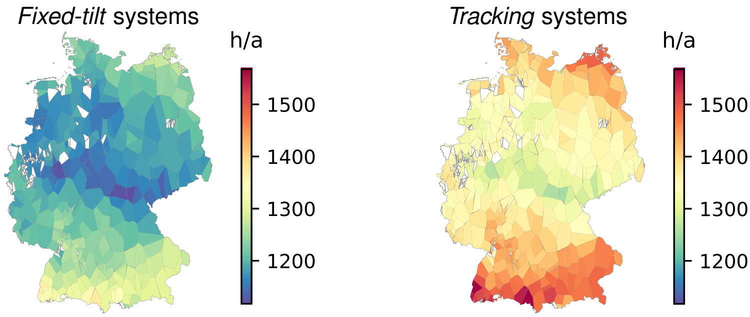

(a) ∅ FLHs: 1210 h **(b)** ∅ FLHs: 1377 h

Figure 4.19: Full load hours (FLHs) of PV open-field (*Fixed-tilt & Tracking*) systems in the scenarios (weather year 2013). Regions marked in white do not hold any capacities.

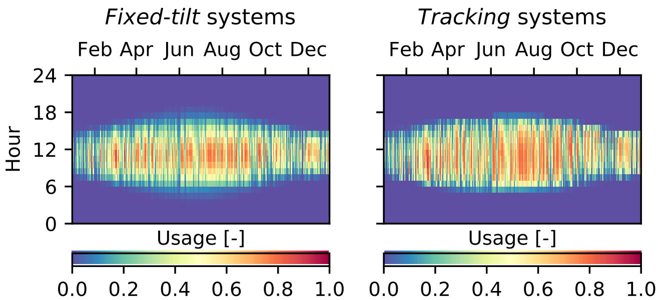

Figure 4.20: Representative electricity generation patterns from PV rooftop systems (weather year 2013).

The two PV open-field systems are modeled as *Source* components in *FINE* with a shared, maximum capacity potential. The simulated regional electricity generation series serve as an upper bound on the electricity generation of the systems. From a full load hour perspective, the open-field systems with *Tracking* are more attractive to the energy system. However, as described above, they are more expensive than the systems with a *Fixed-tilt*. Thus, both technology classes are provided to the energy system model with a shared potential constraint.

Run-of-river (R-o-r) Hydroelectricity Plants

The placements and time series of run-of-river (r-o-r) hydroelectricity plants are based on the work of *Syranidis* [114]. The placements of these plants are visualized in Figure 4.21, aggregated to the *Voronoi* regions. For Germany, plant capacities with a total of 3.8 GW_{el} and an annual generation of 17.3 TWh_{el} are considered.

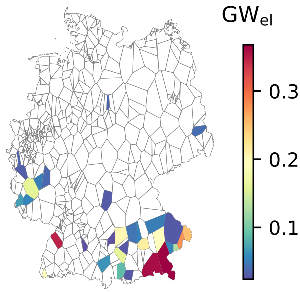

Figure 4.21: Capacities of run-of-river hydroelectricity plants (Σ 3.8 GW_{el}). Regions marked in white do not hold any capacities.

Exemplary heat maps of capacity specific r-o-r generation time series within different regions in Germany are visualized in Figure 4.22.

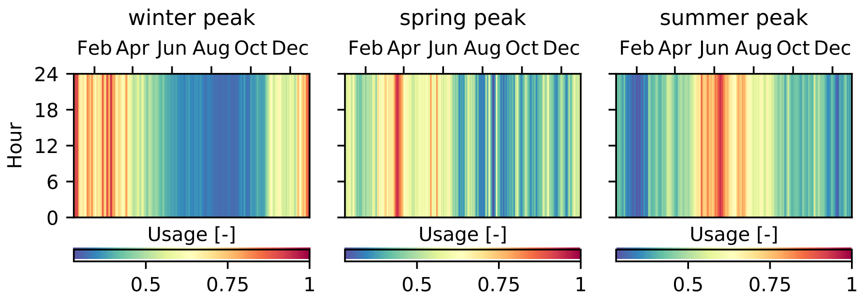

Figure 4.22: Exemplary electricity generation patterns from run-of-river hydroelectricity plants.

Seasonal generation patterns can be observed for all regions. The season in which the peak electricity generation is reached varies for the plants between winter, spring and summer. A *Fast Fourier Transformation* confirms the seasonal generation pattern and does not indicate any other distinct patterns, cf. Figure 4.23.

The run-of-river hydroelectricity plants are modeled as *Source* components in *FINE*. The presented capacities in Figure 4.21 are assumed to be fixed. The regional electricity generation time series serve as an upper bound on their electricity generation.

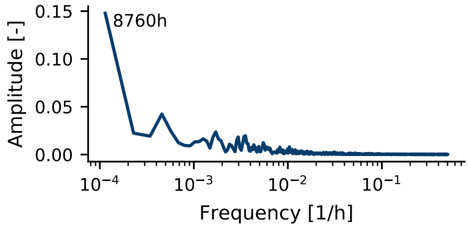

Figure 4.23: *Fast Fourier Transformation* of an electricity generation pattern from run-of-river hydroelectricity plants within one region.

Decentralized Electricity Generation from Wood

Within this thesis, combined heat and power (CHP) plants operated on wood chips are considered. A total wood chip potential of 142 $TWh_{wood,LHV}$ is assumed which translates to an electricity generation potential of 40.5 TWh_{el} when the CHP plants are modeled with a conversion efficiency of 0.285 $kW_{el}/kW_{wood,LHV}$ [120]. The assumption on the total wood potential, i.e. forestry biomass, is based on a study of the *Deutsches Biomasseforschungszentrum* (*German Biomass Research Center*) [116].

Furthermore, it is assumed that the considered cost of the wood chips only covers a transport distance of 20 km [121]. As the modeled regions have a, in general, larger spatial dimension, a “copper plate” assumption for the transport between these regions does not suggest itself. Thus, the total potential must be regionally distributed which is within this study done based on the forest area in Germany as provided by the Corine Land Cover data [117, 118] and by applying the *Python* packages *geokit* [58] and *glaes* [119]. The electricity generation potential from wood chips in the *Voronoi* regions is visualized in Figure 4.24.

The regional distribution of the forestry biomass correlates to the regionally aggregated data presented in the study of the *Deutsches Biomasseforschungszentrum* [116]. A more detailed distribution of the forestry biomass might be of interest in future work. However, the current one already sufficiently correlates the potential of wood chips fired CHP plants to the extent of forestry areas in that region.

Theoretically, also industrial wood residues, waste wood and short-rotation forestry could be additionally considered. The potentials of the former two are smaller than the one of the forestry biomass, 16 and 31 $TWh_{wood,LHV}$ respectively [116],

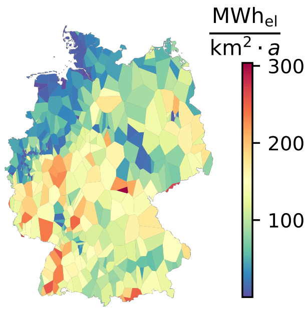

Figure 4.24: Electricity generation potential (Σ 40.5 $\mathrm{TWh_{el}}$) from wood chip fired CHP plants in the *Voronoi* regions.

and are moreover difficult to regionalize. As this is beyond the scope of this work, they are currently not further considered. The short-rotation forestry, as any other short-rotation biomass, is as well not modeled in the scenarios, thus avoiding a *Tank-or-Table* discussion as the arable land can be fully utilized for food production. Expanding these additional potentials and exploring them in further detail is of interest for future work, especially when the heat and transport sector are represented in more detail. In this case, heat and transport fuels can be generated / synthesized by biomass technology pathways.

In general, it must be noted that, in the current scenarios, CHP plants serve the sole purpose of providing electricity. Their heat generation is taken for granted. A future integration of the heat sector will thus provide a more complete picture of the potential applications of CHP plants.

A truck transport of the wood chips between regions is not considered, as only decentral, local wood chip fired CHP plants are modeled. Thus, the plants can be modeled as a *Source* component for electricity in *FINE* with a commodity cost for the wood chips. The regional, annual electricity generation of the plants is limited with an additional constraint.

Decentralized Electricity Generation from Biogas and Hydrogen

Combined heat and power (CHP) plants with a plant size of several megawatts are considered in the scenarios. The CHP plants are equipped with a combustion engine and are operated on either biogas or hydrogen.

Both technologies are modeled as *Conversion* components in *FINE* and have no geographical restrictions.

It must be noted that, in the current scenarios, the CHP plants serve the sole purpose of providing electricity and that their heat generation is taken for granted. A future integration of the heat sector will provide a more comprehensive picture of the potential applications of CHP plants.

Centralized Electricity Generation from Thermal Power Plants

As introduced in section 2.3.1, the power plant landscape will significantly change until the year 2050 as most of the power plants existing in 2018 are either decommissioned or assigned to the cold reserve. It is assumed within thesis that the locations of all nuclear power plants as well as the locations of all lignite, hard coal or natural gas power plants that exceed their technical lifetimes in 2050, cf. the studies by *Markewitz* [127] and *Markewitz et al.* [128], can be reassigned. They are used as potential locations for new thermal power plants. This has the benefit that existing on-site infrastructure might be partly reused and a good connection to the electric grid can be ensured. Appropriately, the capacity of the replaced plant is assumed to serve as an upper capacity bound for the new plant. The required information for this reassignment is obtained from *Open-Power-System-Data* for *Conventional power plants* [130].

In the scenarios, plants operating with an open cycle gas turbine (OCGT) or a combined cycle gas turbines (CCGT) can be built at these sites. The plants can be either operated on methane-rich gas (MRG) or on hydrogen, cf. the study by *Welder et al.* [99] for a more detailed discussion on *Hydrogen-to-Power* (HtP) technology pathways in energy systems. Thus, four types of technologies compete for the available capacity potentials, namely *OCGT (MRG)*, *CCGT (MRG)*, *OCGT (GH_2)* and *CCGT (GH_2)*. The resulting shared capacity potentials are visualized in Figure 4.25.

The four plant types are modeled as *Conversion* components in *FINE*. The capacities presented in Figure 4.25 provide a shared, maximum capacity potential.

Lithium-Ion Batteries

With the background on lithium-ion batteries presented in section 2.3.1 and also with respect to reducing the overall computational load when solving the optimization program stated by the energy system model, only lithium-ion batteries are considered as an electricity storage option with a focus on serving as a daily storage option.

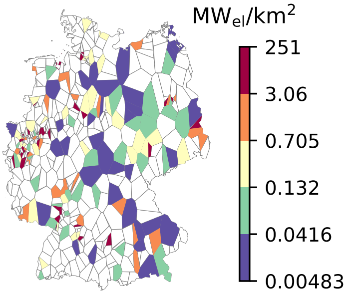

Figure 4.25: Capacity potentials of the competing, centralized thermal power plant technologies ($\Sigma\,66\,\mathrm{GW_{el}}$). Regions marked in white do not hold any capacities.

The lithium-ion batteries are modeled as *Storage* components in *FINE* and without geographical restrictions. The power to energy ratio ($\mathrm{kW_{el}/kWh_{el}}$) of the battery is fixed to a value of 1 so that it can be fully charged and discharged within one hour. This assumption fits well to the currently installed stationary, large-scale lithium-ion battery systems in Germany, for which an average power-to-energy ratio of 1.27 is found by *Stenzel et al.* [132][5]. Thus, the batteries serve as highly flexible energy storage in the hourly regiment.

Pumped Hydroelectric Energy Storage

The existing and planned PHES plants in 2018 provide the basis for the PHES modeling within the scenarios. These plants are categorized into two classes based on their year of construction. The first class, *PHES (existing)*, is comprised of plants built in or after 1970. These plants are still within their technical lifetime of 80 years [133]. For these plants, only operational expenditures of their charging and discharging units, i.e. pumps and turbines, are considered. The second class, *PHES (refurbished)*, is comprised of plants built before 1970 and which can be refurbished. Within this thesis, it is assumed that the refurbishment cost is comprised of the replacement of the PHES plant's pump and turbine as well as the renovation of its storage basins. The resulting regionalized capacities of the two classes, obtained from the database by *Stenzel et al.* [136], are visualized in Figure 4.26.

The PHES plants are modeled as *Storage* components in *FINE*. Pumps and turbines belonging to the PHES plant are not modeled separately but are integrated into the *Storage* component. The power to energy ratio for the charging and

[5] As the scenarios are modeled with an hourly resolution, a power-to-energy ratio above 1 has the same effect as a ratio equal to 1.

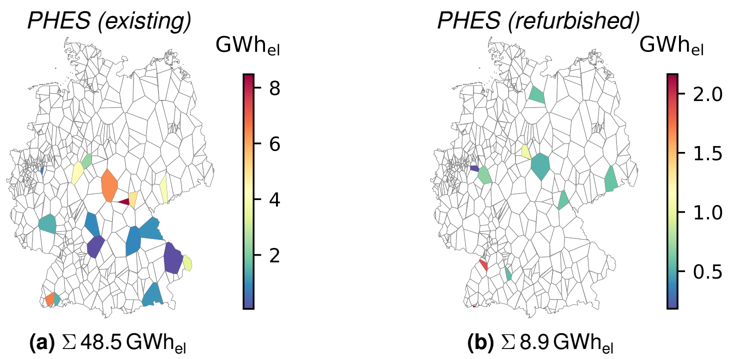

Figure 4.26: Capacities / capacity potentials of PHES plants (existing / refurbished), aggregated to the *Voronoi* regions. Regions marked in white do not hold any capacities.

discharging of the PHES plant is set to 1/7. It must be noted that no external water inflows into the PHES plants are considered to reduce the modeling complexity. These inflows are however small in comparison to other electricity sources as for example run-of-river hydroelectricity, cf. the work of *Syranidis* [114].

AC and HVDC Lines

The scenario *B2025* of the *Netzentwicklungsplan (NEP) Strom* (*network development plan - electricity*) from the year 2015 [107] serves as a data base of the electric lines considered within the scenarios of this thesis, cf. section 2.3.1. The underlying data of the lines is derived from an infrastructure analysis study of *Forschungszentrum Jülich* [106].

Furthermore, the trend of an increasing consideration of DC line expansions in the network development plans, cf. [107, 139, 140], is incorporated in the modeling of the scenarios. With respect to the data available for this thesis, HVDC line expansions along the HVDC lines from the *B2025* scenario of the *NEP* from 2015 are allowed in the scenarios. In the following, the HVDC lines from the *NEP* 2015 are referred to as *DC lines (ex.)*. HVDC lines which can be built in addition to these are referred to as *DC lines (new)*.

The AC lines are modeled in the scenarios as a *Transmission* component with a linearized power flow. The HVDC lines, *DC lines (ex.)* and *DC lines (new)*, are modeled as basic *Transmission* components.

4.3.2 Hydrogen Infrastructure

The technical components associated to the hydrogen infrastructure of the scenarios are presented in the following. The hydrogen infrastructure is thereby subdivided into infrastructure for liquid hydrogen and infrastructure for gaseous hydrogen at medium ($\sim$ 30 bar) and high ($\sim$ 100 bar) pressure levels.

- First, *Conversion* components which produce one of the three hydrogen forms are described. These are
  - electrolyzers which produce gaseous hydrogen at 30 bar from electricity and water,
  - liquefaction plants which liquefy gaseous hydrogen at 30 bar,
  - regasification plants which generate gaseous hydrogen at 100 bar from liquid hydrogen, and
  - compressor stations which compress gaseous hydrogen from 30 bar to 100 bar.
- Next, salt caverns for the storage of gaseous hydrogen at high pressure and pipe systems for gaseous hydrogen storage at medium pressure as well as cryogenic tanks for liquid hydrogen storage are described as *Storage* components.
- Lastly, hydrogen pipelines which are operated at 100 bar are considered and introduced as *Transmission* components.

In addition to the inter-regional transmission infrastructure, a cost surcharge for the hydrogen distribution within the regions is determined. This surcharge models the cost for the intra-regional infrastructure and is considered in the component models of the respective hydrogen demands.

For additional descriptions of hydrogen infrastructure technologies and respective literature references, see subsection 2.3.2.

Electrolyzers

Based on the current trends in PtG projects and the outlook on techno-economic technology parameters, cf. section 2.3.2, electrolyzers (PEMEL) are considered in the scenarios which are connected to the intra-regional hydrogen distribution network (pressure levels around 30 bar). Thus, the electrolyzers can be operated highly flexible. Nevertheless, future studies could include the consideration of HTEL for a less flexible however more efficient hydrogen production. The electrolyzers are modeled as *Conversion* components in *FINE* that convert electricity into hydrogen. The utility water is assumed to be sufficiently available in all regions. No geo-referenced restrictions are considered for the placement of the electrolyzers.

Liquefaction Plants

To convert gaseous hydrogen at 30 bar into liquid hydrogen liquefaction plants for hydrogen are considered in the scenarios and are modeled as a *Conversion* component in *FINE*.

Regasification Plants

Regasification plants are considered to convert liquid hydrogen to pressurized gaseous hydrogen. It is assumed within this thesis that the gaseous hydrogen leaves the evaporator at a pressure of 100 bar and can thus be directly injected into a hydrogen transmission pipeline (pressure levels around 100 bar). The regasification plants are modeled as a *Conversion* component in *FINE*.

Hydrogen Compressor Stations

Hydrogen compressor stations are required at several steps of the hydrogen supply system. The compressors required at storage units are modeled implicitly within the respective *Storage* components. The compressors at fueling stations for hydrogen demands in the mobility sector are considered in the cost for hydrogen distribution within regions. The compressors that are explicitly modeled during optimization are the one that compress hydrogen from a 30 bar level, i.e. after electrolysis, to a pressure level of 100 bar, i.e. for its injection into hydrogen transmission pipelines. The compressors are modeled as a *Conversion* component in *FINE*.

Salt Caverns for Gaseous Hydrogen (GH_2) Storage

Salt caverns are considered as geological hydrogen storage within the scenarios. Here, two classes of salt caverns are considered. On the one hand, in 2017 existing salt cavern locations can be rededicated for hydrogen use. These caverns are modeled with a smaller invest. On the other hand, at eligible locations identified by *Welder et al.* [2], new caverns can be mined. These caverns are modeled with a higher invest which considers the investment for the mining of the caverns. The capacity potentials of the two classes are visualized in Figure 4.27 with the assumption that one cavern can store 212 $GWh_{GH_2,LHV}$ [165].

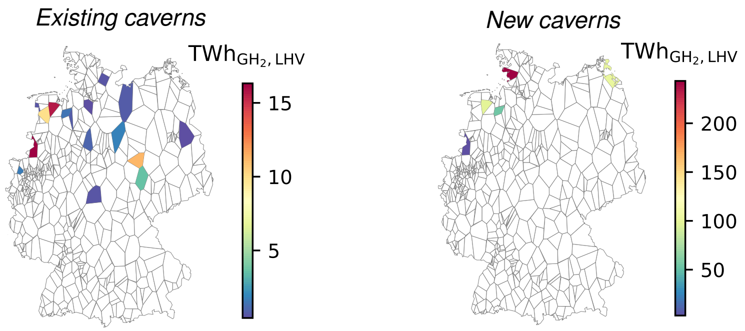

(a) Σ 67 $TWh_{GH_2,LHV}$ **(b)** Σ 504 $TWh_{GH_2,LHV}$

Figure 4.27: Capacity potentials (including cushion gas) for hydrogen filled salt caverns (existing / new). Regions marked in white do not hold any capacities.

The hydrogen filled salt caverns are modeled as *Storage* components in *FINE* which are connected to the hydrogen transmission network. In the scenarios, the salt caverns can also be used to store methane-rich gas. Accordingly, a shared potential constraint is implemented for these component types.

Pipe Systems for Gaseous Hydrogen (GH_2) Storage

Within the scenarios, the hydrogen pipe storage is essentially modeled as an isolated hydrogen pipeline which is connected to the transmission grid with a compressor. The pipe storage system is modeled as a *Storage* component in *FINE*. As local geology restrictions are not considered in the scenarios, due to the considered regions' spatial extents, the pipe storage systems are modeled as having no locational eligibility restrictions.

Cryogenic Tanks for Liquid Hydrogen (LH_2) Storage

Cryogenic tanks for LH_2 storage are modeled as a *Storage* component in *FINE* without locational eligibility restrictions.

Inter-regional Hydrogen Transmission Pipelines

For the transmission of hydrogen between regions, a pipeline system operated on pressure levels between 70 and 100 bar is considered. While the pipeline routes for inter-regional transport are explicitly modeled, the intra-regional transport is considered with to the respective hydrogen demands assigned cost factors, cf. the section on hydrogen distribution within regions.

Within this thesis, an artificial differentiation between the transmission and distribution level is made based on the chosen regional resolution. Inter-regional pipelines are accounted to the transmission level while intra-regional hydrogen supply is accounted to the distribution level. Furthermore, it is assumed that no gas re-compression is required in the transmission and, if existing, in the distribution network.

Potential routes for new pipelines are derived from the study of *Baufumé et al.* [76]. The chosen methodology to aggregate these routes to the respectively considered spatial resolution is, within this thesis, achieved in two steps. First, the centroids of the regions in the scenarios are connected to the candidate grid. Second, if two regions share a candidate line, the shortest path between these two regions alongside the candidate grid is determined. The collectivity of all shortest paths provides the considered eligible routes. These routes are visualized for exemplary, spatially aggregated regions in Figure 4.28.

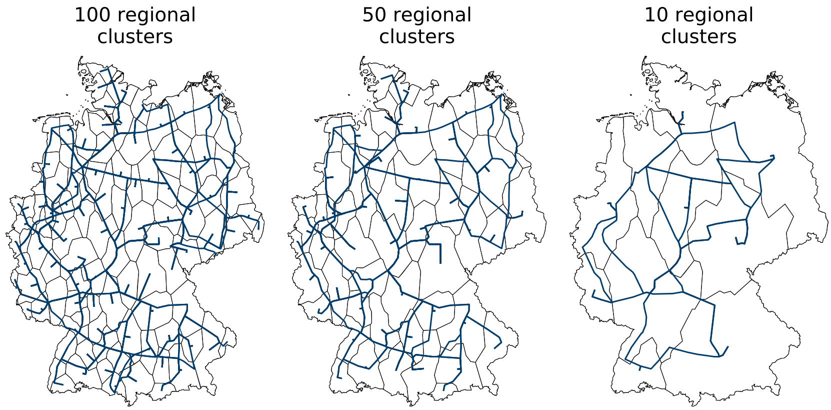

Figure 4.28: Candidate routes (blue) for new inter-regional GH_2 pipelines in the scenarios with centralized hydrogen supply pathways.

To design the pipelines with *FINE*, the flows through the pipelines must be represented as energy flows. This is achieved with a simplified flow model as presented by *Baufumé et al.* [76]. In future work, the methodology presented by *Robinius et al.* [83], to which contributions were made to within the scope of this thesis, could be deployed in the post processing of the optimization. This methodology ensures for tree-shaped network designs a robust, feasible pipeline design under the consideration of pressure losses.

The inter-regional GH_2 pipelines are modeled as a *Transmission* component in *FINE*. The collectivity of all shortest paths provides the eligible connections. The lengths of these connections are considered for the computation of the required investment for the potential new lines. The pipelines can be modeled with binary variables which indicate which connections are built. If a connection is built, its respective binary variable enforces the consideration of a binary cost contribution and a minimum capacity which corresponds to a pipeline diameter of 100 mm. Furthermore, a maximum capacity corresponding to three large-sized pipe diameters of 1,400 mm is considered for each connection.

It must be noted that with this modeling approach, a candidate line can be used by multiple inter-regional connections. These connections are however modeled individually and thus do not have the option to use each other's capacity. The overall pipeline length and required capacity is therefore slightly overestimated. An example to circumvent this effect in future work is to introduce additional, incrementally small regions which model the pipeline junctions. With this approach, it would be possible to avoid the modeling of multiple connections alongside one candidate line.

Hydrogen Distribution within Regions

The assumptions on the hydrogen distribution within regions (intra-regional) are based on results obtained in a study of *Reuß et al.* [80]. For the distribution of hydrogen to fueling stations, GH_2-trucks (trailers with pressurized gas storage in composite vessels) are considered. The identified hydrogen demands in industry are either supplied by pipeline or by GH_2-trucks. Within this thesis, the assumption is made that the trucks are fueled with synthetic, carbon-neutral diesel.

The cost contributions of the required intra-regional infrastructure are summarized in commodity related cost surcharges. These cost surcharges are then considered for the respective hydrogen demands in *FINE* as a commodity cost and are obtained in two steps.

1. The driving distances of the trucks and the total pipeline lengths within each region are estimated based on a formula given by *Yang and Ogden* [175]. This formula was accredited by *Reuß* [153] for the case of national hydrogen supply systems.
2. The regional supply cost contributions are simulated with the methodology and cost parameters used by *Reuß et al.* [80].
    - For the hydrogen demand in the mobility sector, cost contributions for

truck transport and fueling stations are considered. The cost contribution of the truck transport is, inherently, correlated to the spatial extends of the regions. The cost contribution of the fueling stations considers a learning rate and is thus lower for a higher number of fueling stations.

- For the hydrogen demand in the industry sector, only the cost for intra-regional hydrogen transport infrastructure is considered. The least expensive transport mode, either by pipeline or by truck, is in this context determined for each region. For this, the hydrogen demand per consumer is averaged and a minimum pipeline diameter of 100 mm is considered.

Figure 4.29 visualizes the average investment related costs for the intra-regional hydrogen distribution as a function of the spatial resolution. With an increasing

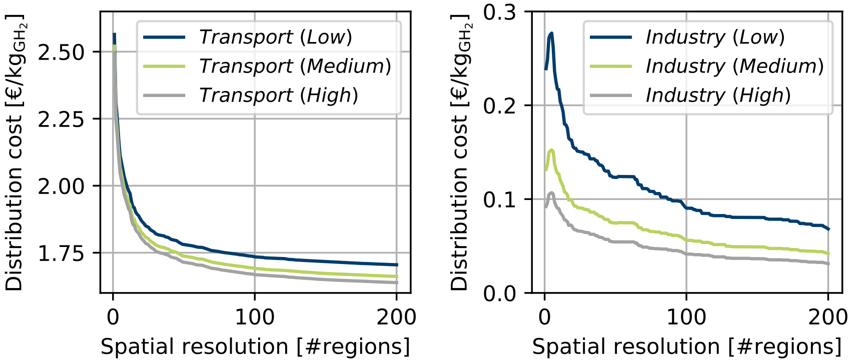

Figure 4.29: Average investment related cost for intra-regional hydrogen distribution as a function of the spatial resolution.

spatial resolution, the costs drop as the intra-regional transport distances are shortened[6]. Oppositely, the cost for the hydrogen transmission infrastructure increases. The decreasing cost for the heuristically modeled distribution thus compensates the increasing cost for the transmission. A geo-referenced visualization of the cost is given for 130 aggregated regions in Figure A.18 in the appendix A.6.

With the presented approach, the required hydrogen supply infrastructure is modeled from production, over storage, transmission and distribution to the end consumer. However, the design of the distribution infrastructure is only heuristically

[6]The initial increase in the cost for industrially used hydrogen results from the demand per customer averaging. This averaging leads to an overestimation of pipeline distribution as the least expensive transport mode.

estimated and does not consider additional energy demands, as for example electricity required for recompression at the fueling stations. Future work could couple *FINE* with existing hydrogen infrastructure simulation models, as presented by *Reuß et al.* [80], or could consider a two-level approach in which *FINE* is once used to model the transmission level and then applied to model the distribution level of each region individually.

4.3.3 Infrastructure for Methane-containing Gases

The scenarios' infrastructure components for methane-containing gases are presented in the following. The infrastructure is subdivided into infrastructure for biogas, which has comparably low methane contents, and methane-rich gas (MRG). MRG is in this context a collective term for natural gas, purified biogas and synthetic methane.

- First, *Conversion* components which produce either biogas or MRG are described. These are
  - biogas plants,
  - biogas purification and grid injection plants which produce MRG from biogas, and
  - methanation plants which produce MRG from hydrogen and carbon dioxide.
- Next, salt caverns and pipe systems for the storage of MRG and double membrane gas storage for raw biogas are described as *Storage* components.
- Lastly, MRG pipelines are considered and introduced as *Transmission* components.

For additional descriptions and literature references of the respective technologies, see subsection 2.3.3.

Biogas Plants

Within this thesis, bio / green waste and liquid manure are considered as residual materials for gaseous biomass production. These potentials need to be spatially distributed for the scenarios investigated within this thesis. They are distributed with simple distribution keys, by using the *Python* packages *geokit* [58] and *glaes* [119], to enforce basic allocation logics. More accurate distribution keys could be applied in future work but are otherwise beyond the scope of this thesis.

- The biogas potential from bio and green waste is distributed based on the population density in Germany in the year 2015 [182]. The resulting spatial distribution of the potential is aggregated to the German federal states and is then compared to literature values on bio / green waste from 2006 and 2017 [180, 181]. The comparison gives a sufficient correlation between the simulated distribution and the literature values. Only the potential of the state of Berlin is notably overestimated. This outlier can be explained by regulations on organic waste bins which were however adapted in Berlin in 2019, cf. [178, 179].
- The biogas potential from manure is distributed based on pasture area given by the *Corine Land Cover* [118]. The distributed data is again aggregated to the German states and then compared with values from literature [116, 180]. Again, the comparison shows a sufficient correlation. Particularly, the study of the *Deutsches Biomasseforschungszentrum* [116] mentions that the largest potentials occur in the north-eastern part of Lower Saxony and the south-eastern part of Bavaria which matches the simulated distribution.

The spatial distributions of the biogas potentials from bio / green waste and manure as well as their summarized potentials are visualized in Figure 4.30.

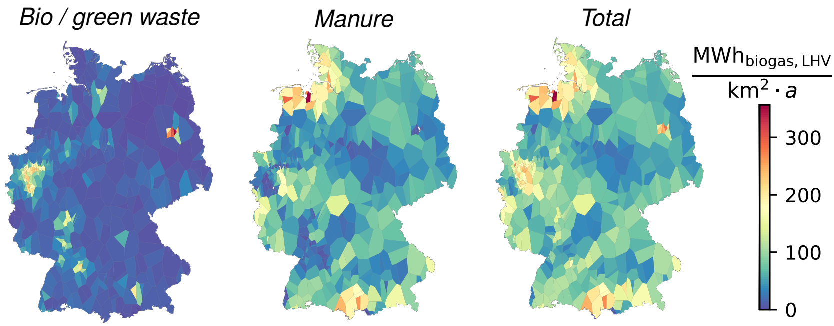

(a) Σ 6 $\mathrm{TWh_{biogas,LHV}/a}$ **(b)** Σ 25 $\mathrm{TWh_{biogas,LHV}/a}$ **(c)** Σ 31 $\mathrm{TWh_{biogas,LHV}/a}$

Figure 4.30: Biogas potentials from bio / green waste and manure.

Biogas plants are modeled as a *Conversion* component in *FINE* which must be operated with a constant operation rate. The determined potentials serve as an upper capacity bound.

Biogas Purification and Grid Injection Plants

To inject biogas into the MRG grid, a purification step is required to increase the methane content and to remove impurities out of the gas. This purification step, alongside with the compression and injection of the gas into the grid, is realized in biogas purification and grid injection plants. Within this thesis, biogas upgrading plants are modeled as *Conversion* components in *FINE*.

Methanation Plants

Methanation plants that convert carbon dioxide, captured from air, and hydrogen into methane are considered within the scenarios. Methanation pathways in energy supply systems have the advantage of using existing natural gas infrastructure at low cost. However, the methane production is associated with comparably high investment cost. Within this thesis, the methanation plants are modeled as *Conversion* components in *FINE*.

Future work could additionally consider carbon dioxide capture from, for example, industry processes or power plants or assume an optional carbon dioxide purchase with a fixed price. As these pathways are however not the focus of this thesis they are not considered further.

Salt Caverns for Methane-rich Gas (MRG) Storage

The storage of methane-rich gases (MRG) in salt caverns is modeled, with respect to its locational eligibility and its techno-economic parameters, similarly to the storage of hydrogen in salt caverns. The total capacity potentials of the caverns are visualized in Figure A.16 in the appendix A.5.

Geological Pore Storage for Methane-rich Gases (MRG)

Within the scenarios, it is assumed that pore storage sites existing in 2016 can be used in 2050 for the storage of methane-rich gases (MRG). The locations of these sites as well as their estimated potential storage capacities[7], cf. the report of underground gas storage in Germany [170], are visualized in Figure 4.31.

The geological pore storage is modeled as a *Storage* component in *FINE*. The capacity potentials presented in Figure 4.31 are set to be fixed values. The actual utilization of this storage type within the scenarios is thus represented by the, during the optimization determined, site specific charging and discharging rates.

[7] Assumed lower heating value: 10 $kWh_{MRG,LHV}/Nm^3$.

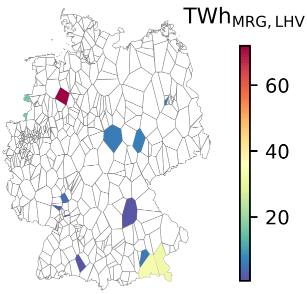

Figure 4.31: Capacity potential (Σ 191 TWh$_{CH_4,LHV}$) of pore storage for methane-rich gases. Regions marked in white do not hold any capacities.

Pipe Systems for Methane-rich Gas (MRG) Storage

Pipe systems are considered as a near-surface storage option for methane-rich gas (MRG). The general concept of the gas storage system is described in section 2.3.3.

In analogy to the hydrogen pipe storage system, the MRG pipe storage system is modeled as an isolated pipeline which is connected to the transmission grid with a compressor station. The pipe storage system is modeled as a *Storage* component in *FINE*. Furthermore, the pipe storage system is modeled without locational eligibility restrictions.

Double Membrane Gas Storage for Raw Biogas

Within this thesis, double membrane gas storage is considered for raw biogas. The double membrane gas storage is modeled as a *Storage* component in *FINE*. No geographical restrictions are considered.

Pipelines for Methane-rich Gas (MRG) Transmission

For the transport of methane-rich gas (MRG), selected routes of the in 2018 existing natural gas pipeline grid are considered, based on the data provided by *Cerniauskas et al.* [85].

It is possible that the determined pipeline capacities will also be used to supply other MRG flows which are not modeled within the scenarios. For example, the scenarios assume a “copper plate” for the natural gas import, supply and export and furthermore do not model all sectors in which a demand for methane-rich gas can arise, e.g. to supply a fuel for heat generation. Thus, the pipeline capacities will have to be shared. To consider this multiple use of the pipelines, it is assumed that the MRG flows within the scenarios can only use a fixed share (default 10%) of the given pipeline capacities.

Furthermore, it must be considered that the existing natural gas pipelines might be reassigned for other applications, e.g. to transport hydrogen. However, this can be investigated with higher informative value when a more complete representation of the energy system is considered. As this is beyond the scope of this thesis, such an investigation is not further pursued but is however of high interest for future work.

The pipelines are modeled as a *Transmission* component in *FINE*. The capacities of the pipelines are assumed to be fixed. Furthermore, the transmission of the gas is assumed to be free of charge as only operational cost arise which are, in comparison to other cost contributions in the supply system, small.

It must be noted that this model of MRG transmission in pipelines is simplistic and could be modeled in greater detail. For example, different pressure levels could be considered, compressor stations modeled, and unidirectional flows considered. This is however beyond the scope of this thesis but could be included in future work. Nevertheless, the simplistic model can give a good first impression of strategies for biogas and synthetic natural gas transmission and is thus included in the scenarios.

4.4 Discussion

The presented scenario setup is assessed in the following with respect to its capabilities. Based on this assessment, the scope of its application is discussed, and potential future work is identified.

With the presented scenario scope, it is possible to design infrastructure systems which are capable of supplying national electricity and hydrogen demands in a future German energy system under the consideration of carbon dioxide reduction targets. Within this scenario scope, Germany is modeled with European and intercontinental energy imports and exports. The scenario scope models the energy supply systems on essential infrastructure levels, covering today's conventional electricity and (natural) gas infrastructure as well as promising future infrastructure with sufficient technology readiness levels.

The scenario scope is hallmarked by its regionally resolved data base. This data base is built upon in literature available data and simulation models. It benefits in this context from the availability of open-data and open-source code provided by the research community and the German state and industry. Particularly the electricity generation from wind turbines and PV panels, key technologies to the German *Energiewende* (energy transition), can thus be considered in high spatial but also temporal resolution. Also, the electric and gas transmission grids are displayed in high spatial detail and geological storage as well as the location of today's power plants are considered on a geo-referenced level. All technologies are assessed in technical detail and associated with techno-economic parameters.

Combined with the modeling framework *FINE*, the scenario scope thus enables the assessment of the considered infrastructure levels in future German energy systems. With respect to the national carbon dioxide reduction targets, the structural changes required to meet them and the ageing of today's infrastructure, such infrastructure assessments are a matter of urgency.

Particularly, the spatially and temporally resolved data base of the scenario scope enables the assessment of energy transmission and storage infrastructure as spatial and temporal balancing options. Spatial discrepancies between energy supply and demand suggest a detailed consideration of spatial balancing options. The identified daily, seasonal and annual patterns within the electricity supply and demand suggest the investigation of balancing options in different temporal regimes. Moreover, the considered commodity conversion technologies enable the modeling of sector-coupling pathways.

Future work could expand the considered scenario scope on several levels.

- More detailed models on energy import and export can be connected and iterated with the modeled scenarios.
- Additional sectoral energy and commodity demands, as for example for heat, should be integrated. The considered electricity demand should be modeled in higher spatial detail. These demands can be added or updated with bottom-up or a top-down modeling approaches. For the latter, a one-node energy system model can be used to generate demand profiles which are then assigned with distribution keys to the considered regions.
- Infrastructure components can be added or modeled in higher technical detail. For example, they could be modeled with nonlinear cost functions and additional operational constraints. Models with higher physical and spatial detail can be applied in the post-processing of the optimization to model / improve the design and operation of the pipeline networks and the electricity transmission grid.
- As already mentioned in section 3.4, pathways which model the energy system transformation from today up until 2050 should be assessed.

In general, it is noted that the presented scenarios are projections into the future and are thus subject to uncertainty. Changes in demography, disruptive events / technologies, policy interventions and per se inherent uncertainties, as for example weather and demand patterns, can and will lead to deviations between actually chosen pathways and the modeled scenarios. Nevertheless, the scenarios provide techno-economic insights into future energy supply systems for Germany and can thus recommend technology pathways and support policy-making.

4.5 Summary

In this chapter the scenario scope investigated within this thesis, named *FINE-CROSSING*, was described. The scenario scope focuses on the modeling of coupled electricity, hydrogen and methane-rich gas infrastructure in a German energy system in the year 2050. The scenario is modeled in such a way that it is compatible with the in chapter 3 presented spatio-temporal energy system modeling mimic.

In section 4.1, the chosen spatial and temporal context of the scenarios was described. The considered regions in Germany are defined based on the structure of the electric grid. An hourly resolution is considered for the temporal context and, if required, typical days are considered together with a seasonal storage formulation. This spatial and temporal context is considered for the spatial and temporal data aggregation, cf. sections 3.1.1 and 3.1.2, of the scenarios' components.

The basic energy and mass flows across the virtual system boundaries of the modeled scenarios were presented in section 4.2. These flows comprise the final energy demands, energy imports and exports as well as carbon dioxide restrictions. As final energy demands, a final electricity demand as well as hydrogen demands in the transport and industry sector are taken into account. For energy imports and exports, European electricity imports and exports as well as intercontinental natural gas and liquid hydrogen imports are considered. The carbon dioxide reduction target of a scenario is set in reference to the 1990's emissions caused by electricity generation. This target is varied between $80-100\%$ of this value. These energy and mass flows are modeled as *Source* and *Sink* components in *FINE*.

A detailed account of all considered infrastructure levels was given in section 4.3. In subsection 4.3.1, the components of the electricity infrastructure were presented. Technologies for the processing of gaseous and liquid hydrogen were described in subsection 4.3.2. The infrastructure for methane containing gases, namely natural gas, biogas and synthetic methane, was presented in subsection 4.3.3.

The infrastructure components are modeled as *Source*, *Conversion*, *Storage* and *Transmission* components in *FINE*. Tables A.1-A.17 in the appendix A give an overview of the components modeling parameters.

In section 4.4, the presented scenario scope was assessed with respect to its capabilities, the potential scope of its application and possible expansions / adaptions of it in future work. The regionally resolved database which the scenario scope provides as well as the capability to model transmission, storage and, in general, sector coupling infrastructure was highlighted.

Chapter 5

Optimized Cross-linked Infrastructure Scenarios for Germany

Three scenario branches for investigating cross-linked infrastructure in a future German energy system are presented within this chapter. The three scenario branches are visualized in Figure 5.1.

- The scenarios within the *BELS* (Basic ELectricity Supply) scenario branch assess basic electricity supply systems without exogenously given hydrogen demands and without a centralized hydrogen infrastructure.
- The scenarios within the *BELS*$^+$ (Basic ELectricity Supply$^+$) scenario branch additionally consider a centralized hydrogen infrastructure.
- The scenarios within the *BLHYS* (Basic eLectricity and HYdrogen Supply) branch additionally consider hydrogen demands in the mobility and industry sector. Here, low, medium and high hydrogen demand scenarios are investigated.

Thus, the second and third scenario branch extend the scope of its respective predecessor. As the first and second scenario branch supply the same final energy demand, they can be compared intuitively with respect to cost, design and operation of the optimized supply systems. The second and third scenario branch are more challenging to compare as the third scenario branch considers an exogenously given, additional final energy demand in the transport and industry sector in form of hydrogen. Naturally, the latter requires additional energy sources and infrastructure and is thus more expensive. However, it also decarbonizes a wider scope of the energy system.

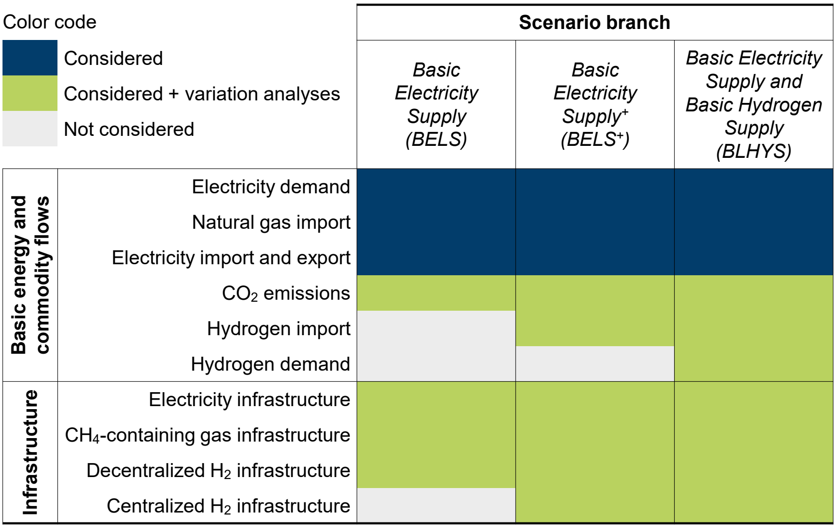

Figure 5.1: Definition of the three main scenario branches.

For each of these scenario branches, optimal energy supply systems are determined by applying the modeling framework *FINE*. Based on the outcome of a spatio-temporal sensitivity analysis, the supply systems are modeled with 75 regions and 30 typical days in a linear program. These settings provide a sufficient trade-off between regional and temporal accuracy and manageable run times[1].

In addition to comparing the scenario branches with respect to cost, design and operation of the optimized supply systems, the long-run marginal costs (LRMCs) for the electricity and, if applicable, hydrogen supply are assessed. These are available with a spatial and temporal resolution and are an output of the optimization. In a figurative sense, these long-run marginal costs represent how much it would cost to supply an additional energy unit within a specific region at a given time step. In this chapter, the LRMCs will be used to serve as an indicator for specific system behavior on the one hand and to qualitatively compare different scenarios with each other on the other hand. Specific conclusions on the electricity market design which might arise from these LRMCs, or marginal cost in general, are not drawn as this field of application is beyond the scope of this thesis but might be of interest in future work.

All scenario branches are presented with the same scheme. First, the optimal

[1] On *Intel® Xeon® Gold 6144* processors, these are, on average, less than a day.

system configurations of the respective reference scenarios in the scenario branches are introduced in an aggregated form for varying carbon dioxide restrictions. Then, a selection of these reference scenarios is visualized and discussed with spatial and temporal detail. Finally, scenario variations, in which certain components are excluded or included to the reference scenarios, are presented. These scenario variations highlight the value of the respectively excluded or included components and are an approach to mimic a simplified sensitivity analysis in the computationally expensive scenario calculations.

SCENARIO VARIATIONS:
To investigate the robustness of the results, a large number of scenario variations / sensitivity analyses can be conducted. However, these are computationally expensive and, with the high number of possible parameter variations, can quickly become convoluted and incomprehensive. Thus, only a selection of scenario variations is presented within this thesis. These are chosen with the intent to foster the understanding of the value of specific infrastructure components.

It is important to keep in mind that the conclusions that can be drawn from these variations are specifically valid for the considered scenario scope. A different scenario scope may reveal different conclusions. Nevertheless, the conclusions which can be drawn from the presented scenario variations can be used as benchmarks which can either confirm assessments from other studies or can be rebutted with well-founded reasons.

The presentation of the cross-linked infrastructure scenarios for Germany is structures as follows. In section 5.1 the scenario results of the *BELS* scenario branch are presented. Consecutively, the *BELS*$^{+}$ and *BLHYS* scenario branch are presented in section 5.2 and section 5.3. The results are compared to literature in subsection 5.4.5. A discussion of the results is already provide alongside the results presentation. However, a concluding discussion is provided in section 5.4. The chapter is summarized in section 5.5.

5.1 *BELS* - Basic ELectricity Supply Scenarios

Within this section, first, the optimal system configurations of the *BELS* reference scenario under varying carbon dioxide reduction targets (80%, 85%, 90%, 95%, and 100%) are presented and compared with each other in subsection 5.1.1. Next, the resulting optimal electricity supply systems for the 80% and 100% reduction target are presented and discussed in detail in sections 5.1.2 and 5.1.3.

Scenario variations of the reference scenario are presented and shortly discussed in subsection 5.1.4.

5.1.1 Optimal System Configurations under Varying CO_2 Reduction Targets

The total annual cost (TAC) of the *BELS* reference scenario under varying carbon dioxide reduction targets, the avoided emissions (in reference to the year 1990) as well as the installed capacities of commodity generating and converting technologies are visualized in Figure 5.2. Additional figures for primary energy sources, general electricity generation and consumption and dispatchable electricity generation are given in the appendix B.1, Figures B.1 – B.4.

The main cost contributions in the 80% CO_2 reduction scenario arise from offshore wind turbines (fixed foundation), onshore wind turbines (*Class I*), open-field PV systems (fixed tilt), gas power plants with open and combined cycle gas turbines, as well as from electricity and natural gas import. The 100% CO_2 reduction scenario inherently excludes natural gas imports and is furthermore characterized by a larger technology portfolio, additionally including onshore wind turbines of *Class II*, rooftop PV (southwards- and eastwards-facing), wood-fired CHPs, biogas plants, electrolyzers, methanation plants, lithium-ion batteries and DC line expansions.

In general, it can be noted that with stricter reduction targets, the amount of imported natural gas and the capacities of power plants operated on methane-rich gas (MRG) are reduced while increasing capacities of renewable energies and infrastructure for spatial and temporal energy balancing are built. In the following, the selection of different components is summarized with respect to increasing carbon dioxide reductions. The optimal system configurations for storage and transmission components will be presented afterwards in more detail.

- Offshore wind turbines with a fixed foundation (*Wind offshore (fixed)*) are selected over the ones with a floating foundation (*Wind offshore (float)*). The ones with a floating foundation are selected once the maximum capacity potential of the ones with a fixed foundation is reached.
- Onshore wind turbines are preferably chosen from *Class I*. Only for the 100% reduction target, turbines of *Class II* appear in the optimal design configuration in larger amounts, even though the turbines in *Class I* are not fully installed. This suggests congestions in the electric grid in the respective supply system.
- Run-of-river power plants (*R-o-r plants*) are modeled with a fixed capacity and are thus installed with the same capacity in all scenarios.

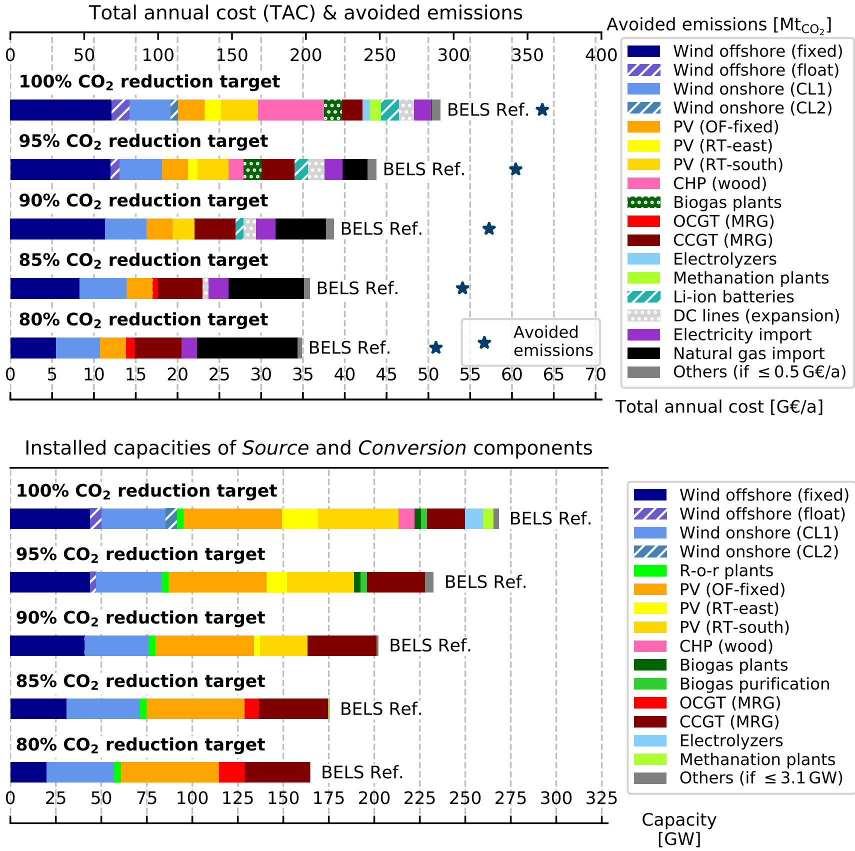

Figure 5.2: Total annual cost, avoided emissions and installed capacities of *Source* and *Conversion* components in the *BELS* reference scenario under varying CO_2 restrictions.

- The PV open-field systems provide an electricity generation profile which partly correlates with electricity demand and the capacity dependent investment for the systems is small. These two factors lead to an overall small levelized cost of electricity of the PV systems. Thus, the available PV open-field potential is maxed out in all scenarios (54 GW_p). The less expensive systems with a fixed tilt (*PV (OF-fixed)*) are in all cases preferred over the ones with a tracking system.

- Increasing shares of rooftop PV are built, preferably southwards-facing ones (*PV (RT-south)*), followed by eastwards-facing ones (*PV (RT-east)*).

- Electricity generation from biomass (biogas and wood) is only chosen in larger quantities for reduction targets of 95% and 100%. In these scenarios, biogas is primarily purified and injected into the gas grid where it is later fed to centralized gas power plants.
- Open cycle gas turbine plants (*OCGT (MRG)*), which are in comparison to combined cycle gas turbine plants (*CCGT (MRG)*) less investment-intensive but also less efficient, are selected for reduction targets of 80% and 85% only. For all reduction targets, power plants with combined cycle gas turbines are considered, however in decreasing amounts. For the less strict reduction targets, these gas turbine plants are operated on natural gas only. For stricter reduction targets, they are also operated on purified biogas and, for the 100% reduction target, also on synthetic methane from the *Power-to-Hydrogen-to-Methane* pathway.
- For a 100% reduction target, a *Power-to-Hydrogen-to-Methane-to-Power* pathway is chosen during optimization by considering electrolyzers and methanation plants in the supply system.
- The cost share of lithium-ion batteries notably increases from about 0% to 4% between the 80% and 100% reduction target.
- DC line expansions are considered starting from the 85% reduction target. The cost contribution increases until the 95% reduction target. A slight decrease is recorded for the 100% reduction target. The decrease is correlated with the consideration of the *Power-to-Hydrogen-to-Methane* pathway which serves, together with the considered gas grid, as an alternative spatial balancing option.

The secured electricity generation capacities of the scenario configurations are visualized in Figure 5.3.

For the 80% reduction target, mainly natural gas operated thermal power plants and PHES constitute the secured generation capacities. Starting from the 90% reduction target, more than half of the secured generation capacities are provided by lithium-ion batteries. Moreover, with stricter reduction targets, the thermal power plants are supplied with increasing amounts of purified biogas or synthetic methane. In comparison to the in 2017 existing secured generation capacities, primarily constituted of fossil power plants, the structure of the secured supply capacities is transformed towards a secure supply from renewable energy sources via storage technologies. The peak in the exogenously given *basic* electricity demand is reached in winter and equals about 83 GW_{el}. Thus, hypothetically, a secure electricity supply cannot be guaranteed for the 80% and 85% reduction target. The integration of a constraint into the modeling framework *FINE* which guarantees a secured electricity generation capacity can be considered in future work.

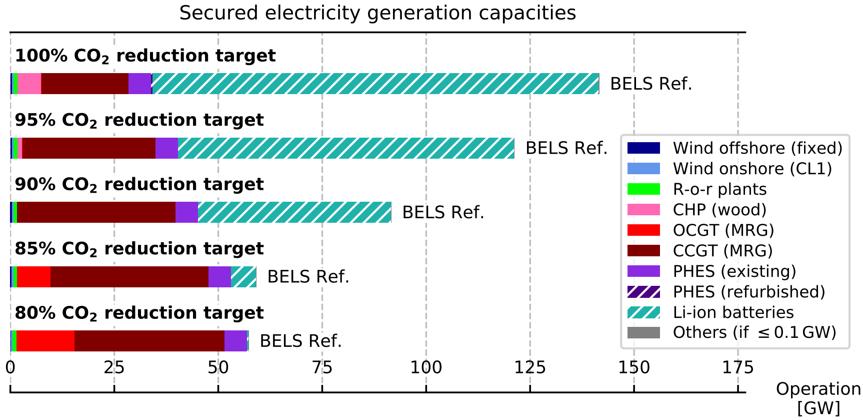

Figure 5.3: Secured electricity generation supply capacities in the *BELS* reference scenario under varying carbon dioxide reduction targets.

Concerning storage and transmissions technologies, only lithium-ion batteries and DC line expansions have notable cost shares in the TAC. However, the system design and operation are also constituted of several other essential storage and transmission technologies.

The capacities of the installed *Storage* components are visualized in Figure 5.4, once for all *Storage* components and once for non-geological *Storage*.

As pore storage is modeled with a fixed capacity of several hundred $TWh_{MRG,LHV}$, it is excluded from the bar plot for improved visibility. Overall, the required storage capacities increase steeply with stricter reduction targets.

- Pumped hydro energy storage which is assumed to not require major refurbishment (*PHES (existing)*) is modeled with a fixed capacity and is invariant to the varying carbon dioxide restrictions.
- Refurbished PHES is only considered for the 100% reduction target.
- The installed lithium-ion battery capacities increase significantly with stricter reduction targets.
- A small number of about five to nine pipe systems for methane-rich gas is built in a remote region in northern *Franconia* / southern *Thuringia*. The systems are not connected to the considered gas grid and thus do not have access to geological storage. These pipe systems are filled with purified biogas which is then fed to CCGT plants in the region.
- The role of low-cost geological storage for high carbon dioxide reduction

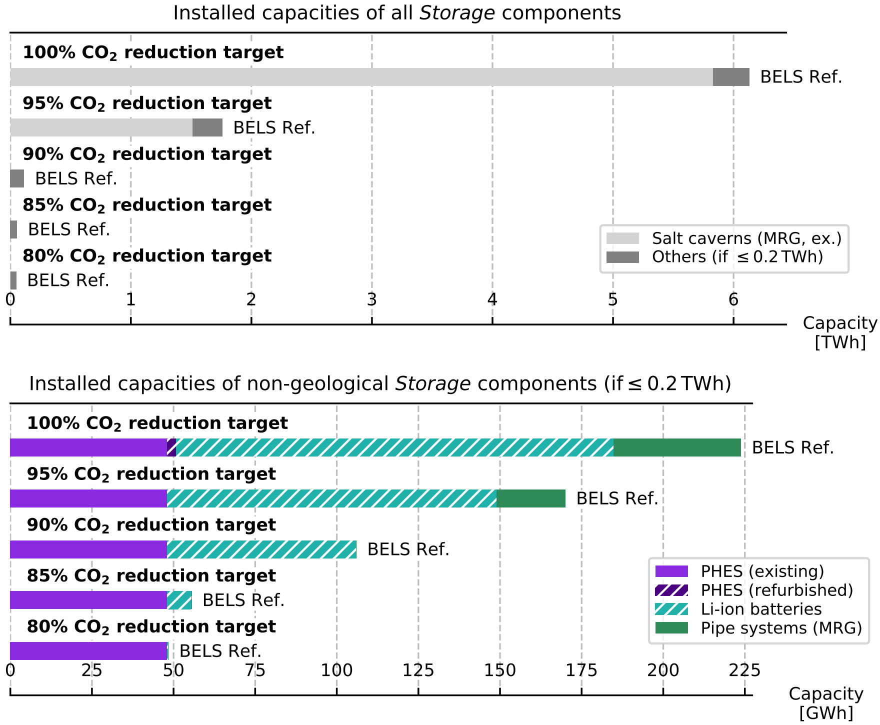

Figure 5.4: Storage design in the *BELS* reference scenario under varying carbon dioxide reduction targets (pore storage excluded).

targets becomes apparent in the optimal design of the MRG-filled salt caverns, which are built at in 2017 existing salt cavern locations (*Salt caverns (MRG, ex.)*), and the operation of the considered pore storage. The installed capacities of the salt caverns and the operation of the pore storage (not visualized) increase steeply for the 95% and 100% reduction target. In the latter, not only purified biogas but also methane produced via the *Power-to-Hydrogen-to-Methane* pathway is stored in geological storage.

For *Transmission* components, the annual commodity exchange between regions is visualized for the different reduction targets in Figure 5.5[2]. In general, it can be noted that the utilization and the number of considered transmission technologies increases with stricter reduction targets.

[2] These values do not consider intra-regional commodity transmission.

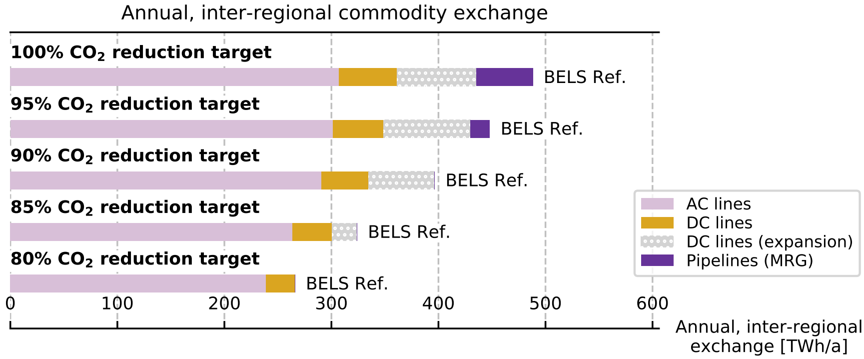

Figure 5.5: Transported commodities in the *BELS* reference scenario under varying carbon dioxide reduction targets.

- The utilization of the considered AC and DC lines, which are modeled with a fixed capacity, increases, indicating increasing spatial mismatches in the electricity generation and demand.
- Starting from the 85% reduction target, DC line expansions are built in increasing quantity. However, the utilization decreases for the 100% reduction target. There, the *Power-to-Hydrogen-to-Methane* pathway provides additional MRG which can be transported in pipelines and thus serves as an additional spatial balancing option.
- The transmission of methane-rich gas, stemming from biogas purification and methanation, becomes prominent for the 95% and 100% reduction target.

It can be summarized that with stricter carbon dioxide reduction targets the technology portfolio becomes more divers and supply pathways for renewable energy sources are built in larger quantities.

5.1.2 Supply System Assessment (80% CO_2 Reduction)

Within this section, the optimal supply system for the *BELS* scenario with an 80% carbon dioxide reduction target (*BELS*-80%) is assessed in techno-economic detail. Table 5.1 presents the installed capacities, TAC contributions and operation characteristics (annual operation, full load hours (FLHs) / turn-over count (TOC)) of the components considered in the optimal supply system.

Table 5.1: Techno-economic parameter overview (*BELS*-80%).

	Capacity	TAC [M€/a]	Operation [TWh/a]	FLHs or TOC [h/a] or [-]
Wind offshore (fixed)	20 GW_{el}	5492	97 (0.9)	4754
Wind onshore (CL1)	37 GW_{el}	5255	88 (0.1)	2356
R-o-r plants	3.8 GW_{el}	451	17.4 (0.0)	4558
PV (OF-fixed)	54 GW_{el}	3136	66 (0.2)	1206
OCGT (MRG)	14 GW_{el}	959	20	1420
CCGT (MRG)	36 GW_{el}	5657	201	5664
PHES (existing)	48 GWh_{el}	76	5.3 | 4.1	96
Li-ion batteries	0.41 GWh_{el}	7.1	0.2 | 0.2	517
AC lines	-	0	238.6	-
DC lines	-	0	27.4	-
Electricity export	-	-0.78	0.8	-
Electricity import	-	1820	40	-
Natural gas import	-	12018	364	-
Electricity demand	-	0	528	-

TAC: Total annual cost. Operation: for *Source* components, if existing, curtailment is listed in parentheses; for *Storage* components: charging | discharging; for *Transmission* components: inter-regional transmission. FLHs or TOC: Full load hours of *Source* and *Conversion* components; turn-over count of *Storage* components.

The values presented in the table will be revisited and discussed with a focus on electricity generation, storage and transmission in the following. Final remarks on the long-run marginal costs of the supply system conclude this section.

Electricity Generation

To put the installed electricity generation capacities into context, they are compared to the electricity generation capacities existing in 2017 in Germany, with data obtained from the *Bundesnetzagentur* (*Federal Network Agency*) [101, 108].

- The capacity of open-field PV systems is quintupled ($11\,GW_p^{2017} \rightarrow 54\,GW_p$).
- Run-of-river plants are installed with a fixed capacity of $3.8\,GW_{el}$[3].
- The capacity of offshore wind turbines is quadrupled ($5.4\,GW_{el}^{2017} \rightarrow 20\,GW_{el}$) and their average full load hours are increased ($3200\,h/a \rightarrow 4750\,h/a$).
- The capacity of onshore wind turbines is below the one installed in 2017 ($50\,GW_{el}^{2017} \rightarrow 37\,GW_{el}$). However, and as for the offshore wind turbines, the average full load hours are significantly increased ($1700\,h/a \rightarrow 2350\,h/a$). The

[3] The run-of-river modeling is based on the work of *Syranidis* [114] who based the run-of-river capacities of Germany on ENTSO-E data [113] from 2015.

increase in the full load hours of the onshore wind turbines is rooted in the future turbine design considered by *Ryberg et al.* [102] and the cost-optimal placement of the wind turbines.

- Moreover, no photovoltaic rooftop systems are installed for the 80% reduction target. This modeling result must be put into a critical perspective. For the given boundary conditions, the PV rooftop systems are not cost-optimal, and PV open-field systems are preferably built. However, as the energy system is not modeled completely (additional energy demands, transition pathways as well as policy and market frameworks are not considered), PV rooftop systems can appear in different scenario settings.
- The centralized gas power plant fleet changes significantly in comparison to the year 2017. As described in section 2.3.1, nuclear and coal power plants are phased out and are thus excluded from the scenario scope. Therefore, they do not appear in the optimal system design. The installed capacity of gas power plants on the other hand increases significantly ($26\,GW_{el}^{2017}$ [101, 130] $\rightarrow 50\,GW_{el}$).
- Biogas is not part of the optimal design solution. Moreover, none of the available CHP technologies (wood / biogas / $GH_{2,\,30\,bar}$) are considered. As for the PV rooftop systems, this result must be critically assessed. Again, the utilization of biogas and the mentioned CHP technologies is not cost-optimal within the investigated scenario scope. However, with an extension of the scenario scope which considers, for example, heat demands or production pathways for bio-fuels, these components can become part of optimal supply pathways.

Overall, a comparably small share of the renewable electricity generation is curtailed.

The optimal regional distribution of the electricity generation capacities is visualized in Figure 5.7. Gas power plants are placed close to electricity load centers / regions, cf. Figure 4.2. Offshore turbines are inherently built in the north of Germany. For the two regions which are connected by DC lines to the south of Germany, offshore capacities of several gigawatts are considered. Onshore turbines and open-field PV systems are considered in multiple regions. The latter dominate the electricity generation in several regions in the east of Germany. The placement of the wind turbines deviates from the wind turbine placements in 2017, cf. [101]. Notable is here that less wind turbines are placed in the northeast of Germany and more turbines are placed in the west and south of Germany. Overall, the placement and structure of the renewable electricity sources deviates from the 2017 system. On the one hand, this is caused by changes in the techno-economic parameters of the technologies. On the other hand, this is also caused by the techno-economic optimality focus of the supply systems which does not take market mechanisms into account.

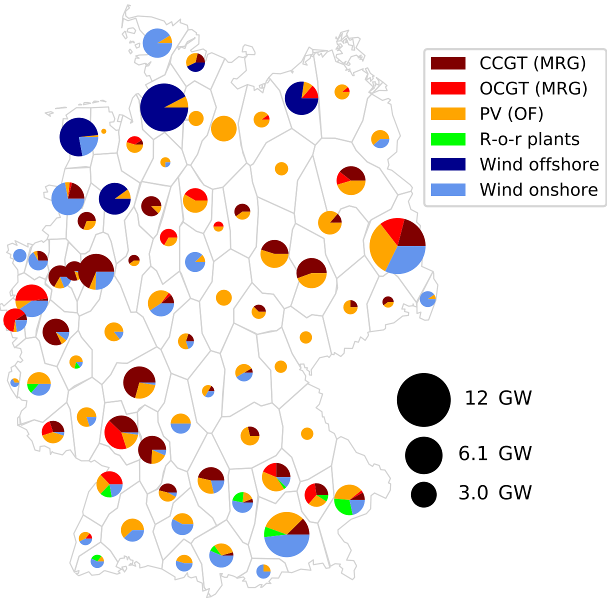

Figure 5.7: Regional distribution of electricity generation capacities (*BELS*-80%).

The gas power plants are flexibly operated to provide electricity when electricity generation from renewable energies, locally or supra-regionally, is not sufficiently available, cf. Figure 5.6.

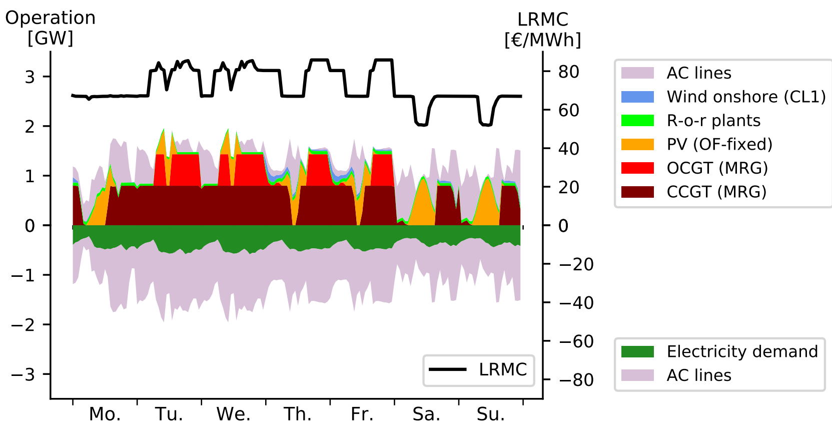

Figure 5.6: Regional electricity sources and sinks (*BELS*-80%, 10th calendar week, Bavaria).

The figure shows electricity sources and sinks for a region in Bavaria, north of Munich, in the 36th calendar week. The nodal long-run marginal cost (LRMC) is visualized as well. A low LRMC correlates with time steps in which the sum of local renewable generation and incoming transmission is sufficient to cover the electricity demand and outgoing electricity transmission. At higher LRMC, CCGT and OCGT are additionally operated. The less investment-intensive but also less efficient OCGT turbines are used to provide electricity when the LRMC reaches its highest values.

Electricity Transmission and Storage

The capacities and utilization of the AC and DC lines is visualized in Figure 5.8.

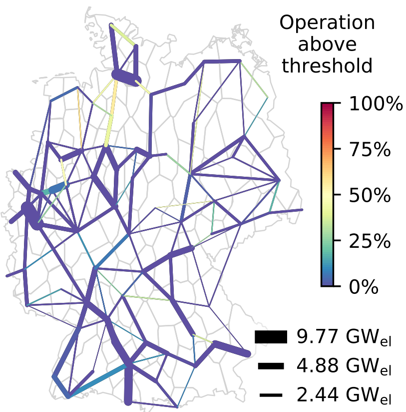

(a) AC lines

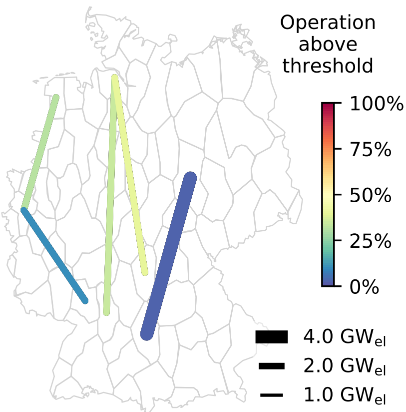

(b) DC lines

Figure 5.8: Operation of AC / DC lines above 80% of their capacity (*BELS*-80%).

The utilization is given in form of the annual operation of a line above 80% of its considered capacity[4]. The figure thus highlights lines which are frequently operated close to their defined maximum transmission potential. When additionally considering Figure 5.6, it is apparent that the integration of the installed offshore capacities leads to stress on selective electric DC lines. Particularly, the DC lines which connect *Schleswig-Holstein* with *Baden-Württemberg* and *Bavaria*, but also the DC lines connecting *Lower Saxony* with *North Rhine-Westphalia* and *North Rhine-Westphalia* with *Baden-Württemberg* appear beneficial to the electricity

[4] I.e. the nominal capacity for DC lines and the nominal capacity times 70% for AC lines.

supply system. However, the DC line between *Saxony-Anhalt* and *Bavaria* seems to be oversized for the considered supply scenario. Higher stress levels can also be found for AC lines which were candidates for congested lines in 2017 and 2018, cf. the quarterly reports on network and system security from the *Bundesnetzagentur* (*Federal Network Agency*) [137, 138]. However, as the here presented electricity supply scenario diverges from these historical system states, they are not straightforward to compare.

The installed storage capacities and the annual charging operation of these storage capacities are visualized in Figure 5.9.

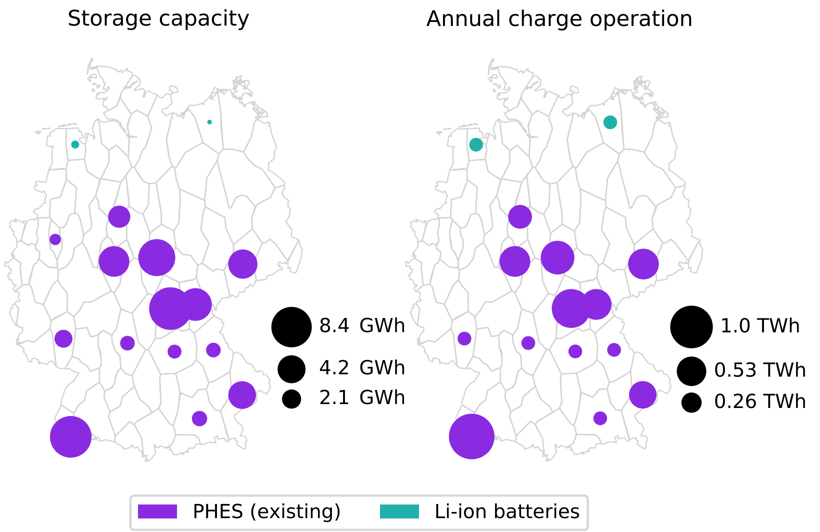

Figure 5.9: Capacities and charging operation of electricity storage (*BELS*-80%).

As the considered PHES is mostly located in the middle and south of Germany, lithium-ion batteries ($\Sigma\, 0.41\, GWh_{el}$) are positioned in the north of Germany for temporal balancing. The ratio between the charging operation and the storage capacities indicates in which operation mode the technologies are used. Table 5.1 gives the average turn-over count (TOC)[5] for the technologies. The average TOC of 517 indicates that the lithium-ion batteries are operated as daily / half-daily electricity balancing options. Moreover, from the TOC, it can be deducted that the operation of the batteries is limited by their cyclic life time (TOC = 12,000/22·0.95).

[5]Sum of the annually charged energy in a storage, if applicable multiplied with the charging efficiency of the storage, divided by the capacity of the storage.

With an average TOC of 96, the PHES seems to be operated as a daily / inter-daily storage option. These assumptions can be confirmed when the operation profiles of the storage technologies are investigated in more detail.

An exemplary profile of a PHES is given in Figure 5.10. While the PHES operates as a daily storage in winter, it is operated as an inter-daily storage during summer in this scenario.

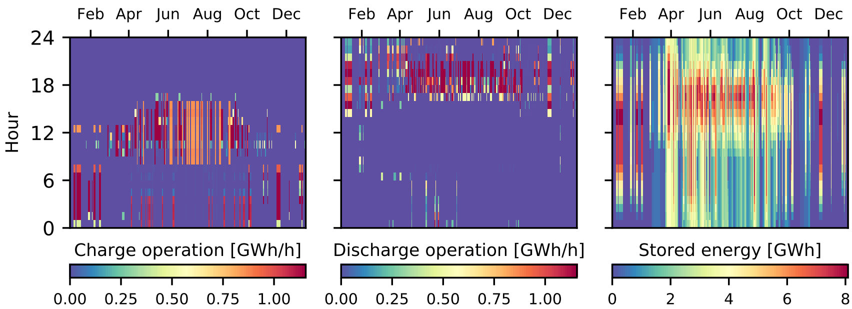

Figure 5.10: Exemplary annual PHES operation (*BELS*-80%).

Long-run Marginal Costs (LRMCs)

The long-run marginal costs for the electricity supply are presented and discussed in more detail to provide additional insights into the supply system behavior and to give an indicator for the cost of electricity supply.

An annual average[6] of 77 €/MWh$_{el}$ is obtained for the long-run marginal cost of the electricity supply for the 80% reduction target. It must be noted that these cost are not equivalent to the average levelized cost of electricity in the system (here 66 €/MWh$_{el}$), but rather represent what, on average and under the assumption of a perfect market, the next unit of electricity would cost.

The regional yearly averages (non-weighted) and duration curves of the long-run marginal costs (LRMC) are visualized in Figure 5.11. With the AC and DC lines being partially congested, regional differences in the LRMC arise. Regions in the north of Germany which have access to low-cost wind electricity display comparably low LRMCs. The most northern region is connected to *Norway*, which provides electricity to Germany at low cost, and displays the lowest LRMCs. The duration

[6] (Σ Regional LRMC profiles $\cdot$ electricity demand) / (Σ electricity demand).

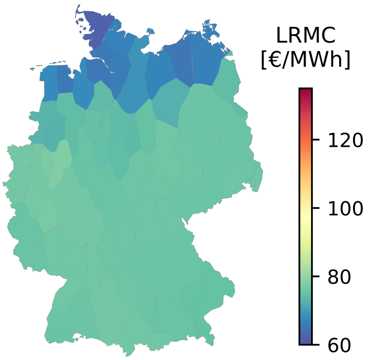

(a) Spatial distribution

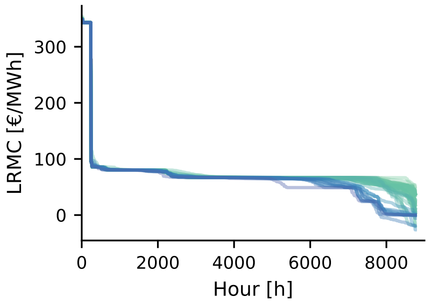

(b) Regional duration curves

Figure 5.11: Yearly average and duration curves of the nodal, long-run marginal costs (*BELS*-80%).

curves of the nodal LRMC indicate for a few number of regions and a small number of times steps, LRMC of about 0 €/MWh$_{el}$. This indicates a rather small amount of surplus electricity / curtailment.

5.1.3 Supply System Assessment (100% CO_2 Reduction)

The techno-economic parameter overview for the *BELS* reference scenario with a 100% reduction target is given in Table 5.2.

In comparison to the *BELS* reference scenario with the 80% reduction target, the considered technology portfolio is more diverse and shifted towards supplying renewable energy only. Of particular interest is in this context the *Power-to-Hydrogen-to-Methane* pathway which is only considered for the 100% reduction target. The parameters of the table will be revisited within this section with a focus on comparing the optimal system design and operation to the one of the 80% reduction target.

Electricity Generation

In comparison to the *BELS* reference scenario with the 80% reduction target, a number of alternative renewable energies are considered for the optimal system design. The renewable energies already considered for the 80% target are, if

Table 5.2: Techno-economic parameter overview (*BELS*-100%).

	Capacity	TAC [M€/a]	Operation [TWh/a]	FLHs or TOC [h/a] or [-]
Wind offshore (fixed)	44 GW_{el}	12111	211 (3.1)	4759
Wind offshore (float)	6.3 GW_{el}	2153	33 (0.1)	5222
Wind onshore (CL1)	35 GW_{el}	4925	80 (0.5)	2285
Wind onshore (CL2)	6.2 GW_{el}	910	9.6 (0.0)	1560
R-o-r plants	3.8 GW_{el}	430	13.2 (4.2)	3462
PV (OF-fixed)	54 GW_{el}	3136	65 (0.9)	1193
PV (RT-east)	20 GW_{el}	2000	22 (0.2)	1107
PV (RT-south)	44 GW_{el}	4432	52 (0.9)	1171
PV (RT-west)	2.8 GW_{el}	284	3.2 (0.0)	1141
CHP (wood)	8.8 GW_{el}	7858	38	4303
Biogas plants	3.5 GW_{biogas}	2164	31	8760
Biogas purification	3.5 GW_{MRG}	172	31	8715
CCGT (MRG)	21 GW_{el}	2448	34	1572
Electrolyzers	9.9 GW_{el}	885	41	4117
Methanation plants	5.5 GW_{MRG}	1332	23	4118
PHES (existing)	48 GWh_{el}	76	9.7 | 7.6	176
PHES (refurbished)	2.8 GWh_{el}	35	0.5 | 0.4	171
Li-ion batteries	134 GWh_{el}	2174	46.3 | 41.1	328
Pipe systems (MRG)	39 GWh_{MRG}	8.9	0.3 | 0.3	11
Pore storage (MRG)	191 TWh_{MRG}	21	20.8 | 20.8	0.24
Salt caverns (MRG, new)	75 GWh_{MRG}	0.57	0.5 | 0.5	9.3
Salt caverns (MRG, ex.)	5.8 TWh_{MRG}	19	24.5 | 24.5	5.9
AC lines	-	0	307	-
DC lines	-	0	54.3	-
DC lines (expansion)	-	1759	73.9	-
Pipelines (MRG)	-	49	53	-
Electricity export	-	-20.24	20	-
Electricity import	-	2086	42	-
Electricity demand	-	0	528	-

Capacity: If applicable, w.r.t the lower heating value (LHV). TAC: Total annual cost. Operation: If existing, curtailment is listed in parentheses; for *Storage* components, charging and discharging operation are listed. FLHs or TOC: Full load hours of *Source* and *Conversion* components; turn-over count of *Storage* components.

possible, built to a larger extend. Logically, and as no carbon dioxide sinks are considered, the amount of imported natural gas is decreased to zero.

- The capacity of installed offshore wind turbines increases between the 80% and the 100% reduction target by a factor of about 2.5 (20 GW_{el} $\rightarrow$ 50 GW_{el}). Now, also offshore wind turbines with a floating foundation are considered.
- The capacity installation of onshore wind turbines increases between the 80% and the 100% reduction target from 37 GW_{el} to 41 GW_{el}. Here, not only

onshore turbines from *Class I* but also from *Class II* are considered.

- In contrast to the scenario with the 80% reduction target, photovoltaic rooftop systems are a part of the optimal design solution and a total of 67 GW_p is built (2017: 31 GW_p, 42 GW_p when PV open-field systems are included, [101, 108]).

- Only CCGT plants are considered in the centralized gas power plant fleet. These are operated on purified biogas and synthetic methane. Overall the gas plant capacities are reduced from 50 GW_{el} to 21 GW_{el} between the 80% and the 100% reduction target.

- Biomass-wise, biogas production and purification plants as well as wood-fired CHPs are now part of the optimal design solution. It must be noted that the decision to include these CHPs is driven by the electricity supply and does not take a heat demand into account. 31 TWh of biogas, i.e. the maximum production potential that is considered in the scenario scope, are injected into the MRG grid. In comparison, in 2017, more than 9 TWh of biogas were injected into the natural gas grid [101].

- Furthermore, a "*Power-to-Hydrogen-to-Methane-to-Power*" pathway is considered to supply renewable electricity. This pathway will be discussed in more detail later in this section.

The regional distribution of electricity generating components is visualized in Figure 5.12. PV rooftop systems are built in larger quantities in the old federal states of Germany. In the new federal states, open-field systems with a fixed tilt are the dominant PV technology. Electricity generation from floating offshore wind turbines is only considered within the offshore capacities that are connected to the region surrounding *Hamburg*. This region is again connected via two DC lines to *Baden-Württemberg* and *Bavaria*. The onshore wind turbines which are considered for the 80% reduction targets in the most northern regions in Germany are omitted. However, the offshore wind turbine capacities in that region are increased and integrated with electrolyzers and methanation plants as a flexibility option into the system[7]. Onshore wind turbines of *Class II* are included in only two regions in the south of *Baden-Württemberg* and reinforce the renewable electricity generation in these regions.

An impression of the electricity generation and consumption in the scenario is given in Figure 5.13 for a region in *Bavaria*.

[7] Cf. Figure 5.17 in the section on methane-rich gas generation, storage and transmission.

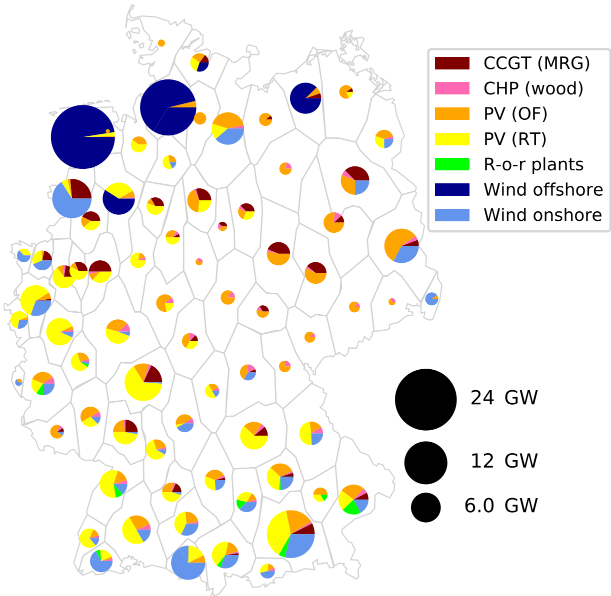

Figure 5.12: Regional distribution of electricity generation capacities (*BELS*-100%).

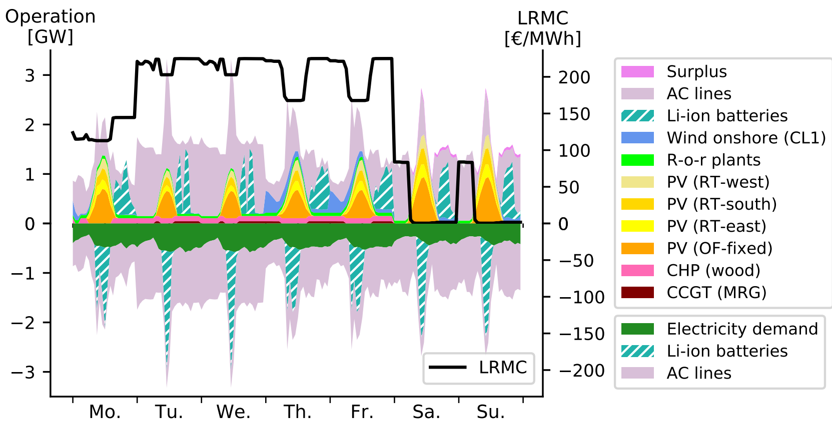

Figure 5.13: Regional electricity sources and sinks (*BELS*-100%, 10th calendar week, *Bavaria*).

Lithium-ion batteries are charged at lower LRMC plateaus before being discharged at comparably higher LRMC plateau. Wood-fired CHPs complement and supplement electricity generation from PV rooftop systems. The operation of CCGT plants correlates with high LRMC plateaus. The electricity generation in the region thus significantly differs between the 80% and the 100% reduction target, cf. Figure 5.6 versus Figure 5.13.

A different operating behavior is observed in the north of *Mecklenburg Western Pomerania*, cf. Figure 5.14.

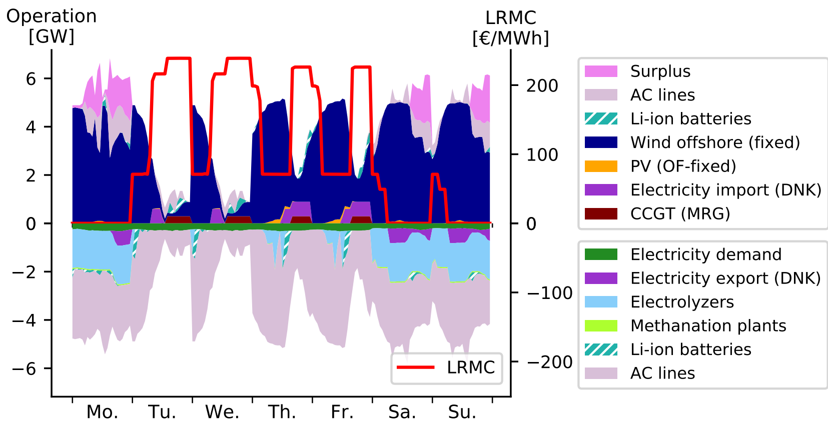

Figure 5.14: Regional electricity sources and sinks (*BELS*-100%, 10th calendar week, north of Germany).

In this region, electricity generation is dominated by offshore wind turbines connected to the region. The figure indicates why the *Power-to-Hydrogen-to-Methane* pathway is considered in the optimization. The operation of the electrolyzers and methanation plants at times of low LRMC puts little additional stress on the electricity generation and is, together with the low-cost transmission and storage infrastructure, overall cost-beneficial.

Electricity Transmission and Storage

The capacities and utilization of the AC and DC lines is presented in Figure 5.15. The utilization is visualized in form of the operation of a line above 80% of its considered capacity[8].

[8] I.e. the nominal capacity for DC lines and the nominal capacity times 70% for AC lines.

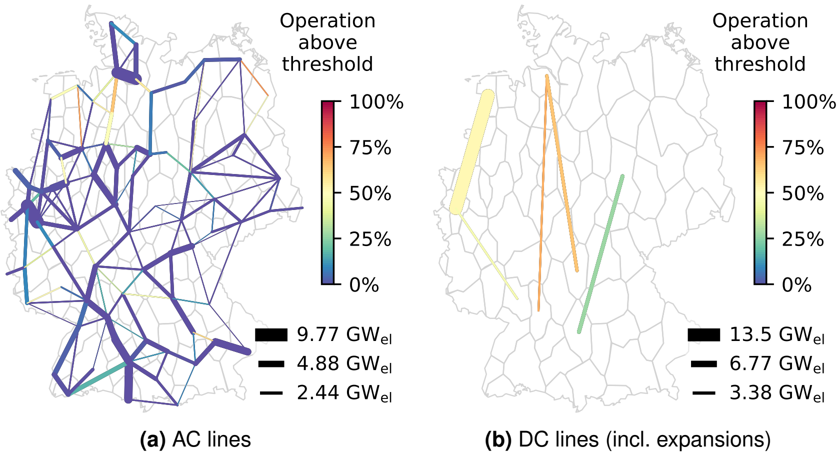

Figure 5.15: Operation of AC / DC lines above 80% of their capacity (*BELS*-100%).

The DC line capacities between *Lower Saxony* and *North Rhine-Westphalia* are significantly reinforced from 2 GW$_{el}$ to about 13.5 GW$_{el}$. Also, the DC line between *Schleswig Holstein* and *Bavaria* is reinforced to a nominal capacity of 3.4 GW$_{el}$. The DC line between *Saxony-Anhalt* and *Bavaria* is, in comparison to the *BELS*-80% scenario, better integrated into the system.

The electricity storage design for the 100% reduction target is visualized in the appendix B.1 in Figure B.5. In comparison to the 80% reduction target, the considered capacity of lithium-ion batteries is significantly increased (0.41 GWh$_{el}$ $\rightarrow$134 GWh$_{el}$). Also, a refurbishment of PHES is considered.

Exemplary operation profiles of a lithium-ion battery and a PHES are given in Figure 5.16. Lithium-ion batteries have a more explicit daily operation profile in the 100% reduction target case. Their charging operation is strongly correlated with the electricity generation from PV systems. However, during winter days, the batteries are also sometimes charged at night when electricity from wind turbines is abundantly available. PHES serves again as a daily and inter-daily storage. However, its operation is distinctively different from the one for the 80% reduction target. While lithium-ion batteries are mostly operated to shift electricity from the morning and early afternoon to the evening, PHES is in most cases used to shift electricity from the morning and late afternoon to the early morning hours of the next day. The average storage duration inside the PHES is thus longer. An explanation of these different operating behaviors can be found in the self-discharge of the technologies. The self-discharge is assumed to be zero for

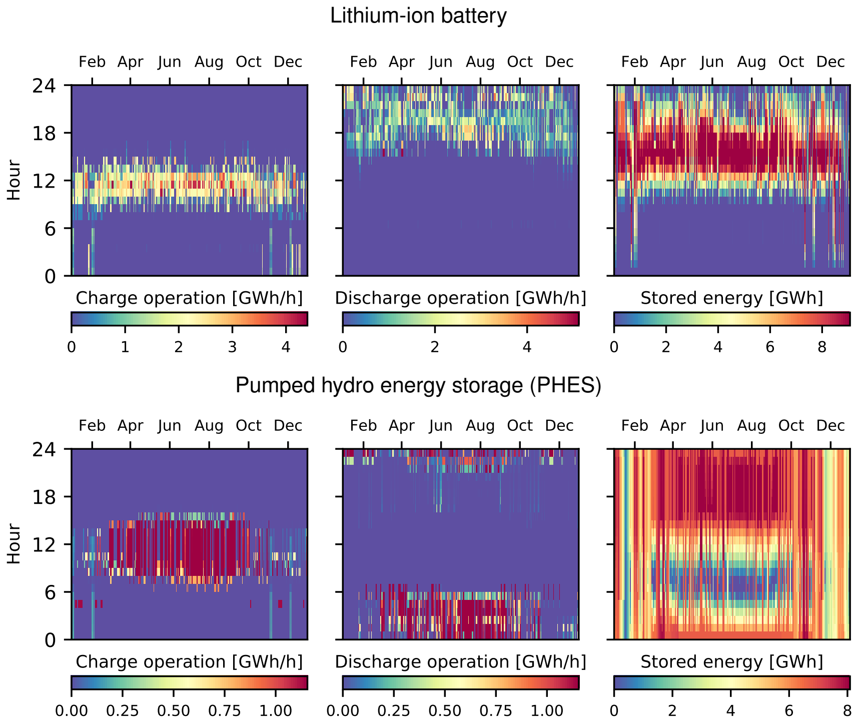

Figure 5.16: Exemplary operation profiles of lithium-ion batteries and PHES (*BELS*-100%).

PHES and 3% per month for lithium-ion batteries. Another explanation can be found in the power-to-energy ratios of the technologies. For the battery operation profile, the ratio of discharged energy and installed storage capacity is in the evening often above 1/4. A PHES with the same storage capacity would, with a modeled power-to-energy ratio of 1/7, not be able to fully supply this demand.

Methane-rich Gas Generation, Transmission and Storage

Methane-rich gas (MRG) is produced via biogas purification and methanation of hydrogen and carbon dioxide, extracted from ambient air, in the scenario. Regional distributions of the production and consumption sites for MRG are visualized in Figure 5.17. Biogas purification units are considered at each biogas production site and are distributed across Germany. Methanation units of in total 5.5 $GW_{MRG,LHV}$

are located at electrolysis sites with a total capacity of 9.9 GW_{el}. These are again mainly operated on surplus electricity from offshore wind turbines / at times of low LRMC, cf. Figure 5.14.

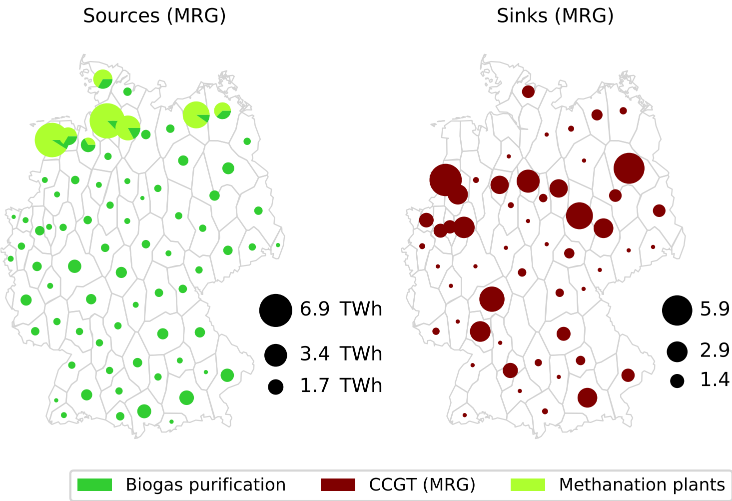

Figure 5.17: Regional distribution of MRG sources and sinks (*BELS*-100%).

The transmission of the produced MRG to the CCGT plants takes place via pipeline. A further analysis into the pipeline grid reveals above average utilizations of pipeline capacities considered in the north of Germany. Some pipelines even show frequent congestions. These congestions could be avoided by increasing the share of the original natural gas pipeline capacities which are dedicated to the transmission of purified biogas and synthetic methane (here: 10%). This would however reduce the transmission potentials for MRG demands that are not explicitly modeled in the scenario scope.

In contrast to the 80% reduction target case in which MRG storage is not considered, MRG storage in pore storage, existing and new salt caverns and pipe systems is pursued in large scale. The optimal capacities and annual charging operation of MRG storage are visualized in Figure 5.18. The ratio between the charging operation and the installed capacities indicates the operation mode of the different storage options. Salt caverns have a turn-over count 5.9 / 9.1 (existing / new caverns) and are used as seasonal storage.

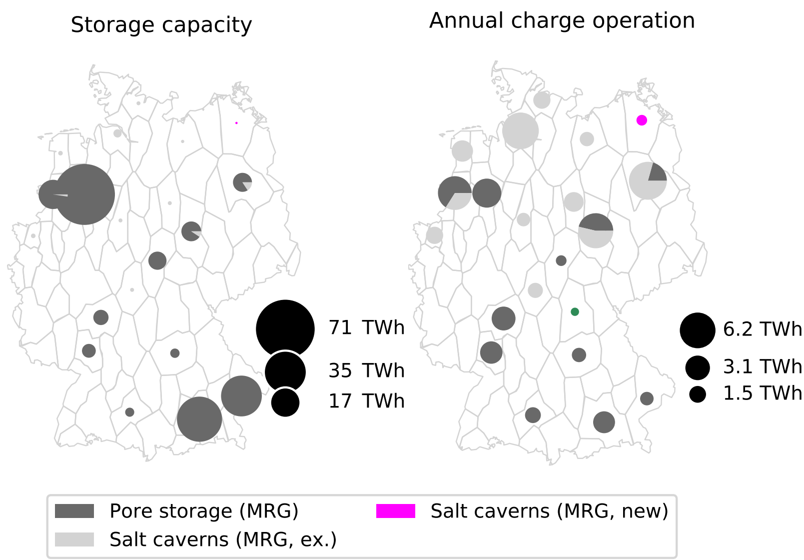

Figure 5.18: Capacities and charging operation of MRG storage (*BELS*-100%).

Long-run Marginal Costs (LRMCs)

An annual average of 128 €/MWh$_{el}$ is obtained for the long-run marginal cost of the electricity supply for the 100% reduction target (*BELS*-80%: 77 €/MWh$_{el}$). The duration curves of the regional LRMC are visualized for the 80% and 100% reduction target side by side in Figure 5.19.

The number of time steps in which the LRMCs are above 100 €/MWh$_{el}$ is significantly increased. However, also the number of time steps in which the LRMC are close to 0 €/MWh$_{el}$, which correlate to time steps in which electricity from intermittent renewable energies is available and not supplied to the *basic* electricity demand, is significantly increased. At these time steps, hydrogen is produced via electrolysis in the supply system, cf. Figure 5.20[9].

The electrolyzers are primarily operated with their maximum production rate when the LRMC are equal to 0 €/MWh$_{el}$. However, they can also be operated at times when the LRMC are smaller than 71.2 €/MWh$_{el}$. Overall, the electrolyzers are operated with an annual, average LRMC of 17.5 €/MWh$_{el}$.

[9]For improved visibility, operation curves are sorted and only shown for regional capacities above 0.5 GW$_{el}$.

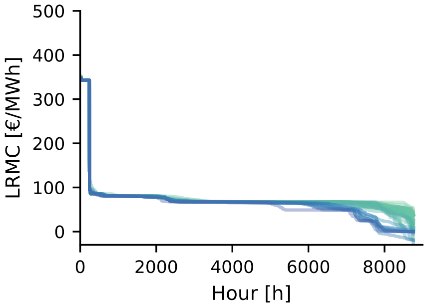

(a) *BELS*, 80% CO_2 reduction target

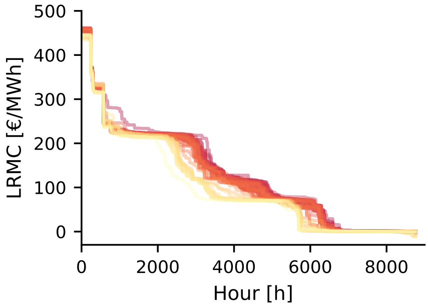

(b) *BELS*, 100% CO_2 reduction target

Figure 5.19: Duration curves of the nodal, long-run marginal cost (*BELS*-80% & *BELS*-100%; color $\sim \varnothing$ LRMC of a region).

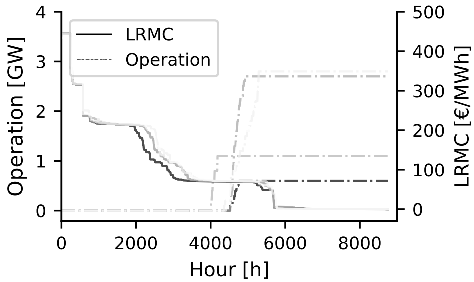

Figure 5.20: LRMC duration curves in regions with electrolyzers and corresponding electrolyzer operation profiles (*BELS*-100%).

With larger amounts of low-cost electricity being available, the conversion losses of the *Power-to-Hydrogen-to-Methane-to-Power* pathway become subordinate. When the comparably low investment cost of the pathway, the very small self-discharge of the gas storage and the availability of an alternative transmission infrastructure are additionally considered, favorable operating conditions are presented to the pathway. The pathway is thus considered in the optimal system design.

5.1.4 Scenario Variations

For the *BELS* scenario branch, the following scenario variations are considered.

1. Value of transmission infrastructure components:

(a) The system is modeled without DC line expansions (*w/o DC line exp.*).
(b) The system is modeled without DC lines in general (*w/o DC lines*).
(c) The system is modeled without MRG transmission and biogas injection into gas pipelines (*w/o pipelines (MRG)*).

2. Value of storage infrastructure components:
   (a) The system is modeled without PHES (*w/o PHES*).
   (b) The system is modeled without lithium-ion batteries (*w/o Li-ion batteries*).
   (c) The system is modeled without underground MRG storage (*w/o UGS (MRG)*).
3. Value of selected source and conversion components on the storage and transmission infrastructure design:
   (a) The system is modeled without any biomass, i.e. without wood-fired CHPs and biogas production / purification / storage / CHPs (*w/o biomass*).
   (b) The system is modeled without methanation plants (*w/o methanation*).

For all scenario variations, the TAC and the installed capacities of *Source* and *Conversion* components are visualized side by side in Figure 5.21 and Figure 5.22. The plots for the secured electricity generation capacities, primary energy sources, general electricity generation and consumption, flexible electricity generation, installed *Storage* capacities and the inter-regional commodity transmissions can be found in the appendix B.1, cf. Figures B.6 – B.13. Only the scenario variations which have a notable difference from the reference scenario are shown for each carbon dioxide reduction target. In the following, each scenario variation is shortly described, compared to the reference scenario and the main conclusions which can be drawn from the variation are summarized.

The Value of DC Line Expansions / Domestic DC Lines (1a & 1b)

Depending on the CO_2 reduction target, the removal of DC line expansions / all domestic DC lines leads to a cost increase of 0 - 3% / 1.8 - 7.9%, respectively. From the presented scenario variations, the removal of domestic DC lines in general is the second most expensive scenario variation.

The removal of DC line expansions / DC lines in general leads to a more challenging integration of offshore wind turbines which are therefore installed with smaller capacity. The optimization compensates the reduced offshore electricity generation by building additional onshore wind turbines and PV rooftop systems. Also, the

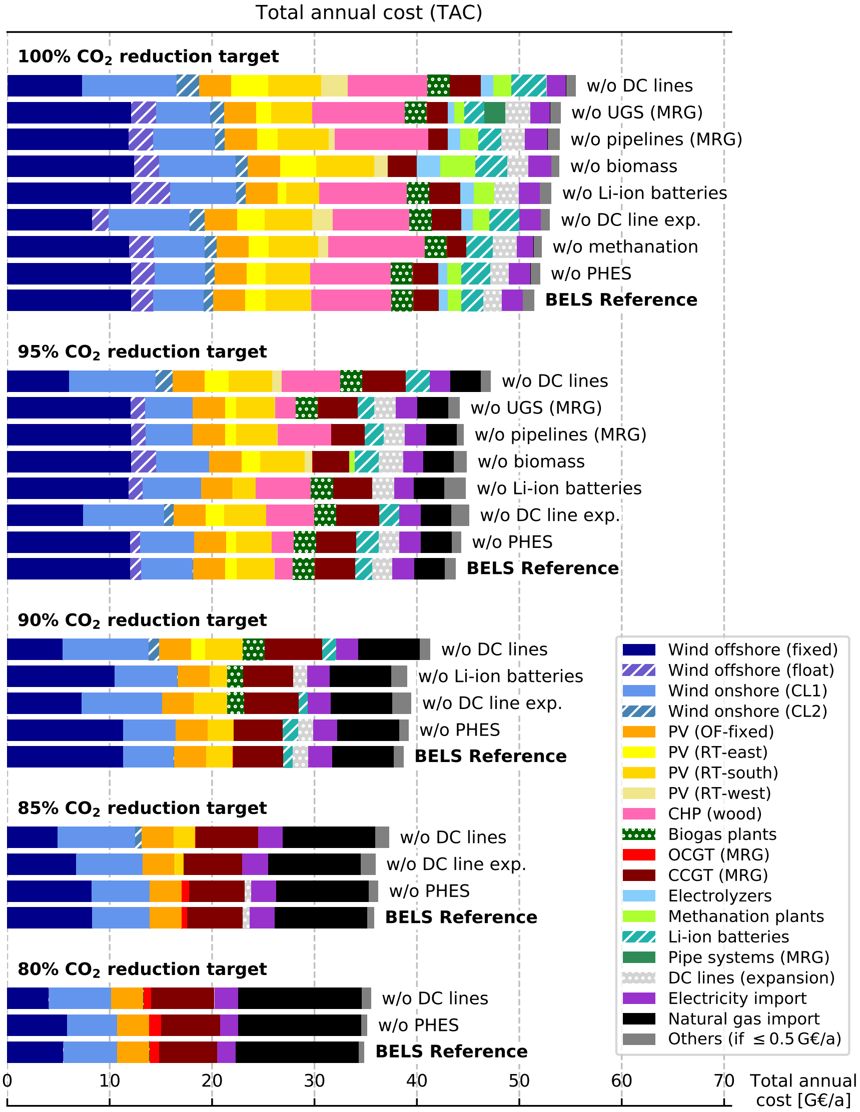

Figure 5.21: Total annual cost in the *BELS* scenario variations.

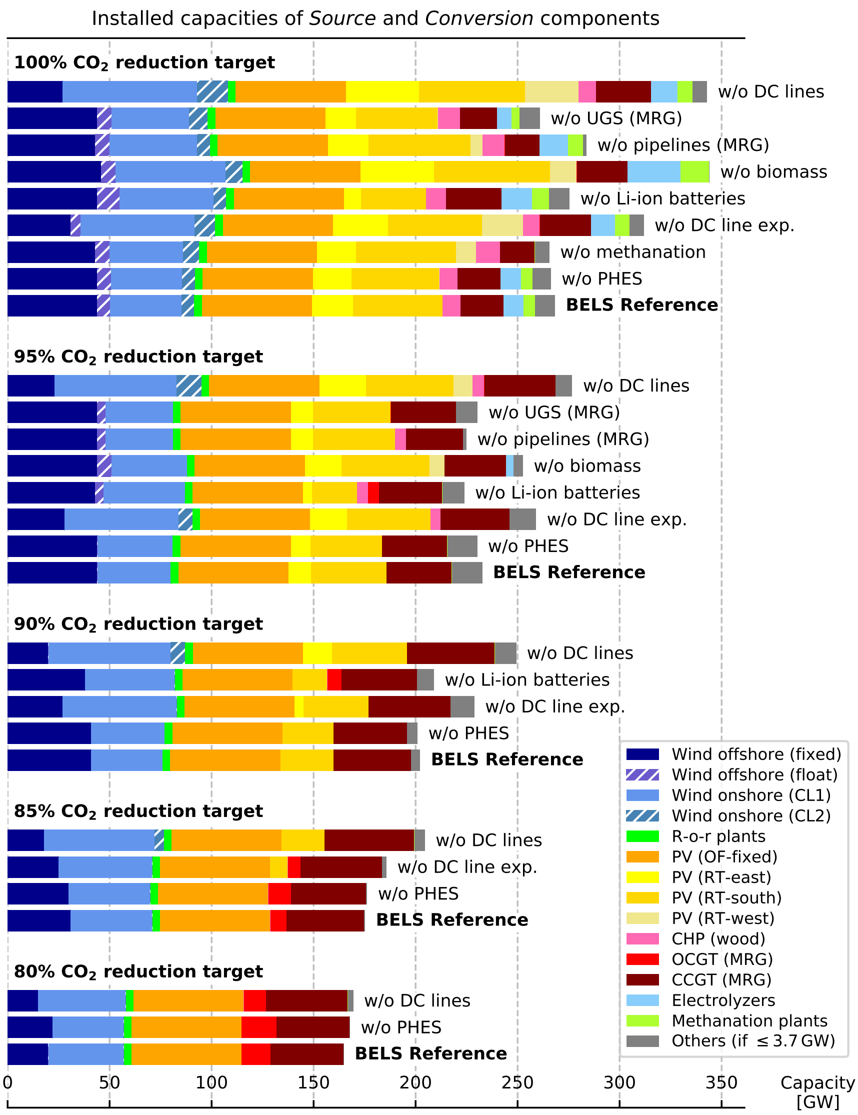

Figure 5.22: Capacities of *Source* and *Conversion* components in the *BELS* scenario variations.

consideration of biogas plants and wood-fired CHPs is considered earlier on and in larger quantities. Overall, the electricity generation is more decentralized. Electrolyzers and methanation plants are solely built in north of Germany. They are built in larger capacities and operated with higher full load hours, benefitting from bottlenecks in the grid.

With the more prominent, intermittent, decentralized electricity generation from onshore wind turbines and PV rooftop systems, larger capacities of daily and, for the 100% reduction target, seasonal storage are required. For the 100% reduction target, pipe systems for gaseous hydrogen storage are built which function as a weekly storage and buffer the production profiles of the electrolyzers for the methanation plants.

Without DC lines as a spatial balancing option, the optimal design solution already includes spatial balancing by the transmission of purified biogas for the 90% reduction target. Even though the considered AC line capacities are unchanged, they are utilized to a smaller amount which is rooted in the more decentralized electricity generation.

Even though the DC lines are removed as a major infrastructure component, a large number of other infrastructure components, as for example lithium-ion batteries, gas storage or renewable electricity generation in general, must be significantly expanded in order to reach a cost optimal design solution within the considered scenario scope.

The Value of Methane-rich Gas Transmission and Biogas Injection into Gas Pipelines (1c)

The value of MRG transmission stemming from biogas purification or methanation is particularly notable for high carbon dioxide reduction targets. While for reduction targets of 80%, 85% and 90% no change in the TAC can be observed, the TAC increases by 1.8% for the 95% reduction target and by 4.8% for the 100% reduction target when they are removed from the supply system.

For the 95% reduction target, the removal of the MRG transmission and biogas purification is compensated with additional wood-fired CHP plants.

For the 100% reduction target, the removal of the MRG transmission and the biogas purification leads to a structural change in the optimal supply system design. On the one hand, electrolyzers are built in larger quantities and are not only placed in the north of Germany but are distributed across Germany, cf. Figure B.14 in the appendix B.1. On the other hand, biogas plants are still operated even though biogas purification and injection into the gas grid are omitted. The biogas is in this context used to fuel decentral CHPs and is stored in double membrane gas storage installations.

UGS storage is omitted in the scenario variation for reduction targets between 80% and 95%. However, for the 100% reduction target, UGS capacities are increased as more MRG is produced by the distributed methanation plants and needs to be stored locally. Moreover, the produced hydrogen is in some cases stored locally in pipe storage systems (GH_2) to buffer the production profiles of the electrolyzers.

For the 100% reduction target, an increase in the utilization of the electric grid and an increase in the installed DC line expansions can be noted. With the omission of the MRG pipelines as a spatial balancing option, the electric grid needs to be utilized more heavily for an optimal design solution and congestions become more likely.

This scenario variation should be taken into consideration when arguing for or against transmission options for gases from *Power-to-X* pathways or biogas purification. It should moreover be considered when arguing for a decentral heat supply from biogas plants. For the latter case, the cost of prohibiting a renewable fuel for centralized electricity generation and the cost of alternative heat supply options must be weighed against each other.

The Value of PHES (2a)

The changes in the TAC which arise from the omission of PHES are comparably small but nevertheless notable and range between 0.8% and 1.1%.

The removal of PHES is compensated with an increased capacity of lithium-ion batteries. For reduction targets of 80% and 85%, the removal is also compensated by additional OCGT capacities which are however operated with lower full load hours (1420 h/a (Reference-80%) $\rightarrow$ 1027 h/a (w/o PHES-80%)).

The omission of the low-tech technology specifically leads to an increase in high-tech lithium-ion batteries for the given scenario scope which could be of interest when a life cycle assessment of the supply system is considered.

The Value of Lithium-ion Batteries (2b)

The impact of removing lithium-ion batteries for the 80% and 85% reduction target is small and is thus not visualized in the bar plots. However, it becomes more prominent with stricter reduction targets. For the 100% reduction target, the TAC increases by 3.2%.

The omission of lithium-ion batteries leads to a reduced capacity of PV rooftop systems. Their reduction is compensated by an increase in the capacities of wind turbines. Furthermore, biogas plants are considered already for the 90% reduction target.

To compensate the omission of lithium-ion batteries as a temporal balancing option, more refurbished PHES is considered. Also, OCGT plants are built until the 95% reduction target to flexibly cover peak loads. Furthermore, for the 100% reduction target, higher capacities of electrolyzers, methanation plants and salt caverns are built to store energy in form of gas.

Concerning transmission infrastructure, the integration of the additionally built wind turbines leads to larger DC line expansions. The increased capacities of electrolyzers and methanation plants lead to an increased MRG transmission between regions.

The scenario variation demonstrates the value of daily, high-efficient energy storage which promotes the integration of PV systems into the energy supply system.

The Value of Underground MRG Storage (2c)

Removing underground storage (UGS) of MRG from the energy supply system leads to a cost increase of up to 5%. As UGS is not part of the optimal design solution for the 80%, 85% and 90% reduction target, no change in the TAC can be observed for these targets.

For the 95% reduction target, the overall structural change of the optimal supply system design is small. The most significant change is the large-scale utilization of pipe storage systems to store the MRG (Σ 1.3 $TWh_{MRG,LHV}$).

With the omission of new and existing salt caverns as well as pore storage, all low-cost storage options are removed from the *Power-to-Hydrogen-to-Methane-to-Power* pathway considered for the 100% reduction target. To compensate their omission, the optimal system design switches to MRG storage in pipe systems and reduces the installed capacities of electrolyzers, methanation plants and CCGT plants by about 30%. Moreover, wood-fired CHPs are built in larger quantities.

For both reduction targets, MRG pipelines are used less often. The DC lines are on the other hand further expanded and more electricity is transmitted through them.

Overall, the scenario variation shows that energy storage in gas is a robust design solution for high carbon dioxide reduction targets. When UGS is not eligible, pipe storage systems may serve as a storage alternative. However, UGS is often more cost-lucrative.

The Value of Biomass (3a)

The change in TAC by the omission of biomass ranges between 0% and 4.8%.

The omission of biogas plants and wood-fired CHPs forces the optimization to build alternative renewable energy sources in larger quantities. Specifically, the capacities of offshore wind turbines and PV rooftop systems are notably increased.

To compensate the omission of biogas and wood, which can both be stored at low cost, refurbished PHES and lithium-ion batteries are considered in larger quantities and small installations of pipe systems (GH_2) are built. Moreover, electrolyzers and methanation plants are built in larger quantities and are already part of the optimal design solution for the 95% reduction target. To store these larger amounts of MRG, also new salt cavern locations are considered.

With the expansion of offshore wind turbine capacities, larger DC line expansions are considered and utilized to a higher degree. Likewise, with the increased capacities of methanation plants, the pipelines for MRG are more frequently used.

Overall, the scenario variation demonstrates that with the omission of biomass, other renewable energies such as wind turbines and PV systems have to be built. These cannot provide energy as flexible as the biomass pathways and thus require additional energy storage.

The Value of Methanation Plants (3b)

The value of methanation plants is investigated for the 100% reduction target. There, a cost increase of 1.4% can be registered when methanation plants are omitted.

The omission of methanation plants leads to a notable increase in wood-fired CHP plants and PV rooftop systems. The integration of the additional PV systems is supported by additional lithium-ion battery capacities. Salt caverns are built in smaller quantities and are dedicated to the sole purpose of storing purified biogas.

Inherently, MRG pipelines are utilized less. As electricity from offshore wind turbines is not used for electrolysis, methanation and spatial balancing by pipeline transmission anymore, more electricity needs to be transported via DC lines from the north to the south of Germany. Thus, more DC line expansions are built and more electricity is transmitted. Nevertheless, the curtailment in this scenario variation is doubled in comparison to the reference scenario (30 $TWh_{el} \rightarrow$ 65.5 TWh_{el}, incl. electricity export which is supplied from surplus electricity only). This is also reflected in the long-run marginal costs of the electricity supply which are more often close to 0 €/MWh, cf. Figure B.15 in the appendix B.1.

5.2 *BELS+* - Basic ELectricity Supply with a Centralized H_2-Infrastructure

The *BELS+* scenario branch extends the *BELS* scenario branch by the consideration of additional, more centralized hydrogen infrastructure components. These comprise pipelines for gaseous hydrogen (GH_2), GH_2 storage in salt caverns, liquid hydrogen (LH_2) import, LH_2 storage in cryogenic tanks, regasification terminals, liquefaction plants, and finally GH_2 operated OCGT and CCGT plants.

In analogy to the previous section, first, the optimal system configurations of the *BELS+* reference scenario under varying carbon dioxide reduction targets (80%, 85%, 90%, 95%, and 100%) are presented and are compared to the ones of the *BELS* reference scenario in subsection 5.2.1. In subsection 5.2.2, the resulting optimal electricity supply system for the 100% reduction target is presented and discussed in detail. Scenario variations of the reference scenario are presented and shortly discussed in subsection 5.2.3.

5.2.1 Optimal System Configurations under Varying CO_2 Reduction Target

The TAC of the *BELS* and *BELS*$^+$ reference scenarios are visualized side by side in Figure 5.23 for varying carbon dioxide reduction targets. In the figure, also the avoided emissions (in reference to the year 1990) are indicated.

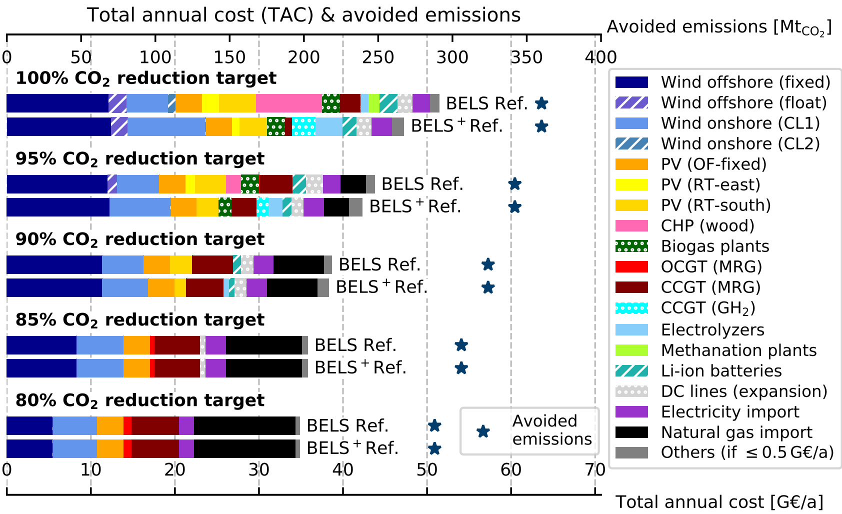

Figure 5.23: Total annual cost and avoided emissions in the *BELS* and *BELS*$^+$ reference scenario under varying CO_2 restrictions.

For the 80% and 85% reduction target, no change in the TAC is observed. However, for the 90%, 95%, and 100% reduction target, the TAC decreases by 0.9%, 3.4%, and 8.8% respectively. For these reduction targets, the cost contributions of onshore wind turbines (*Class I*), CCGT (GH_2) and electrolyzers increase while the costs of onshore wind turbines (*Class II*), PV rooftop systems, wood-fired CHPs, biogas plants, CCGT (MRG), methanation plants and lithium-ion batteries decrease. More specifically, wood-fired CHPs and methanation plants are not considered in the optimal system configuration for any of the reduction targets.

The installed capacities of the respective *Source* and *Conversion* components are visualized for these reduction targets side by side in Figure 5.24. The installed capacity of gaseous hydrogen-fueled CCGT is 3.8 GW_{el} for the 90% reduction target and reaches a value of 22 GW_{el} for the 100% reduction target. Thus, it

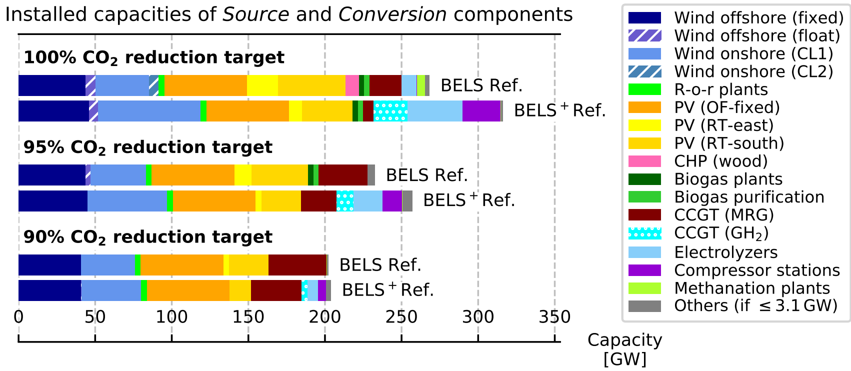

Figure 5.24: Installed capacities of *Source* and *Conversion* components in the *BELS* and *BELS+* reference scenario under varying CO_2 restrictions.

can be concluded that centralized reconversion of hydrogen to electricity, i.e. a *Power-to-Hydrogen-to-Power* pathway, has a pivotal role for the cost optimal design of the energy supply systems with high carbon dioxide reduction targets. The power plants also contribute to the secured electricity generation capacities, which are, alongside with figures for primary energy sources, general electricity generation and consumption, and dispatchable electricity generation given in the appendix B.2, Figures B.16 – B.20.

Besides lithium-ion batteries and DC line expansions, several other *Storage* and *Transmission* components significantly contribute to the supply systems' functionality but have only a small share on the TAC.

The capacities of the installed *Storage* components in the *BELS* and *BELS+* reference scenario are visualized side by side in Figure 5.25, once for all *Storage* components and once for non-geological *Storage*[10]. The change in the installed storage fleet is assessed component-wise in the following.

- Pumped hydro energy storage which is assumed to not require major refurbishment (*PHES (existing)*) is modeled with a fixed capacity and is thus invariant.
- Refurbished PHES, only considered for the 100% reduction target, is built with a smaller capacity in the *BELS+* scenario branch.

[10] As pore storage is modeled with a fixed capacity of several hundred $TWh_{MRG,LHV}$, it is excluded from the bar plot for improved visibility.

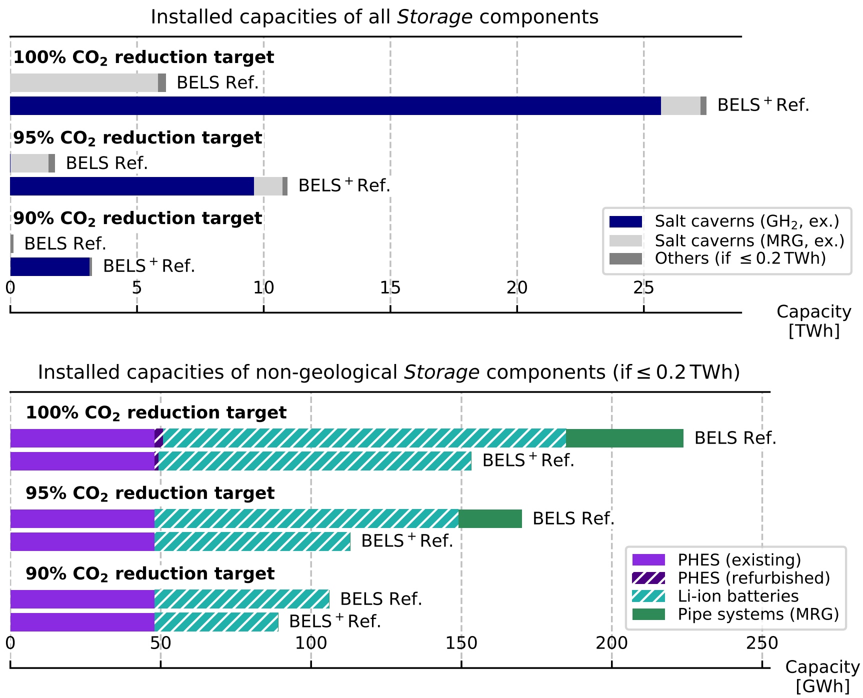

Figure 5.25: Storage design in the *BELS* and *BELS*+ reference scenario under varying carbon dioxide reduction targets (pore storage excluded).

- Within the *BELS*+ scenario branch, smaller amounts of lithium-ion batteries are installed.
- Pipe systems (MRG) are not considered in the *BELS*+ scenario branch.
- Within the *BELS*+ scenario branch, smaller capacities of MRG-filled salt caverns are considered. However, about 15 to 121 hydrogen-filled salt caverns (3.1 / 25.7 TWh_{GH_2}) are considered at in 2017 existing salt cavern locations (*Salt caverns (GH_2, ex.)*) in the *BELS*+ scenario branch. Thus, the considered geological storage capacities have multiplied.

Three conclusions can be drawn from these results. First, the amount of high-efficient, more investment-intensive electricity storage is decreased. Second, a significant increase in low-efficient, low investment-intensive electricity storage via a *Power-to-Hydrogen-to-Power* pathway is considered. Third, by the omission of the less efficient *Power-to-Hydrogen–to-Methane-to-Power* pathway and the reduced demand of biogas, the role of MRG storage becomes less prominent.

For *Transmission* components, the annual commodity exchange between regions is visualized for the *BELS* and *BELS*+ scenario branch side by side in Figure 5.26[11]. Several observations can be deducted from the bar plot.

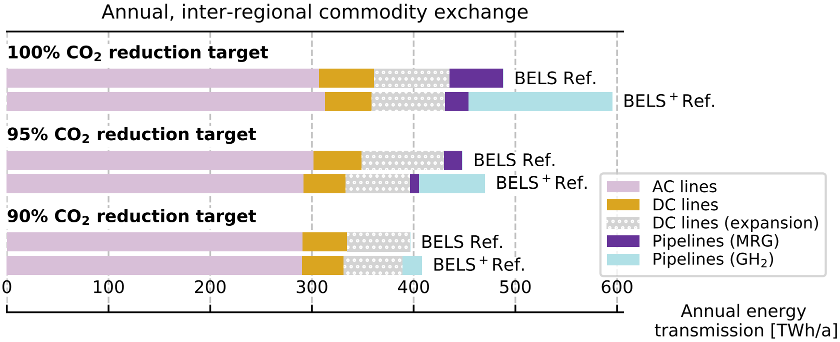

Figure 5.26: Transported commodities in the *BELS* and *BELS*+ reference scenario under varying carbon dioxide reduction targets.

- In total, the utilization of the considered AC and DC lines is smaller in the *BELS*+ scenario branch.
- Also, the utilization of the considered MRG pipelines is smaller in the *BELS*+ scenario branch.
- Starting from the 90% reduction target, gaseous hydrogen pipelines are considered as an additional *Transmission* component.

Overall, more energy is transmitted in the *BELS*+ scenario branch.

The annual average of the long-run marginal cost of electricity supply[12] are visualized side by side in Figure 5.27 for the *BELS* and *BELS*+ reference scenario. The average LRMCs correlate to a certain degree to the TAC of the two scenario branches. For the 90%, 95% and 100% reduction target, the average LRMC is reduced by 5.7%, 9% and 11% respectively.

In general, the consideration of the centralized hydrogen infrastructure leads to a less expensive supply system, specifically for strict carbon dioxide reduction targets. With the introduction of a *Power-to-Hydrogen-to-Power* pathway, which is comprised of electrolyzers, pipelines, salt caverns and CCGT plants (GH_2), the capacities of biogas plants, wood-fired CHPs, PV rooftop systems and lithium-ion

[11] These values do not consider the intra-regional commodity transmission.
[12] (Σ Regional LRMC profiles $\cdot$ electricity demand) / (Σ electricity demand).

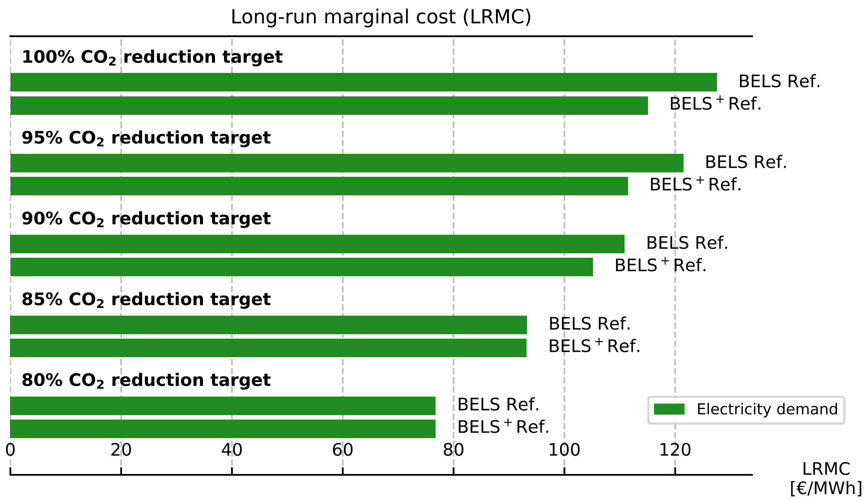

Figure 5.27: Weighted long-run marginal cost in the *BELS* and *BELS*$^+$ reference scenario under varying carbon dioxide reduction targets.

batteries are notably reduced while the capacities of onshore wind turbines are increased. Apparently, the *Power-to-Hydrogen-to-Power* pathway plays a pivotal role in the energy supply systems when high carbon dioxide reduction targets are considered. For the 100% reduction target, it has an overall cost share of 14% on the TAC to which the installed electrolyzer and CCGT plants contribute the largest shares. Thus, the assessment of this pathway will be the focus throughout the rest of this section.

5.2.2 Supply System Assessment (100% CO_2 Reduction)

The techno-economic parameter overview for the *BELS*$^+$ reference scenario with the 100% reduction target is given in Table 5.3. In comparison to the *BELS* reference scenario with the 100% reduction target, cf. Table 5.2, the most notable change in the parameters occurs in the consideration of the additional hydrogen infrastructure for the centralized *Power-to-Hydrogen-to-Power* pathway and the omission of wood-fired CHPs and methanation plants. The parameters of the table will be revisited throughout this section with a focus on comparing the optimal system design and operation to the one from the *BELS* scenario branch with the 100% reduction target.

Table 5.3: Techno-economic parameter overview (*BELS*$^+$-100%).

	Capacity	TAC [M€/a]	Operation [TWh/a]	FLHs or TOC [h/a] or [-]
Wind offshore (fixed)	46 GW_{el}	12432	220 (0.1)	4813
Wind offshore (float)	5.8 GW_{el}	1971	30 (0.0)	5245
Wind onshore (CL1)	67 GW_{el}	9289	167 (0.3)	2482
R-o-r plants	3.8 GW_{el}	439	15.0 (2.4)	3929
PV (OF-fixed)	54 GW_{el}	3136	66 (0.1)	1209
PV (RT-east)	8.4 GW_{el}	838	9.6 (0.0)	1141
PV (RT-south)	33 GW_{el}	3311	40 (0.0)	1205
PV (RT-west)	0.89 GW_{el}	89	1.0 (0.0)	1132
Biogas plants	3.5 GW_{biogas}	2127	30	8760
Biogas purification	3.5 GW_{MRG}	169	30	8751
OCGT (MRG)	0.37 GW_{el}	25	0.18	490
CCGT (MRG)	6.9 GW_{el}	873	19	2742
CCGT (GH_2)	22 GW_{el}	2740	54	2445
Electrolyzers	36 GW_{el}	3238	123	3396
Compressor stations	25 GW_{GH_2}	167	86	3396
PHES (existing)	48 GWh_{el}	76	9.7 | 7.6	176
PHES (refurbished)	1.3 GWh_{el}	17	0.2 | 0.2	150
Li-ion batteries	104 GWh_{el}	1687	34.0 | 30.6	310
Salt caverns (GH_2, ex.)	26 TWh_{GH_2}	278	88.6 | 88.6	5.2
Pore storage (MRG)	191 TWh_{MRG}	10	10.5 | 10.5	0.12
Salt caverns (MRG, new)	75 GWh_{MRG}	0.57	0.5 | 0.5	8.8
Salt caverns (MRG, ex.)	1.6 TWh_{MRG}	5	8.9 | 8.9	8
AC lines	-	0	313.1	-
DC lines	-	0	45.9	-
DC lines (expansion)	-	1738	72.1	-
Pipelines (MRG)	-	15	22.8	-
Pipelines (GH_2)	-	137	141.3	-
Electricity export	-	-8.72	8.7	-
Electricity import	-	2481	50	-
Electricity demand	-	0	528	-

Capacity: If applicable, w.r.t the lower heating value (LHV). TAC: Total annual cost. Operation: If existing, curtailment is listed in parentheses; for *Storage* components, charging and discharging operation are listed. FLHs or TOC: Full load hours of *Source* and *Conversion* components; turn-over count of *Storage* components.

Electricity Generation, Transmission and Storage

In comparison to the *BELS* scenario, the *BELS*$^+$ scenario has a stronger focus on onshore wind turbines as a renewable energy source and reduces / omits electricity generation from PV / wood in the optimal design solution. Furthermore, the *BELS*$^+$ scenario takes use of its additional hydrogen infrastructure options and considers a *Power-to-Hydrogen-to-Power* pathway to provide electricity flexibly. For each electricity providing component, the changes between the two scenarios are summarized in the following.

- The considered amount of offshore wind turbines only varies slightly between the two scenarios.
- The capacity of onshore wind turbines increases notably from 41 GW_{el} to 67 GW_{el} in the *BELS*$^+$ scenario. Moreover, onshore turbines from *Class II* are not considered.
- As for all previous scenarios, the capacity potential for PV open-field systems with a fixed tilt is maxed out.
- Inverse to the increased onshore wind turbine capacity, the considered capacity of photovoltaic rooftop systems is reduced from 67 GW_p to 42 GW_p in the *BELS*$^+$ scenario.
- Biomass-wise, both scenarios consider about the same amount of biogas for their optimal supply system design. However, wood-fired CHPs are not considered for the *BELS*$^+$ scenario.
- For the *BELS*$^+$ scenario, OCGT plants and CCGT plants operated on MRG are considered (Σ 7 GW_{el}) in the centralized gas power plant fleet. The capacity of MRG operated centralized power plants is thus, in comparison to the *BELS* scenario (21 GW_{el}), significantly reduced. The omission of this flexible electricity supply option is compensated by the installation of hydrogen operated CCGT plants with a total capacity of 22 GW_{el}.

Overall, the amount of remaining surplus electricity is reduced by the consideration of the centralized hydrogen infrastructure. While in the *BELS*-100% scenario 9.9 TWh_{el} from curtailment and 20 TWh_{el} of non-mandatory electricity export are considered, these values are reduced to 2.9 TWh_{el} and 8.7 TWh_{el} in the *BELS*$^+$-100% scenario configuration.

The regional distribution of electricity generating components is visualized in Figure 5.28. In comparison to Figure 5.12, which visualized the regional distribution of electricity generating components for the *BELS* scenario with the 100% reduction target, the consideration of onshore wind turbines is less dominant in the south of Germany but is more prominent in the north of Germany. Hydrogen operated CCGT plants are considered close to load centers but can also be found in larger numbers in the new federal states of Germany in regions without local PV rooftop systems and lithium-ion batteries (the latter are not visualized).

With the consideration of more onshore wind turbines in the north of Germany, the AC grid lines there are utilized more frequently, and congestions become more likely. However, the consideration of the *Power-to-Hydrogen-to-Power* pathway,

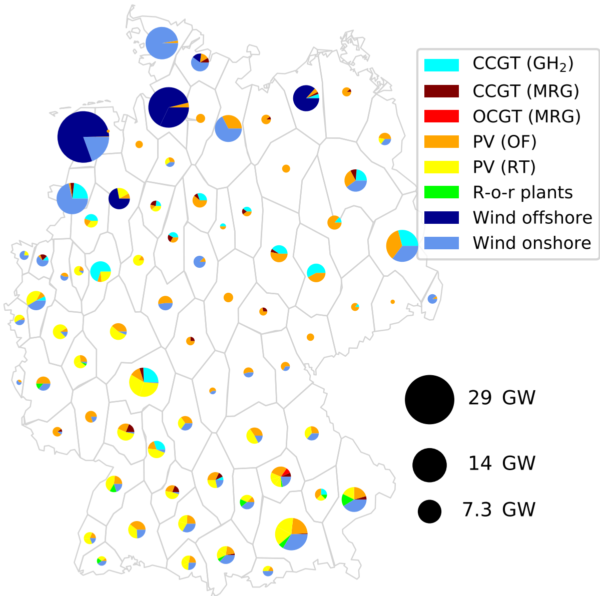

Figure 5.28: Regional distribution of electricity generation capacities (*BELS+*-100%).

which provides an additional spatial balancing option, supports the energy transmission between the north and south of Germany and thus slightly less DC line expansions are built, cf. Figure B.21 in the appendix B.2.

In correlation with the reduction of PV capacities, the installed capacities of lithium-ion batteries are reduced by about a quarter and less refurbished PHES is built. The turn-over counts and operation profiles of the installed lithium-ion batteries and PHES resemble the one from the *BELS* scenario.

Generation, Storage and Transmission of Methane-rich Gas

With methanation plants not being selected for the optimal design solution, MRG is solely produced via biogas purification. Consequently, the MRG pipelines are utilized less frequently and the considered salt cavern capacities for MRG storage is reduced by two thirds and the operation of pore storage is halved.

Generation, Storage and Transmission of Hydrogen

In the *BELS*⁺ scenario, the capacity of electrolyzers is, in comparison to the *BELS* scenario, increased by a factor of three and a half. The spatial distribution of hydrogen production sites is visualized in Figure 5.29.

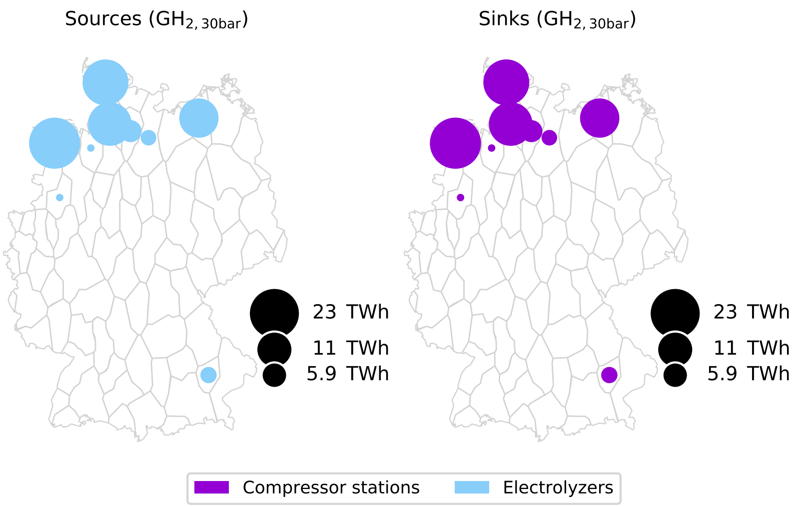

Figure 5.29: Regional distribution of hydrogen sources and sinks (*BELS*⁺-100%).

In contrast to the *BELS* scenario, the produced hydrogen is not processed in methanation plants but is compressed in compressor stations and then injected into hydrogen pipelines. There, it is either transmitted to salt caverns or to CCGT plants in regions of concurrently low electricity supply. In the scenario, electrolyzers are not only placed in the north of Germany but also in one region in *Bavaria*.

The electrolyzers are not primarily operated on electricity from offshore wind turbines, as in the *BELS* scenario, but also draw electricity from onshore wind turbines. An example for the latter is visualized in Figure 5.30 for a region in the north of Germany. Hydrogen is again produced at times of low long-run marginal cost, but not exclusively at 0 €/MWh. The electrolyzer plants located in the region in *Bavaria* are primarily supplied with electricity from onshore wind turbines from surrounding regions.

Energy storage in hydrogen filled salt caverns at in 2017 existing salt cavern locations is considered with 26 $TWh_{GH_2,LHV}$ (about 121 caverns). The spatial distribution of the capacities is visualized in Figure 5.31.

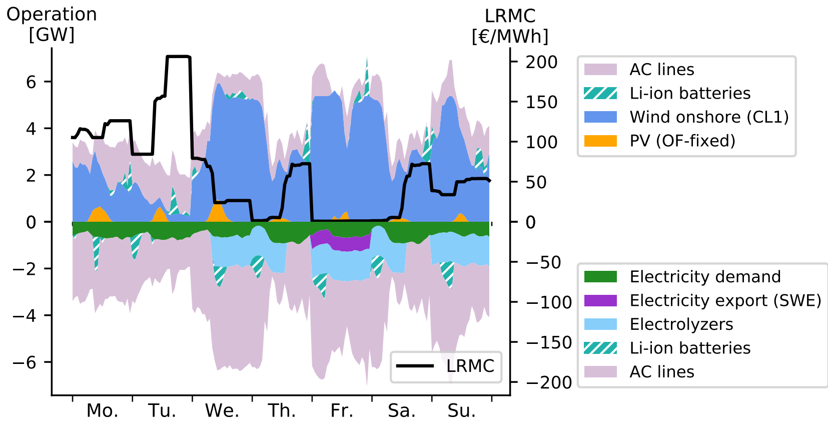

Figure 5.30: Electricity sources (>0) and sinks (<0) in region in the north of Germany, connected to Sweden (SWE), 50th calendar week (*BELS*+-100%).

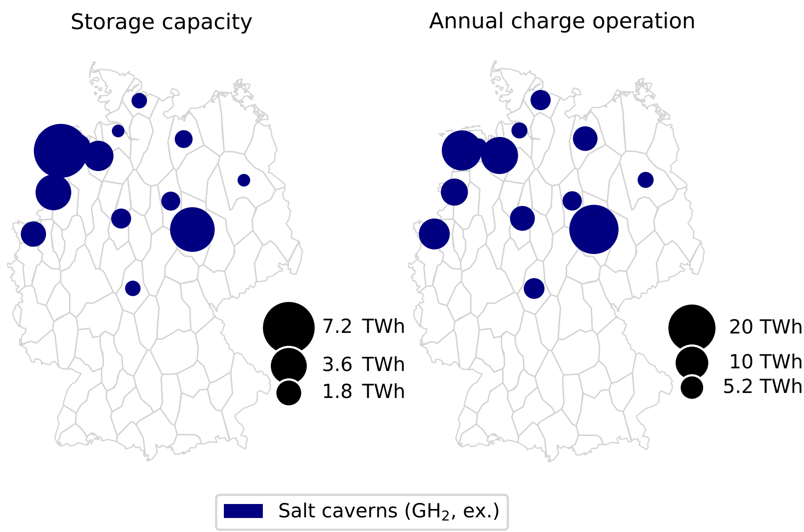

Figure 5.31: Capacities and charging operation of hydrogen energy storage (*BELS*+-100%).

The caverns are preferably placed in the north of Germany, close to the production sites. Several locations can also be found in the middle of Germany.

The salt caverns are primarily used as seasonal energy storage. Correlated to the seasonal dependent electricity supply from wind turbines, they are charged during winter and spring and then are discharged during summer and fall, cf. Figure 5.32.

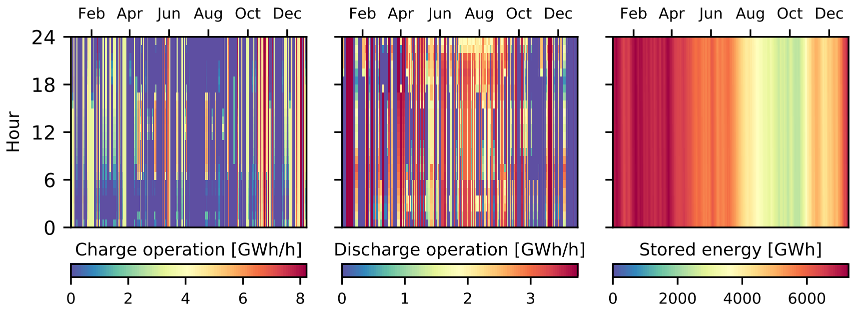

Figure 5.32: Exemplary operation profile of hydrogen-filled salt caverns (*BELS*$^{+}$-100%).

Overall, the salt caverns contribute 278 M€/a to the TAC of the supply system, i.e. they have a share of 0.6% on the TAC.

The gaseous hydrogen is transmitted from the compressor stations to salt cavern locations and CCGT plants via pipeline at about 100 bar. The pipelines capacities and average utilization are visualized in Figure 5.33. The size of a pipeline is determined by its peak fluid flow while the average utilization of the pipelines is determined by the operation of the electrolyzers, salt caverns and CCGT plants at each time step. A low average utilization indicates that a pipeline is designed to transmit specific peak fluid flows from a production or to consumption site. The pipeline installation contributes 137 M€/a to the TAC of the supply system, i.e. it has a share of 0.3% on the TAC.

The hydrogen pipeline grid is assessed and quantified with techno-economic parameters within this section to draw conclusions on *Power-to-Hydrogen-to-Power* pathways. However, the construction of a hydrogen pipeline system that is solely dedicated to transmitting hydrogen for reconversion purposes is a rather theoretical concept and must be perceived as such. A more application-oriented assessment would be to include the majority of potential hydrogen consumers when determining the pipeline design. In section 5.3, hydrogen demands in the transport and industry sector will be added as additional consumers, and thus a more application-oriented pipeline design will be revealed.

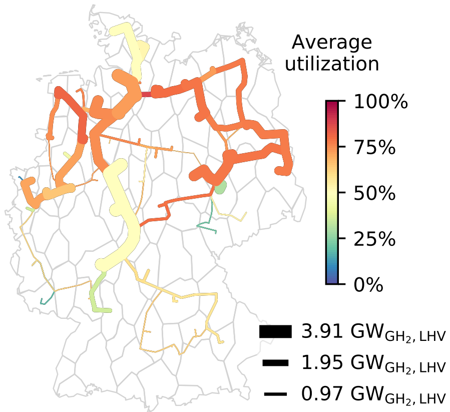

Figure 5.33: Installed capacities and average utilization of hydrogen pipelines (*BELS*+-100%).

Long-run Marginal Costs (LRMCs)

An annual average[13] of 115 €/MWh_{el} is obtained for the long-run marginal cost of the electricity supply for the 100% reduction target (*BELS*-100%: 128 €/MWh_{el}). The duration curves of the regional LRMC are visualized for the *BELS* and *BELS*+ scenario with a 100% reduction target side by side in Figure 5.34.

In comparison to the *BELS* scenario, the number of time steps in which the LRMCs are above 200 €/MWh_{el} are significantly reduced in the *BELS*+ scenario. However, also the number of time steps in which the LRMC are close to 0 €/MWh_{el} are reduced. The latter indicates a better integration of intermittent renewable energies by the centralized hydrogen infrastructure, overall leading to smaller amounts of surplus electricity.

The LRMC duration curves in regions with electrolyzers and the corresponding electrolyzer operation profiles are visualized side by side in Figure 5.35 for the two scenarios[14].

[13] (Σ Regional LRMC profiles · electricity demand) / (Σ electricity demand).

[14] For improved visibility, operation curves are sorted and only shown for regional capacities above 0.5 GW_{el}.

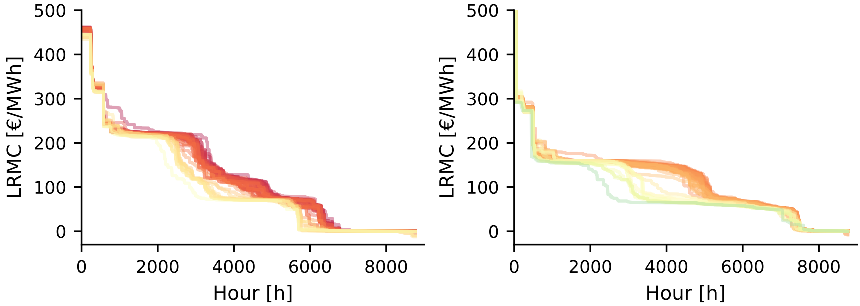

(a) *BELS*, 100% CO_2 reduction target **(b)** *BELS*⁺, 100% CO_2 reduction target

Figure 5.34: Duration curves of the nodal, long-run marginal cost (*BELS*-100% & *BELS*⁺-100%; color ∼ ∅ LRMC of a region).

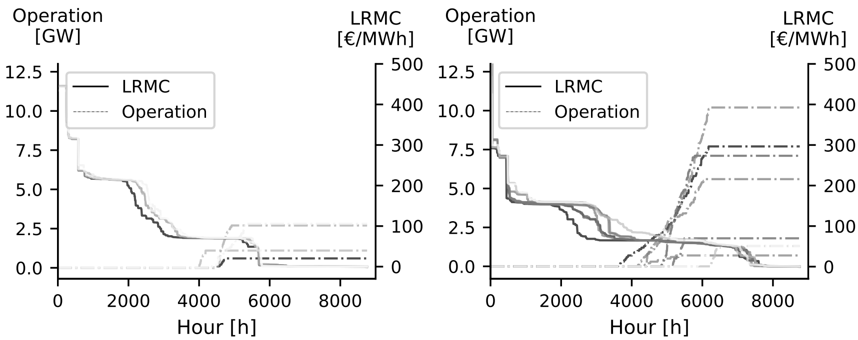

(a) *BELS*, 100% CO_2 reduction target **(b)** *BELS*⁺, 100% CO_2 reduction target

Figure 5.35: LRMC duration curves in regions with electrolyzers and corresponding electrolyzer operation profiles (*BELS*-100% & *BELS*⁺-100%).

The electrolyzers are again operated with their maximum production rate when the LRMC is equal to 0 €/MWh_{el}. They can also be operated when the LRMC is smaller than 71.2 €/MWh_{el} (*BELS*) or 64.5 €/MWh_{el} (*BELS*⁺). For the *BELS*⁺ scenario, this results in higher full load hours in regions close to shore and in less full load hours in inland regions. The annual average of the LRMC used by the electrolyzers is equal to 17.5 €/MWh_{el} in the *BELS*-100% scenario. As the downstream infrastructure for hydrogen reconversion to electricity is less expensive in the *BELS*⁺-100% scenario, this value increases to 32.2 €/MWh_{el}.

5.2.3 Scenario Variations

For the *BELS*$^+$ scenario branch, the following scenario variations are considered.

1. Value of transmission infrastructure components:
    (a) The system is modeled without DC line expansions (*w/o DC line exp.*).
    (b) The system is modeled without DC lines in general (*w/o DC lines*).
    (c) The system is modeled without hydrogen pipelines (*w/o pipelines (GH_2)*).
2. Value of storage infrastructure components:
    (a) The system is modeled without lithium-ion batteries (*w/o Li-ion batteries*).
    (b) The system is modeled without hydrogen storage in existing salt caverns (*w/o ex. caverns (GH_2)*).
    (c) The system is modeled without hydrogen storage in salt caverns (*w/o caverns (GH_2)*).
    (d) The system is modeled without underground storage (*w/o UGS (MRG & GH_2)*).
3. Value of selected *Source* and *Conversion* components on the storage and transmission infrastructure design:
    (a) The system is modeled without MRG transmission and biogas injection into gas pipelines (*w/o biomass*).
    (b) The system is modeled without electrolyzers (*w/o electrolyzers*).
    (c) The system is modeled with a lower capacity specific investment cost for electrolyzers (300 €/kW_{el}) (*w/- low electrolyzer cost*).

The omission of either MRG transmission, biogas purification and injection, MRG storage in UGS or biomass in general all display nearly the same optimization results. Therefore, only the *w/o biomass* scenario variation is shown representatively.

A scenario variation with low hydrogen import cost (105 €/$MWh_{LH_2,LHV}$ instead of 120 €/$MWh_{LH_2,LHV}$) was performed as well. However, deviations from the reference scenario could not be observed and are therefore not presented.

The presentation scheme of the scenario variations resembles the one from the *BELS* scenario branch. For all scenario variations, the total annual cost (TAC) and the installed capacities of *Source* and *Conversion* components are visualized side by side in Figure 5.36 and Figure 5.37. The plots for the secured electricity generation capacities, primary energy sources, general electricity generation and consumption, flexible electricity generation, installed *Storage* capacities and the inter-regional commodity transmissions can be found in the appendix B.2, cf. Figures B.22 – B.29. In the following, each scenario variation is shortly presented, compared to the reference scenario and, if applicable, to the results from the *BELS* scenario branch.

The Value of DC Line Expansions / Domestic DC Lines (1a & 1b)

The omission of DC line expansion / domestic DC lines in general leads to a cost increase of up to 2.8% / 7.9% respectively. In contrast to the *BELS* scenario branch, the removal of domestic DC lines in general is only for the 90% and 95% reduction target the second most expensive scenario variation. For the 100% reduction target, the removal of centralized hydrogen infrastructure components causes higher cost increases.

As for the *BELS* scenario, the removal of the lines leads to a more challenging integration of offshore wind turbines, which are thus built in smaller capacities, and leads to an increase in onshore wind turbines, PV rooftop systems, biogas plants and lithium-ion batteries. Also, electrolyzers and CCGT (GH_2) plants are built in larger capacities and are operated with higher full load hours. With the more decentralized electricity generation, the electrolyzers are distributed more widely across Germany. The CCGT plants on the other hand are more concentrated in and around regions of high electricity demands.

While AC lines are utilized less due to the more decentralized electricity generation, GH_2 pipelines are used more frequently. They serve as an alternative spatial balancing option to the DC lines which can transmit energy from the north of Germany to the rest of the country. While most of the produced hydrogen is directly stored in salt caverns and thus temporally detached from its consumption, a small share of the produced hydrogen is directly sent to CCGT plants in other regions. Thus, it provides a concurrent compensation of spatial generation and demand mismatches.

With increasing restrictions on the carbon dioxide emissions and the eligibility of DC lines, overall more hydrogen is stored in salt caverns. For the 100% reduction target, less salt cavern capacities are considered in comparison to the reference case. However, these are operated with a higher turn-over count, i.e. they are charged and discharged more frequently over the year.

Similar conclusions as for the *BELS* scenario branch can be drawn. Even though the DC lines are removed, a large number of other infrastructure components must be significantly expanded to reach a cost optimal supply system. It must be

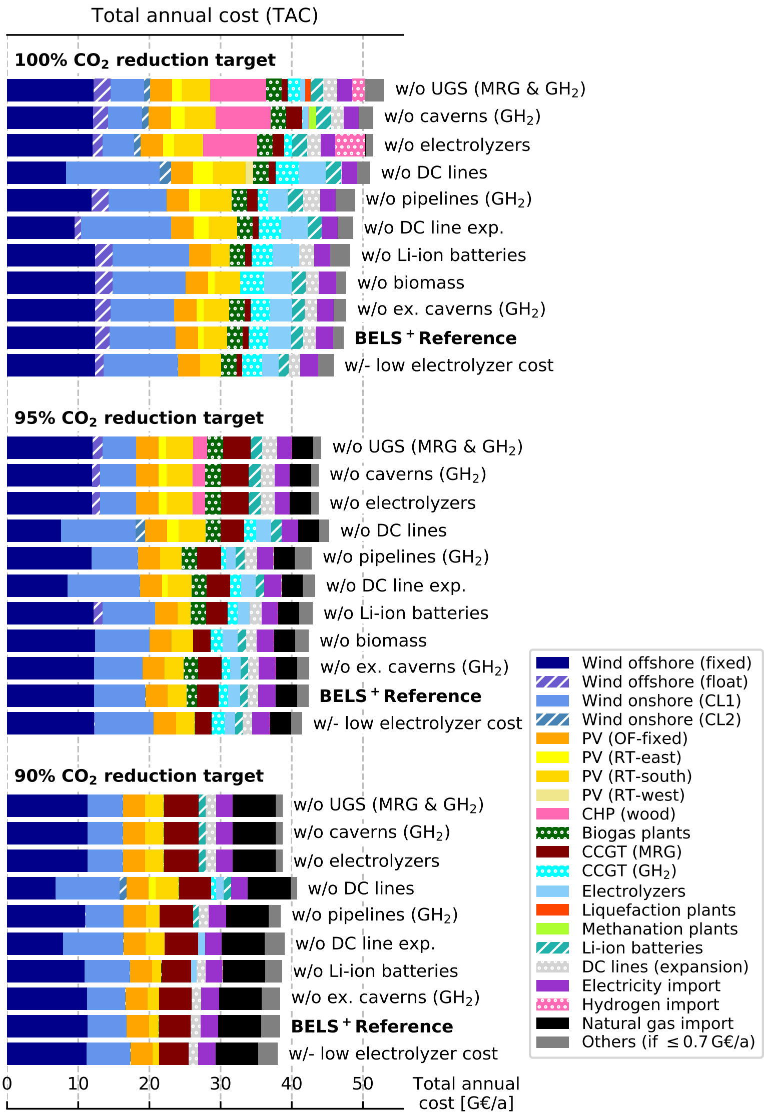

Figure 5.36: Total annual cost in the *BELS+* scenario variations.

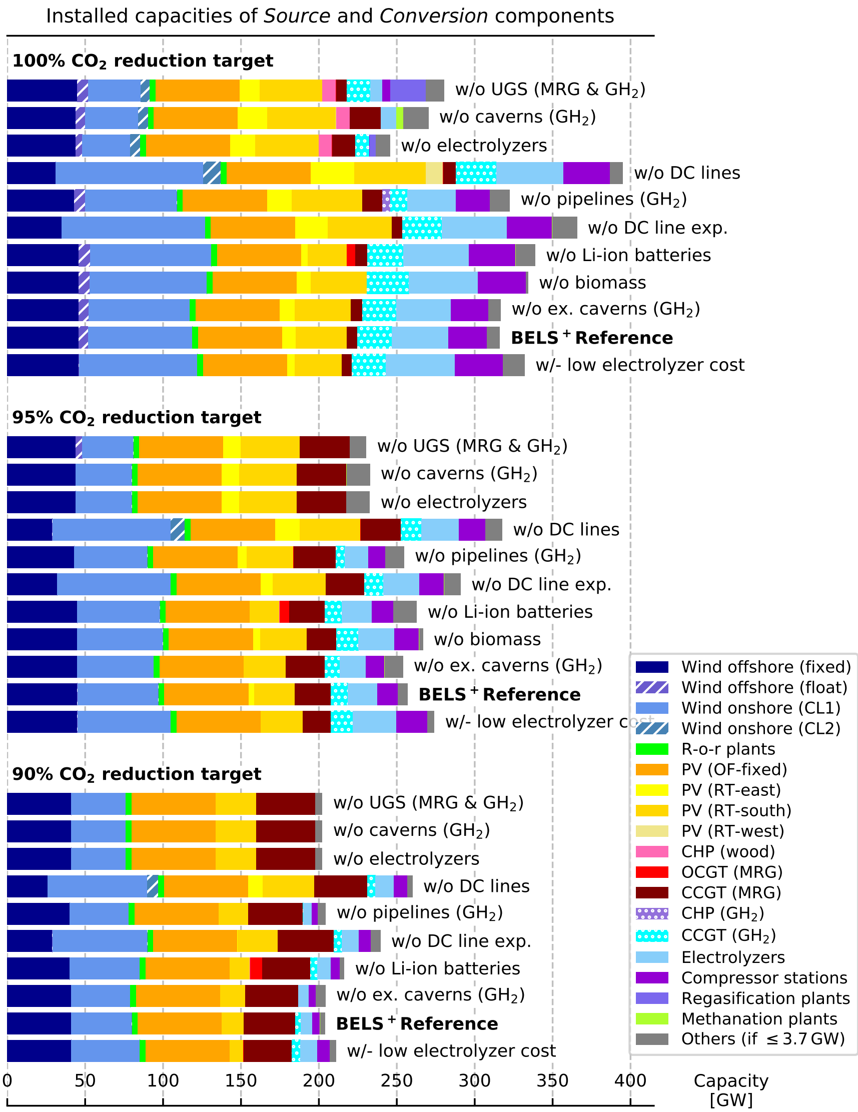

Figure 5.37: Capacities of *Source* and *Conversion* components in the *BELS*$^{+}$ scenario variations.

additionally noted that the considered hydrogen infrastructure plays a key role in buffering the negative effects of the omitted DC lines.

The Value of Hydrogen Transmission in Gas Pipelines (1c)

In this scenario variation, hydrogen transmission pipelines which connect regions are omitted. However, intra-regional sub-networks of electrolyzers, salt caverns and CCGT / OCGT power plants are still eligible.

With the omission of the inter-regional hydrogen transmission by pipeline, the TAC increases in comparison to the *BELS*$^+$ reference case by 0.3-3.3%.

The omission of the pipelines leads to a decrease in onshore wind turbines and an increase in PV rooftop systems. Moreover, the composition and regional distribution of the power plant fleet changes notably. The change is induced by the regional distribution of the electrolyzers which are distributed across North and upper Central Germany in regions which have access to salt caverns. In these regions, intra-regional networks of electrolyzers (31 GW_{el}), hydrogen operated CCGT and CHP plants (11 GW_{el} and 5 GW_{el}) and salt caverns are formed. In comparison to the reference case, less plant capacities for hydrogen reconversion are built. CCGT plants operated on methane-rich gas are primarily built in Central and South Germany and are more centered around electricity demand centers. In comparison to the reference case, the considered plant capacities are increased, however their full load hours are reduced.

Correlated to the increase of PV rooftop systems, the considered lithium-ion battery capacities are increased. Overall, less hydrogen-filled salt caverns are considered. Even though less salt cavern capacities are considered, also more expensive new salt cavern locations are considered.

Without the inter-regional transmission by hydrogen pipeline, the regional mismatch between electricity supply in the North and demand in the inland must be mitigated by alternative means. AC lines are used more frequently. DC lines are further expanded, and more electricity is transmitted through them. Also, MRG pipelines are used more frequently, since less purified biogas is used locally but is transmitted to the electricity demand centers in Central and South Germany.

Even though inter-regional hydrogen transmission is not eligible, intra-regional hydrogen supply networks are still cost-lucrative in combination with the intermittent electricity generation from wind turbines. Thus, the centralized hydrogen supply infrastructure is not only cost-lucrative when it serves as a national spatial balancing option but also in local co-operation, even if this requires the construction of new salt caverns.

The Value of Lithium-ion Batteries (2a)

The impact of the omission of lithium-ion batteries leads to cost increases by 0.8%, 1.4% and 2% for the 90%, 95% and 100% respectively. The relative cost increase is thus less prominent for the *BELS*$^+$ scenario branch than for the *BELS* scenario branch.

Like the *BELS* scenario, the omission of lithium-ion batteries leads to a decrease in PV rooftop systems and an increase in wind turbines, thermal power plants, PHES and DC line expansions for the *BELS*$^+$ scenario. Furthermore, the *Power-to-Hydrogen-to-Power* pathway is considered with larger capacities.

Particularly notable is the increase in OCGT plant capacities, both for MRG and GH_2. For the 100% target, 5.6 GW_{el} (MRG) and 3.4 GW_{el} (GH_2) are considered in the scenario variation while in the corresponding reference case only 0.4 GW_{el} of OCGT plants (MRG) are considered. The OCGT plants are operated with full load hours below 500 h/a and serve to cover peak electricity demands.

As for the *BELS* scenario branch, the scenario variation demonstrates the value of daily, high-efficient energy storage which facilitates the integration of PV systems into the energy supply system. It also highlights the value of the centralized hydrogen infrastructure which buffers the effects resulting from omission of the batteries more robustly.

The Value of Hydrogen Storage in Existing Salt Caverns (2b)

The omission of hydrogen storage in existing salt caverns leads to only small increases in the TAC (0.1%-0.8% for the 90%-100% reduction targets).

In comparison to the reference scenario, the considered capacities for PV rooftop systems, biogas plants and lithium-ion batteries are slightly increased while the capacities of wind turbines, electrolyzers, salt caverns (GH_2) and CCGT plants (GH_2) are reduced. Instead of existing salt cavern locations, new salt cavern locations are selected which are solely located in the north of Germany.

The scenario variation demonstrates that even if new salt caverns for hydrogen storage must be specifically mined, they are still selected in significant numbers (up to 105 caverns). Thus, hydrogen storage in salt caverns is a robust design decision in the considered scenario scope for high carbon dioxide reduction targets.

The Value of Hydrogen Storage in Salt Caverns (2c)

The increase in TAC resulting from the entire omission of hydrogen storage in salt caverns ranges between 0.9% and 8.8% (90%-100% reduction target). For the 90% and 95% reduction target, centralized hydrogen infrastructure components are not considered in any form. Thus, the optimal supply systems correspond to the ones from the *BELS* reference scenario. However, for the 100% reduction target, structural changes appear in the optimal supply system design which are discussed in the following.

For the 100% reduction target, the supply system displays several similarities to the corresponding *BELS* reference scenario. Less wind turbines and more PV rooftop systems and lithium-ion batteries are considered. Also, wood-fired CHPs and the *Power-to-Hydrogen-to-Methane-to-Power* pathway are again considered. However, hydrogen reconversion to electricity is not completely excluded from the system. Hydrogen is supplied by electrolyzers (28 $TWh_{GH_2,LHV}$) and liquid hydrogen (LH_2) import (3.7 $TWh_{GH_2,LHV}$) in the scenario. The LH_2 arrives via shipping in the north of Germany where it is either stored in cryogenic tanks or converted to GH_2 at 100 bar in regasification terminals and subsequently injected into hydrogen transmission pipelines. Gaseous hydrogen in general is either used in methanation plants (4.3 $GW_{MRG,LHV}$) or fed to hydrogen operated CCGT plants (1.9 GW_{el}) to which it is transmitted by pipeline (GH_2). Pipe storage systems (GH_2) are considered as buffer storage at its production and consumption sites.

Even though the system displays structural changes, its overall cost is almost equal to the one of the *BELS* reference scenario with the 100% reduction target (Δ0.06%).

This scenario variation demonstrates the value of hydrogen storage in salt caverns in the investigated scenario scope. Without them, the system falls back to the more conventional supply pathways considered in the *BELS* scenario. With them, electricity generated from wind turbines can be more efficiently integrated into the supply system. All in all, the storage of synthetic gas which was produced via electricity at low LRMC is a robust design decision in the considered scenario scope for high carbon dioxide reduction targets.

The Value of Underground Storage (MRG & GH_2) (2d)

The omission of all underground storage options has a comparably small effect for the 90% reduction target (0.9% cost increase). However, for the 100% reduction target, it leads to the highest cost increase of all scenario variations (12%). Nevertheless, in this case it is still 1.9% less expensive than its counterpart in the

BELS scenario branch (*BELS* - 100% - *w/o UGS (MRG)*).

For all cases, but particularly for the 90% and 95% reduction target, strong resemblances to the supply systems in the *BELS* reference scenarios can be observed. Less onshore wind turbines are built and larger capacities of PV rooftop systems, wood-fired CHPs, biogas plants and lithium-ion batteries are considered.

For the 100% reduction target, the scenario variation substitutes the omission of UGS with 3 $TWh_{MRG,LHV}$ of pipe storage systems for purified biogas. Additionally, cryogenic tanks with a capacity of 6.6 $TWh_{LH_2,LHV}$ are considered. The cryogenic tanks are thereby used as seasonal hydrogen storage. Pipe storage systems (0.5 $TWh_{GH_2,LHV}$) are additionally used as a weekly storage. All in all, a total of 14.8 $TWh_{LH_2,LHV}$ of liquid hydrogen is imported and the hydrogen produced by electrolysis (21 $TWh_{GH_2,LHV}$) is partly liquefied.

Overall, the possibility to import and domestically produce liquid hydrogen, store it in cryogenic tanks and distribute it after regasification via pipeline to hydrogen fueled CCGT plants leads to the above-mentioned cost decrease of 1.9% for the 100% reduction target in comparison to the *BELS* - 100% - *w/o UGS (MRG)*.

In general, the scenario variation highlights the significance of UGS as a low-cost storage option for both, MRG and hydrogen. It also identifies alternative but more expensive storage options, i.e. pipe storage systems and cryogenic tanks.

The Value of Biomass (3a)

Like the *BELS* reference scenario, changes in the TAC only occur for the 95% and 100% reduction target when biogas injection into the pipelines and thus inter-regional MRG transmission is omitted. This results in a full omission of biomass (biogas / wood-fired CHPs). However, these changes are notably smaller (*BELS*$^+$: 0.1%-0.8% (95%-100% reduction target); *BELS*: 1.8%-4.8% (95%-100% reduction target)).

In contrast to the *BELS* reference scenario, significant structural changes in the supply system design do not occur. The capacities of wind turbines and PV rooftop systems are slightly increased. Furthermore, the temporal balancing that was provided by the storage of the purified biogas is compensated by an increase in lithium-ion batteries and an expansion of the *Power-to-Hydrogen-to-Power* pathway. The omission of the spatial balancing option that was provided by the MRG pipelines is mitigated by a slightly increased electricity and hydrogen transmission.

This scenario variation has overall only a small effect on the TAC. It moreover highlights that biogas, and biomass in general, plays only a minor role in the *BELS*$^+$ reference scenario. In general, it demonstrates that the consideration of a centralized *Power-to-Hydrogen-to-Power* pathway can limit the role of biomass in the supply system.

The Value of Electrolyzers (3b)

In this scenario variation, the optimal supply system corresponds to the one from the *BELS* reference scenario for the 90% and 95% reduction target. This means that centralized hydrogen infrastructure components are not considered. The supply systems achieving a 100% reduction target also displays similarities to the corresponding *BELS* reference scenario. However, as it considers additional technologies it is slightly less expensive. In comparison to the *BELS*$^+$ reference scenario, a cost increase by 8.8% is determined.

The omission of electrolyzers leads to a significant decrease in onshore wind turbines for the 100% reduction target which is partly compensated by additional PV rooftop systems, lithium-ion batteries and wood-fired CHP plants. Even though a domestic hydrogen production is not eligible anymore, a *Hydrogen-to-Power* pathway is still considered by importing 35.3 $\mathrm{TWh}_{\mathrm{LH_2,LHV}}$ of liquid hydrogen.

The imported hydrogen is converted to gaseous hydrogen at regasification terminals. There, it is injected into hydrogen pipelines and then transmitted to hydrogen salt caverns or hydrogen-fueled CCGT plants. However, overall fewer salt caverns and hydrogen-fueled CCGT plants compared to the *BELS*$^+$ reference scenario are considered.

The scenario variation demonstrates the value of domestic hydrogen production by electrolysis for high carbon dioxide reduction targets. Also, the scenario variation once more shows that the consideration of hydrogen storage in caverns and reconversion in CCGT plants is a robustly reoccurring design decision for high carbon dioxide reduction targets.

The Value of Low Capacity Specific Investment Cost for Electrolyzers (3c)

As in the *BELS* scenario branch, the capacity specific investment of electrolyzers is set to 300 €/$\mathrm{kW_{el}}$ (initial value: 500 €/$\mathrm{kW_{el}}$) for this scenario variation. For the *BELS*$^+$ scenario branch, the effect of the reduced electrolyzer cost is more notable than in the *BELS* scenario branch. For the 100% reduction target, the TAC decreases by 3%. For the 90% reduction target, the TAC still decreases by 0.8%.

With the consideration of less expensive electrolyzers, the capacities of PV rooftop systems, lithium-ion batteries, PHES and DC line expansions are reduced while the capacities of onshore wind turbines and components of the *Power-to-Hydrogen-to-Power* pathway are increased. For example, the installed capacity of electrolyzers increases from 36 GW_{el} (FLHs: ∅ 3396 h/a) to 44 GW_{el} (FLHs: ∅ 3126 h/a).

This scenario variation gives a perspective of the additional potential of electrolyzers if their capacity specific investment were to drop below 500 €/kW_{el}.

5.3 *BLHYS* - Basic ELectricity and HYdrogen Supply Scenarios

The *BLHYS* scenario branch extends the *BELS*+ scenario branch by the consideration of an exogenously given, low (L-GH_2, 85.5 $TWh_{GH_2,LHV}$), medium (M-GH_2, 167.9 $TWh_{GH_2,LHV}$) or high (H-GH_2, 243.7 $TWh_{GH_2,LHV}$) *basic* hydrogen demand, cf. section 4.2.1. The hydrogen demands cover demands in the transport and industry sector. The hydrogen demand in the energy sector (reconversion to electricity) is endogenously determined during the optimization of the energy supply systems.

In analogy to the previous two sections, first, the optimal system configurations of the *BLHYS* reference scenario under varying carbon dioxide reduction targets (80% and 100%) and hydrogen demands (L-GH_2, M-GH_2 and H-GH_2) are presented and are compared to the ones of the *BELS* and *BELS*+ reference scenarios in subsection 5.3.1. To cover the two extremes of the reference scenario, first the scenario with the 80% reduction target and the L-GH_2 demand is presented and discussed in detail in subsection 5.3.2 and then the scenario with the 100% reduction target and the H-GH_2 demand is presented and discussed in detail in subsection 5.3.3. Scenario variations of the reference scenario are presented and shortly discussed in subsection 5.3.4.

Throughout this section, a specific focus is given on electrolyzers as the key technology to cross-linked infrastructure design in the scenarios. Moreover, hydrogen-related storage and transmission technologies required to supply the additional hydrogen demands are assessed in detail.

5.3.1 Optimal System Configurations under Varying CO_2 Reduction Targets and GH_2 Demands

The total annual cost (TAC) of the *BELS*, *BELS⁺* and *BLHYS* reference scenarios are visualized side by side in Figure 5.38 for varying carbon dioxide reduction targets and, if applicable, for varying hydrogen demands. In the figure, also an estimate of the avoided emissions is given for each of the scenario configurations (in reference to the year 1990, see also Table B.1 in the appendix B.3).

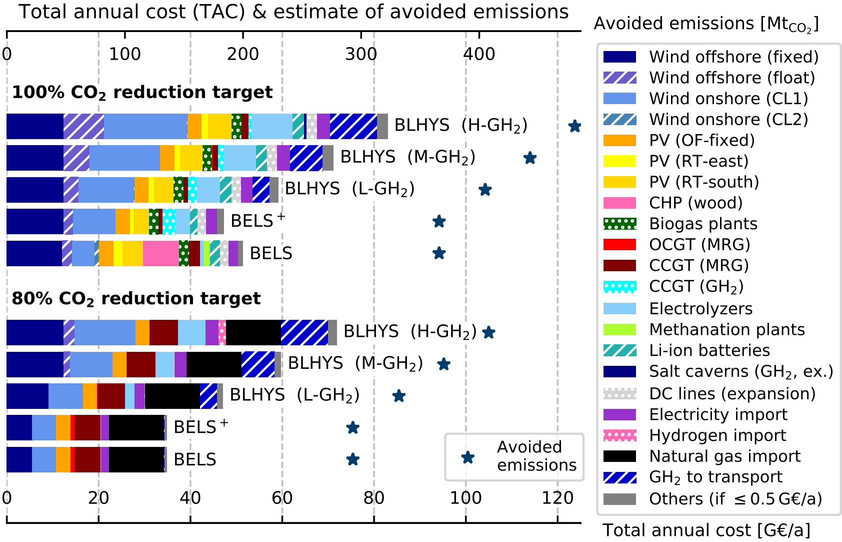

Figure 5.38: Total annual cost and estimate of avoided emissions in the *BELS*, *BELS⁺* and *BLHYS* reference scenario under varying CO_2 restrictions.

In the *BLHYS* scenario and with respect to the *BELS⁺* scenario, the TACs increase by 35% (L-GH_2), 71% (M-GH_2) and 106% (H-GH_2) for the 80% reduction target. For the 100% reduction target, the total annual costs increase by 25% (L-GH_2), 51% (M-GH_2) and 75% (H-GH_2) respectively. These cost increases are accompanied by a larger decarbonization of the energy system, i.e. by increases in the avoided emissions. Prominent increases in the cost contributions occur for onshore and offshore wind turbines, electrolyzers and the intra-regional distribution cost for the hydrogen demand in the transport sector (*GH_2 to transport*). An increase in the cost for PV rooftop systems can be observed as well but is however of smaller magnitude. Only for the 100% reduction target and the H-GH_2 demand, the cost contribution from salt caverns is above 0.5 G€/a. As these components are the key elements of the hydrogen supply chain, these cost increases are reasonable.

In contrast to these components, the cost contribution of hydrogen-fueled CCGT plants decreases with increasing hydrogen demands. Instead of balancing the electricity demand with hydrogen reconversion, the demand is more often satisfied concurrently. While for the L-GH_2 demand, 99.6 TWh_{el} of the electricity demand cannot be directly covered by wind turbines, PV systems and run-of-river plants, this value decreases to 86.3 TWh_{el} for the M-GH_2 demand and to 73.3 TWh_{el} for the H-GH_2 demand. In other words, with an increasing hydrogen demand, more renewable energy sources are built, and a larger share of the electricity demand can be directly supplied, leading to less balancing options for the electricity supply.

Notable is also the consideration of a hydrogen import for the 80% reduction target and the H-GH_2 demand. This anomaly will be explained later in this section in context with the long-run marginal cost of the hydrogen supply.

Further insights into the installed capacities of the considered *Source* and *Sink* components are given in Figure 5.39.

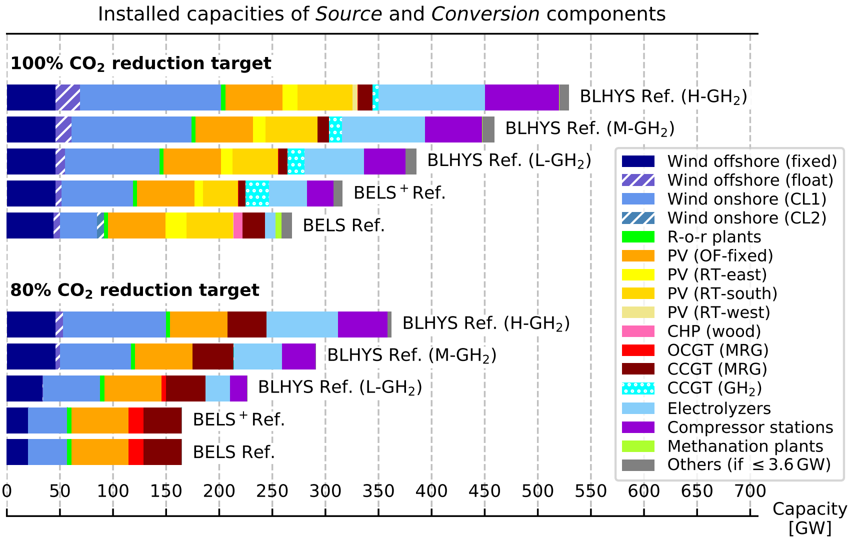

Figure 5.39: Installed capacities of *Source* and *Conversion* components in the *BELS*, *BELS*⁺ and *BLHYS* reference scenario under varying CO_2 restrictions.

The observations which can be made for each component are summarized in the following.

- The capacity potential for offshore wind turbines with a fixed foundation is for the 100% reduction target and all supply systems with a M-GH_2 or H-GH_2 demand almost fully exploited, i.e. close to 46 GW_{el} of turbines are built. For these scenarios, also offshore wind turbines with a floating foundation are considered. For the 100% reduction target and the H-GH_2 demand, a total of 69 GW_{el} of offshore wind turbines is built.

- The amount of additionally considered onshore wind turbines appears to be strongly linked to the increase in the exogenously given hydrogen demands. Between 37 and 133 GW_{el} are installed in the different scenarios. It must be noted that in the 80% reduction target, additional onshore wind turbines are considered to provide electricity for electrolysis instead of, for example, additional PV rooftop systems. These results highlight the synergies arising from the combined consideration of wind turbines and electrolyzers.
- Run-of-river plants are modeled with a fixed capacity of in total 3.8 GW_{el}.
- In all scenarios, the capacity potential of PV open-field systems is fully exploited, i.e. 54 GW_p are built. The systems with a fixed tilt are thereby chosen over the ones with a tracking system.
- PV rooftop systems are only considered for the 100% reduction target. For the scenarios with an exogenously given hydrogen demand, between 54 to 71 GW_p are considered.
- OCGT plants operated on methane-rich gas are only considered for the 80% reduction target in the *BELS*, *BELS*$^+$ and *BLHYS*-L-GH_2 scenario. For all other scenarios, MRG is only converted in the more expensive but also more efficient CCGT plants.
- For the 80% reduction target, the installed capacity of CCGT plants is between 36-39 GW_{el} in all scenarios. For the 100% reduction target, the capacities of CCGT plants increases with increasing exogenously given hydrogen demand. Even though these capacities increase, the generated amount of electricity stays constant at about 19 TWh_{el} in all scenarios except of the *BELS* scenario. The plants are thus operated with lower full load hours and are designed to cover increasing peak loads in the electricity demand.
- Hydrogen reconversion is again not considered for the 80% reduction target but only for the 100% reduction target. As already described previously, the amount of CCGT plants decreases with increasing hydrogen demands.
- The amount of considered electrolyzer capacities increases significantly throughout the scenarios. While for the 80% reduction target no electrolyzer plants are considered in the *BELS* and *BELS*$^+$ scenario, up to 100 GW_{el} are considered for the 100% reduction target. The electrolyzers in the *BLHYS* scenario are operated for the 80% reduction target with average full load hours around 5000 h/a. The full load hours decrease for the 100% reduction target, resulting in average full load hours around 3500 h/a.

- The amount of considered compressor stations is linked to the considered electrolyzers which are modeled with an efficiency of 70%.

Additional figures for the secured electricity generation capacities, primary energy sources, general electricity generation and consumption, and dispatchable electricity generation are given in the appendix B.3 in Figures B.30 – B.34.

Besides lithium-ion batteries and DC line expansions, which have notable contributions to the TAC for the 100% reduction target, several other *Storage* and *Transmission* components again significantly contribute to the supply systems' functionality but have only a small share on the TAC.

The capacities of the installed *Storage* components are visualized side by side in Figure 5.40 for all scenarios, once for all *Storage* components and once for non-geological *Storage*[15].

The installed storage capacities are component-wise assessed and compared with each other.

- Only for the *BELS*-80% and *BELS*$^+$-80% scenario, salt caverns are neither considered for MRG storage nor for hydrogen storage. In all other scenarios, between 7 and 280 salt caverns are considered for the optimal supply systems. These caverns are in all cases placed at in 2017 existing salt cavern locations. Salt caverns for methane-rich gas are filled with purified biogas and, only for the *BELS*-100% scenario, with gas from methanation plants. Hydrogen-filled salt caverns are used to store hydrogen produced by electrolysis and, only for the *BLHYS*-80%-H-GH$_2$ demand, imported hydrogen. Overall, the amount of considered salt caverns is multiplied between the 80% and the 100% reduction target for the respective scenarios and increases with increasing hydrogen demands in the transport and industry sector.
- Existing PHES is modeled with a fixed capacity of 48 GWh$_{el}$. Only for the 100% reduction target, refurbished PHES is considered but is never exploited to its full capacity potential ($<$ 8.9 GWh$_{el}$).
- Lithium-ion batteries are not considered for the 80% reduction target in the *BELS* and *BELS*$^+$ reference scenario but are part of the optimal supply system in all other scenarios. Several observations can be made for the different scenarios.
  - The required battery capacities multiply between the 80% and the 100% reduction targets in all scenarios.

[15] As pore storage is modeled with a fixed capacity of several hundred TWh$_{MRG,LHV}$, it is excluded from the bar plot for improved visibility.

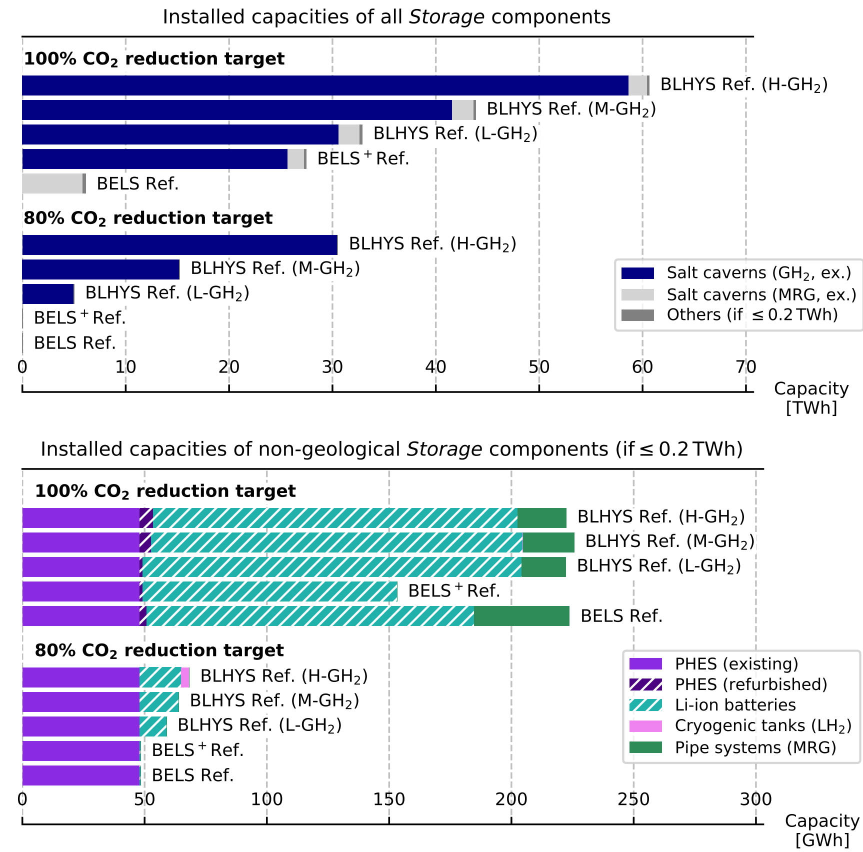

Figure 5.40: Storage design in the *BELS*, *BELS*$^+$ and *BLHYS* reference scenario under varying carbon dioxide reduction targets (pore storage excluded).

- With the option of hydrogen reconversion being available in the *BELS*$^+$ scenario, less battery capacities are required for the 100% reduction target than in the respective *BELS* scenario.
- The increase in the capacities between the *BELS*$^+$ and *BLHYS* scenarios can be explained based on the operation profiles of the CCGT plants. These indicate an increasing focus on the integration of wind turbines into the supply systems. The freed-up integration of PV systems is then undertaken by lithium-ion batteries.
- The required battery capacities in the *BLHYS* scenarios increase

with increasing hydrogen demands for the 80% reduction target and decrease with increasing hydrogen demands for the 100% reduction target. The increase for the 80% reduction target can be linked to the omission of OCGT plants for the M-GH_2 and L-GH_2 demand. The decrease for the 100% reduction can be linked to the fact that a larger share of the electricity demand can be directly supplied with an increasing hydrogen demand and thus less electricity storage is required.

- For the *BLHYS*-80%-H-GH_2 demand scenario, cryogenic liquid hydrogen tanks are installed at the shipping terminal to buffer arriving hydrogen imports.
- Pipe systems are again installed in regions that are not connected to the natural gas grid. There, they store purified biogas and supply MRG to small scale power plants.

The consideration of the additional hydrogen demands thus leads to additional electricity storage capacities in the order of several gigawatt hours. More prominent is however the consideration of several terawatt hours of underground gas storage which are additionally considered in the optimal design of the supply systems.

For *Transmission* components, the annual commodity exchange between regions is visualized side by side in Figure 5.41 for all scenarios[16].

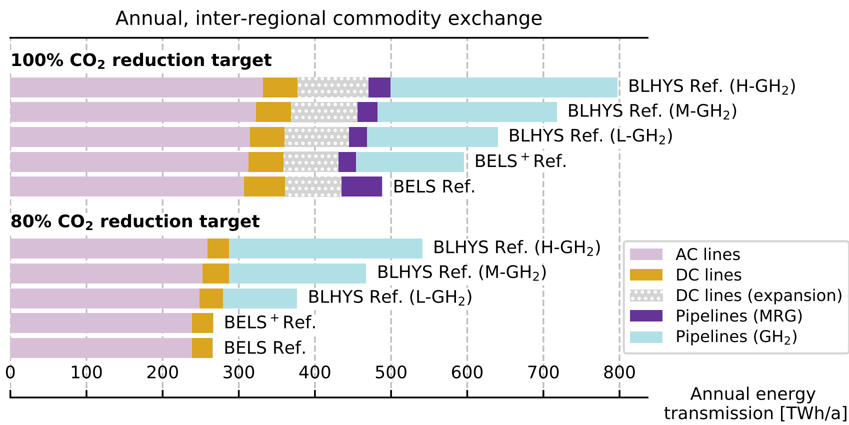

Figure 5.41: Transported commodities in the *BELS*, *BELS*⁺ and *BLHYS* reference scenario under varying carbon dioxide reduction targets.

Several observations can be made for the different transmission technologies.

[16] These values do not consider the intra-regional commodity transmission.

- In general, the additional consideration of hydrogen demands in the transport and industry sector lead to an increased inter-regional electricity exchange and, for the 100% reduction target, also to increased DC line expansions.
- The slight increase in inter-regional MRG transmission within the *BLHYS* scenario can be linked to the decreasing full load hours of the MRG operated CCGT plants, i.e. less MRG is directly consumed but is first transmitted to storage facilities.
- Most prominent is the increased inter-regional hydrogen transmission which is accompanied by an expansion of the considered hydrogen pipeline grid. The contribution of the hydrogen pipeline grid to the TAC equals 169 M€/a for the L-GH_2, 218 M€/a for the M-GH_2 and 266 M€/a for the H-GH_2.

Overall, it can be concluded that with stricter carbon dioxide reduction targets and additional energy demands inter-regional energy exchanges increase and a more divers technology portfolio emerges.

The annual average of the long-run marginal cost (LRMC) of electricity and hydrogen supply[17] are visualized side by side in Figure 5.42 for the *BLHYS* reference scenario.

As for the *BELS* and *BELS*$^+$ scenario, the average LRMC of the electricity supply increases between the 80% and 100% reduction target with less low-cost electricity providers being available. For the 80% reduction target, the LRMCs for the electricity supply increase with an increasing hydrogen demand. However, for the 100% reduction target, the LRMCs for the electricity supply slightly decrease with an increasing hydrogen demand. A reason for this system behavior can be found when assessing the remaining, not utilized RES potentials in the system. For the 80% reduction target, the levelized cost of electricity (LCOE) of the next available, low-cost electricity generator increases notably between the L-GH_2 and H-GH_2 demand scenario. However, for the 100% reduction target, the LCOE of the next available, low-cost electricity generator stays at an almost constant level as most low-cost electricity generators are already utilized to their full potential. The small decrease in the LRMCs can be explained by considering that, as previously explained, a larger share of the electricity demand can be directly supplied with an increasing hydrogen demand. Overall, the additional hydrogen demand increases the LRMCs of the electricity supply in comparison to the *BELS*$^+$ scenario by 5.2% / 9.5% / 14% for the 80% reduction target and by only 3.5% / 3.0% / 2.6% for the 100% reduction target, cf. Figure 5.27 in the previous section.

The difference in the LRMCs for the hydrogen supply to the transport and industry sector is, for a given demand scenario and reduction target, only caused by the

[17] (Σ Regional LRMC profiles $\cdot$ demand) / (Σ demand).

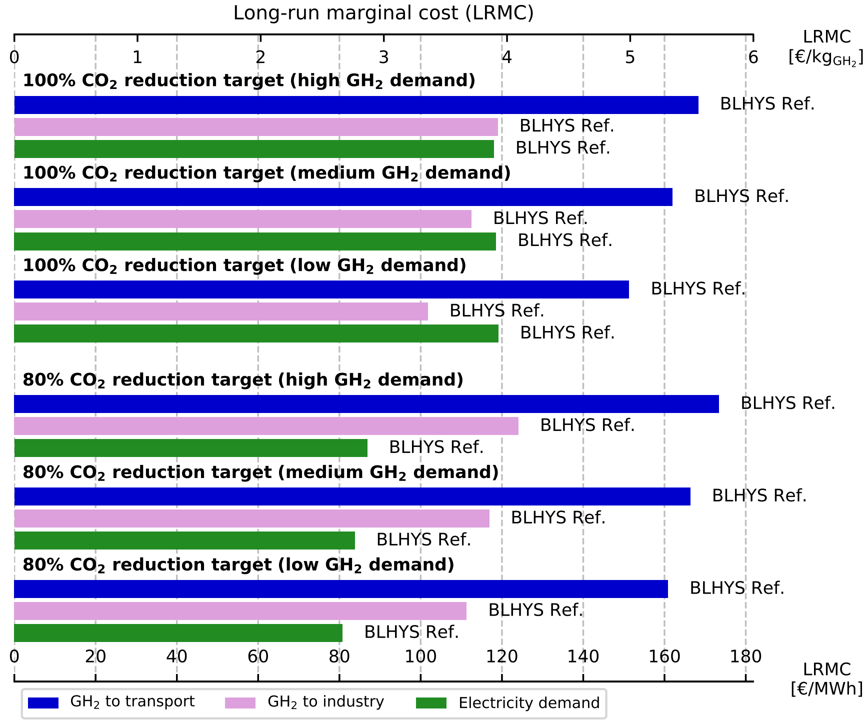

Figure 5.42: Weighted long-run marginal cost in the *BLHYS* reference scenario under varying carbon dioxide reduction targets.

different intra-regional distribution cost. However, most notable is the fact that the LRMCs for the hydrogen supply drop between the 80% and the 100% reduction target. With the omission of natural gas, the capacities of intermittent renewable electricity sources to supply the electricity demand must be significantly expanded. A by-product of this expansion is, in comparison to the 80% reduction target, the larger amount of low-cost electricity which cannot be directly used to supply the electricity demand. The electrolyzers in the 100% reduction target are thus able to operate on “less expensive” electricity, i.e. at times when the LRMCs for the electricity supply is low. Overall, this results in less expensive LRMCs for the hydrogen supply for the 100% reduction target. Thus, Figure 5.42 also indicates why only for the 80% reduction target and the H-GH_2 demand liquid hydrogen import is considered. Only in this configuration, the LRMC of the hydrogen supply is high enough so that liquid hydrogen import becomes a cost-lucrative option.

Summarizing, it can be stated that the consideration of additional hydrogen demands leads to additional infrastructure expansions. Most prominent is here the increase in onshore and offshore wind turbines, electrolyzers, intra-regional hydrogen distribution infrastructure, hydrogen-filled salt caverns, and inter-regional hydrogen transmission pipelines. Less prominent increases can also be observed for PV systems, lithium-ion batteries and DC line expansions. Only hydrogen-fueled CCGT plants are considered in decreasing capacities as a larger share of the electricity demand can be directly supplied with an increasing hydrogen demand. The additional hydrogen demands increase the LRMC cost for the electricity supply by 5.2%-14% for the 80% reduction target and by about 3% for the 100% reduction target. The LRMCs for the hydrogen supply to the transport and industry sector on the other hand decrease between the 80% and 100% reduction target by 2.9%-8.6%.

The following two techno-economic system assessments will focus on the design and operation of the hydrogen supply infrastructure.

5.3.2 Supply System Assessment (L-GH_2, 80% CO_2 Reduction)

The techno-economic parameter overview for the *BLHYS* reference scenario with the 80% reduction target and the L-GH_2 demand is given in Table 5.4. In comparison to the *BELS* reference scenario with the 80% reduction target, cf. Table 5.1, the most prominent changes occur in the considered capacities for wind turbines, electrolyzers, hydrogen-filled salt caverns and hydrogen pipelines. The design and operation of the hydrogen related infrastructure will be the focus of this section.

Electricity Generation, Transmission and Storage

In the following, the electricity generation, transmission and storage infrastructure of the scenario are compared to the reference scenario of the *BELS* scenario branch with an 80% reduction target (*BELS*-80% = *BELS*$^+$-80%).

The considered electricity generation capacities mainly change with respect to the installed wind turbine capacities and the considered thermal power plants. The installed offshore and onshore wind turbine capacities increase by 14 GW_{el} and 17 GW_{el} respectively. The considered capacities of MRG-fueled OCGT plants are reduced by 9.6 GW_{el} while the ones of MRG-fueled CCGT plants are increased by 1 GW_{el}. Peak loads arising from PV generation, which were formerly covered by OCGT plants, are now also partly covered by lithium-ion batteries (+10.6 GWh_{el}).

Table 5.4: Techno-economic parameter overview (*BLHYS*-80%-L-GH_2).

	Capacity	TAC [M€/a]	Operation [TWh/a]	FLHs or TOC [h/a] or [-]
Wind offshore (fixed)	34 GW_{el}	9179	164 (0.3)	4781
Wind onshore (CL1)	54 GW_{el}	7415	133 (0.3)	2485
R-o-r plants	3.8 GW_{el}	450	17.1 (0.3)	4489
PV (OF-fixed)	54 GW_{el}	3136	66 (0.1)	1209
OCGT (MRG)	4.4 GW_{el}	297	4.8	1082
CCGT (MRG)	37 GW_{el}	6056	223	5979
Electrolyzers	23 GW_{el}	2035	122	5375
Compressor stations	16 GW_{GH_2}	105	86	5375
PHES (existing)	48 GWh_{el}	76	7.3 | 5.7	133
Li-ion batteries	11 GWh_{el}	186	3.6 | 3.1	300
Salt caverns (GH_2, ex.)	5.0 TWh_{GH_2}	54	25.4 | 25.4	7.6
AC lines	-	0	248.6	-
DC lines	-	0	31	-
Pipelines (GH_2)	-	77	96.9	-
Electricity export	-	-0.89	0.9	-
Electricity import	-	2276	48	-
Natural gas import	-	12018	364	-
Electricity demand	-	0	528	-
GH_2 to transport	-	3682	70	-
GH_2 to industry	-	51	15.6	-

Capacity: If applicable, w.r.t the lower heating value (LHV). TAC: Total annual cost. Operation: If existing, curtailment is listed in parentheses; for *Storage* components, charging and discharging operation are listed. FLHs or TOC: Full load hours of *Source* and *Conversion* components; turn-over count of *Storage* components.

Overall, the electricity generation capacities are increased and, for thermal power plants, shifted towards plants with higher efficiency.

The regional distribution of electricity generating components is visualized in Figure 5.43. In comparison to the *BELS* scenario with the 80% reduction target, the CCGT plant capacities are redistributed and partly substitute former OCGT plants. The remaining OCGT plant capacities are distributed across Germany. Particularly in the north of Germany, onshore wind turbine capacities are significantly increased.

Again, in comparison to the *BELS* scenario with the 80% reduction target, the grid utilization is slightly increased, cf. Figure 5.8 and Figure B.36 in the appendix B.3. The DC lines between *Lower Saxony*, *North Rhine-Westphalia*, *Baden-Württemberg* and *Bavaria* are more often operated close to their maximum transmission capacity. However, DC line expansions are still not considered.

The regional distribution of the installed electricity storage, along with its annual charging operation, is visualized in Figure 5.44.

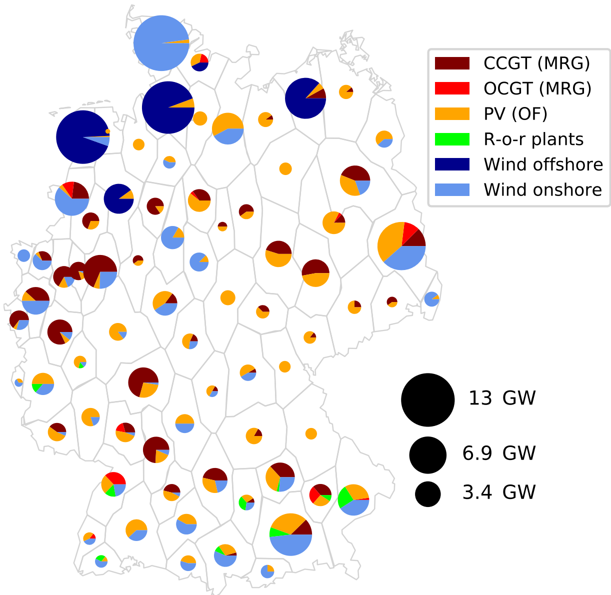

Figure 5.43: Regional distribution of electricity generation capacities (*BLHYS*-80%-L-GH_2).

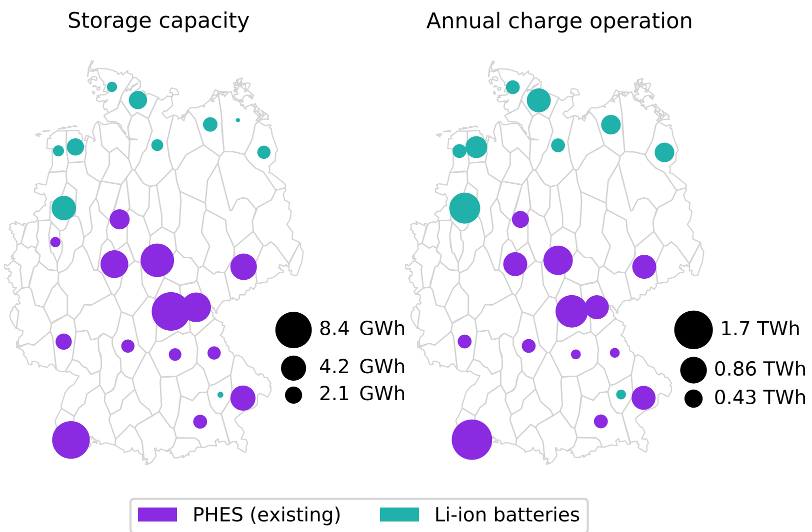

Figure 5.44: Capacities and charging operation of electricity storage (*BLHYS*-80%-L-GH_2).

Lithium-ion batteries are primarily placed in regions in the north of Germany where no existing PHES is available. These regions are often characterized by high wind turbines capacities. However, a closer investigation of the time series of the electricity sources and sinks reveals that the batteries are still primarily used to buffer peaks in the electricity generation caused by PV systems.

Hydrogen Generation, Transmission and Storage

In the scenario, the hydrogen production is located in four regions in the north of Germany which are characterized by large wind turbine capacities, cf. Figure 5.45. From these regions, hydrogen is transmitted to either storage locations or consumers in the transport and industry sector.

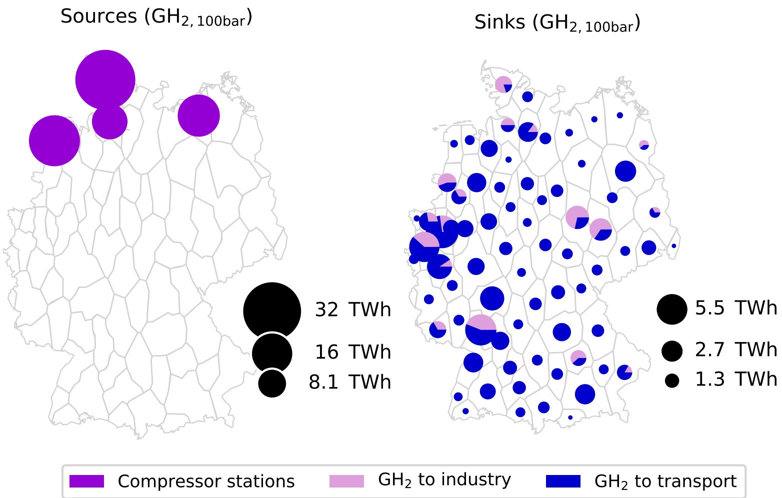

Figure 5.45: Regional distribution of hydrogen sources and sinks (*BLHYS*-80%-L-GH_2; electrolyzers are connected to the compressor stations).

The electrolyzers' production profiles are comparable to the ones presented in Figure 5.14 and Figure 5.30. The former figure represents a typical production profile of an electrolyzer operated on electricity from offshore wind turbines. The latter represents a typical production profile of an electrolyzer operated on electricity from onshore wind turbines.

The regional distribution of salt caverns that are provided for hydrogen storage is visualized in Figure B.35 in the appendix B.3. The storage capacities are located closely to the electrolyzer sites. Within these regions between about one and eight salt caverns are built. An average turn-over count of about 7.6 indicates a seasonal storage operation of the salt caverns which is confirmed when the storage inventories of the caverns are investigated in more detail.

The optimized hydrogen pipeline network is visualized in Figure 5.46. In total, about 6600 km of pipelines are built.

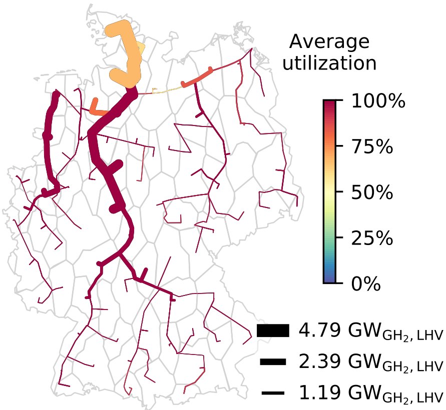

Figure 5.46: Installed capacities and average utilization of hydrogen pipelines (*BLHYS*-80%-L-GH_2).

The main arteries of the pipeline network start at the production and storage locations and then decrease in their capacities towards the end-consumer. The pipeline routes between production and storage facilities are not always used up until their maximum transport capacity, due to the fluctuating production profiles of the electrolyzers. Their capacities are determined based on the maximum production, storage injection or storage withdrawal rates in the connected regions. The pipeline routes that solely transmit hydrogen to the end-consumers, which have constant demand profiles in this scenario, are operated with a constant flow rate and thus have a 100% utilization over the year.

About 75% of the pipeline connections have a transmission capacity of less than 0.45 GW_{GH_2}, which is below the flow capacity modeled for a minimum pipeline diameter of 100 mm. If the minimum pipeline transmission capacity is set to 0.45 GW_{GH_2} and a fixed cost contribution of 340 €/m and operational cost of 5 €/(m·a) are assumed, cf. subsection 4.3.2, the TAC contribution for the pipeline grid adds up to 437 M€/a. The pipeline cost is thus underestimated which results from modeling the supply systems as a linear program instead of a mixed integer linear program. Nevertheless, the transmission pipeline network still contributes with less than 1% to the TAC of the supply system which is a magnitude smaller than the cost contribution for intra-regional hydrogen distribution cost (Σ 3733 M€/a).

Overall, several simplifications are made for the pipeline modeling. For example, the fluid velocity is set to a fixed value even though higher velocities might be eligible, pressure losses are disregarded, parallel pipelines can occur which could be aggregated, the cost for the distribution is estimated based on region diameters and the cost function of the pipelines is linearized. In future work, a more physical accurate pipeline model could be coupled with the optimization output of *FINE* to improve the overall pipeline design and give the regionally resolved supply system design an even higher value, cf. [15, 98].

Long-run Marginal Costs (LRMCs)

Annual averages[18] of 81 €/MWh$_{el}$ / 111 €/MWh$_{GH_2}$ / 162 €/MWh$_{GH_2}$ are obtained for the long-run marginal cost of the electricity / hydrogen to industry / hydrogen to transport supply. Duration curves of the regional LRMCs of the electricity supply and hydrogen supply to the transport sector are visualized in Figure 5.47 together with exemplary LRMC profiles[19].

The duration curves of the electricity supply strongly resemble the profiles of the *BELS*-80% scenario, cf. Figure 5.19, i.e. a few time steps are characterized by a peak in the LRMCs and, for a few regions, about 800 h/a of low LRMCs arise. The profiles of the LRMC display a daily but also seasonal pattern. On average, the LRMCs are highest in the early evening hours in summer. Higher LRMCs correlate with time steps in which lithium-ion batteries are discharged.

The hydrogen supply is on the other hand characterized by comparably constant, regionally invariant LRMCs. A slight decrease in the average LRMC of the hydrogen supply can be observed from the north to the south of Germany (not visualized). The profiles of the LRMC of the hydrogen supply are closely linked to the discharging of hydrogen-filled salt caverns, i.e. they are slightly more expensive in summer when most caverns are being discharged. It can thus be concluded that the availability of low-cost hydrogen transmission and storage infrastructure leads to regionally and temporally balanced LRMCs of the hydrogen supply. Moreover, it

[18] (Σ Regional LRMC profiles · demand) / (Σ demand).

[19] Regional LRMCs of the hydrogen supply to the industry sector = Regional LRMCs of the hydrogen supply to the transport sector - a cost factor for intra-regional distribution.

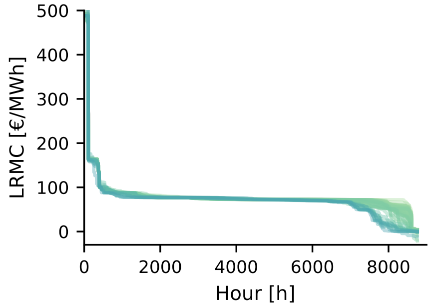

(a) Regional duration curves (electricity)

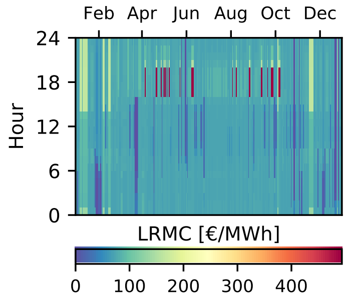

(b) Exemplary profile (electricity)

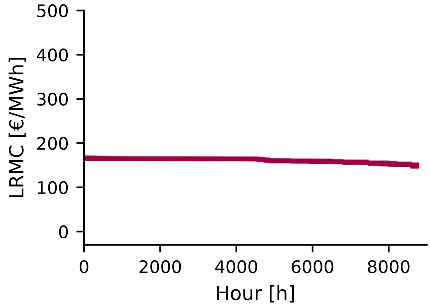

(c) Regional duration curves (GH_2 to transport)

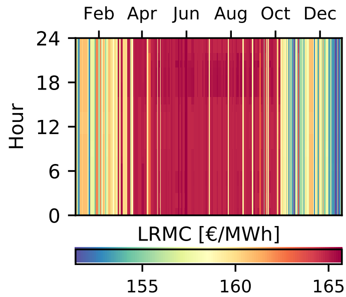

(d) Exemplary profile (GH_2 to transport)

Figure 5.47: Duration curves and profiles of the nodal, long-run marginal cost (*BLHYS*-80%-L-GH_2; duration curve plots: color $\sim \varnothing$ LRMC of a region).

can be concluded that the major cost contributions for the LRMCs of the hydrogen supply arise from cost of hydrogen production and intra-regional distribution.

The electrolyzers in the scenario are operated once the LRMCs of the electricity supply fall below 77.1 €/MWh_{el}. On average, they are operated with LRMCs of 56.3 €/MWh_{el}. For the 100% reduction target and the L-GH_2 demand, this average value drops, with more low-cost LRMCs being available, to 38.1 €/MWh_{el}.

5.3.3 Supply System Assessment (H-GH_2, 100% CO_2 Reduction)

The *BLHYS* reference scenario with the 100% reduction target and the H-GH_2 demand poses with the strictest carbon dioxide reduction target and the highest final energy demand the highest requirements on the supply system. The techno-economic parameter overview for the scenario is given in Table 5.4.

Table 5.5: Techno-economic parameter overview (*BLHYS*-100%-H-GH_2).

	Capacity	TAC [M€/a]	Operation [TWh/a]	FLHs or TOC [h/a] or [-]
Wind offshore (fixed)	46 GW_{el}	12432	220 (0.3)	4808
Wind offshore (float)	23 GW_{el}	8752	123 (0.0)	5276
Wind onshore (CL1)	133 GW_{el}	18153	330 (2.6)	2479
Wind onshore (CL2)	1.1 GW_{el}	165	1.9 (0.0)	1651
R-o-r plants	3.8 GW_{el}	443	15.7 (1.7)	4126
PV (OF-fixed)	54 GW_{el}	3090	64 (0.6)	1199
PV (OF-tracking)	0.8 GW_{el}	61	1.2 (0.0)	1451
PV (RT-east)	14 GW_{el}	1432	16.0 (0.2)	1114
PV (RT-south)	52 GW_{el}	5184	61 (0.6)	1178
PV (RT-west)	4.8 GW_{el}	476	5.4 (0.1)	1127
Biogas plants	3.5 GW_{biogas}	2148	31	8760
Biogas purification	3.5 GW_{MRG}	170	31	8730
CCGT (MRG)	14 GW_{el}	1526	19	1418
CCGT (GH_2)	5.7 GW_{el}	635	7.6	1326
Electrolyzers	100 GW_{el}	8932	365	3662
Compressor stations	70 GW_{GH_2}	460	256	3662
PHES (existing)	48 GWh_{el}	76	8.9 | 7.0	162
PHES (refurbished)	5.5 GWh_{el}	69	1.0 | 0.8	158
Li-ion batteries	149 GWh_{el}	2411	44.0 | 38.9	281
Salt caverns (GH_2, ex.)	59 TWh_{GH_2}	634	129.8 | 129.8	3.3
Pipe systems (MRG)	20 GWh_{MRG}	4.5	0.2 | 0.2	14
Pore storage (MRG)	191 TWh_{MRG}	18	17.5 | 17.5	0.2
Salt caverns (MRG, ex.)	1.8 TWh_{MRG}	5.7	6.2 | 6.2	4.8
AC lines	-	0	331.8	-
DC lines	-	0	45.7	-
DC lines (expansion)	-	2262	92.7	-
Pipelines (MRG)	-	24	29.3	-
Pipelines (GH_2)	-	266	297.5	-
Electricity export	-	-10.03	10	-
Electricity import	-	2839	56	-
Electricity demand	-	0	528	-
GH_2 to transport	-	10233	202	-
GH_2 to industry	-	60	42	-

Capacity: If applicable, w.r.t the lower heating value (LHV). TAC: Total annual cost. Operation: If existing, curtailment is listed in parentheses; for *Storage* components, charging and discharging operation are listed. FLHs or TOC: Full load hours of *Source* and *Conversion* components; turn-over count of *Storage* components.

In comparison to all of the previously presented scenarios, the considered capacities for wind turbines, electrolyzers, hydrogen-filled salt caverns and hydrogen pipelines are again notably expanded. Within this section, the design and operation of the hydrogen related infrastructure of the *BLHYS*-100%-H-GH_2 scenario will be compared to the one from the *BLHYS*-80%-L-GH_2 scenario.

Electricity Generation, Transmission and Storage

In the following, the electricity generation, transmission and storage infrastructure of the scenario are compared to the *BELS*$^+$ scenario branch with an 100% reduction target.

Prominent changes in the electricity generation capacities between the *BLHYS*-100%-H-GH_2 scenario and the *BELS*$^+$-100% scenario can be found in almost all components. The considered capacity of intermittent renewable energies is multiplied. Wind turbine capacities are increased by 17.2 GW_{el} / 66 GW_{el} (offshore / onshore). PV rooftop system capacities are increased from 42 GW_p to 71 GW_p. Also, the amount of MRG-fueled power plants is increased (+7 GW_{el}). The capacity of hydrogen-fueled CCGT plants is however reduced (-16.3 GW_{el}).

The regional distribution of electricity generating components is visualized in Figure 5.48.

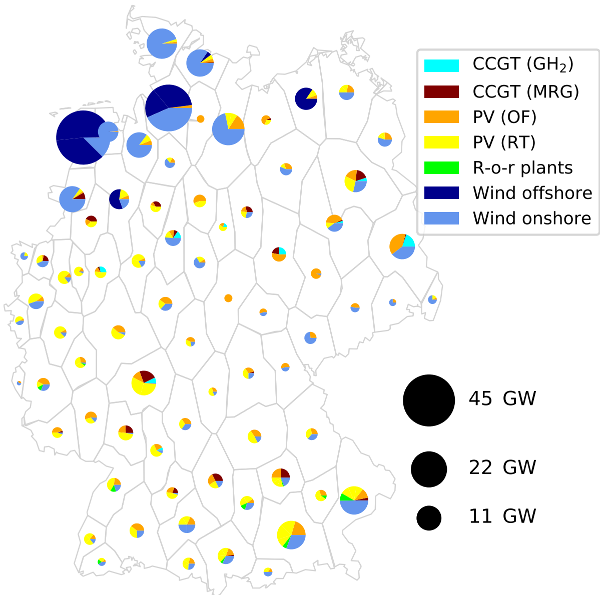

Figure 5.48: Regional distribution of electricity generation capacities (*BLHYS*-100%-H-GH_2).

Onshore wind turbines are primarily placed in the *Lower Saxony* and

Mecklenburg-Western Pomerania. Several gigawatts of capacity are also placed in southern *Bavaria* and North-Eastern Germany. Rooftop PV systems are not considered for several regions in the new federal states of Germany. However, in these regions, electricity generation from open-field PV systems is prominent.

The utilization of the electric grid is similar to the *BELS*$^{+}$-100% scenario, cf. Figure B.21 and Figure B.37 in the appendix B.3. The same AC lines indicate congestions, however, in the *BLHYS*-100%-H-GH_2 scenario with a higher frequency. The DC lines between the *North Sea* and *North Rhine-Westphalia* as well as the one between the *North Sea* and *Northern Bavaria* are expanded. These expansions are larger in the *BLHYS*-100%-H-GH_2 scenario (+2.5 GW_{el} and +1 GW_{el}). The DC line connecting the east and south of Germany is once more not well adapted into the supply system and appears to be oversized.

Electricity storage is widely distributed across Germany. Several regions with low storage capacities are supported by CCGT plants to balance local demand. Lithium-ion batteries are again primarily used as a daily storage option, i.e. they store electricity during noon and then discharge it in the evening. However, in several regions, they are also used to store electricity during noon to balance downtimes of wind turbines during night.

Hydrogen Generation, Storage and Transmission

In the *BLHYS*-100%-H-GH_2 scenario, hydrogen production sites can not only be found in the north of Germany but also in the west and south of Germany. In general, these sites are either located in regions which have ample renewable energies or in regions which are well connected to other regions with ample renewable energies. From these production sites, the hydrogen is sent via pipeline to either salt caverns or end-consumers in the electricity, transport or industry sector, cf. Figure 5.49.

A closer investigation reveals the differences in the operation of electrolyzers that are located close to the *North-* and *Baltic Sea* versus the ones that are positioned in the inland. Exemplary operation profiles are given in Figure 5.50. In general, two patterns can be observed in the operation profiles. One displays similarities to the electricity generation of wind turbines and the other displays similarities to the electricity generation of PV systems. The closer the electrolyzers are positioned to the shore, the more dominant the former profile becomes (FLHs: 3120-4750 h/a). Oppositely, the closer the electrolyzers are located in the inland, the more dominant the latter profile becomes (FLHs: 2800-3340 h/a).

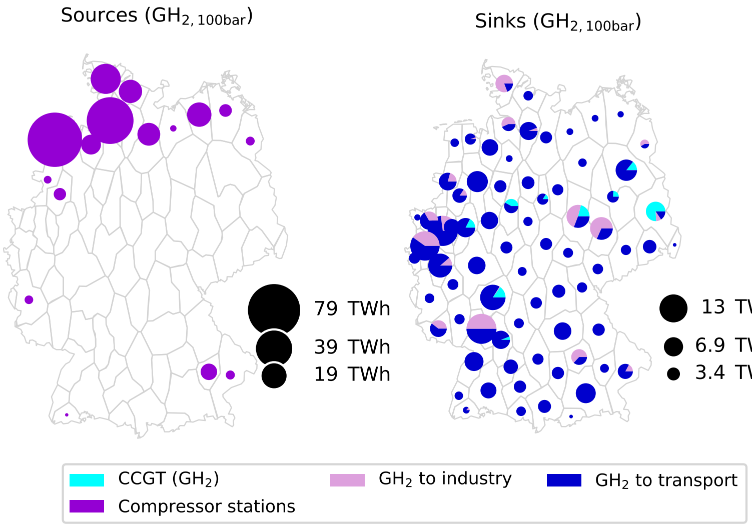

Figure 5.49: Regional distribution of hydrogen sources and sinks (*BLHYS*-100%-H-GH_2; electrolyzers are connected to the compressor stations).

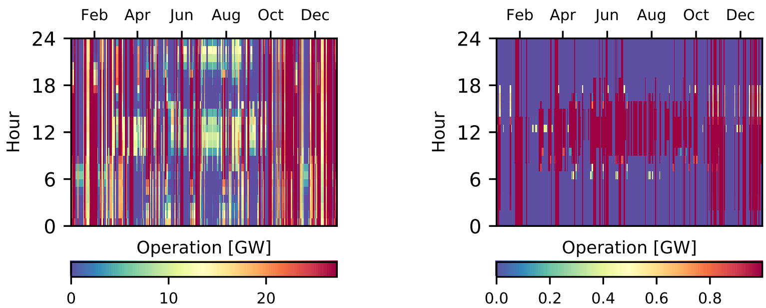

(a) Shore (*East Frisia*, FLHs: 4165 h/a) **(b)** Inland (*NRW*, FLHs: 2803 h/a)

Figure 5.50: Electrolyzer operation close to shore and in the inland (*BLHYS*-100%-H-GH_2, *NRW*: *North Rhine-Westphalia*, FLHs: full load hours).

The considered hydrogen-filled salt cavern capacities and their annual charging operation are visualized in Figure 5.51.

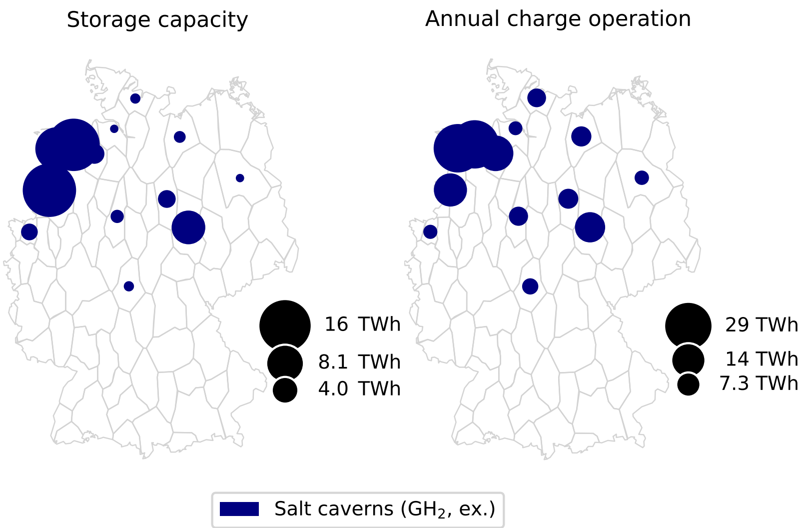

Figure 5.51: Capacities and charging operation of hydrogen storage (*BLHYS*-100%-H-GH_2).

In comparison to the *BLHYS*-80%-L-GH_2 scenario, salt caverns are not only positioned in North Germany but also in Central Germany. In these regions, between 2 and 77 salt caverns are considered. In total, a capacity of 59 $TWh_{GH_2,LHV}$ is utilized, i.e. 278 salt caverns, in the scenario (maximum capacity potential: 67 $TWh_{GH_2,LHV}$). The salt caverns are again used as for seasonal storage, cf. Figure 5.52. They are primarily charged when the electricity generation from wind turbines is high, i.e. in fall, winter and the beginning of spring, and are discharged during spring and summer to overcome downtimes in the hydrogen production at electrolyzer sites.

The optimized hydrogen pipeline network is visualized in Figure 5.53. About 7000 km of pipelines are considered for the scenario. The main arteries of the pipeline network start again at the production and storage sites and then decrease in their capacities towards the end-consumer. With the considered thermodynamical assumptions on the fluid flow, a maximum pipeline diameter of about 1200 mm is considered in the pipeline grid.

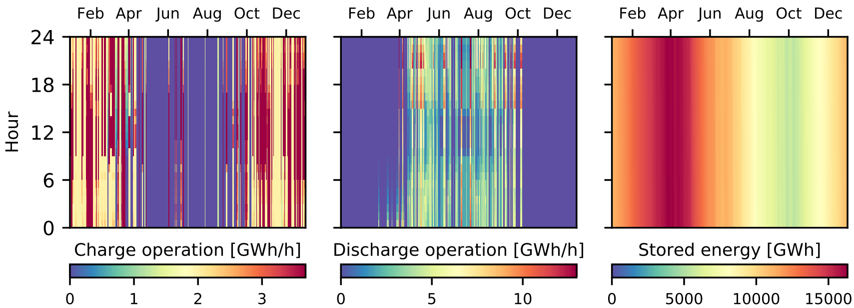

Figure 5.52: Exemplary operation profile of hydrogen-filled salt caverns (*BLHYS*-100%-H-GH_2).

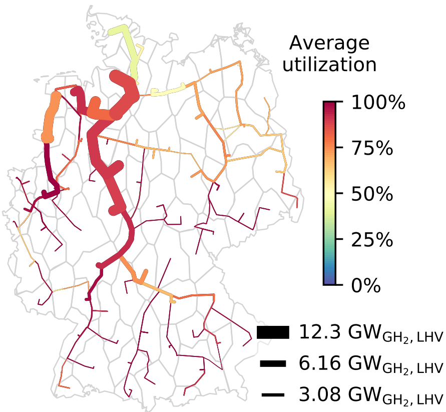

Figure 5.53: Installed capacities and average utilization of hydrogen pipelines (*BLHYS*-100%-H-GH_2).

In comparison to the *BLHYS*-80%-L-GH_2 scenario, a higher number of pipeline segments does not display an average utilization of 100% during the year. This is on the one hand caused by the wider geographical distribution of the electrolyzers but on the other hand also by the consideration of hydrogen-fueled CCGT plants. The latter have, in contrast to the demands in the transport and industry sector, fluctuating demand profiles.

In the scenario, 68% of the pipelines connections have a transmission capacity below 0.45 GW_{GH_2} (*BLHYS*-80%-L-GH_2: 75%). If the minimum pipeline transmission capacity is again set to 0.45 GW_{GH_2}, i.e. to a pipeline diameter of 100 mm, and a fixed cost contribution of 340 €/m and operational cost of 5 €/(m·a) are assumed, cf. subsection 4.3.2, the TAC contribution for the pipeline grid adds up to 608 M€/a. It thus contributes with 1% and not 0.5% to the TAC of the supply system. This cost share is again a magnitude smaller than the cost contribution for intra-regional hydrogen distribution (Σ 10296 M€/a).

Long-run Marginal Costs (LRMCs)

Annual, average long-run marginal costs[20] of 118 €/MWh_{el} / 119 €/MWh_{GH_2} / 168 €/MWh_{GH_2} are obtained for the electricity / hydrogen to industry / hydrogen to transport supply.

Duration curves of the regional LRMCs of the electricity supply are visualized in Figure 5.54 for the *BLHYS*-80%-H-GH_2 and *BLHYS*-100%-H-GH_2 scenario. An

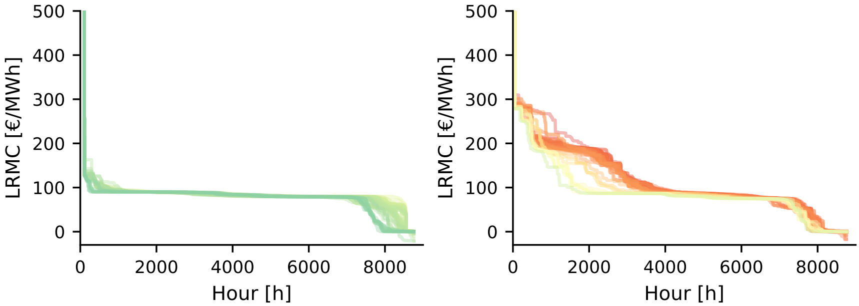

(a) *BLHYS*-80%-H-GH_2 **(b)** *BLHYS*-100%-H-GH_2

Figure 5.54: Duration curves of the nodal, long-run marginal cost (*BLHYS*-80%-H-GH_2 vs. *BLHYS*-100%-H-GH_2).

increase in the number of time steps in which the LRMCs are close to 0 €/MWh and an increase in the number of time steps in which the LRMCs are above 100 €/MWh can be noted. Similar observations were made for the *BELS* and *BELS*$^+$ scenario, cf. Figure 5.19 and Figure 5.34.

The LRMC duration curves in regions with electrolyzers and the corresponding

[20] (Σ Regional LRMC profiles · demand) / (Σ demand).

electrolyzer operation profiles are visualized for the *BLHYS*-80%-H-GH_2 and the *BLHYS*-100%-H-GH_2 scenario in Figure 5.55[21].

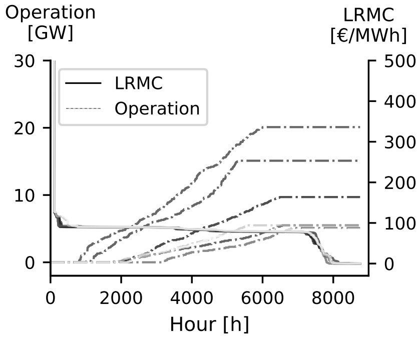

(a) *BLHYS*-80%-H-GH_2

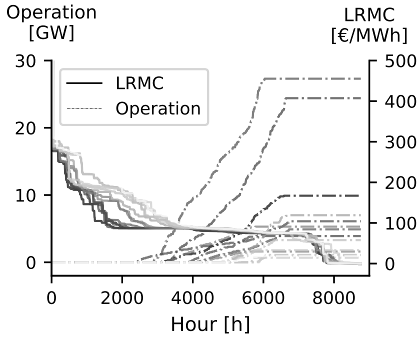

(b) *BLHYS*-100%-H-GH_2

Figure 5.55: LRMC duration curves in regions with electrolyzers and corresponding electrolyzer operation profiles (*BLHYS*-80%-H-GH_2 vs. *BLHYS*-100%-H-GH_2; color $\sim \varnothing$ LRMC of a region).

The electrolyzers are again operated with their maximum production rate when the LRMC is equal to 0 €/MWh_{el}. They can also be operated when the LRMC is smaller than 90 €/MWh_{el} (80%-H-GH_2) or 86.7 €/MWh_{el} (100%-H-GH_2). The annual average of the LRMCs used by the electrolyzers are equal to 64.1 €/MWh_{el} (80%-H-GH_2) and 53.2 €/MWh_{el} (100%-H-GH_2). This difference in the operational cost of the electrolyzers is directly linked to the differences between the average LRMCs for the hydrogen supply for the 80% and 100% reduction target.

The regional time series of the hydrogen supply's LRMCs are again characterized by seasonal profiles with a small amplitude and only small regional differences. Thus, also for this scenario configuration, the LRMCs for the hydrogen supply indicate that the cost impact of storage and transmission infrastructure is comparably small, because of their low cost, and that the major cost contributions to the LRMCs arise from the hydrogen production and intra-regional distribution.

5.3.4 Scenario Variations

For the *BLHYS* scenario branch, the following scenario variations are considered.

[21] For improved visibility, operation curves are sorted and only shown for regional capacities above 0.5 GW_{el}.

1. Value of transmission infrastructure components:
   (a) The system is modeled without DC line expansions (*w/o DC line exp.*).
   (b) The system is modeled without DC lines in general (*w/o DC lines*).
   (c) The system is modeled without hydrogen pipelines (*w/o pipelines (*GH_2*)*).
2. Value of storage infrastructure components:
   (a) The system is modeled without lithium-ion batteries (*w/o Li-ion batteries*).
   (b) The system is modeled without hydrogen storage in existing salt caverns (*w/o ex. caverns (*GH_2*)*).
   (c) The system is modeled without hydrogen storage in salt caverns (*w/o caverns (*GH_2*)*).
   (d) The system is modeled without underground storage (*w/o UGS (MRG &* GH_2*)*).
3. Value of selected *Source* and *Conversion* components on the storage and transmission infrastructure design:
   (a) The system is modeled without biomass (*w/o biomass*).
   (b) The system is modeled without centralized hydrogen reconversion (*w/o* GH_2 *reconversion*).
   (c) The system is modeled without electrolyzers (*w/o electrolyzers*).
   (d) The system is modeled with lower cost for liquid hydrogen import (105 €/$MWh_{LH_2,LHB}$) (*w/- low* LH_2 *import cost*).
   (e) The system is modeled with a lower capacity specific investment cost for electrolyzers (300 €/kW_{el}) (*w/- low electrolyzer cost*).

The presentation scheme of the scenario variations resembles the one from previously presented branches. The results of the variations are only shown for the 80% and 100% carbon dioxide reduction target but there for all hydrogen demand scenarios (L-GH_2 / M-GH_2 / H-GH_2). The total annual cost (TAC) and the installed capacities of *Source* and *Conversion* components are visualized side by side in Figure 5.56 – Figure 5.59. The plots for the secured electricity generation capacities, primary energy sources, general electricity generation and consumption, flexible electricity generation, installed *Storage* capacities and the inter-regional commodity transmissions can be found in the appendix B.3, cf. Figures B.38 – B.53. Each scenario variation is shortly presented, compared to the reference scenario and, if applicable, to the results from the *BELS* and *BELS*$^+$ scenario branch.

The Value of DC Line Expansions / Domestic DC Lines (1a & 1b)

The omission of DC line expansions / domestic DC lines in general leads to an increase of up to 3% / 7.6% in the TAC.

As for the scenario variations in the *BELS* and *BELS*$^+$ scenario branch, the capacity of offshore wind turbines is reduced as it is more difficult to distribute their electricity without the consideration of DC lines. Onshore wind turbines and PV rooftop systems are built with increased capacities to compensate the reduced electricity generation from offshore wind turbines. For the 100% reduction target, wood-fired CHPs are additionally considered.

For the 80% reduction target, additional capacities for electrolyzers are considered but operated with smaller full load hours. Also for the 100% reduction target, additional capacities for electrolyzers are considered and broadly distributed across Germany. In contrast to the 80% reduction target, these are operated with higher full load hours. The additionally produced hydrogen is used in the energy sector, i.e. the amount of electricity provided by hydrogen operated CCGT plants is increased.

With the hydrogen reconversion pathway being most cost-lucrative in the L-GH_2 demand scenario, the considered amount of lithium-ion batteries is reduced in comparison to the corresponding reference scenario. However, in the H-GH_2 demand scenario, the reconversion pathway is less attractive and additional lithium-ion batteries are built as a balancing option.

Again, AC lines are utilized less in the scenario variations while hydrogen pipelines are utilized more. The latter results from an interplay of increased hydrogen storage, a broader distribution of the electrolyzer sites and the additional hydrogen demands in the energy sector.

Similar conclusions as in the previously presented scenario variations can be drawn. When DC lines are not expanded / removed, a large number of other infrastructure components must be significantly expanded to reach a cost optimal supply system. The spatial and temporal balancing options provided by the hydrogen infrastructure can buffer the negative effects of the removal of the lines to a certain extent. Overall, the annual LRMCs of both, electricity and hydrogen supply, are increased.

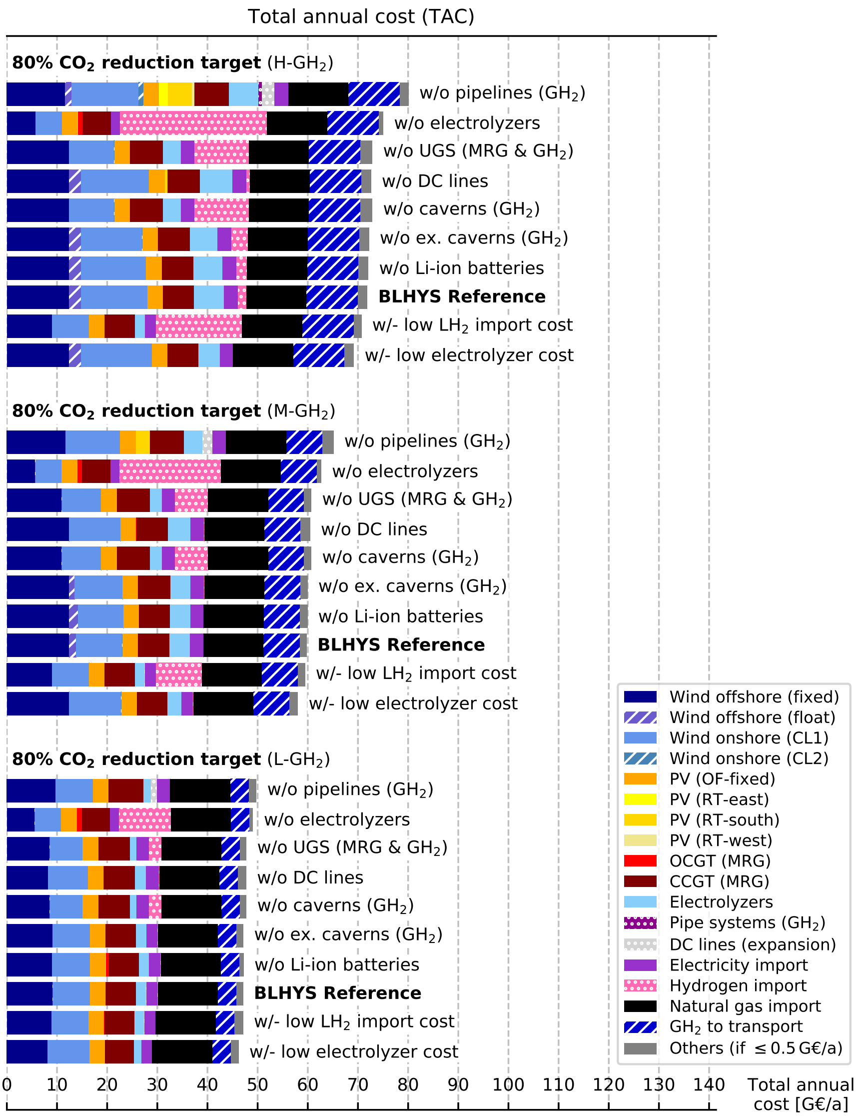

Figure 5.56: Total annual cost in the *BLHYS*-80% scenario variations.

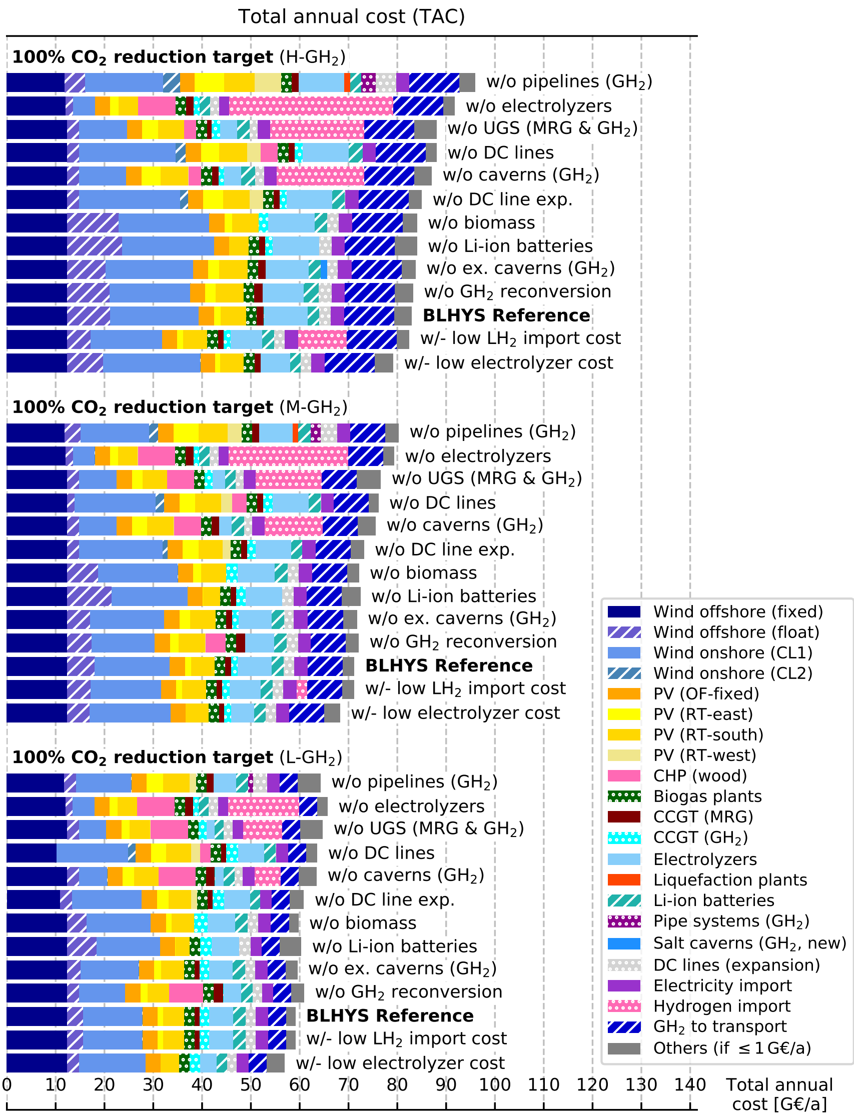

Figure 5.57: Total annual cost in the *BLHYS*-100% scenario variations.

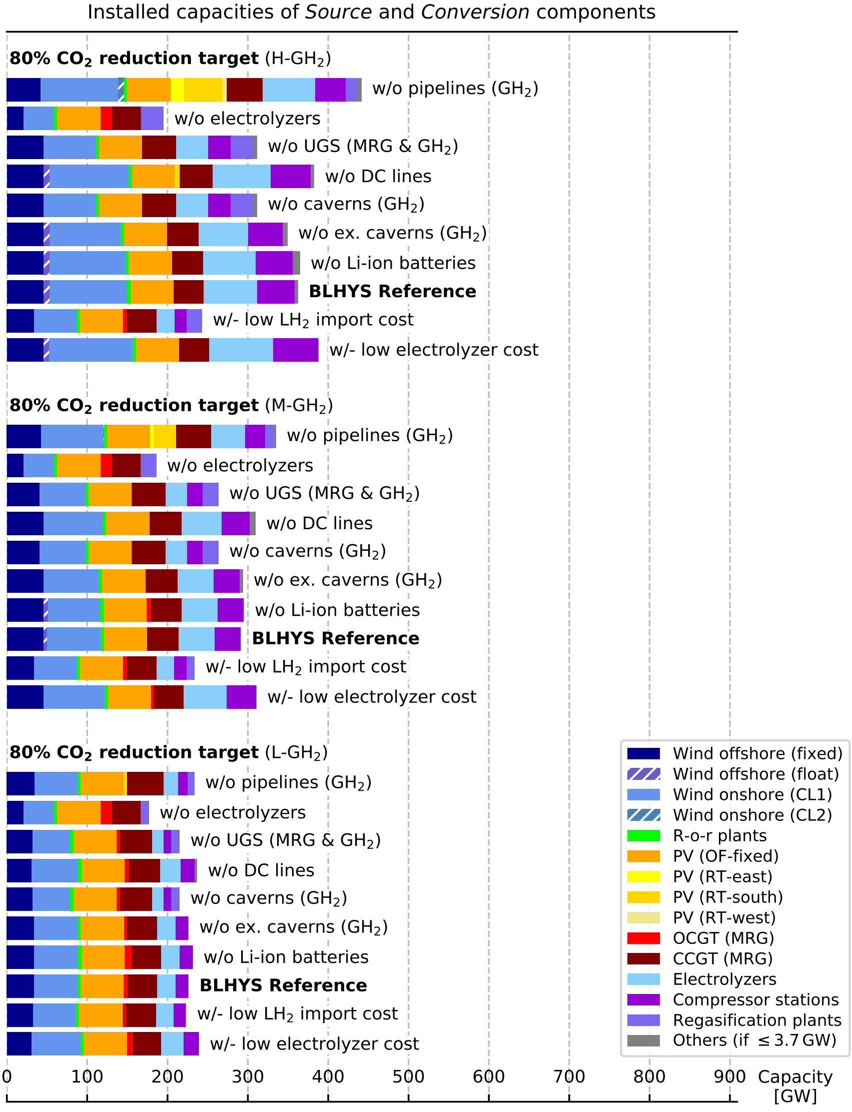

Figure 5.58: Capacities of *Source* and *Conversion* components in the *BLHYS*-80% scenario variations.

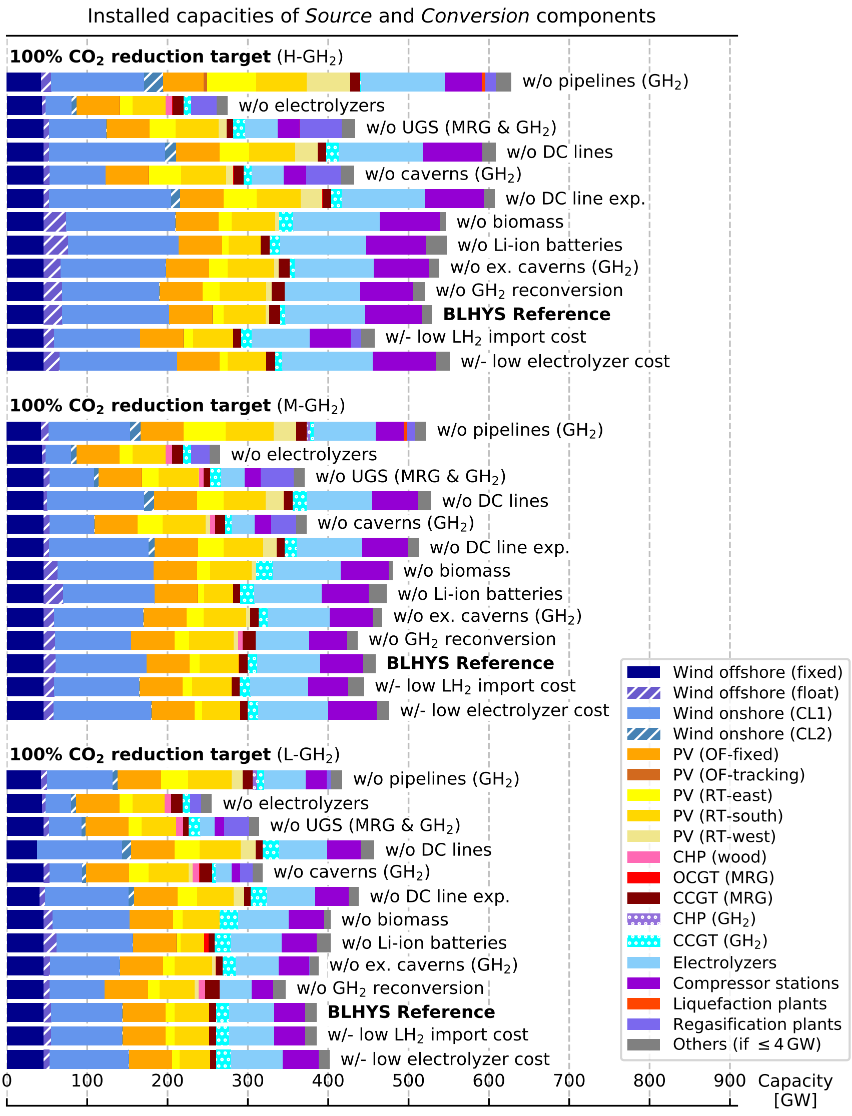

Figure 5.59: Capacities of *Source* and *Conversion* components in the *BLHYS*-100% scenario variations.

The Value of Hydrogen Transmission in Gas Pipelines (1c)

The omission of inter-regional hydrogen transmission pipelines has a far-reaching impact on the structural design of the energy supply systems and leads to the most expensive system designs within the considered scenario variations. For the 80% reduction target, the omission of the pipelines leads to a cost increase of 5.7% / 9.0% / 11.4% for the L-GH_2 / M-GH_2 / H-GH_2 demand, respectively. For the 100% reduction target, the omission of the pipelines leads to a cost increase of 8.8% / 12.8% / 15.7% for the L-GH_2 / M-GH_2 / H-GH_2 demand, respectively.

In the scenario variation, regions which have large wind turbine potentials with good full load hours cannot be used to supply hydrogen via large-scale, centralized electrolyzers to other regions anymore. Thus, for all scenario configurations, the total capacity of wind turbines is reduced and hydrogen imports are fully omitted. The turbines which are considered are distributed more widely across Germany and even large amounts of wind turbines from *Class II* are considered. With the omission of the hydrogen pipelines as a spatial balancing option, DC lines are expanded further to transmit the electricity from offshore wind turbines from the north to the south of Germany. In general, more electricity is transmitted between regions.

As a larger amount of electricity needs to be generated in each region to produce hydrogen locally for the demands in the industry and transport sector, the installed capacities of PV rooftop systems are significantly increased, almost reaching the maximum defined potential. For some regions, even the more expensive PV open-field systems with a tracking system are considered instead of the ones with a fixed angle to increase the full load hours of the electricity supply.

For the 100% reduction target, flexible electricity generation is still provided by MRG-operated CCGT plants but also by hydrogen-fueled CCGT plants. However, the latter are built in smaller capacity. Additionally, in the north of Germany, hydrogen-fueled CHP plants are considered for the L-GH_2 and M-GH_2 demand. The hydrogen-fueled power plants form, together with electrolyzers, salt caverns, pipe systems and cryogenic tanks, local, intra-regional supply networks.

Electrolyzers are located in each region. For the 80% reduction target, they are built in smaller capacity but are operated with larger full load hours. For the 100% reduction target, they are on average built in smaller capacity but are also operated with smaller full load hours. The reduced hydrogen production is linked to the reduced hydrogen-fueled CCGT plant capacities. For hydrogen storage, a wider portfolio of storage technologies is considered. Wherever possible, hydrogen is stored in existing salt caverns or, as a second option, in newly built caverns. Overall fewer salt caverns are built as they only have to buffer the local hydrogen production in a few regions. If salt caverns cannot be built in the regions, a mixture of cryogenic tanks, together with liquefaction and regasification plants, and pipe storage systems is considered. The cryogenic tanks are used as a monthly / seasonal storage while the pipe storage systems buffer daily fluctuations.

Overall, the scenario variation clearly demonstrates the benefits of the hydrogen pipeline system for the considered demand scenarios. As the considered hydrogen demands are larger than the one endogenously arising in the *BELS*$^+$ scenario branch, the effect of the omission of the pipelines is consequently larger. This effect could be mitigated to a certain extent if alternative hydrogen transmission options were considered in the supply system, as for example trucks for gaseous or liquid hydrogen transport. It can be concluded that, from a cost-perspective, a cost-efficient hydrogen transmission technology is indispensable in future energy systems with notable, regionally distributed hydrogen demands.

The Value of Lithium-ion Batteries (2a)

The omission of lithium-ion batteries only has a small effect on the scenarios with the 80% reduction target (TAC increase $< 0.2\%$). For the 100% reduction target however, a TAC increase of up to 2% can be observed.

For the 80% reduction target, the omission of the batteries is partly compensated by OCGT plants (MRG). Overall, the LRMCs of the electricity and hydrogen supply increase, leading to additional hydrogen imports and reduced domestic hydrogen production in the H-GH_2 demand scenario. The reduced domestic hydrogen production leads to reduced salt cavern capacities for seasonal hydrogen storage.

For the 100% reduction target, correlated to the omission of lithium-ion batteries, the considered PV rooftop systems are reduced. The reduction of the PV capacities is compensated on the one hand by additional refurbished PHES and on the other hand by a notable increase in the offshore and onshore capacities of wind turbines. The increase of wind turbine capacities is accompanied by further expansions of DC lines. Both, electrolyzers and hydrogen-fueled CCGT plants, are built with increasing capacities and are operated with increasing full load hours. The latter leads to an increased number of salt caverns for hydrogen storage with an overall increased turn-over count.

As for the *BELS* and *BELS*$^+$ scenario branch, the scenario variation demonstrates the value of daily, high-efficient energy storage which facilitates the integration of PV systems into the energy supply system.

The Value of Hydrogen Storage in Existing Salt Caverns (2b)

The omission of hydrogen storage in salt caverns that existed in 2017 leads to a maximum cost increase of 0.9% for the 100% reduction target. For the 80% reduction target, the increase is below 0.5%.

The more expensive new salt caverns lead to a cost increase in the *Power-to-Hydrogen-to-Power* pathway. The pathway is thus considered less prominently, i.e. it is designed with smaller electrolyzer, salt cavern and CCGT plant capacities. The amount of wind turbines and the capacities of DC lines in their vicinity are also reduced. To compensate the reduced capacities of wind turbines and hydrogen-operated CCGT plants, additional PV rooftop systems and lithium ion batteries are built. For the 80% target with the H-GH_2 demand, domestic hydrogen production becomes less cost-attractive and more hydrogen is imported.

As in the *BELS*$^+$ branch, this scenario variation demonstrates that the mining of new salt caverns instead of the reassignment of already existing salt cavern locations does not have a significant impact on the cost. In all but one scenario configuration, hydrogen is exclusively domestically produced. For the reference scenario, between 144-277 salt caverns are built for hydrogen storage. For the scenario variation, still between 128-249 salt caverns are newly mined.

The Value of Hydrogen Storage in Salt Caverns (2c)

In contrast to the *BELS*$^+$ scenario branch, the omission of hydrogen storage in salt caverns already has an impact on the 80% reduction target since the caverns are a key infrastructure component to supply hydrogen to the mobility and transport sector. The complete omission of hydrogen storage in salt caverns leads to cost increases of up to 1.6% for the 80% reduction target and up to 7.4% for the 100% reduction target.

In general, the omission of salt caverns as hydrogen storage leads to reductions of offshore and onshore wind turbine capacities, which again leads to a reduction of the considered DC line expansions, and, for the 100% reduction target, to an increase in PV rooftop systems and wood-fired CHPs.

The reduction of the wind turbine capacities has a prominent effect on the domestic hydrogen production which, however, varies between the L-GH_2, M-GH_2 and H-GH_2 demand. A shift from domestic hydrogen production towards hydrogen imports takes place with increasing hydrogen demands and stricter carbon dioxide reduction targets.

For all but two scenario configurations, the domestically produced hydrogen is not stored anymore but is directly sent to the end-consumers. The considered electrolyzer capacities are thus indirectly limited by the peak hydrogen demand in the system. Only the imported, liquid hydrogen is stored in cryogenic tanks which are used as monthly / seasonal storage.

For the 100% reduction target and the L-GH_2 and M-GH_2 demand, the installed electrolyzer capacities exceed the hydrogen demand peaks. In these cases, the technology pathway "domestic electrolyzer - pipe storage system - compressor" is partly cost-competitive against the technology pathway "hydrogen import - cryogenic tank - regasification". This is caused by sufficiently available low-cost electricity, i.e. low LRMCs of the electricity supply. Consequently, pipe storage systems are considered in these two supply systems, 444 $GWh_{GH_2,LHV}$ for the L-GH_2 demand and 138 $GWh_{GH_2,LHV}$ for the M-GH_2 demand[22].

For the 100% reduction target and the L-GH_2 demand, a small share of the produced hydrogen is even used in methanation plants to produce 4.4 TWh_{MRG} of MRG which is then stored in salt caverns. Consequently, also the considered CCGT plant (MRG) capacities are increased.

The scenario variation once more demonstrates the importance of salt caverns in national hydrogen supply chains or, more generally, the value of synthetic gas storage in salt caverns to integrate seasonal electricity generation. It moreover shows that hydrogen import can become an alternative hydrogen supplier when domestic hydrogen production becomes less cost-lucrative.

The Value of Underground Storage (MRG & GH_2) (2d)

The omission of all UGS options leads to an increase in the TAC of up to 1.6% for the 80% reduction target and up to 9.5% for the 100% reduction target.

This scenario variation can be regarded as a sequel of the previous scenario variation in which UGS was only omitted for hydrogen storage. Consequently, similarities in the changes can be observed. For the 80% reduction target in which UGS of MRG does not play a role, the two scenario variations display the same results. However, for the 100% reduction target, a few additional changes can be observed. The omission of UGS for MRG leads to the consideration of pipe storage systems for purified biogas. MRG-fueled CCGT plants are built with smaller capacities but are operated with higher full load hours, providing, in total, the same

[22]With an increasing hydrogen demand, the domestically produced hydrogen is more often sent directly to the end-consumer and thus less gaseous hydrogen storage is required.

amount of electricity. As purified biogas can be stored locally, the total amount of transported MRG is also reduced. For the L-GH_2 demand, methanation is not considered anymore as UGS for MRG is omitted. In comparison to the previous scenario variation, hydrogen-fueled CCGT plant capacities are increased.

In comparison to the *BELS*$^+$ scenario variation which does not consider UGS, the domestically produced hydrogen is not liquefied as only the imported, liquid hydrogen is stored in seasonal storage. Domestically produced hydrogen is either directly sent to the consumer or, in the 100%-L-GH_2 configuration, stored in pipe storage systems which function as a daily buffer storage.

In general, the scenario variation highlights once more the significance of UGS as a low-cost storage option for MRG or hydrogen and identifies alternative, but more expensive, storage options.

The Value of Biomass (3a)

The omission of biomass, i.e. biogas and wood-fired CHPs, does not have an effect on the 80% reduction target. However, for the 100% reduction target, the TAC of the supply systems is increased by up to 1.3%.

In all scenario configurations, the omission of biomass leads to an increase in wind turbines, electrolyzers and hydrogen-fueled CCGT plants[23] as well as an increase in PV rooftop systems and lithium-ion batteries. The expanded *Power-to-Hydrogen-to-Power* pathway additionally leads to an increase in hydrogen storage and transmission. MRG storage and transmission is omitted.

The scenario variation gives an outlook on the supply system design if the biomass (biogas and wood) would be used to supply different demands in the energy system, e.g. to supply heat or be used in *Power-to-Fuel* pathways.

The Value of Centralized Hydrogen Reconversion (3b)

The omission of hydrogen reconversion to electricity in centralized thermal power plants only has an effect for the 100% reduction target. There, increases of 3% (L-GH_2), 1.3% (M-GH_2) and 0.3%(H-GH_2) occur in the TAC. The changes in the supply systems strongly depend on the considered hydrogen demand in the industry and transport sector. Nevertheless, a common factor between the different demand scenarios is the reduction of wind turbine and electrolyzer capacities and the increase of PV rooftop capacities.

[23] Up to 23 GW_{el} of CCGT plants (GH_2) are considered.

The L-GH_2 demand is affected strongest by the omission. For the scenario configuration, enough low-cost electricity is available to consider a methanation pathway for the supply system. Consequently, methanation plants are built, MRG transmission and storage is increased and more MRG-operated CCGT plants are considered. As less electrolyzers operate flexibly on intermittent electricity, wood-fired CHPs are built with a capacity of 8.2 GW_{el} and operated with full load hours of on average 3942 h/a to balance the electricity generation.

For the H-GH_2 demand, an increase in PV and lithium-ion battery capacities as well as further DC line expansion are sufficient to compensate the omission of the centralized, hydrogen-fueled power plants. For this scenario configuration, the high number of electrolyzers provides a large amount of flexibility to integrate intermittent, renewable electricity generation. Thus, the capacity of wood-fired CHPs is significantly decreased to 0.7 GW_{el} and only operated with full load hours of 2964 h/a, i.e. their average LCOE is notably increased in comparison to the supply system with the L-GH_2 demand.

Overall, it can be concluded that hydrogen-fueled, centralized thermal power plants are particularly valuable in supply systems in which their balancing potential supports the integration of intermittent electricity generation. The extent to which they are considered in the supply systems depends on competing flexibility providers, as for example alternative hydrogen consumers or alternative flexible electricity providers.

The Value of Electrolyzers (3c)

The omission of electrolyzers leads to an increase of 4.2%-4.8% in the TAC for the 80% reduction target and to an increase of 10.6%-11.4% for the 100% reduction target.

The omission of electrolyzers forces the hydrogen demands in the transport and industry sector to be fulfilled with imported, liquid hydrogen. Up to 280 $TWh_{LH_2,LHV}$, or 8.4 $Mt_{LH_2,LHV}$, are imported. Furthermore, offshore and onshore wind turbines which were formerly integrated into the supply system by domestic electrolyzers are built in significantly smaller numbers. To balance the intermittent electricity supply for the 80% reduction target, additional MRG-fueled OCGT plants are considered. For the 100% reduction target, about 14 GW_{el} of MRG-fueled CCGT plants, which provide 19 TWh_{el}/a of electricity per year, are considered, independent of the hydrogen demand. Wood-fired CHPs are considered in the scenario variation for the 100% reduction target as additional electricity suppliers. Overall, the electricity supply systems show strong similarities with the *BELS* reference scenario configurations (80% and 100%).

The hydrogen related infrastructure is primarily dedicated to the hydrogen supply in the transport and industry sector. For the 100% reduction target, about 9.4 GW_{el} of hydrogen-fueled CCGT plants, which provide 23 TWh_{el} of electricity annually, are considered, independent of the hydrogen demand. Salt caverns for hydrogen storage are completely omitted for the 80% reduction target, as the imported hydrogen is directly sent to the end-consumers. For the scenario configurations with the 100% reduction target, hydrogen-fueled CCGT plants enter the supply system as variable consumers and again salt caverns are considered for seasonal storage, however in smaller numbers than in the reference configurations.

The average LRMCs for the electricity supply are reduced to 77 €/MWh_{el} for the 80% reduction target and increased to 126 €/MWh_{el} for the 100% scenario, independent of the exogenously given hydrogen demand. For the 80% reduction target, the electricity supply system benefits from the omitted RES expansion. The increase for the 100% reduction target can be linked with the increased hydrogen reconversion cost. The LRMC cost of the hydrogen supply are almost constant between the different carbon dioxide reduction targets and the hydrogen demands[24]. For the industry sector, an average LRMC of 125 €/$MWh_{GH_2,LHV}$, or 4.2 €/$kg_{GH_2,LHV}$, is obtained. For the transport sector, an average LRMC of 174 €/$MWh_{GH_2,LHV}$, or 5.8 €/$kg_{GH_2,LHV}$, arises.

In general, it can be noted that electricity supply is largely decoupled from the hydrogen supply in the scenario variation.

The Value of Low Hydrogen Import Cost (3d)

Reducing the cost of the liquid hydrogen import from 120 €/MWh to 105 €/MWh leads to a cost decrease of 0%-2.7%, for the 80% reduction target, and of 0%-0.6%, for the 100% reduction target. The smaller reduction span for the 100% reduction target results from the lower LRMCs of the hydrogen supply with stricter reduction targets.

For the L-GH_2 demand, the supply systems remain unchanged. However, for the M-GH_2 and H-GH_2 demand, additional hydrogen imports are considered for the supply system operation. This effect is more prominent for the 80% reduction target and less prominent for the 100% reduction target. To store the constantly arriving imported liquid hydrogen, cryogenic tanks are built at the shipping terminals and the required amount of salt caverns for gaseous hydrogen storage is reduced. With the increased import, less onshore and offshore wind turbines are required for the operation of the domestic electrolyzers. The electrolyzers are again built

[24] Different intra-regional distribution costs are considered for the different hydrogen demands.

with smaller capacities and are moreover operated with smaller full load hours. For the 100% reduction target, the less expensive hydrogen supply again leads to increased capacities of hydrogen-fueled CCGT plants.

The average LRMC of electricity and hydrogen supply are visualized for the scenario variation side by side in Figure B.54 in the appendix B.3. The LRMCs for the electricity supply are at 81 €/MWh$_{el}$ for the 80% reduction target and at 119 €/MWh$_{el}$ for the 100% scenario, independent of the hydrogen demand in the transport and industry sector. The LRMCs of the hydrogen supply are almost constant between the different carbon dioxide reduction targets and the M-GH$_2$ and L-GH$_2$ demand. For the industry sector average, an annual LRMC of 3.7 €/kg$_{GH_2,LHV}$ is obtained. For the transport sector, an average LRMC of 5.3 €/kg$_{GH_2,LHV}$ arises.

It can thus be concluded that, specifically for larger hydrogen demands and supply systems which do not have access to low-cost, intermittent electricity generation, the supply system benefits from the liquid hydrogen import. Furthermore, the scenario variation indicates that the assumed hydrogen import cost is a sensitive parameter which, amongst other factors, determines the split between domestic hydrogen production and considered hydrogen import.

The Value of Low Capacity Specific Investment Cost for Electrolyzers (3e)

The reduction of the capacity dependent investment of the electrolyzers from 500 €/kW$_{el}$ to 300 €/kW$_{el}$ leads to a cost reduction of up to 3.7%, for the 80% reduction target, and of up to 4.5%, for the 100% reduction target.

In the scenario variation, higher electrolysis capacities with lower cost contributions are considered for the different scenario variations. For the 100% reduction target with the H-GH$_2$ demand, 113 GW$_{el}$ instead of only 100 GW$_{el}$ are considered. The electrolyzers are operated with lower full load hours but with their increased capacities they generate more hydrogen over the year in total. With the increase in the domestic hydrogen production, more salt caverns for hydrogen storage are considered and the inter-regional hydrogen transmission is increased. For the operation of the electrolyzers, additional offshore and onshore wind turbines are built. However, the PV rooftop capacities are slightly reduced and along with them the considered amount of lithium-ion batteries.

For the 100% reduction target, the more profitable conditions for the domestic hydrogen production lead to higher capacities of hydrogen-fueled CCGT plants on the one hand. On the other hand, they also lead to a decrease of hydrogen import for the L-GH$_2$ demand and the 80% reduction target. However, theoretically, the assumed commodity cost of the hydrogen import should decrease as well, as the assumed oversea supply chain also includes electrolyzers.

In total, the scenario variation leads to reduced LRMCs of both the electricity and hydrogen supply, cf. Figure B.55 in the appendix B.3. The average annual LRMCs of the electricity supply drop to 78-82 €/MWh$_{el}$ for the 80% reduction target and to 114 €/MWh$_{el}$ for all scenario configurations with the 100% reduction target. Thus, on average, the cost is 4 €/MWh$_{el}$ less expensive than in the reference case. The LRMC for the hydrogen supply to the industry sector drop to 3.1-3.6 €/kg$_{GH_2,LHV}$ for the 80% reduction target and to 3.4-3.7 €/kg$_{GH_2,LHV}$ for the 100% reduction target. The LRMC for the hydrogen supply to the transport sector drops to 5.0-5.3 €/kg$_{GH_2,LHV}$ for the 80% reduction target and to 4.8-5.2 €/kg$_{GH_2,LHV}$ for the 100% reduction target.

Thus, the scenario variation demonstrates the effect which the introduction of less-investment intensive electrolysis has on the optimal electricity and hydrogen supply. As the previous scenario variation, it also indicates that the split between domestic hydrogen production and liquid hydrogen import is critically determined by the cost difference of the two supply chains.

5.4 Scenario Cross-cutting Discussions

Within this section, scenario cross-cutting discussions are presented. For this, first, electricity and hydrogen supply concepts in a future German energy system under varying carbon dioxide restrictions are discussed in subsection 5.4.1. Next, the role of individual infrastructure technologies and international imports and exports are abstracted from the scenario run in subsection 5.4.2 and subsection 5.4.3. The opportunities and synergies which arise from a cross-linked infrastructure are discussed in subsection 5.4.4. The overall modeling setup of the scenarios as well as their results are compared to literature in subsection 5.4.5. Finally, the scenario results are compared to the German energy supply infrastructure existing in 2017 / 2018 in subsection 5.4.6.

5.4.1 Electricity and Hydrogen Supply Concepts in a Future German Energy System under Varying CO_2 Reduction Targets

Based on the scenarios investigated within this thesis, general conclusions for future German energy supply concepts are deducted with respect to varying carbon dioxide reduction targets. In this context, general concepts for the energy supply system structure, including electricity and hydrogen production, storage and transmissions, and the LRMCs of the electricity and hydrogen supply are discussed.

80% Carbon Dioxide Reduction Target

For an 80% reduction target, it can be concluded that natural gas operated OCGT and CCGT plants, offshore and onshore wind turbines, open-field PV systems, r-o-r plants as well as electricity imports will play a key role in the electricity supply in a future German energy system. With the additional consideration of hydrogen demands, also electrolyzers, salt caverns, pipelines and intra-regional distribution infrastructure are required for hydrogen production, storage, transmission and distribution. If hydrogen demands are high and only small amounts of "surplus electricity" are available, also liquid hydrogen imports should be considered.

For temporal balancing, existing PHES and smaller amounts of lithium ion batteries are sufficient and CCGT and OCGT plants can provide flexible electricity generation. Hydrogen production can be cost-efficiently buffered in salt caverns and, if hydrogen imports are considered, in cryogenic tanks.

For spatial balancing, the electricity grid of the *NEP* from 2015 is sufficient [107] and hydrogen pipelines should be considered as a cost-efficient hydrogen transmission option. All in all, for an 80% reduction target, major expansions of storage and transmission infrastructure are primarily required for the hydrogen supply.

For an 80% reduction target, the average LRMC of the electricity supply increases with an increasing electricity consumption. The increase of the LRMC is rooted in the depletion of the more cost-lucrative RES with an increasing electricity consumption. However, alongside with the increasing electricity consumption, also a wider section of the energy system can be decarbonized.

Also the average LRMCs of the hydrogen supply to the industry and transport sector increase with increasing hydrogen demands. The increases in the supply cost are directly linked to the decreasing availability of low-cost electricity for electrolysis operation with an increasing hydrogen demand. Particularly high operational cost of the domestic electrolyzers thereby results in the additional consideration of international liquid hydrogen imports.

Increasing Carbon Dioxide Reduction Targets

With stricter carbon dioxide reduction targets, the considered RES storage and transmission technology portfolio has to become more divers to achieve a cost-optimal energy supply. Supply pathways for RES have to be either added or reinforced. Offshore and onshore wind turbines are required in increasing capacities and also PV rooftop systems and biogas plants have to contribute with major shares to the electricity supply. Without a centralized hydrogen infrastructure, also wood-fired CHPs should be considered. With a centralized hydrogen infrastructure, hydrogen-fueled CCGT can contribute to a secured electricity supply. The utilization of natural gas and the amount of MRG operated power plants can on the other hand be reduced. However, MRG-fueled CCGT plant capacities are still an option for flexible electricity provision via purified biogas and, when centralized hydrogen reconversion is not available, also synthetic methane.

For temporal balancing, also refurbishment of PHES should be considered and lithium-ion battery capacities further increased. *Power-to-Hydrogen-to-Methane-to-Power* or *Power-to-Hydrogen-to-Power* pathways should be considered for a cost-optimal supply system with a particularly high reduction target. Here, it has to be noted that in the investigated scenarios, the methanation pathway is not part of the optimal design solution anymore once centralized hydrogen reconversion is considered. Additional options for flexible electricity supply should be provided by CCGT plants operated on purified biogas if the biogas is not required in other sectors. In general, seasonal gas storage in salt caverns is pivotal and is of interest for the temporal shifting of biogas, hydrogen and synthetic methane.

For spatial balancing, the DC line capacities suggested in the *NEP* from 2015 [107] have to be multiplied and MRG and hydrogen transmission considered. Hydrogen transmission serves in this context as a spatial balancing option for both, the electricity and hydrogen supply.

For a 100% reduction target, the average LRMC of the electricity supply is decreased when a centralized hydrogen infrastructure is considered as it enables a cost-lucrative *Power-to-Hydrogen-to-Power* pathway. The average LRMCs of the electricity supply vary for the 100% reduction target only slightly when additional hydrogen demands are considered. This means that for high reduction targets, the additional hydrogen demands affect the electricity supply only slightly while decarbonizing a wider section of the energy system at the same time.

For a 100% reduction target, the average LRMC of the hydrogen supply are in comparison to the average LRMC of the hydrogen supply for an 80% reduction target smaller. The hydrogen production profits from the “surplus electricity” arising from the basic electricity supply, i.e. for the higher reduction targets, more low-cost electricity is available for the electrolyzers.

5.4.2 The Role of Individual Infrastructure Technologies

Based on the presented reference scenarios and scenario variations in the *BELS*, *BELS*$^+$ and *BLHYS* scenario branch, the roles of the individual infrastructure technologies are identified. Hereby, the role of an infrastructure component is identified based on the conclusions which can be made on, if applicable,

- its chosen design, i.e. when and to which extent a component is considered in the energy supply system,
- its operation, e.g. when and which specific operation patterns occur,
- its contribution to the TAC of the energy supply systems,
- the effect which the omission of the component has on the optimal supply system, and
- the correlation which can be observed between different technologies.

The roles of the individual infrastructure technologies are first identified for electricity infrastructure technologies, then for hydrogen infrastructure technologies and finally for technologies for methane-containing gases.

The Role of Individual Electricity Infrastructure Technologies

For individual electricity infrastructure technologies, the following conclusions can be drawn.

- *Wind turbines*: Offshore and onshore wind turbines provide more than half and, in some cases, even more than two thirds of the annually generated electricity in the supply systems. They are thus a corner stone of the renewable electricity supply within the scenarios.
  - *Offshore wind turbines*: Offshore wind turbines with fixed and floating foundations are considered within the scenarios. The turbines with a fixed foundation, which are closer to shore, less expensive but also have smaller full load hours, are preferably considered in the scenarios. Only after their capacity potential is maxed out, offshore wind turbines with floating foundations are considered. In comparison to the capacities existing in 2017, the considered capacities are multiplied in all scenarios. Their integration into the energy supply system is linked with the

availability of DC line connections. Without DC lines, their installation is decreased, and, at the same time, larger amounts of curtailment arise. This effect is particularly strong when alternative, cost-efficient spatial balancing options are not available.

- *Onshore wind turbines*: Not always, only the LCOE-wise least expensive onshore wind turbines are considered in the supply systems which points towards congestions in the electric grid. With the considered spatial resolution, the bottlenecks in the electric grid can be detected during optimization and the wind turbines which lead to an overall cost-optimal system design, which are not necessarily the turbines with the lowest LCOE, are considered for the optimal energy supply systems. This statement is confirmed when DC lines / DC line expansions are omitted from the supply systems. In this case, the turbine placements are shifted from the north to the center and south of Germany, overall with increased capacity. In general, the wind turbines in the scenarios have, on average, higher full load hours than the onshore wind turbines existing in 2017. This is on the one hand caused by the further improved design of the turbines but on the other hand also by the cost-optimal turbine selection, i.e. suboptimal turbine locations which were considered in 2017 are not considered in the supply systems which again results in, on average, higher full load hours.

Furthermore, throughout the scenarios, the highly intermittent, seasonal electricity generation of the wind turbines requires a number of flexibility options to be cost-efficiently integrated into the energy supply systems. For lower carbon dioxide reduction targets, these can be power plants operated on natural gas. However, for higher reduction targets, the presence of electrolyzers, serving as a flexible electricity consumer, crucially decide to which extent wind turbines are considered in the energy supply systems.

- *Photovoltaic systems*: Independent of the technology type, PV systems show notable synergies with daily storage options throughout the scenario branches, i.e. lithium-ion batteries and PHES. The quantities with which they are considered depends on the technology type and the reduction target.
  - *Photovoltaic open-field systems*: The considered capacity potential for PV open-field systems are fully exploited throughout all scenarios. In all scenarios, mainly the less expensive systems with a fixed tilt are considered. A tracking system, which provides higher full load hours, is only considered when specifically high local electricity demands occur in each region of the modeled supply system. The PV open-field systems supply are characterized with the, on average, second lowest LCOE of all electricity generators. Moreover, their electricity generation has a high correlation with the considered electricity demands. Arising excess electricity is stored during daytime in lithium-ion batteries and is

discharged in the late afternoon / evening hours.

  - *Photovoltaic residential rooftop systems*: PV residential rooftop systems are modeled with notably higher investment cost and are therefore considered in smaller quantities. For the 80% reduction target, PV rooftop systems are not considered in the optimal supply system. However, for the 100% reduction target they are, after the wind turbines, together with the PV open-field systems the second corner stone of the renewable electricity supply.

- *Run-of-river hydroelectric plants*: Within the considered scenario scope, run-of-river hydroelectric plants are modeled with a fixed capacity and only operational expenditures are considered. As these operational expenditures are comparably low, the technology has the lowest LCOE of all electricity generators.

- *Decentralized electricity generation*: The decentralized electricity generation in CHP plants is considered in only a selected number of scenarios. This is partly because their concurrent heat generation is taken for granted in the scenarios. Nevertheless, in the scenarios where they are considered, they serve as flexible electricity providers which moreover contribute to the secured electricity generation capacities in the scenarios.

  - *Wood-fired CHP plants*: Wood-fired CHP plants are only considered in scenarios in which centralized hydrogen reconversion is either not available or, due to a technology omission in the *Power-to-Hydrogen-to-Power* pathway, not cost-attractive.
  - *Biogas-fueled CHP plants*: Biogas-fueled CHP plants are only considered in the *BELS* scenario branch in which biogas injection into the MRG grid is not eligible. In this case, the locally produced biogas can be stored in double membrane gas storage systems and is fed to the CHP plants.
  - *Hydrogen-fueled CHP plants*: Hydrogen-fueled CHP plants are also only considered in a small number of scenarios. They are considered when hydrogen pipelines are omitted as a hydrogen transport option. In this case, they appear in intra-regional sub-networks in regions which have access to salt caverns, i.e. regions in which low-cost hydrogen storage is available.

- *Centralized electricity generation from thermal power plants*: Centralized thermal power plants are used within the scenarios to flexibly balance positive residual loads in the electricity supply. With the availability of gas from either imports or large-scale storage systems, the plants significantly contribute to the secured electricity generation capacities throughout the scenarios. Which technology type and which fuel is used in these plants depends on the scenario settings.

- *MRG operated OCGT and CCGT plants*: MRG operated power plants are fueled with either natural gas, purified biogas or synthetic methane. For the 80% reduction target, only natural gas is considered as a fuel in all scenario branches. From there, with increasing reduction targets, also purified biogas and, for a small number of scenarios, also synthetic methane is considered as a fuel. The less efficient but also less expensive OCGT plants are considered only for small reduction targets and when high-efficient/ highly flexible electricity storages (lithium-ion batteries / PHES) are omitted from the supply systems. The OCGT plants are in general operated with small full load hours and are used to supply peaks in the positive residual loads in the supply systems.
- *Hydrogen operated OCGT and CCGT plants*: In the scenarios, hydrogen operated power plants are not considered for the 80% reduction targets but can become a corner stone of a secure electricity supply with increasing reduction targets. The extent to which they are considered in the supply systems generally depends on several factors. Here, the availability of low-cost electricity, which increases with stricter carbon dioxide restrictions, to produce hydrogen at low cost is one factor. Another factor is that the usage of renewably produced hydrogen in thermal power plants competes with energy supply pathways for this low-cost electricity. For example, when increasing, exogenously given hydrogen demands are considered, the installed capacities of hydrogen operated thermal power plants is decreased. In a small number of scenario variations, also hydrogen-fueled OCGT plants are considered. Similarly to the MRG-fueled OCGT plants, they are then operated to cover peaks in the positive residual loads in the supply system.

• *Lithium-ion batteries*: In the scenarios, lithium-ion batteries serve as a daily storage option. Their operation is prominently linked to the electricity generation from PV systems. In most cases, the decrease / increase in the capacity of one of the components leads to a decrease / increase in the other component. Thus, the consideration of PV systems and lithium-ion batteries appears to be highly correlated. Often, the batteries are charged between morning and afternoon and are then discharged in the evening to cover local electricity demands. During winter, they are also sometimes charged with intermittent electricity generation peaks from wind turbines. In regions with large capacities of wind turbines, batteries are also operated to overcome downtimes of these turbines. However, when the batteries are operated as an intra-daily energy storage, and are thus charged more than once a day, their cyclic lifetime becomes a limiting factor of their operation. In a few cases, lithium-ion batteries are operated as a night storage, i.e. the electricity charged during daytime is stored during night and is then discharged in the early morning hours of a day. Alongside their support of integrating intermittent renewable energies, specifically PV systems, into the energy supply systems, the batteries provide secured electricity generation capacities. Starting around the 90% reduction target, they often supply more than half of these secured capacities.

- *Pumped hydroelectric energy storage*: The larger part of the considered PHES is modeled with a fixed capacity in the investigated scenarios. However, a certain share of PHES is only available if it is refurbished. The refurbishment of this PHES is, capacity-wise, slightly less expensive than the installment of new lithium-ion batteries and is, moreover, modeled without a self-discharge. However, in comparison to the lithium-ion batteries, they are associated with higher losses during charging and discharging operation and, moreover, have a smaller power-to-energy ratio and are thus not as flexible as the batteries. In general, this leads to only small refurbishment rates in the optimal supply system designs. Throughout the scenarios, it can be observed that PHES is more often than batteries operated as a night storage. This can be linked to its negligible self-discharge and to the higher flexibility of lithium-ion batteries which are better suitable for covering peak positive residual loads occurring in the evening.
- *National AC and HVDC lines*: National AC and HVDC lines are the energetic most efficient means to distribute generated or imported electricity throughout the country. Consequently, they are frequently used, and selected lines even indicate frequent congestions. All in all, they contribute in all scenarios to more than half of the transmitted energy. However, with increasing carbon dioxide reduction targets and increasing hydrogen demands in the transport and industry sector, gas, and particularly hydrogen, transmission becomes a second corner stone of intra-regional energy exchanges.
  - *National AC lines*: AC lines are modeled with fixed capacities in the scenarios. Without the possibility for expansion, they display frequent congestions, particularly in the north of Germany. The scenario variations in the *BELS*+ and *BLHYS* scenario branch clearly demonstrate that the consideration of hydrogen pipelines can, at least partly, take the strain off the grid. Nevertheless, AC line expansions should also be pursued further. The presented scenario scope and a further development of *FINE* would allow for such an assessment.
  - *National HVDC lines*: DC line routes starting in the north of Germany are used in the scenarios to transmit electricity of offshore wind turbines to Western and Southern Germany. These lines thus provide the opportunity to distribute centralized, renewable electricity generation with comparably high full load hours to the load centers of Germany. Even though DC expansions are assumed to be about 20-times more expensive than hydrogen pipelines, they are still considered in large capacities in most scenarios. It must be further noted that one of

the lines proposed in the network development plan of 2015 [107] is, in most scenarios, not well adapted in the system. Summarizing all off these observations, it becomes obvious that the considered expansions considered in the network development plan must be drastically expanded, or even alternative / new routes considered, to guarantee a cost-optimal energy supply within the considered scenario scope. Only for low reduction targets or in cases where they or offshore wind turbines are omitted, they do not appear within the optimal energy supply system. In general, a strong correlation between the capacity expansion of offshore wind turbines and DC line expansions can be observed throughout the scenarios. However, also onshore wind turbines are affected by limitations on DC line expansions. If DC line expansions, or domestic DC lines in general, are omitted from the supply system, the placement of onshore wind turbines is shifted to the center and south of Germany.

The Role of Individual Hydrogen Infrastructure Technologies

Conclusions for individual hydrogen infrastructure components are presented in the following.

- *Electrolyzers*: Electrolyzers are the corner stone of cross-linked infrastructure design within this thesis. In the scenarios, they have several purposes. On the one hand, they provide the electricity, transport and industry sector with renewably produced hydrogen and thus foster their decarbonization. On the other hand, they indirectly support the electricity system as a flexible electricity consumer and thus significantly contribute to a cost-efficient integration of onshore wind turbines into the electricity supply system. For small annual hydrogen productions and lower reduction targets, electrolyzers are primarily operated on electricity from offshore wind turbines[25] and are correspondingly placed in regions with access to offshore wind turbines. With an increasing domestic hydrogen production and increasing reduction targets, also onshore wind turbines in the north of Germany significantly contribute to the hydrogen production. For high demands and high reduction targets, also electrolyzer operation patterns which partly mirror electricity generation from PV systems can be observed. In general, wind-driven operation patterns can be observed closer to shore while PV-driven operation patterns are more prominent in the inland. The former are, on average, characterized by higher full load hours while the latter are characterized by smaller full load hours. The

[25] An exact identification of which electricity is used for what application is often difficult, if not even impossible. Nevertheless, certain correlations can be identified.

omission of electrolyzers from scenarios with either higher reduction targets or hydrogen demands in the mobility / industry sector leads to significant increases in the TAC and causes dependencies on liquid hydrogen import. For high reduction targets, their omission, and thus the omission of a flexibility provider, even causes increases in the average LRMC of the regular electricity supply.

- *Salt caverns for gaseous hydrogen storage*: In scenarios with either higher reduction targets or exogenously given hydrogen demands, hydrogen storage in salt caverns is an essential corner stone for cost-efficient energy supply system design. Even though their share on the supply systems' TAC is in all scenarios below 1%, the TAC can increase significantly when they are omitted (up to 9%). In all considered scenarios, the in 2017 existing salt cavern locations are sufficient to satisfy the storage demands. A rededication of these caverns for hydrogen storage thus provides new business cases for storage operators. However, even if the existing salt cavern locations were not available for hydrogen storage, the optimal supply system cost would only slightly increase if the mining of new salt caverns were considered. The purpose of hydrogen storage in salt caverns can be identified when their operation profiles are investigated. The caverns primarily serve as a seasonal storage. They are preferably charged during late fall, winter and early spring when electricity generation from wind turbines is highest. Then, during the remainder of the year and specifically in summer, they are discharged. Their omission in the energy supply systems is compensated by the consideration of liquid hydrogen storage in cryogenic tanks, for inter-monthly/seasonal storage, and with gaseous hydrogen storage in pipe systems, for daily and weekly storage.
- *Hydrogen transmission pipelines*: Hydrogen transmission pipelines are the second corner stone to a cost-efficient hydrogen infrastructure. As for the salt caverns for hydrogen storage, they have in general cost shares below 1% on the TAC of the supply systems. In scenarios with high hydrogen demands, their omission leads to TAC increases of up to 15.7%. However, it must be considered here that, in these cases, hydrogen must be produced locally within each region. An alternative transmission option, as for example trucks for gaseous or liquid hydrogen transport, would reduce this cost increase again. The relative increase has thus to be perceived as the cost increase when inter-regional hydrogen transmission is, in general, omitted.
- *Hydrogen distribution within regions*: In the *BLHYS* scenario branch, the intra-regional hydrogen distribution infrastructure for the hydrogen demands in the transport sector (1.6-1.75 €/kg$_{GH_2}$), which are primarily constituted of the cost for the fueling stations, contribute notably to the TAC of the supply systems. However, in general, the intra-regional transmission, both for the hydrogen demands in the industry and transport sector, contributes with only

minor shares to the TAC.

- *Pipe systems for gaseous hydrogen storage*: Pipe systems for hydrogen storage are considered in only selected scenarios. In the *BELS* scenario branch, they are considered to buffer the hydrogen production of the electrolyzers to operate the methanation plants with higher full load hours. In the remaining scenarios they are considered for daily storage when hydrogen transmission pipelines or hydrogen storage in salt caverns is omitted. In both cases they are often combined with cryogenic tanks for liquid hydrogen storage which provide additional monthly and seasonal storage.
- *Cryogenic tanks for liquid hydrogen storage*: Cryogenic tanks are built in the supply systems when either hydrogen imports are considered or when hydrogen pipelines or hydrogen storage in salt caverns are omitted and a larger hydrogen demand is considered in the system. In the former case, they buffer the constantly arriving hydrogen imports and are discharged when the domestic electrolyzers are not in operation. It the latter case, they serve as inter-monthly / seasonal storage while pipe systems buffer daily fluctuations. Their seasonal storage operation is caused by their rather costly and energy intensive charging process (liquefaction) and their, in comparison to the pipe systems, rather low storage capacity related investment. In this context, their comparably high self-discharge is an accepted side-effect.
- *Regasification plants*: Regasification plants are required as soon as liquid hydrogen is considered in the energy supply system. Their overall cost contributions and energy demands are in general small.
- *Liquefaction plants*: Liquefaction plants are considered in scenarios with larger hydrogen demands when, as already mentioned previously, hydrogen pipelines or hydrogen storage in salt caverns are omitted from the supply systems. In this context, they enable seasonal liquid hydrogen storage in cryogenic tanks.

The Role of Individual Infrastructure Technologies for Methane-containing Gases

Lastly, conclusions on infrastructure technologies for methane-containing gases are presented.

- *Biogas plants & biogas purification and grid injection plants*: Biogas plants are frequently considered in the scenarios with higher reduction targets. When biogas plants are considered, they are most often considered with biogas purification and grid injection plants. The electricity supply chain “biogas plant - purification and grid injection - transmission -

geological storage - centralized thermal power plant” is in this context more cost-attractive than the electricity supply chain “biogas plant - double membrane biogas storage - decentralized CHP plant”. When the former supply chain is not available due to the omission of one of its technologies, the second pathway is in some scenarios considered. As already previously mentioned, the utilization of biogas in centralized power plants is also partly caused by the neglection of regional heat demands or the consideration of bio-fuels for the transport sector. Nevertheless, even if they were considered, a regional availability of biogas might not be guaranteed, and a means of biogas transport might have to be considered.

- *Double membrane gas storage for raw biogas*: Biogas storage is only considered in larger amounts in the *BELS* scenario variation in which MRG pipelines and biogas injection into the grid are omitted. In this scenario variation, they provide a temporal balancing option for local biogas production. In the other two scenario branches, the omission of MRG pipelines and biogas injection into the grid is primarily buffered with an expansion of the *Power-to-Hydrogen-to-Power* pathway.
- *Methanation plants*: Methanation plants are only considered in a few scenario variations. Particularly in the *BELS* scenario branch, they have a key role for the 100% reduction target. There, they provide means to access low-cost, seasonal, geological energy storage. In general, as soon as a centralized hydrogen infrastructure becomes fully available, methanation plants are completely disregarded. A different picture might present itself if the carbon dioxide would not be captured from ambient air but was available from, for example, industry processes at low cost. Nevertheless, the efficiency losses which are connected to the methanation are not negligible and the only benefit of the pathway is, in the considered scenario scope, the usage of existing transmission and storage infrastructure which, overall, has only a small influence on the TAC.
- *Geological storage for MRG*: Geological storage for MRG is considered in all scenarios in which either biogas and its purification and injection into the MRG grid is eligible or a methanation pathway is considered. If the cost contributions of the respective storage options are related to their operation, they are all operated with a levelized cost of discharged energy of 1 €/$MWh_{MRG,LHV}$. In general, geological storage is used to provide low-cost seasonal storage.
  - *Pore storage for MRG*: Pore storage is modeled with a fixed capacity and has, with its small power-to-energy ratio, a comparably small turn-over count.
  - *Salt caverns for MRG storage*: Salt caverns, which have a higher power-to-energy ratio, are operated with higher turn-over counts. New

salt cavern locations are only considered for two scenario variations in the *BELS* scenario branch. The consideration of the new salt cavern locations is in this context correlated to congestions in the MRG pipeline grid. In general, the storage of purified biogas or synthetic methane provides another business case for cavern operators. All in all, a maximum of 13 salt caverns is considered in the scenario variations. In comparison to salt cavern usage for hydrogen storage, which is considered with up to 294 salt caverns, this value is small.

- *Pipe systems for MRG storage*: In an energy supply system in which all regions have access to geological gas storage, pipe systems for MRG storage is not considered. However, as soon as geological storage is not available, pipe systems are used to store purified biogas and, in some scenario variations, even synthetic methane.
- *MRG transmission pipelines*: The partial consideration of the existing natural gas grid, it is assumed that 10% of its capacity is available in the scenarios, provides an additional spatial balancing option in the energy supply system. The pipelines are primarily used for purified biogas transmission in the scenarios, but for selected scenarios they are also used to transmit synthetic methane. Specifically the use of low-cost geological storage as well as the option to generate electricity in the more efficient centralized power plants, makes the usage of the pipeline grid cost-attractive.

5.4.3 The Role of International Energy Imports and Exports

Based on the presented reference scenarios and scenario variations in the *BELS*, *BELS*$^+$ and *BLHYS* scenario branch, roles of international energy imports and exports are identified. First, the role of electricity imports and exports, then the role of natural gas imports and finally the role of liquid hydrogen imports is discussed.

The Role of International Electricity Imports and Exports

In the scenarios, electricity imports and exports to and from Germany are modeled based on positive and negative residual loads in countries interconnected to Germany. Electricity imports from a specific country are associated with the average LCOE of the renewable energy mix in that country. For electricity exports, marginal revenues of 1 €/MWh$_{el}$ are considered.

In all scenarios, Germany is a net electricity importer. In one scenario, a net import of 54 TWh$_{el}$/a occurs. Consequently, an omission of electricity imports and exports would lead to a significant increase in the cost. In comparison, between 2008 and

2017, Germany was a net electricity exporter [101]. In the scenarios, Germany's role in the European electricity market is thus reversed.

It has to be noted that electricity export is only served by "surplus electricity" and is thus more prominent for strict reduction targets. In reality, the actual international electricity market is more complex and is modeled in this thesis with only very basic assumptions. These modeling assumptions can be approved upon in future work. For example, iterations between the optimization of single countries and their electricity exchange can be made. Also, the underlying scenario assumptions for each country can in this context be harmonized.

The Role of International Natural Gas Imports

Natural gas imports are modeled with a commodity cost of 33 €/MWh$_{\mathrm{MRG,LHV}}$ and are available in all regions, i.e. they are modeled with a "copper plate assumption" and are thus not accounted for in the considered MRG grid.

International natural gas imports play a key role in the flexible electricity supply in the scenarios with reduction targets below 100%. For scenarios with an 80% reduction target, 364 TWh$_{\mathrm{MRG,LHV}}$/a of natural gas are imported. With stricter reduction targets, the role of centralized, flexible electricity generation is partly assumed by thermal power plants operated on either hydrogen or purified biogas / synthetic methane.

A more complete picture of the role of natural gas imports can be identified in future work by connecting a gas market model to the scenario modeling workflow. Then, also exports to interconnected countries can be considered and natural gas transmission in the pipeline grid can be modeled. Furthermore, more sophisticated assumptions on the cost of natural gas import can be made. Also the security of supply which Germany provides to the European gas market with the storage of natural gas in UGS can be assessed. In the context of a transition to highly renewable energy systems, the manifestation of this security of supply is likely to change and the storage of renewably generated gases (hydrogen, purified biogas, synthetic methane) will gain in importance.

The Role of International Liquid Hydrogen Imports

Hydrogen imports are modeled based on the work of *Heuser et al.* [150] and *Robinius et al.* [98] who model international hydrogen import-export relations in detail.

Throughout the scenarios, it is noticeable that the extent to which liquid hydrogen imports are considered depends mainly on several factors. Crucial is the cost difference between the supply chains of domestically produced hydrogen versus the one of imported hydrogen. Here, a lower hydrogen import cost or the omission of cost-efficient domestic infrastructure components leads to a shift towards hydrogen imports. Also, the availability of low-cost electricity in the domestic electricity supply system and the competition for this low-cost electricity has a decisive influence. Here, a high availability and low competition lead to a shift towards domestic hydrogen production. For increasing hydrogen demands and less strict reduction targets, less low-cost electricity, or “surplus electricity” resulting from the basic electricity supply, is available.

5.4.4 Cross-linked Infrastructure: Opportunities and Synergies

Throughout the investigated scenarios, it can be noted that electrolysis is the key component to a cross-linked infrastructure design. It thus enables the supply and decarbonization of the industry and transport sector by supplying renewable hydrogen.

For high reduction targets, this one-directional link between the electricity and gas infrastructure is complemented with options to reconvert hydrogen / synthetic methane to electricity. In the investigated scenarios, hydrogen reconversion is preferred over the reconversion of synthetic methane. Thus, the centralized hydrogen infrastructure is not only used to supply exogenously given hydrogen demands but is also used in the electricity sector as a flexible electricity provider.

These cross-links between the electricity and gas infrastructure provide additional spatial and temporal balancing options. The operation of the electrolyzers on low-cost electricity and the low investment-intensive hydrogen storage and transmission infrastructure provides, in comparison to for example onsite hydrogen production or additional electricity infrastructure, cost-lucrative supply pathways.

Particularly with increasing carbon dioxide reduction targets, synergies between the hydrogen and the electricity supply infrastructure become apparent.

- On the one hand, the electricity supply system benefits from the consideration of electrolyzers as a flexibility provider. The electrolyzers provide access to RES which would otherwise be challenging to integrate and thus not considered in an optimal supply system. Specifically, they enable a cost-efficient integration of wind turbines into the energy system, thus leading to notable smaller amounts of “surplus electricity” within the electricity system. Moreover, with the provided hydrogen reconversion options, positive residual loads can be flexibly covered on a renewable basis. The additional stress on the energy supply system which is caused by the additionally considered hydrogen demands leads for strict carbon dioxide reduction targets to negligible cost increases for the electricity supply.

- On the other hand, with increasing carbon dioxide reduction targets, the hydrogen supply infrastructure benefits from increasing amounts of "surplus electricity" which arises out of the decarbonization of the electricity supply. Electrolyzers can be operated on lower LRMCs of the electricity supply, and thus leads to cost decreases in the LRMC of a renewable hydrogen supply between the 80% and the 100% reduction target.

It can thus be concluded that electrolyzers and the reconversion of synthetic gases to electricity have the potential to play a vital role in the cost-optimal design of future energy systems.

5.4.5 Scenarios in Comparison to Literature

In this section, the results of the presented scenarios are first compared to the individual modeling of future German electricity and hydrogen infrastructure scenarios in literature and, if applicable, to their modeling results. Then, the results are compared to one-nodal energy system scenarios of Germany, which investigate all sectors of the energy system.

Future German Electricity Infrastructure in Literature

Within this section, the scenarios investigated within this thesis are compared to studies from literature presented in subsection 2.2.1. In analogy to subsection 2.2.1, they are compared with respect to chosen spatial and temporal resolution, modeling approach and considered technology portfolio. It has to be noted that the studies are set up for different purposes. For example, a study might focus on a complex power plant dispatch and thus only considers a comparably low temporal resolution. The goal of the literature comparison is in this context to highlight that the chosen scenario modeling setup of this thesis is suitable for its purpose.

- *Spatial and temporal resolution*: In comparison to the listed literature, this thesis' scenarios provide the highest spatially resolved future German supply system representation when an annually interconnected, hourly resolved timeframe is considered. This in turn enables the modeling of both, transmission infrastructure and seasonal storage.

- *Chosen modeling approach*: Even though MILPs give valuable insights into energy system design, they come at the expense of increased computational runtimes. For the scope of this thesis' scenarios, which aim for a detailed representation of storage and transmission infrastructure, an LP formulation is thus more expedient. A standardized post-discretization could however improve the scenarios in future work.
- *Technology portfolio and scenario results*: Concerning the design and operation or storage and transmission technologies, several parallels can be drawn between the scenarios from literature and this thesis' scenarios.
  - Correlations between "battery - PV" and "wind - hydrogen storage" are also observed by *Schlachtberger et al.* [23] and *Victoria et al.* [24].
  - The study by *Victoria et al.* [24] on "the role of storage technologies throughout the decarbonization of a sector-coupled European energy system" gives a comprehensive overview over electricity, hydrogen and heat storage in future interconnected European energy systems. Here, hydrogen storage becomes relevant starting from an 80% reduction target and then increases with stricter reduction targets. This result is in agreement with the results obtained in this thesis' scenarios. The slope of the TAC curve, which rises with stricter reduction targets,displays similarities to the expressions of the TAC presented for the *BELS* reference scenarios. Hydrogen transmission and intra-regional distribution is not considered with technical or economic parameters in the study by *Victoria et al.* [24].
  - Specific grid expansions for Germany are determined by *Ludig et al.* [64] (5 regions, 3 days for each season, 5 year transformation pathway), *Kemfert et al.* [66] (21 regions, annual hourly resolution, fixed generation and storage technologies) and *Neumann and Brown* [12] (20-100 regions, 100-400 time steps, storage omitted). All of these studies identify the connection between the *North Sea* to the *South-West* of Germany as an essential connection in the German electricity grid.
    - For this connection, *Ludig et al.* [64] identify a capacity expansion requirement of 17 GW_{el}.
    - *Kemfert et al.* [66] suggest expansions of more than 10 GW_{el} for this connection.
    - The most sophisticated approach to identify DC and AC line expansions is proposed by *Neumann and Brown* [12]. The authors consider, in comparison to this thesis' scenarios, a newer version of the electricity network development plan, but nevertheless expand the "*North Sea* - *South-West*" and the "*North Sea* - *South*" DC line connection to 5 GW_{el} for a Germany 2040 scenario with a 65% share of renewable electricity. Moreover, they also identify several AC line expansion requirements. AC line expansions are not considered in

the scope of this thesis and should be included in future work.

These findings are in agreement with the findings of this thesis' scenarios. In general, the studies identify recent network development plants as being inadequate for achieving a cost-optimal future energy system with high carbon dioxide reduction targets.

– As in this thesis, *Kluschke and Neumann* [71] also investigate shadow prices of the electricity supply in their study and extrapolate nodal hydrogen cost in this context. They determine values around 6 €/kg_{H_2} for the hydrogen supply which is about 1 €/kg_{H_2} more expensive than the values determined within this thesis' scenarios. Moreover, their nodal hydrogen costs vary significantly. To analyze this deviation with respect to this thesis scenarios, the by *Kluschke and Neumann* assumed input parameters have to be investigated more closely. Their techno-economic parameters for the electricity infrastructure and electrolyzers are in a similar range as the ones considered within this thesis, their considered hydrogen storage cost is more expensive, hydrogen transmission is not considered and the demand specific cost contributions from fueling stations is less expensive. Thus, it can be concluded that the lower hydrogen cost obtained in this thesis is connected to the consideration of low cost hydrogen transmission and storage, i.e. by pipeline and salt caverns. Moreover, with the consideration of a hydrogen transmission network, the effect of varying nodal cost for the hydrogen supply is significantly reduced.

Infrastructure scenarios which include a comprehensive investigation of cross-linked transmission technologies are not presented in the studies. Thus, with respect to the listed literature, it can be derived that this thesis provides novel cross-linked infrastructure scenarios for Germany.

Future German Hydrogen Infrastructure in Literature

Within this section, the scenarios investigated within this thesis are compared to the studies from literature presented in subsection 2.2.2. Again, several assets and drawbacks of these studies can be identified when comparing their results against the results obtained in this thesis. These are again categorized with respect to spatial and temporal resolution, considered technology portfolio and chosen modeling approach.

- *Spatial resolution*: Within this thesis, the transmission infrastructure is designed for only 75 regions with spatial detail, however the endogenous placement of electrolyzers and storage locations is considered. Thus, for example, electrolyzers are not exclusively built in the north of Germany.

Moreover, hydrogen distribution infrastructure is, for each fueling station and each consumer in industry, also considered by estimating the distribution cost with the model from *Reuß* [153]. The chosen spatial resolution of 75 regions can be assessed in context with a spatial sensitivity analysis conducted by *Reuß et al.* [80]. *Reuß et al.* determine for their scenarios an cost-optimal cluster size of around 40 / 80 / 120 regions[26] for their low (1 Mt_{GH_2}) / medium (2 Mt_{GH_2}) / high (3 Mt_{GH_2}) demand scenario for Germany when transmission pipelines and GH_2 trucks are considered for the hydrogen supply. Thus, the considered 75 regions provide an already good estimate of the transmission level. Nevertheless, the spatial detail, as provided by the other studies is not given. Here, a model-coupling suggests itself for future work: The transmission level could be optimized with *FINE* and the presented modeling scope while for the distribution level is the model of *Reuß* [153] could be applied, benefitting from the strength of both approaches.

- Temporal resolution: An hourly resolution across the year, as it is considered for the scenarios of this thesis, is, besides in the study of *Welder et al.* [2], not considered for any of the studies. This temporal resolution allows several additional investigation options for the hydrogen infrastructure. It allows to identify operation strategies for the complete hydrogen infrastructure chain. Cost-optimal locations of electrolyzers are determined based on endogenously determined electricity generation profiles. Their operation can be linked to the LRMCs of the electricity supply which provides an option to determine their operational expenditures in more detail. Also, for each storage technology, charging and discharging profiles as well as storage inventories are provided and hybrid storage systems can be designed.
- Chosen modeling approach: The chosen modeling approach of this thesis' scenarios can be compared with scenarios which are capable of modeling high spatial resolutions, with scenarios which model higher technical details, e.g. pressure losses and with the modeling of storage in the scenarios.
  - Within this thesis, an endogenous cross-linked infrastructure optimization for electricity, hydrogen and parts of methane-containing gas is considered. This approach guarantees optimality of the overall design and enables the consideration of hydrogen reconversion. However, it comes at the cost of a less detailed spatial resolution as for example considered in the scenarios by *Robinius et al.* [9], *Reuß et al.* [80] or *Cerniauskas et al.* [81].
  - As tested for the scenarios within this thesis, MILPs are in this context computationally expensive and are not considered for the benefit of obtaining a higher spatial resolution. To consider binary or integer modeling decisions, either algorithmic improvements of the formulation

[26] About 100 fueling stations per cluster. However, the presented objective function is flat around the optimal solution and cluster sizes of 20-200 fueling stations still provide a close to optimal solution.

and / or optimization of the MILPs are required or model-coupling workflows can be considered, as for example suggest by *Reuß et al.* [15].

– In comparison to the listed studies from literature, the endogenous storage design and operation is one of the strengths of this thesis' scenarios.

- *Technology portfolio*: The scenario scope of this thesis does not cover the exhaustive hydrogen infrastructure portfolio considered by *Reuß et al.* [80]. Instead, it focuses on providing a technology portfolio for electricity infrastructure as well as the handling of methane-containing gas. With the resulting cross-linked infrastructure setup, the consideration of hydrogen reconversion pathways, which are not considered within the studies from literature, is enabled.

Energy System 2050 Scenarios for Germany

A direct comparison between the results obtained in this study to results in literature from one-nodal energy system scenarios, which investigate all sectors of the energy system, is challenging for several reasons. Each scenario is modeled with its own set of input parameters, has its own workflow to determine its supply system design, which is not necessarily optimized, and considers different system boundaries. Nevertheless, a few studies considering "Germany - 2050" scenarios are selected to provide a general overview of how the supply systems designed within this thesis fit into literature, cf. subsection 2.2.3. In contrast to the scenarios within this thesis, which only considers the energy sector and parts of the industry and transport sector, only studies from literature are selected which investigate all sectors of the energy system. Moreover, only scenarios which have at least an 80% reduction target are considered. A short list with the titles of the studies and, if necessary, the title of the considered scenarios is given in the following.

1. "Klimaschutz: Der Plan Energiekonzept für Deutschland", 90% reduction target [86]
2. "Was kostet die Energiewende? Wege zur Transformation des deutschen Energiesystems bis 2050", 85% reduction target [87]
3. "Erfolgreiche Energiewende nur mit verbesserter Energieeffizienz und einem klimagerechten Energiemarkt –Aktuelle Szenarien 2017 der deutschen Energieversorgung" [88]
   (a) "KLIMA -17 MEFF", medium efficiency measures, 95% reduction target
   (b) "KLIMA -17 HEFF", high efficiency measures, 95% reduction target
4. "Klimaschutzszenario 2050" [89]

   (a) 80% reduction target
   (b) 90% reduction target
5. “Klimaschutzszenario 2050” [90]
   (a) 80% reduction target
   (b) 95% reduction target
6. “Entwicklung der Energiemärkte - Energiereferenzprognose”, 80% reduction target [91]
7. “Die Energiewende nach COP 21 – Aktuelle Szenarien der deutschen Energieversorgung”, 95% reduction target [92]
8. “Langfristszenarien und Strategien für den Ausbau der erneuerbaren Energien in Deutschland bei Berücksichtigung der Entwicklung in Europa und global”, medium RES expansions, 80% reduction target [93]
9. “Langfristszenarien für die Transformation des Energiesystems in Deutschland Modul 10.a: Reduktion der Treibhausgasemissionen Deutschlands um 95% bis 2050”, base scenario, 85% reduction target [94]
10. “Leitstudie Integrierte Energiewende” [95]
    (a) “Elektrifizierungsszenario”, 80% reduction target
    (b) “Elektrifizierungsszenario”, 95% reduction target
    (c) “Technologiemixszenario”, 80% reduction target
    (d) “Technologiemixszenario”, 95% reduction target
11. “Energiesystem Deutschland 2050”, 80% reduction target [96]
12. “Pathways to deep decarbonization in Germany” [97]
    (a) 80% reduction target
    (b) 85% reduction target
    (c) 90% reduction target
13. “Kosteneffiziente und klimagerechte Transformationsstrategien für das deutsche Energiesystem bis zum Jahr 2050” [98]
    (a) “Szenario 80”, 80% reduction target
    (b) “Szenario 95”, 95% reduction target

Figure 5.60 presents the annual electricity generation and consumption for these scenarios and the scenario investigated within this thesis side by side. While the greenhouse gas reduction targets for scenarios from literature refer to the full set of emissions from 1990, the reduction targets for the scenarios of this thesis refer only to the ones of electricity generation in 1990. Nevertheless, the electricity consumption assumed within this thesis is within the range presented in literature. This is mainly caused by two factors: On the one hand, as the electricity demand is based on the year 2013, efficiency measures are not considered, and electricity demands in certain sectors are not reduced. On the other hand,

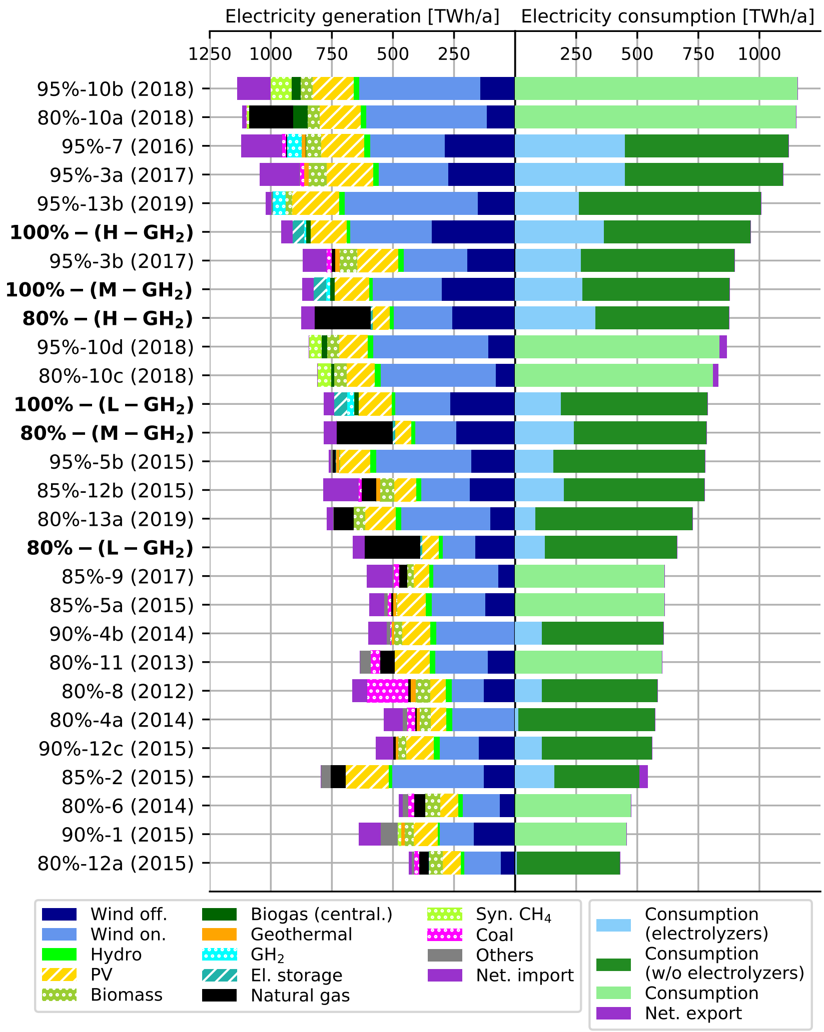

Figure 5.60: Annual electricity generation and consumption in German energy scenarios, sorted by consumption. The reduction targets of this thesis' scenarios (*BLHYS*: 80% / 100% - L-GH_2 / M-GH_2 / H-GH_2) only relate to the electricity sector. The studies from literature are numbered according to the previously given list.

additional electricity demands, e.g. for battery electric vehicles, considered in the studies from literature are not considered within this thesis.

Several observations can be made.

- The electricity consumption of electrolyzers is considered in several scenarios. Here, scenarios *3a* and *7* display higher electricity consumptions of electrolyzers than the one considered in the *BLHYS*-100%-H-GH_2 scenario of this thesis.
- Several scenarios, particularly older ones, still consider electricity generation by coal-fired power plants in larger quantities. In these studies, a statutory coal phase out was not determined yet.
- Geothermal electricity generation is considered in several scenarios, however only with minor shares to the annual electricity generation.
- Biomass in form of CHP plants plays only a minor role in the scenarios within this thesis. However, in literature, major contributions from biomass to the electricity generation are considered.
- The usage of synthetic methane and biogas in centralized power plants is considered in larger extends in study *10*. The amounts of gas which are used for this purpose are above the amounts considered in this thesis' scenarios.
- Hydrogen reconversion to electricity is considered prominently in scenarios *7* and *13b*. The amount of electricity generated by the reconversion is in both cases more than double of what is generated in the *BLHYS*-100%-L-GH_2 scenario.
- The electricity generation from natural gas in scenario *10a* (80% reduction) and the scenarios of this thesis with an 80% reduction target are in a similar range.
- In all but three scenarios, i.e. *2*, *10c* and *10d*, Germany is a net electricity importer.

Figure 5.61 gives a more detailed look on the installed capacities for electricity generation. Due to partially not available data, not all scenarios are visualized. Again, several observations can be made.

- The *BLHYS*-100%-H-GH_2 scenario has the highest installed capacity of offshore turbines. However, scenarios *3a* and *7* install offshore wind turbines with similar capacities.
- The considered onshore wind turbines capacities in this thesis' scenarios are, for the respective reduction targets well within the range of literature. Only scenarios *2*, *5b*, *13a* and *13b* consider notably higher capacities.

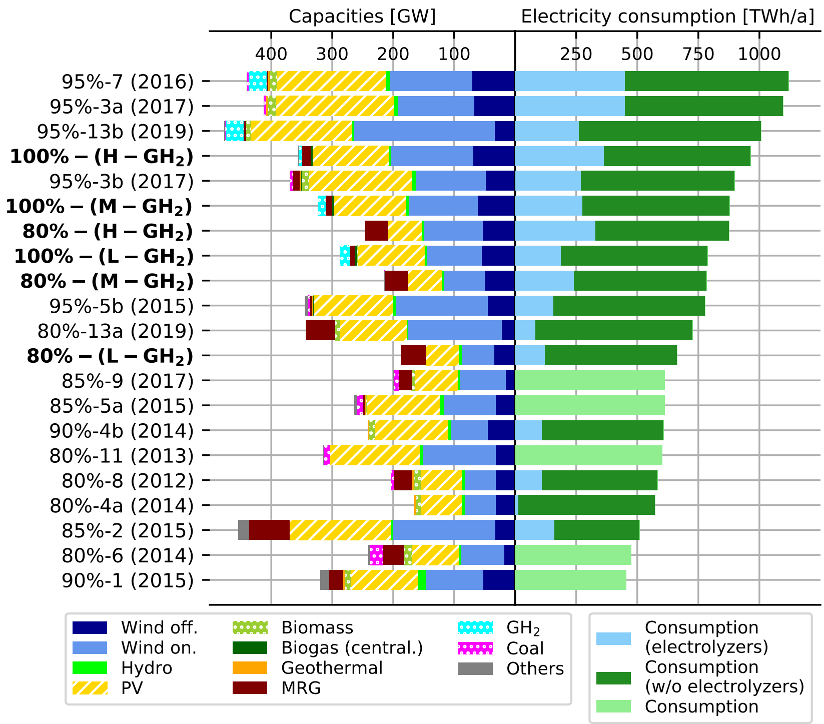

Figure 5.61: Renewable electricity generation capacities and annual electricity consumption in German energy scenarios. Storage is not considered; reduction targets of this thesis' scenarios only relate to the electricity sector.

- The PV generation capacities considered within this thesis' scenarios are rather moderate. This is more prominent for the 80% reduction target and less prominent for the 100% reduction target.
- For an 80% reduction target, the capacities of natural gas fueled power plants (MRG) are mostly above 30 GW_{el} in the scenarios.
- Among the scenarios with high reduction targets, the scenarios within this thesis have comparably large thermal power plant capacities (MRG and GH_2). Here, scenarios *7* and *13b* are exceptions.
- The installed capacity of hydrogen reconversion plants in scenarios *7* and *13b* is more than twice as high as in the *BLHYS*-100%-L-GH_2 scenario.

In general, the installed electricity generation capacities of this thesis' scenarios are moderate but still within the range of literature.

To which extent storage and transmission infrastructure are considered in these scenarios is often difficult to determine. Most scenarios model, if at all, energy storage with basic assumptions and do not consider a regional resolution for their system design. This is partly rooted in the intended purpose of the studies which rather focus on a detailed representation of the energy system and not on its infrastructure design. However, some studies couple their output with sophisticated electricity and gas grid models for feasibility testing.

Nevertheless, the benefits of seasonal storage, restrictions in RES expansions due to limitations of the electric grid or the identification of transmission infrastructure expansions are thus not captured in detail. Consequently, also the interplay of cross-linked infrastructure is more difficult to capture in the respective scenario setups. Thus, potential supply pathways are either not considered at all or they are considered, but then only in an aggregated manner.

The strength of the scenarios investigated within this thesis is that not only the magnitudes of the installed capacities are determined but also it is determined where they are placed under the endogenous consideration of storage and transmission infrastructure.

Several conclusions can be drawn when comparing this thesis' scenarios to comprehensive one-nodal energy system scenarios for Germany in the year 2050. It can be concluded that this thesis' scenarios fit, with respect to electricity generation and consumption, within the range of literature. The consideration of large-scale hydrogen reconversion is not considered in many scenarios. However, as shown in the *BELS* and *BELS*$^{+}$ scenario comparison, the energy supply system's cost can be decreased notably by its consideration when high reduction targets are considered. The utilization of geothermal energy and biomass is underestimated within this thesis' scenarios. In general, this thesis' scenarios would profit from a more detailed representation of future energy demands and the energy system's sector in general.

Concluding Remarks

With the chosen trade-off between spatial and temporal resolution, considered technology portfolio and applied modeling approach, novel cross-linked infrastructure scenarios with a focus on storage and transmission infrastructure could be expediently modeled. Specifically the consideration and endogenous design of cross-linked electricity and hydrogen transmission infrastructure for Germany is not considered in the reviewed literature. However, with respect to one-nodal energy system models, the energy demands in the considered sectors are modeled in this thesis with only basic assumptions. Concluding remarks on the application of a cross-linked infrastructure design approach as well as future work which could increase the sectoral representation in the design approach are presented in the following.

As a concluding remark on cross-linked infrastructure design, its application in the design of future energy supply pathways is discussed. The study by *Buddeke et al.* [70] suggests an integrated RES, storage and (electricity) grid development strategy to design future energy supply pathways. Also *Kluschke and Neumann* [71] suggest a co-optimization of multiple energy sectors in the context of power system investment planning to exploit synergies. This thesis suggests to go one step further and proposes an integrated cross-linked infrastructure development strategy for both power and all relevant gas systems, i.e. including transmission infrastructure design. Individual, separate pathways to (a) first design the electricity supply system without cross-linked infrastructure (e.g. the *BELS*-100% reference scenario) and then the required infrastructure for hydrogen (e.g. the *BLHYS*-100% reference scenario) or to (b) design the energy supply system without hydrogen pipelines (*BLHYS-w/o pipelines (GH_2)*), would lead to incompatibilities and / or significant additional cost.

Furthermore, future work which could increase the sectoral representation of the overall workflow with which the scenarios are created is suggested. In future work, a one / few nodal energy system model could be run first. Then, solely the demands could be regionally distributed. Finally, the multi-nodal, cross-linked infrastructure model could be run and, if required, for each region the distribution infrastructure with an approach similar to *Reuß et al.* [80] could be determined. Thus, a full energy system design with a highly detailed spatial representation for cross-linked infrastructure could be provided.

5.4.6 An Urgent Need for Change - Comparison to German Energy Supply Infrastructure in 2017 / 2018

In this section, the energy supply systems in the reference scenarios of the three scenario branches are compared to the in 2017 or 2018, depending on the literature source, existing German energy supply infrastructure.

Procurement, Transmission and Storage of Electricity

The differences in the electricity generation capacities between the scenarios and the electricity generation capacities existing in 2017 are discussed component-wise. The generation capacities in the year 2017 and their full load hours, are obtained from the *Bundesnetzagentur* (*Federal Network Agency*) [101, 108].

- The capacity installations of offshore wind turbines range in the scenarios between 20 GW_{el} and 69 GW_{el}. The in 2017 existing 5.4 GW_{el} are thus significantly increased. Also, the within the scenarios considered turbines have higher full load hours (up to on average 5000 h/a, 2017: 3200 h/a) and thus the overall generated electricity is multiplied. Not only turbines with a fixed foundation, but also turbines with a floating foundation are considered when the stress on the supply system is high, i.e. strict reduction targets and additional final energy demands.
- The in the scenarios considered capacities of onshore wind turbines range between 37 GW_{el} and 133 GW_{el}. In 2017, 50 GW_{el} of onshore turbines were installed which operated with average full load hours of about 1700 h/a. The full load hours of the onshore wind turbines within the modeled scenarios, which are obtained from the work of *Ryberg et al.* [102], are on average higher (*BLHYS*-100%-H-GH_2: 2479 h/a) within the wind turbines class *Class I*.
- A fixed capacity of 3.8 GW_{el} is considered for the run-of-river plants[27].
- The capacity installations of open-field PV systems are in comparison to the in 2017 existing open-field installations quintupled (11 $GW_p \rightarrow 54\ GW_p$).
- Between 0 GW_p and 70.8 GW_p of PV rooftop systems are considered within the scenarios. In the *BLHYS*-100%-H-GH_2 scenario, the in 2017 existing capacities of 31 GW_p are thus more than doubled.
- The centralized gas power plant fleet changes throughout all scenarios significantly in comparison to the year 2017. Nuclear and coal power plants are not eligible in the considered scenario scope. However, different gas-fueled power plants are considered in all scenarios. 0 GW_{el}-14 GW_{el} of MRG-fueled OCGT plants, 6.9 GW_{el}-39 GW_{el} of MRG-fueled CCGT plants and 0 GW_{el}-22 GW_{el} of hydrogen-fueled CCGT plants are considered. In comparison, in 2017, about 26 GW_{el} [101, 130] of gas power plants were installed in Germany.

In this that context, it has to be noted that the determined maximum capacity potential of 620 GW_{el} for onshore wind turbines, 82 GW_{el} for offshore wind turbines and 190 GW_p of PV rooftop systems is in all scenarios not reached. However, for PV open-field systems, the maximum available potential of 54 GW_p is in all scenarios fully utilized.

In all scenarios, in an addition to the domestic electricity generation, Germany is a net electricity importer. In the *BLHYS* reference scenario, net imports of

[27] The run-of-river modeling is based on the work of *Syranidis* [114] who based the run-of-river capacities of Germany on ENTSO-E data [113] from 2015.

up to 54 TWh_{el} occur (80%-H-GH_2). In contrast, in 2017, Germany was with an import-export balance of -50.6 TWh_{el}[28] a net electricity exporter [101].

With the consideration of the network development plan of 2015 [107], several new AC lines and five new DC lines, are considered. However, particularly for scenarios with a high carbon dioxide reduction target, the DC line connections are expanded even further. In the *BLHYS*-100%-H-GH_2 scenario, expansions of up to 13 GW_{el} for a line are considered. Thus, for higher reduction targets, the need for a further grid expansion becomes apparent and decisive measures are suggested if these targets are to be realized cost-efficiently.

Concerning electricity storage, the scenarios display mixed results. For the 80% reduction target, the considered 48.5 GWh_{el} of PHES[29] are sufficient to balance a large share of the renewable electricity generation together with several gigawatt hours of lithium-ion batteries. For the *BELS*-80% scenario, 410 MWh_{el} of battery storage are considered which is less than what was installed in 2018 [132]. For higher reduction targets, the need for electricity storage increases significantly. Battery installations of up to 155 GWh_{el} are considered and also PHES refurbishment is considered. Moreover, *Power-to-Hydrogen-to-Power* pathways are considered. Thus, for high carbon dioxide reduction targets, also a requirement for additional electricity storage becomes apparent.

Procurement, Transmission and Storage of Methane-containing Gases

Only a section of possible applications for methane-containing gases, i.e. biogas, purified biogas, synthetic methane and natural gas, are considered within this thesis. Nevertheless, several conclusions can be drawn from the scenario results with respect to the in 2017 MRG supply system.

Concerning the procurement of methane-containing gases, several changes can be summarized. In general, for high carbon dioxide reduction targets close to 100%, natural gas will not be considered in energy supply systems when carbon dioxide sinks, e.g. carbon capture and storage (CCS) or carbon capture and utilization (CCU) without carbon dioxide emissions further along the process chain, are not considered. Thus, if at all, alternatively procured methane-containing gases will play a more prominent role in future energy systems.

For reduction targets below 100%, still small amounts of natural gas imports

[28] Actual, physical load flows.

[29] A share of the in 2017 existing PHES, which is assumed to not require refurbishment, + the PHES expansions, which will be made within the next few years.

are considered in the scenarios. For scenarios with the 80% reduction target, 364 $TWh_{MRG,LHV}$ of natural gas are imported and fed to gas power plants. In comparison, in 2017, 936 $TWh_{MRG,LHV}$ of natural gas were domestically consumed [101]. Of these, roughly 134 $TWh_{MRG,LHV}$ of natural gas were fed to power plants[30].

Biogas, generated from residual materials, and synthetic methane, generated from electrolysis, carbon capture from ambient air and subsequent methanation, are considered in the scenarios for higher reduction targets to provide an alternative energy carrier for flexible electricity supply.

- The annual biogas usage ranges between 0 and 31 $TWh_{biogas,LHV}$. In the reference scenarios, the biogas is fully purified and injected into the MRG grid. In comparison, in 2017, 9 $TWh_{biogas,LHV}$ were injected into the natural gas grid. As discussed before, the usage of purified biogas in centralized thermal power plants might change when heat and additional fuel demands are considered in an extended scenario scope.
- A methanation pathway is only considered for the *BELS*-100% scenario. There, 9.9 GW_{el} of electrolyzers and 5.5 $GW_{MRG,LHV}$ of methanation plants are considered which generate 23 $TWh_{MRG,LHV}$ of synthetic methane. In comparison, in 2017, a total of 12.6 MW_{el} of electrolyzers was installed in Germany [156].

In the scenarios, purified biogas and synthetic methane can be transmitted via former natural gas pipelines throughout Germany. There, the maximum transport capacity is limited to 10% of the available capacity to provide enough capacity to additional MRG demands which are not modeled. In general, this reduced pipeline grid is rarely if not at all congested. The additionally considered renewable gases thus cause little stress on the pipeline grid.

Also, the existing UGS is only used to a small extent in the scenarios. At a maximum, 8 salt caverns and the existing German pore storage sites are considered for MRG storage. In contrast, 278 of the in 2017 existing salt caverns are used for hydrogen storage in the *BLHYS*-100%-H-GH_2 scenario. The utilization of the existing salt caverns for hydrogen must be reflected in context with a security of supply. With less storage available for natural gas, its security of supply is, inherently, reduced. Nevertheless, pore storage is still exclusively dedicated to MRG storage. Moreover, with the profound changes which will occur in the German energy system, it is questionable if a large security of supply for natural gas will still be required or if hydrogen will take over as a flexible energy carrier which can be

[30] In 2017, gas-fueled power plants generated 72.3 TWh_{el} of electricity, emitting 27 Mt_{CO_2} [101]. If an emission factor of 0.201 $kg_{CO_2}/kWh_{MRG,LHV}$ is assumed [192], this results in 134 $TWh_{MRG,LHV}$ of consumed natural gas.

stored and transmitted at low cost.

Procurement, Transmission and Storage of Hydrogen

Further far-reaching changes in the energy supply system are observed for hydrogen in the scenarios.

In the scenarios, domestic hydrogen generation by electrolysis and liquid hydrogen imports are considered as procurement options to supply renewable hydrogen to the energy, transport and industry sector.

- In the reference scenarios, up to 100 GW_{el} of electrolyzer capacities are installed. In comparison, in 2017, 31 MW_{el} of installed electrolysis capacities existed in Germany [156].
- In one of the reference scenarios (*BLHYS*-80%-H-GH_2), also liquid hydrogen imports are considered. Analogies between the import of liquid hydrogen and liquid natural gas (LNG) can be drawn in this context. As of 2018, no larger LNG terminal existed in Germany, however several sites are concurrently under discussion for future sites.

The construction of a nationwide hydrogen transmission pipeline grid, and its corresponding distribution infrastructure, has the most visible effect in the infrastructural changes, despite its overall minor cost contribution. An option to reduce this construction work is the rededication of former natural gas pipelines, which was not considered in this thesis. Nevertheless, such an assessment is possible with the presented modeling framework *FINE*. Moreover, the considered scenario database provides a good starting point for such an assessment. However, for such an assessment, the consideration of an international gas market and a broader consideration of potential future MRG end-consumers would be advisable.

In the reference scenarios, the utilization of existing salt caverns for hydrogen storage is sufficient to guarantee a secured hydrogen supply. As discussed above, the reduced availability of natural gas storage must be seen in context with a secured natural gas supply. The scenario variations demonstrate that even the consideration of new salt caverns would not lead to a significant cost increase.

An Urgent Need for Change

When comparing the optimal energy supply scenarios investigated within this thesis to the energy supply system infrastructure in 2017 / 2018, it be becomes evident that the German energy supply infrastructure requires drastic changes to guarantee a highly renewable, cost-optimal energy supply in the year 2050.

Concerning electricity infrastructure, the scenarios demonstrate that RES capacities have to be multiplied, e.g. for some scenarios offshore wind turbine capacities are increased more than tenfold and PV open-field systems are in general quintupled. Furthermore, coal and nuclear power plants have to be fully phased out and gas power plant capacities have to be increased. Concerning transmission and storage infrastructure, the electric grid has to be expanded beyond existing grid development plans, and additional electricity storage needs to be built, e.g. for some scenarios up to 150 GWh_{el} are installed.

Concerning infrastructure for methane-containing gas, only a few statements can be made as the in 2017 / 2018 existing natural gas infrastructure is only considered in parts in the scenarios. Nevertheless, the scenarios indicate that the MRG pipeline grid is required for the transmission of purified biogas and, when a full decarbonization is not considered, natural gas which are both used for buffering the intermittent electricity generation from wind turbines and PV systems. Existing UGS is partly used for the seasonal buffering of biogas production. However, a high number of salt caverns currently used for natural gas storage is to be repurposed as hydrogen storage.

The consideration of additional hydrogen demands in the transport and industry sector but also just the option to provide electricity via hydrogen reconversion pathway leads to the cost-optimal consideration of a nationwide hydrogen infrastructure comprised of electrolyzers in the gigawatt scale, a comprehensive pipeline grid and hydrogen storage in salt caverns in the terawatt hour scale. When centralized hydrogen reconversion is considered, also hydrogen-operated CCGT plants are built and in selected scenarios also liquid hydrogen imports are considered. Hydrogen storage falls in this context back on in 2017 / 2018 existing salt caverns and thus additional caverns do not need to be built. However, strategies for the construction of electrolyzers, pipeline routes and power plants should be made.

Naturally, the scenarios just provide one example on how a highly renewable electricity supply system and a partly decarbonization of the transport and industry sector could be realized. Other technology options, efficiency measures or the consideration of stronger international interactions might shift technology specific assessments. However, as not all sectors of the energy system are covered, the required energy supply system might even be underestimated. Nevertheless, the scenarios provide exemplary insights and highlight the urgent need for change the Germany energy supply system has to undergo to reduce its carbon dioxide emissions and thus reduce its impact on climate change.

5.5 Summary

Within this chapter, three scenario branches for future German energy supply systems in the year 2050 were investigated. In the *BELS* and *BELS*$^+$ scenario branch, a basic electricity supply of 528 TWh_{el}/a is supplied, once without and once with a centralized hydrogen infrastructure. In the *BLHYS* scenario branch, which builds on the *BELS*$^+$ scenario branch, also a low / medium / high hydrogen supply in the transport and industry sector of 2.56 / 5.04 / 7.30 Mt_{H_2}/a is considered. In the scenario branches, carbon dioxide reduction targets were varied between 80 and 100%, with respect to the emissions caused by electricity generation in 1990. The scenarios in the branches were modeled as a linear program in the developed modeling framework *FINE* with 75 regions and 30 typical days which are inter-connected by a seasonal storage formulation. For each scenario, the design and operation of the supply system was optimized and the results of these computations were presented in the chapter in aggregated form. Additionally scenario variations were performed to determine the value of individual technologies / components in the system.

In the reference scenarios, the corner stones of the annual renewable energy supply are, with roughly similar shares, offshore and onshore wind turbines, followed by electricity generation from PV (open-field and rooftop) systems. The regional distribution of these RES is not exclusively selected based on their minimum levelized cost of electricity as in some cases congestions in the grid can restrict their cost-optimal placements. Run-of-river plants and renewable electricity imports also contribute to the renewable energy supply and, for high reduction targets, biomass from residues is considered as a primary energy source. Several technology classes contribute to the temporal balancing of the supply systems.

- Existing German PHES is used as daily and inter-daily storage throughout the scenarios.
- The installed capacities of lithium-ion batteries, which are also operated as daily storage, increase significantly with stricter reduction targets. In this context, a high correlation between the operation and design of lithium-ion battery capacities was observed throughout the scenarios.
- Power plants are used for flexible balancing. They are either operated on natural gas or, with stricter reduction targets, on purified biogas or synthetic gases, i.e. hydrogen or methane. The renewable gases are in this context stored in UGS.
- Underground storage is considered for particularly high reduction targets as electricity storage and when hydrogen demands in the mobility and transport sector are considered. The UGS is operated with prominent seasonal profiles and either purified biogas or synthetic gas, i.e. synthetic methane or

hydrogen, is stored.

- If liquid hydrogen imports are selected during optimization, cryogenic tanks are considered at shipping terminals.
- Electrolyzers are either used in the context of seasonal electricity storage or to supply hydrogen to the transport and industry sector. In both cases, they provide flexibility to the electricity system by operating as a flexible electricity consumer. In this context, they contribute to the integration of fluctuating electricity generation from wind turbines in the electricity supply system.

Electricity and gas grids contribute to the spatial balancing of the supply systems.

- AC and DC lines are the corner stones for the spatial balancing of the electricity supply. With increasing reduction targets, DC line expansions of several gigawatts are considered which facilitate the integration of offshore wind turbines into the electricity system.
- For particularly high reduction targets and when hydrogen demands in the mobility and transport sector are considered, spatial balancing by hydrogen pipeline contributes to the cost optimal energy supply.
- Biogas injection and, if centralized hydrogen reconversion is not eligible, synthetic methane transmission via in 2017 existing gas pipelines provide an additional spatial balancing option.

The *BELS* and *BELS*$^{+}$ reference scenarios diverge from each other for reduction targets equal or above 90%. For these reduction targets, centralized hydrogen reconversion is considered in the *BELS*$^{+}$ scenario branch by building hydrogen transmission pipelines, salt cavern storage and hydrogen operated CCGT plants. The consideration of the hydrogen reconversion pathway promotes the cost-efficient integration of wind turbines, causing an increase in wind turbine capacities and a decrease in PV, biomass and methanation capacities. All in all, in comparison to the *BELS* reference scenarios, cost reductions of up to 8.8% are achieved.

With consideration of additional energy demands in the mobility and transport sector in the *BLHYS* scenario branch, the total annual cost of the supply system inherently increases as a wider section of the energy system is decarbonized. Specifically wind turbines, both offshore but primarily onshore, are expanded and additional hydrogen infrastructure (electrolyzers, pipelines, salt caverns and intra-regional distribution infrastructure) is built. If cost-lucrative domestic hydrogen production is maxed out, liquid hydrogen imports are additionally considered. For the investigated scenarios, this is the case in the high hydrogen demand scenario with an 80% reduction target as there, in comparison to the other scenarios, only small amounts of low cost electricity from intermittent RES is available for domestic hydrogen production. If hydrogen reconversion is considered for a given reduction target, the amount of reconverted hydrogen decreases with increasing, exogenously given hydrogen demands in the mobility and transport sector. This is again linked to the availability of low cost electricity.

An overview of the average annual cost of the final energy demands as well as the variable operational expenditures (OPEX) of the electrolyzers in the reference scenarios are presented in Table 5.6. They were obtained by the investigation of the long-run marginal cost of the electricity and hydrogen supply, which can be interpreted as commodity costs in an ideal market.

Table 5.6: Average cost of the final energy demands and variable operational expenditures of the electrolyzers for the 80% and 100% reduction target (based on average long-run marginal cost as a cost indicator).

Cost type	Final energy demand: Electricity [€/MWh_{el}]		Final energy demand: H_2-industry [€/kg_{H_2}]		Final energy demand: H_2-mobility [€/kg_{H_2}]		Variable OPEX electrolyzers [€/MWh_{el}]	
Scenario	80%	100%	80%	100%	80%	100%	80%	100%
BELS	77	128	-	-	-	-	-	17.5
BELS$^+$	77	115	-	-	-	-	-	32.2
BLHYS - L-GH$_2$	81	119	3.71	3.39	5.36	5.04	56.3	38.1
BLHYS - M-GH$_2$	84	119	3.89	3.75	5.54	5.40	60.6	47.5
BLHYS - H-GH$_2$	87	118	4.13	3.96	5.78	5.61	64.1	53.2

The table points to several key findings of the scenario investigation:

- The cost of the electricity supply increases with increasing reduction targets. Furthermore, it decreases with the consideration of a centralized hydrogen infrastructure (*BELS* vs. *BELS*$^+$) and increases with the consideration of additional hydrogen demands (*BELS*$^+$ vs. *BLHYS*). The increase in the latter is less prominent for higher reduction targets and is in this case still notably less expensive than when a centralized hydrogen infrastructure is not considered (*BELS*). At a tipping point, the cost of the electricity supply is reduced with increasing hydrogen demands: while for small hydrogen to electricity demand ratios, the hydrogen production benefits from the intermittent, renewable electricity production for the final electricity demand, this effect is reversed for larger hydrogen to electricity demand ratios.
- The hydrogen costs in the industry and transport sector differ from each other within a scenario only by their intra-regional distribution cost. When stricter reduction targets are deployed on a scenario, the costs decrease. This is caused by the increased availability of low-cost electricity from intermittent RES which can be used flexibly for hydrogen production. This is also reflected

in the variable OPEX of the electrolyzers.

- With increasing hydrogen demands in the mobility and transport sectors, the variable OPEX of the electrolyzers increases as less low-cost electricity, which is generated as a by-product of the final electricity supply, is available. This is one indicator of why hydrogen reconversion is decreased with increasing hydrogen demands.
- In comparison to the *BELS*$^{+}$ scenario, electrolyzers can only be operated with low variable OPEX in the *BELS* scenario under the premise of optimality. This is caused by the less efficient and in total more expensive downstream infrastructure, after electrolysis, of the methanation pathway.

With the considered spatial and temporal resolution, considered technology portfolio and applied modeling approach, in comparison to literature novel infrastructure scenarios were determined for Germany. Specifically with the considered spatial and temporal resolution, cross-linked storage and transmission infrastructure for electricity, methane and hydrogen could be modeled and their interactions investigated in detail. Here, the computationally efficient implementation via interconnected typical days was enabled by the developed modeling framework *FINE*. Scenarios which investigate infrastructure scenarios for Germany in this detail can, to the best knowledge of the author, currently not be found in literature.

In future work, additional demands, for example heat demands, and correspondingly required technologies can be included in the scenario setup and the final electricity demand be modeled in more detail. In this way, the value of CHPs, *Power-to-Heat* and heat storage could, for example, be modeled in detail. Such an additional modeling detail could be obtained by running a one-nodal energy system model with a high sectoral detail first and then distributing its resulting energy demands across Germany. Furthermore, the modeling detail could be increased even further if a detailed technical assessment of the transmission infrastructure is performed in the post-processing of the optimization. Here, for example, post-discretization approaches of the linear program could be performed, pressure losses assessed, spatial disaggregation approaches considered and grid stability tested.

Based on the scenario results obtained in this thesis, an integrated cross-linked infrastructure development strategy for electricity and all relevant gas supply systems was proposed for Germany. Individual, separate pathways to first design the electricity supply system without cross-linked infrastructure and then the required infrastructure for hydrogen or to design the energy supply system without hydrogen pipelines would lead to incompatibilities and / or additional cost. Furthermore, when comparing the results of the scenarios to the German energy supply system in 2017 / 2018, an urgent need for change was exposed which should be taken into genuine consideration by all share and stakeholders.

Chapter 6

Summary and Concluding Remarks

Within this chapter, a final summary and discussion of this thesis is given. For this purpose, first the defined scope and objective are recapitulated in section 6.1. Then, the chosen modeling approach is summarized in section 6.2. In section 6.3, the results of the scenario investigations are presented and put into perspective. Finally, the key conclusions are drawn in section 6.4.

6.1 Scope and Objective

With the increasing share of renewable energies in the German energy system and the target to decarbonize all sectors of the energy system, concepts to determine cross-linked energy supply systems are brought into a new focus.

A number of studies exist in literature which investigate future German electricity and hydrogen supply scenarios individually. However, cross-linked infrastructure assessments, including both energy storage and transmission technologies, have not been the focus of these studies yet. For the assessement of such cross-linked storage and transmission infrastructure scenarios, the current energy system modeling landscape can be improved upon. Most existing *Python*-based modeling frameworks do not consider energy transmission with additional technical constraints and storage is often modeled by simplified means. Moreover, approaches for temporal complexity reduction which maintain the ability to model seasonal storage are often not considered.

In this context, the objective of this thesis was formulated twofold. On the one hand, a modeling framework which is suitable for cross-linked infrastructure investigations must be developed. On the other hand, comprehensive cross-linked infrastructure scenarios must be investigated for Germany, including a detailed representation of all relevant storage and transmission technologies. This led to the following research questions to be investigated:

- What is the optimal cross-linked infrastructure design and operation for a future German energy system scenario under varying carbon dioxide restrictions?
- What is the role of individual technologies in such a scenario, i.e. when are specific technologies considered and how are they operated?
- Which opportunities and synergies but also challenges arise from such a cross-linked infrastructure design?

6.2 Chosen Modeling Approach

The considered modeling approach is twofold. On the one hand, a workflow was created which is capable of generating generic spatially and temporally resolved energy supply system models. On the other hand, a scenario scope for the investigation of cross-linked infrastructure in a future German energy system in the year 2050 was set up.

The presented workflow includes the pre-processing of geo-referenced and temporally resolved energy system data. In the pre-processing, the input data is, if applicable, discretized, clustered and aggregated to provide a compatible input for the subsequently created energy system model. While the workflow is capable of modeling detailed supply system models in theory, the workflow is often limited by the availability of the required input data in practice. Regional disaggregation approaches, for example via distribution keys, can be applied to increase the spatial resolution of coarsely resolved data. They have to be well justified / validated to a large extent, as otherwise a spurious modeling accuracy is suggested. Here, open-data initiatives can contribute to the research field.

The second part of the workflow is the determination of an optimal supply system design. In this context, the novel modeling framework *FINE*, a Framework for INtegrated Energy system assessement was developed. The framework is capable of modeling energy transmission and storage in technical detail, has a feature to reduce temporal complexity while maintaining the capability to model seasonal storage and can furthermore model non-linear cost-capacity correlations and thus an economy of scale. The framework was generically formulated via an object-oriented programming approach. As such, the framework can be applied to model energy system levels ranging from single households, over districts and one-nodal energy systems to multi-regional national and international energy supply systems. The framework was published open-source and does not require commercial software.

To model cross-linked infrastructure scenarios for Germany, first infrastructure components which can be of interest for a future energy supply system were assessed. Technologies for the procurement, conversion, storage and / or transmission of electricity, gaseous and liquid hydrogen, biogas and methane-rich gas, i.e. natural gas, purified biogas and synthetic methane, were investigated and their techno-economic data as well as in literature existing approaches about their geo-referenced modeling identified. In this context, also international electricity imports and exports as well as natural gas and liquid hydrogen imports were discussed.

Based on this input data and the defined modeling workflow, geo-referenced data was aggregated and the scenario scope formulated in terms of input parameters required for the modeling framework *FINE*. The scenario scope is set in Germany in the year 2050 and investigates the supply of a basic electricity demand of 528 TWh_{el}/a and a low, a medium, and a high hydrogen demand scenario in the transport and industry sector, with a demand of 2.56, 5.04, and 7.30 Mt_{H_2}/a, respectively. Additional electricity and hydrogen demands for domestic hydrogen production and hydrogen reconversion to electricity can arise endogenously in the scenario setup. The scenario scope is intended to investigate carbon dioxide reduction targets between 80% and 100%, with respect to the emissions arising from electricity generation in the year 1990. For the supply infrastructure, the in 2017 / 2018 existing energy supply infrastructure and its technological aging was taken into account, i.e. the scenario scope goes beyond a green-field modeling approach. In this context, the existing, or in the near-future planned, electric grid, the natural gas grid, conventional power plants, pumped-hydro energy storage, run-of-river plants and underground gas storage were considered.

6.3 Scenario Results

Three scenario branches for future German energy supply systems in the year 2050 were investigated. In the *BELS* and *BELS*$^+$ scenario branches, only the basic electricity supply is considered, once without and once with a centralized hydrogen infrastructure. In the *BLHYS* scenario branch, which builds on the *BELS*$^+$

scenario branch, also the low / medium / high hydrogen supply in the transport and industry sector is considered. For these scenarios, the optimal design and operation of the supply systems were investigated. In this context, the role of individual infrastructure technologies and synergies of the cross-linked infrastructure design were determined.

In the scenarios, offshore and onshore wind turbines, followed by electricity generation from open-field and rooftop PV systems were identified as the corner stones of renewable electricity procurement. PHES, batteries, the storage of methane-rich gas and hydrogen as well as flexible electricity demands from electrolyzers contribute to the temporal balancing of the supply systems. The electric grid, as well as the transport of methane-rich gas and a newly built hydrogen pipeline grid provide spatial balancing options. Hydrogen imports are chosen for selected scenarios and the interaction within the European electricity supply system contributes to a cost-optimal energy supply system. In general, it could be observed that with stricter carbon dioxide reduction targets, renewable energy procurement is increased and the considered technology portfolio becomes more divers.

The benefit of a centralized, to the electricity infrastructure cross-linked hydrogen infrastructure becomes apparent when the *BELS* and *BELS*$^+$ reference scenarios are compared. The scenarios diverge from each other for reduction targets equal or above 90%. There, a centralized hydrogen reconversion pathway via hydrogen transmission pipelines and salt cavern storage is considered. The consideration of this pathway promotes the cost-efficient integration of wind turbines, causing an increase in wind turbine capacities and a decrease in PV, biomass and methanation capacities. In the scenarios, this pathway is more cost-efficient than the consideration of a methanation pathway. All in all, in comparison to the *BELS* reference scenarios, cost reductions of up to 8.8% are achieved.

In the *BLHYS* scenario branch, the total annual cost of the supply system is inherently increased as a wider section of the energy system is decarbonized. Wind turbine capacities of both offshore but primarily onshore are furthermore expanded and additional hydrogen infrastructure, i.e. electrolyzers, pipelines, salt caverns and intra-regional distribution infrastructure, is built.

In the scenarios, the cost of the electricity supply increases with stricter carbon dioxide reduction targets. When the average long-run marginal cost of the electricity supply is consulted as a cost indicator, 77-87 €/MWh_{el} and 115-128 €/MWh_{el} are determined for the reference scenarios with an 80% and 100% reduction target, respectively. The electricity supply cost decreases with the consideration of a centralized hydrogen infrastructure (*BELS* vs. *BELS*$^+$) and increases with the consideration of additional hydrogen demands (*BELS*$^+$ vs. *BLHYS*). The increase in the latter is less prominent for higher reduction targets and it is still notably smaller compared to a centralized hydrogen infrastructure not being considered (*BELS*).

When the average long-run marginal cost of the hydrogen supply is consulted as a cost indicator, hydrogen cost in the industry sector of 3.71-4.13 €/kg$_{H_2}$ and 3.39-3.96 €/kg$_{H_2}$ (80% reduction target) as well as hydrogen cost in the transport sector of 5.36-5.78 €/kg$_{H_2}$ and 5.04-5.61 €/kg$_{H_2}$ (100% reduction target) were determined for the reference scenarios respectively[1]. Within a scenario, the hydrogen costs in the industry and transport sector differ from each other only by their intra-regional distribution cost. The decrease in the hydrogen supply cost with increasing carbon dioxide reduction targets is caused by the increased availability of low-cost electricity from intermittent RES which can be used flexibly for hydrogen production. This is also reflected in the variable OPEX of the electrolyzers which decreases from 56.3-64.1 €/MWh$_{el}$ in the 80% *BLHYS* reference scenarios to values of 38.1-53.2 €/MWh$_{el}$ in the 100% *BLHYS* reference scenarios.

With increasing hydrogen demands in the mobility and transport sectors, the variable OPEX of the electrolyzers increases as less low-cost electricity, which is generated as a by-product of the final electricity supply, is available. Thus, the endogenously determined capacities of the technologies in the hydrogen reconversion pathway are reduced with increasing hydrogen demands.

With the chosen scenario set and the developed modeling framework *FINE*, novel infrastructure scenarios for Germany were determined. In reflection with literature and with the experience gained during the elaboration of the scenarios, also future work was identified. In this context, future work can include further developments of *FINE* and the application of model-coupling and optimization heuristics to increase the representation of sectoral energy demands and technical modeling detail.

Individual, separate pathways to first design the electricity supply system without cross-linked infrastructure and then the required infrastructure for hydrogen or to design the energy supply system without hydrogen pipelines would lead to incompatibilities and / or additional cost. Thus, based on the scenario results obtained in this thesis, an integrated cross-linked infrastructure development strategy for electricity and all relevant gas supply systems is proposed for Germany.

The modeling results are put into perspective when comparing them to the German energy supply system in 2017 / 2018. Here, an urgent need for change is exposed which should be taken into genuine consideration by decision makers.

[1] The lower end of the costs arises for the low hydrogen demand scenario while the higher end of the costs arises for the high hydrogen demand scenario.

6.4 Conclusions

Finally, the objectives posed at the beginning of this thesis are repeated and reflected upon.

What is the optimal cross-linked infrastructure design and operation for a future German energy system scenario under varying carbon dioxide restrictions?

The optimal cross-linked infrastructure design and operation for a future German energy system is comprised of a multifaceted technology portfolio which has to be strategically placed across Germany. Onshore and offshore wind turbines, rooftop and open-field PV systems and renewable electricity imports will be the corner stones of renewable energy procurement. PHES, batteries, geological storage of synthetic gas, electricity and hydrogen networks and deferrable electricity demands of electrolyzers guarantee a temporally and spatially balanced energy supply.

What is the role of individual technologies in such a scenario, i.e. when are specific technologies considered and how are they operated?

With the large number of scenario variations, the role of each considered technology type could be investigated with respect to when the technologies are considered and how they are operated. As this list is comprehensive, the reader is referred to subsection 5.4.2 for more details. In general, it can be concluded that for a future electricity and hydrogen supply system, hydrogen pipelines, underground storage of both hydrogen and methane-rich gas as well as AC and DC lines are key storage and transmission infrastructure components to guarantee a cost-efficient system design.

Which opportunities and synergies but also challenges arise from such a cross-linked infrastructure design?

On the one hand, the electricity supply system benefits from the consideration of electrolyzers as a flexibility provider. The electrolyzers provide access to RES which would otherwise be challenging to integrate and thus not considered in an optimal supply system. Specifically, they enable a cost-efficient integration of wind turbines into the energy system, thus leading to smaller amounts of “surplus electricity” within the electricity system. Moreover, with the provided hydrogen reconversion options, positive residual loads can be flexibly covered on a renewable basis. The additional stress on the energy supply system which is caused by the additionally considered hydrogen demands leads to negligible cost increases for the electricity supply for strict carbon dioxide reduction targets. On the other hand, with increasing carbon dioxide reduction targets, the hydrogen supply infrastructure benefits from increasing amounts of “surplus electricity” which arises out of the decarbonization of the electricity supply. Electrolyzers can be operated on lower LRMCs of the electricity supply, and thus lead to cost decreases in the LRMC of a renewable hydrogen supply between the 80% and the 100% reduction target. Moreover, with the cross-link between the electricity and hydrogen infrastructure, a wider decarbonization of the energy system’s sectors is enabled.

Appendix A

Appendix - Model Input Parameters

A.1 *Basic* Electricity Demand

In analogy to a figure given by Robinius [14], Figure A.1 visualizes snapshots of the minimum and maximum *basic* electricity demand that occurs in the time series data of the electricity demand.

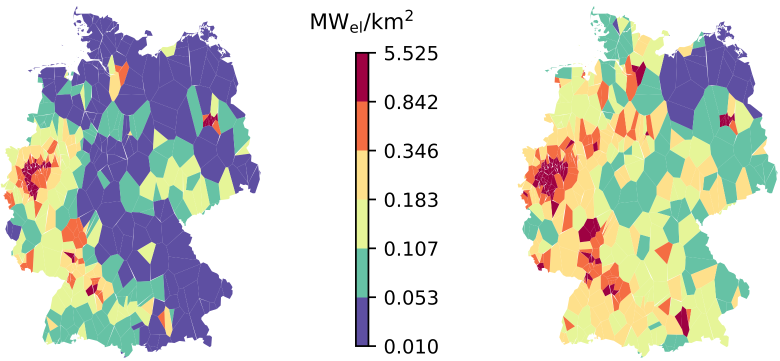

(a) Minimum load **(b)** Maximum load

Figure A.1: Snapshots of the minimum *basic* electricity load (2. July, 7 am, Σ 37 GW_{el}) and the maximum *basic* electricity load (5. December, 6 pm, Σ 83 GW_{el}) in the scenarios.

A.2 *Basic* Hydrogen Demand

The considered *medium* hydrogen demand scenario is based on geo-referenced data from *Cerniauskas et al.* [81] and aggregated to the German federal states visualized in Figure A.2.

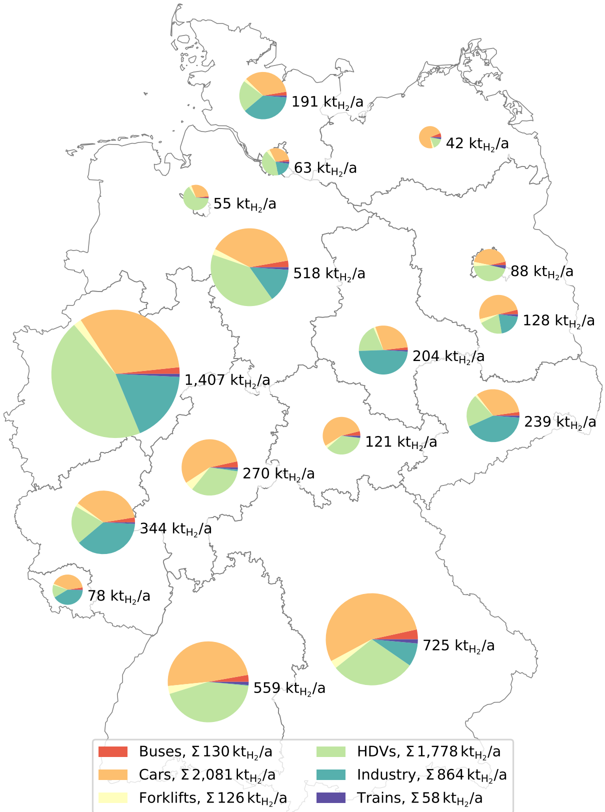

Figure A.2: Annual *basic* hydrogen demands in the *medium* hydrogen demand scenario, aggregated to the German federal states (HDVs: heavy duty vehicles, geo-referenced data from [81]).

A.3 Electricity Imports and Exports

Potential international electricity imports and exports which are considered in the scenarios of this thesis [114].

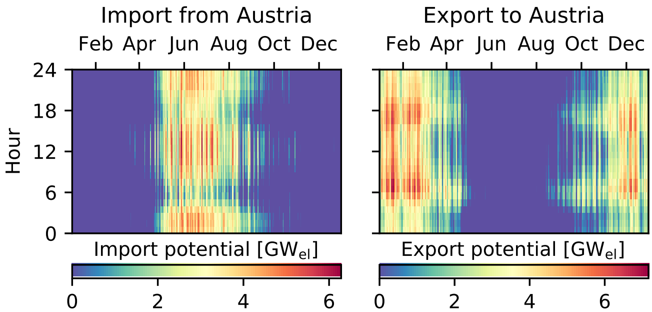

Figure A.3: Electricity imports and exports from and to Austria.

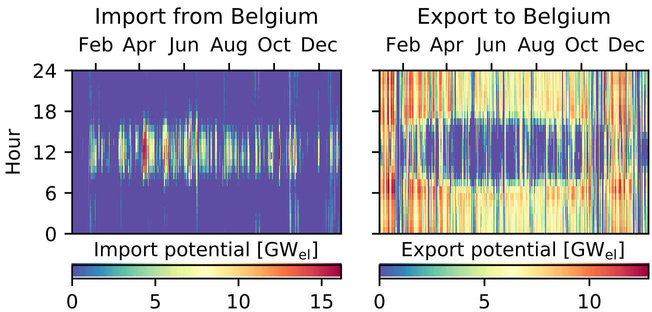

Figure A.4: Electricity imports and exports from and to Belgium.

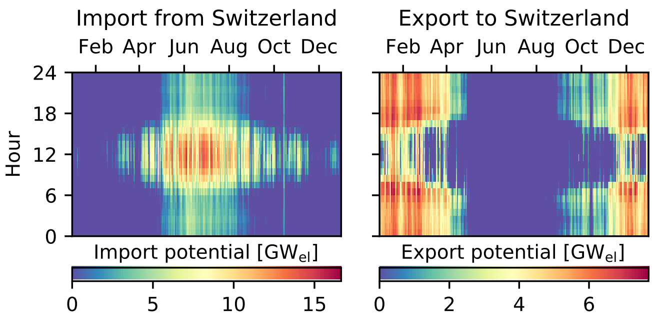

Figure A.5: Electricity imports and exports from and to Switzerland.

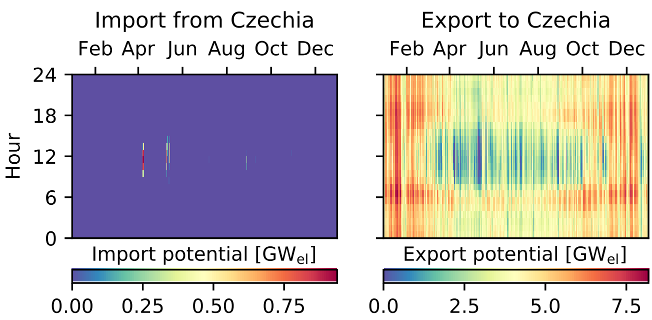

Figure A.6: Electricity imports and exports from and to Czechia.

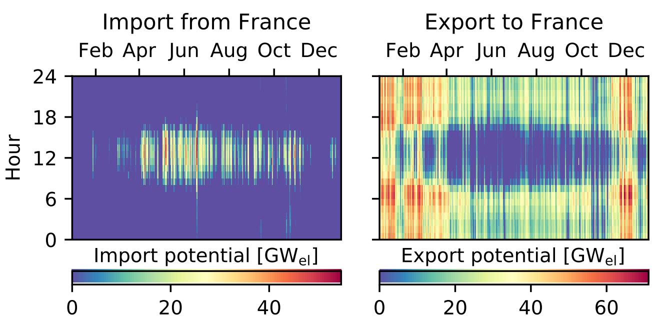

Figure A.7: Electricity imports and exports from and to France.

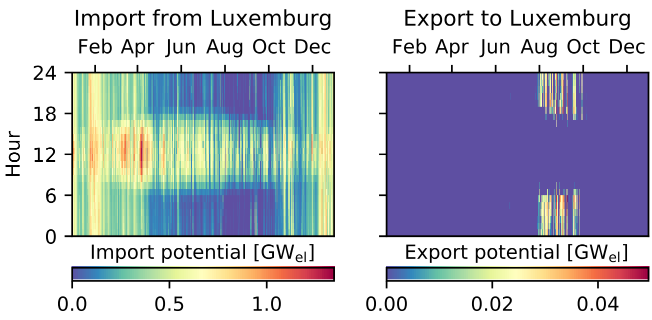

Figure A.8: Electricity imports and exports from and to Luxembourg.

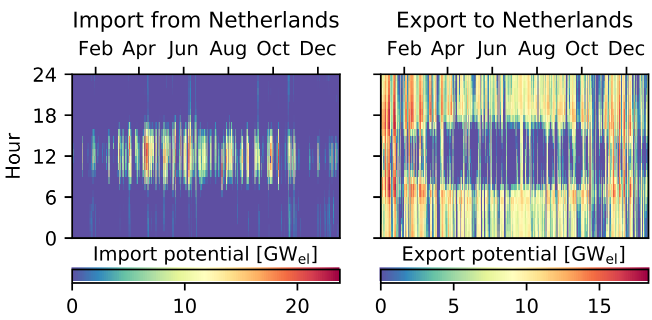

Figure A.9: Electricity imports and exports from and to Netherlands.

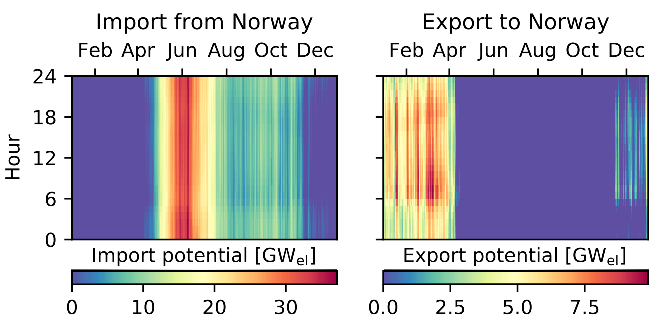

Figure A.10: Electricity imports and exports from and to Norway.

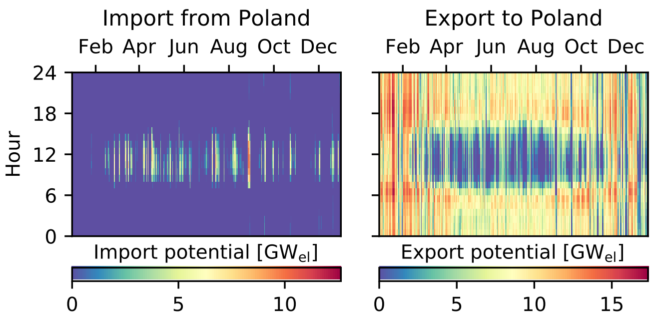

Figure A.11: Electricity imports and exports from and to Poland.

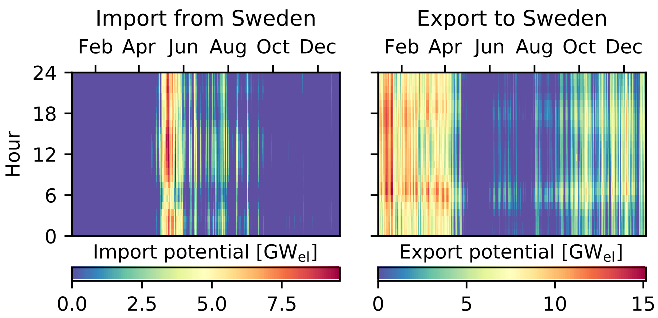

Figure A.12: Electricity imports and exports from and to Sweden.

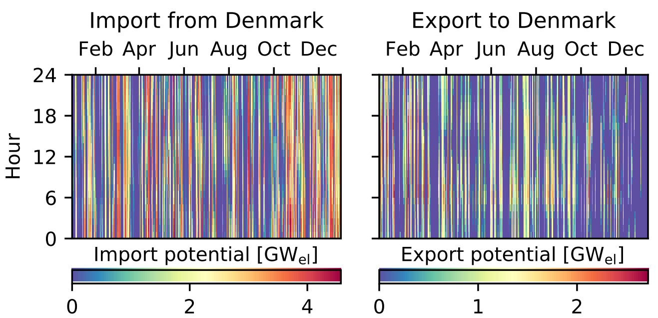

Figure A.13: Electricity imports and exports from and to Denmark.

A.4 Offshore Wind Turbines

Capacity specific invest and long-run average full load hours of offshore wind turbines in the North and Baltic Sea, based on the work of *Caglayan et al.* [105].

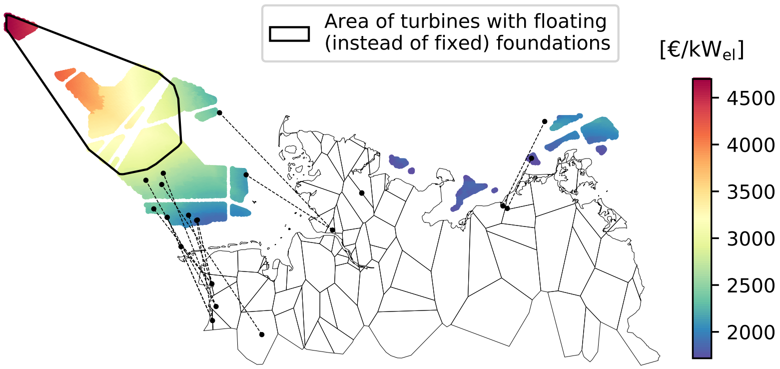

Figure A.14: Capacity specific invest of potential offshore wind turbines in the North and Baltic Sea.

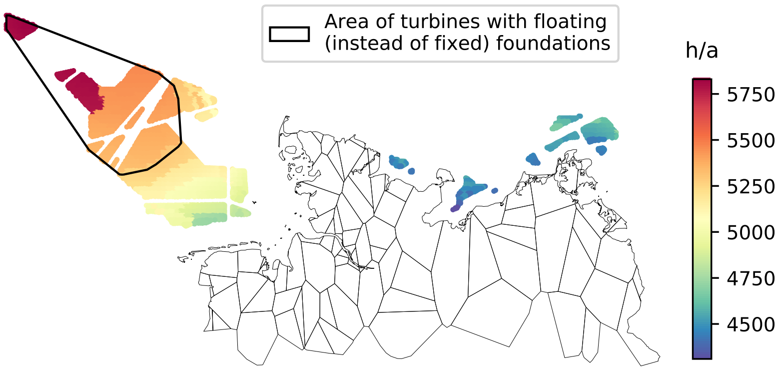

Figure A.15: Full load hours of potential offshore wind turbines in the North and Baltic Sea (long-run average of multiple decades of weather years).

A.5 Storage of Methane-rich Gases in Salt Caverns

Geo-referenced capacity potentials for the storage of methane rich gases in salt caverns, modeled based on existing salt cavern locations in Germany [168].

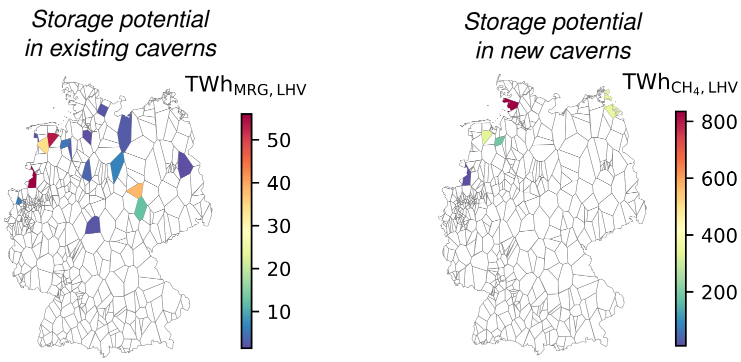

(a) $\Sigma\,231\,TWh_{CH_4}$ **(b)** $\Sigma\,1728\,TWh_{CH_4}$

Figure A.16: Capacity potentials for methane-rich gas storage in salt caverns (existing/ new), aggregated to the *Voronoi* regions. Regions marked in white do not hold any capacities.

A.6 Hydrogen Transmission and Distribution

Hydrogen transmission cost for different magnitudes of demand and transport distance [153]. The most cost-effective combinations of storage and transmission/ distribution technologies are displayed for the different areas of the function.

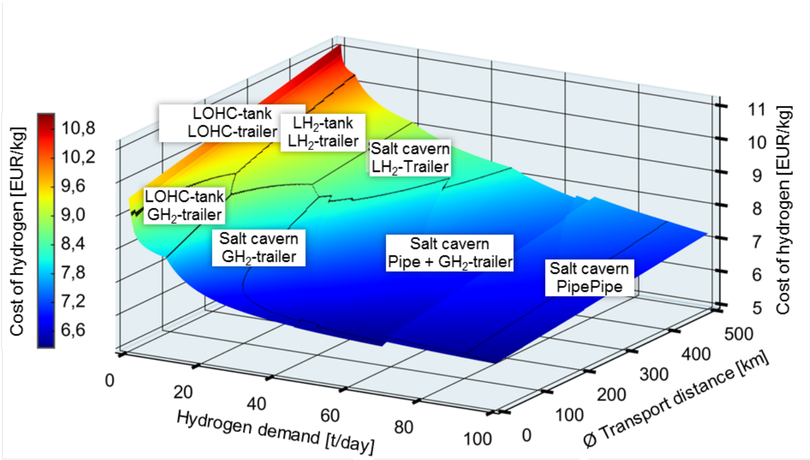

Figure A.17: Cost of hydrogen, given as a function of a daily hydrogen demand and an average transport distance. Figure from Reuß [153], translated from German into English.

Geo-referenced distribution of regional hydrogen distribution cost, modeled based on *Reuß* [153].

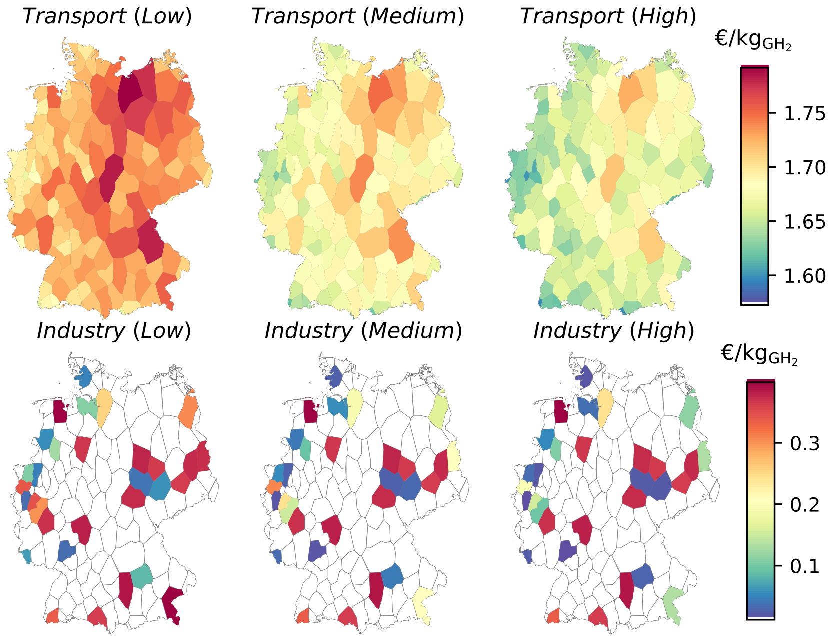

Figure A.18: Infrastructure cost of intra-regional hydrogen distribution (130 aggregated regions).

A.7 Model Parameter Tables

An overview of the parameters used to model the components of the scenarios in *FINE* is given in the following. The expression "f(reg)" refers to parameters with region-specific information.

Table A.1: Parameter overview of *Source* components (Part 1).

	Hydrogen import	Hydrogen import-	Natural gas import
commodity	LH_2	LH_2	MRG
hasCapacityVariable	True	True	False
operationRateFix	f(reg)	f(reg)	-
commodityCost	0.12	0.105	0.033
commodityLimitID	-	-	CO2max
yearlyLimit	-	-	f(scenario)
tsaWeight	0.01	0.01	-
scenarioBranch1	-	-	x
scenarioBranch2	x	x	x
scenarioBranch3	x	x	x

Table A.2: Parameter overview of *Source* components (Part 2).

	Wind onshore (CL1)	Wind onshore (CL2)	Wind offshore (fixed)	Wind offshore (float)
commodity	electricity	electricity	electricity	electricity
hasCapacityVariable	True	True	True	True
capacityMax	f(reg)	f(reg)	f(reg)	f(reg)
operationRateMax	f(reg)	f(reg)	f(reg)	f(reg)
investPerCapacity	f(reg)	f(reg)	f(reg)	f(reg)
opexPerCapacity	f(reg)·0.02	f(reg)·0.02	f(reg)·0.02	f(reg)·0.02
interestRate	0.08	0.08	0.08	0.08
economicLifetime	20	20	25	25
tsaWeight	1	1	1	1
scenarioBranch1	x	x	x	x
scenarioBranch2	x	x	x	x
scenarioBranch3	x	x	x	x

Table A.3: Parameter overview of *Source* components (Part 3).

	PV (rooftop-eastwards)	PV (rooftop-southwards)	PV (rooftop-westwards)
commodity	electricity	electricity	electricity
hasCapacityVariable	True	True	True
capacityMax	f(reg)	f(reg)	f(reg)
operationRateMax	f(reg)	f(reg)	f(reg)
investPerCapacity	880	880	880
opexPerCapacity	17.6	17.6	17.6
interestRate	0.08	0.08	0.08
economicLifetime	25	25	25
tsaWeight	1	1	1
scenarioBranch1	x	x	x
scenarioBranch2	x	x	x
scenarioBranch3	x	x	x

Table A.4: Parameter overview of *Source* components (Part 4).

	PV (OF-fixed)	PV (OF-tracking)	PV (OF-fixed+)	PV (OF-tracking+)
commodity	electricity	electricity	electricity	electricity
hasCapacityVariable	True	True	True	True
capacityMax	f(reg)	f(reg)	f(reg)	f(reg)
operationRateMax	f(reg)	f(reg)	f(reg)	f(reg)
investPerCapacity	520	710	520	710
opexPerCapacity	8.84	10.65	8.84	10.65
interestRate	0.08	0.08	0.08	0.08
economicLifetime	25	25	25	25
sharedPotentialID	PV-OF	PV-OF	PV-OF	PV-OF
tsaWeight	1	1	1	1
scenarioBranch1	x	x	x	x
scenarioBranch2	x	x	x	x
scenarioBranch3	x	x	x	x

Table A.5: Parameter overview of *Source* components (Part 5).

	R-o-r plants	CHP (wood)	Biogas plants
commodity	electricity	electricity	biogas
hasCapacityVariable	True	True	True
capacityMax	-	-	f(reg)
capacityFix	f(reg)	-	-
operationRateMax	f(reg)	-	-
operationRateFix	-	-	f(reg)
investPerCapacity	-	3300	-
opexPerCapacity	95.54	141.9	-
opexPerOperation	0.005	0.0039	-
commodityCost	-	0.098	0.07
interestRate	0.08	0.08	-
economicLifetime	60	25	-
annualOperationMax	-	f(reg)	-
tsaWeight	1	-	0.01
scenarioBranch1	x	x	x
scenarioBranch2	x	x	x
scenarioBranch3	x	x	x

Table A.6: Parameter overview of *Source* components (Part 6).

	Electricity import (LUX)	(POL)	(CHE)	(NLD)
commodity	electricity	electricity	electricity	electricity
hasCapacityVariable	True	True	True	True
capacityFix	f(reg)	f(reg)	f(reg)	f(reg)
sharedOperationRateMax	f(reg)	f(reg)	f(reg)	f(reg)
commodityCost	0.094	0.075	0.053	0.074
tsaWeight	1	1	1	1
scenarioBranch1	x	x	x	x
scenarioBranch2	x	x	x	x
scenarioBranch3	x	x	x	x

Table A.7: Parameter overview of *Source* components (Part 7).

	Electricity import (AUT)	(DNK)	(CZE)	(FRA)
commodity	electricity	electricity	electricity	electricity
hasCapacityVariable	True	True	True	True
capacityFix	f(reg)	f(reg)	f(reg)	f(reg)
sharedOperationRateMax	f(reg)	f(reg)	f(reg)	f(reg)
commodityCost	0.037	0.049	0.068	0.057
tsaWeight	1	1	1	1
scenarioBranch1	x	x	x	x
scenarioBranch2	x	x	x	x
scenarioBranch3	x	x	x	x

Table A.8: Parameter overview of *Source* components (Part 8).

	Electricity import		
	(BEL)	(SWE)	(NOR)
commodity	electricity	electricity	electricity
hasCapacityVariable	True	True	True
capacityFix	f(reg)	f(reg)	f(reg)
sharedOperationRateMax	f(reg)	f(reg)	f(reg)
commodityCost	0.08	0.042	0.024
tsaWeight	1	1	1
scenarioBranch1	x	x	x
scenarioBranch2	x	x	x
scenarioBranch3	x	x	x

Table A.9: Parameter overview of *Conversion* components (Part 1).

	CHP		OCGT		CCGT	
	(biogas)	(GH_2)	(MRG)	(GH_2)	(MRG)	(GH_2)
physicalUnit	GW_{el}	GW_{el}	GW_{el}	GW_{el}	GW_{el}	GW_{el}
hasCapacityVariable	True	True	True	True	True	True
CF electricity	1	1	1	1	1	1
CF MRG	-	-	-2.22222	-	-1.5873	-
CF biogas	-2.12766	-	-	-	-	-
CF $GH_{2,30\mathrm{bar}}$	-	-2.12766	-	-	-	-
CF $GH_{2,100\mathrm{bar}}$	-	-	-	-2.22222	-	-1.5873
capacityMax	-	-	f(reg)	f(reg)	f(reg)	f(reg)
investPerCapacity	850	850	550	550	850	850
opexPerCapacity	8.5	8.5	16.5	16.5	21.25	21.25
opexPerOperation	0.006	0.006	0.002	0.002	0.011	0.011
interestRate	0.08	0.08	0.08	0.08	0.08	0.08
economicLifetime	25	25	30	30	30	30
sharedPotentialID	-	-	CTPP	CTPP	CTPP	CTPP
scenarioBranch1	x	x	x	-	x	-
scenarioBranch2	x	x	x	x	x	x
scenarioBranch3	x	x	x	x	x	x

Table A.10: Parameter overview of *Conversion* components (Part 2).

	Electrolyzers	Electrolyzers-	Liquefaction plants	Regasification plants
physicalUnit	GW_{el}	GW_{el}	$GW_{\mathrm{LH_2,LHV}}$	$GW_{\mathrm{GH_2,LHV}}$
hasCapacityVariable	True	True	True	True
CF electricity	-1	-1	-0.2	-0.02
CF $GH_{2,\mathrm{30bar}}$	0.7	0.7	-1.02	-
CF $GH_{2,\mathrm{100bar}}$	-	-	-	1
CF LH_2	-	-	1	-1
investPerCapacity	500	300	1500	24
opexPerCapacity	15	9	120	0.72
interestRate	0.08	0.08	0.08	0.08
economicLifetime	10	10	20	10
scenarioBranch1	x	x	-	-
scenarioBranch2	x	x	x	x
scenarioBranch3	x	x	x	x

Table A.11: Parameter overview of *Conversion* components (Part 3).

	Compressor stations	Valve	Purification plants (biogas)	Methanation plants
physicalUnit	$GW_{\mathrm{GH_2,LHV}}$	$GW_{\mathrm{GH_2,LHV}}$	$GW_{\mathrm{MRG,LHV}}$	$GW_{\mathrm{MRG,LHV}}$
hasCapacityVariable	True	False	True	True
CF electricity	-0.02	-	-0.043	-0.05
CF MRG	-	-	1	1
CF biogas	-	-	-1	-
CF $GH_{2,\mathrm{30bar}}$	-1	1	-	-1.25
CF $GH_{2,\mathrm{100bar}}$	1	-1	-	-
investPerCapacity	42	-	343	1800
opexPerCapacity	1.68	-	8.575	72
interestRate	0.08	-	0.08	0.08
economicLifetime	15	-	15	25
scenarioBranch1	-	x	x	x
scenarioBranch2	x	x	x	x
scenarioBranch3	x	x	x	x

Table A.12: Parameter overview of *Storage* components (Part 1).

	Li-ion batteries	PHES (existing)	PHES (refurbished)
commodity	electricity	electricity	electricity
capacityMax	-	-	f(reg)
capacityFix	-	f(reg)	-
chargeRate	1	0.142857	0.142857
dischargeRate	1	0.142857	0.142857
chargeEfficiency	0.95	0.88	0.88
dischargeEfficiency	0.95	0.89	0.89
selfDischarge	4.23036e-05	-	-
cyclicLifetime	12000	-	-
stateOfChargeMin	0	0	0
stateOfChargeMax	1	1	1
investPerCapacity	150	-	130
opexPerCapacity	1.5	1.56	1.56
interestRate	0.08	0.08	0.08
economicLifetime	22	40	40
scenarioBranch1	x	x	x
scenarioBranch2	x	x	x
scenarioBranch3	x	x	x

Table A.13: Parameter overview of *Storage* components (Part 2).

	Pipe systems (MRG)	Biogas storage	Pipe systems (GH_2)	Cryogenic tanks (LH_2)
commodity	MRG	biogas	$GH_{2,30\mathrm{bar}}$	LH_2
chargeRate	0.0119048	0.12	0.0119048	1
dischargeRate	0.0119048	0.12	0.0119048	1
chargeEfficiency	1	1	1	1
dischargeEfficiency	1	1	1	1
selfDischarge	-	-	-	1.25018e-05
stateOfChargeMin	0.26	0.1	0.31	-
stateOfChargeMax	1	0.9	1	1
investPerCapacity	2.3	4	7	0.75
opexPerCapacity	0.023	-	0.07	0.015
interestRate	0.08	0.08	0.08	0.08
economicLifetime	30	8	30	20
scenarioBranch1	x	x	x	x
scenarioBranch2	x	x	x	x
scenarioBranch3	x	x	x	x

Table A.14: Parameter overview of *Storage* components (Part 3).

	Salt caverns (MRG, existing)	Salt caverns (MRG, new)	Pore storage (MRG)
commodity	MRG	MRG	MRG
capacityMax	f(reg)	f(reg)	-
capacityFix	-	-	f(reg)
chargeRate	0.00212264	0.00212264	0.000384615
dischargeRate	0.00212264	0.00212264	0.000384615
chargeEfficiency	1	1	1
dischargeEfficiency	1	1	1
stateOfChargeMin	0.29	0.29	0.55
stateOfChargeMax	1	1	1
investPerCapacity	0.02	0.07	-
opexPerCapacity	0.0014	0.0014	-
opexPerChargeOperation	-	-	0.001
interestRate	0.08	0.08	-
economicLifetime	30	30	-
sharedPotentialID	Existing SC	New SC	-
scenarioBranch1	x	x	x
scenarioBranch2	x	x	x
scenarioBranch3	x	x	x

Table A.15: Parameter overview of *Storage* components (Part 4).

	Salt caverns (GH_2, existing)	Salt caverns (GH_2, new)
commodity	$GH_{2,100\mathrm{bar}}$	$GH_{2,100\mathrm{bar}}$
capacityMax	f(reg)	f(reg)
chargeRate	0.00212264	0.00212264
dischargeRate	0.00212264	0.00212264
chargeEfficiency	1	1
dischargeEfficiency	1	1
stateOfChargeMin	0.33	0.33
stateOfChargeMax	1	1
investPerCapacity	0.07	0.23
opexPerCapacity	0.0046	0.0046
interestRate	0.08	0.08
economicLifetime	30	30
sharedPotentialID	Existing SC	New SC
scenarioBranch1	-	-
scenarioBranch2	x	x
scenarioBranch3	x	x

Table A.16: Parameter overview of *Transmission* components.

	AC lines	DC lines	DC lines (expansion)	Pipelines (GH_2)	(MRG)
commodity	electricity	electricity	electricity	$GH_{2,100\mathrm{bar}}$	MRG
hasIsBuiltBinaryVariable	False	False	False	True	False
bigM	-	-	-	60	-
capacityMin	-	-	-	0.45	-
capacityMax	-	-	-	47.4	-
capacityFix	f(reg)	f(reg)	-	-	f(reg)
investPerCapacity	-	-	f(reg)	0.144	-
investIfBuilt	-	-	-	0.34	-
opexIfBuilt	-	-	-	0.005	-
opexPerOperation	-	-	-	-	f(reg)
interestRate	-	-	0.08	0.08	0.08
economicLifetime	-	-	40	40	40
powerFlow	x	-	-	-	-
scenarioBranch1	x	x	x	-	x
scenarioBranch2	x	x	x	x	x
scenarioBranch3	x	x	x	x	x

Table A.17: Parameter overview of *Sink* components (Part 1).

	Hydrogen demand (transport, low)	(transport, medium)	(transport, high)
commodity	$GH_{2,100\mathrm{bar}}$	$GH_{2,100\mathrm{bar}}$	$GH_{2,100\mathrm{bar}}$
hasCapacityVariable	False	False	False
operationRateFix	f(reg)	f(reg)	f(reg)
opexPerOperation	f(reg)	f(reg)	f(reg)
tsaWeight	0.01	0.01	0.01
scenarioBranch1	-	-	-
scenarioBranch2	-	-	-
scenarioBranch3	x	x	x

Table A.18: Parameter overview of *Sink* components (Part 2).

	Hydrogen demand (industry, low)	(industry, medium)	(industry, high)
commodity	$GH_{2,100\mathrm{bar}}$	$GH_{2,100\mathrm{bar}}$	$GH_{2,100\mathrm{bar}}$
hasCapacityVariable	False	False	False
operationRateFix	f(reg)	f(reg)	f(reg)
opexPerOperation	f(reg)	f(reg)	f(reg)
tsaWeight	0.01	0.01	0.01
scenarioBranch1	-	-	-
scenarioBranch2	-	-	-
scenarioBranch3	x	x	x

Table A.19: Parameter overview of *Sink* components (Part 3).

	Electricity demand	Electricity export (LUX)	(POL)	(CHE)
commodity	electricity	electricity	electricity	electricity
hasCapacityVariable	False	True	True	True
capacityFix	-	f(reg)	f(reg)	f(reg)
operationRateFix	f(reg)	-	-	-
sharedOperationRateMax	-	f(reg)	f(reg)	f(reg)
commodityRevenue	-	0.001	0.001	0.001
tsaWeight	1	1	1	1
scenarioBranch1	x	x	x	x
scenarioBranch2	x	x	x	x
scenarioBranch3	x	x	x	x

Table A.20: Parameter overview of *Sink* components (Part 4).

	Electricity export (NLD)	(AUT)	(DNK)	(CZE)
commodity	electricity	electricity	electricity	electricity
hasCapacityVariable	True	True	True	True
capacityFix	f(reg)	f(reg)	f(reg)	f(reg)
sharedOperationRateMax	f(reg)	f(reg)	f(reg)	f(reg)
commodityRevenue	0.001	0.001	0.001	0.001
tsaWeight	1	1	1	1
scenarioBranch1	x	x	x	x
scenarioBranch2	x	x	x	x
scenarioBranch3	x	x	x	x

Table A.21: Parameter overview of *Sink* components (Part 5).

	Electricity export (FRA)	(BEL)	(SWE)	(NOR)
commodity	electricity	electricity	electricity	electricity
hasCapacityVariable	True	True	True	True
capacityFix	f(reg)	f(reg)	f(reg)	f(reg)
sharedOperationRateMax	f(reg)	f(reg)	f(reg)	f(reg)
commodityRevenue	0.001	0.001	0.001	0.001
tsaWeight	1	1	1	1
scenarioBranch1	x	x	x	x
scenarioBranch2	x	x	x	x
scenarioBranch3	x	x	x	x

Appendix B

Appendix - Scenario Results

B.1 *BELS* Branch

In the following, additional figures generated in the *BELS* scenario branch are displayed.

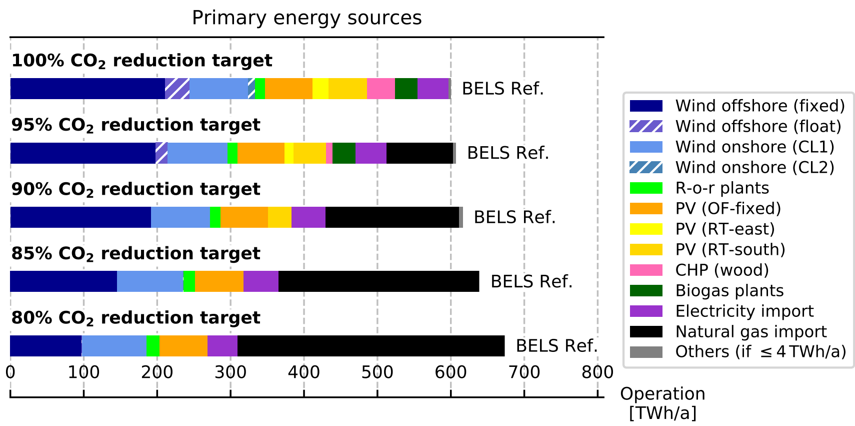

Figure B.1: Primary energy sources in the *BELS* reference scenario.

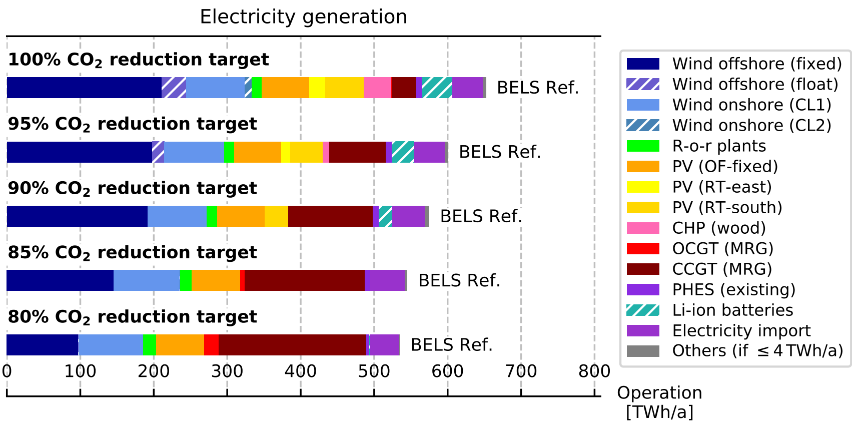

Figure B.2: Annual electricity generation in the *BELS* reference scenario.

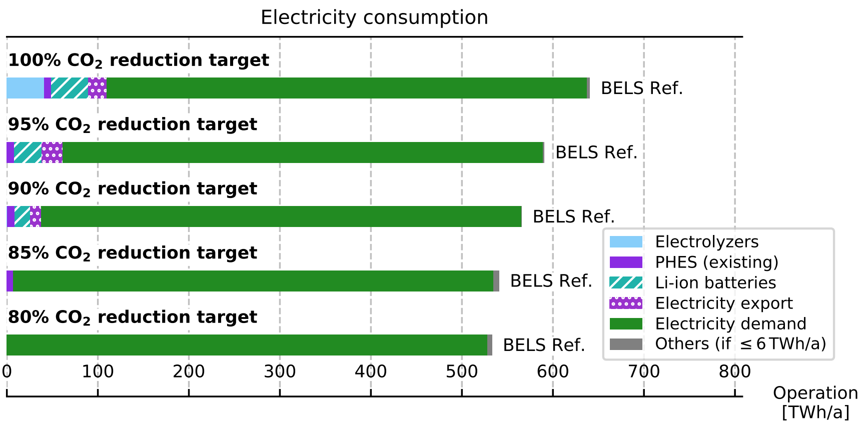

Figure B.3: Annual electricity consumption in the *BELS* reference scenario.

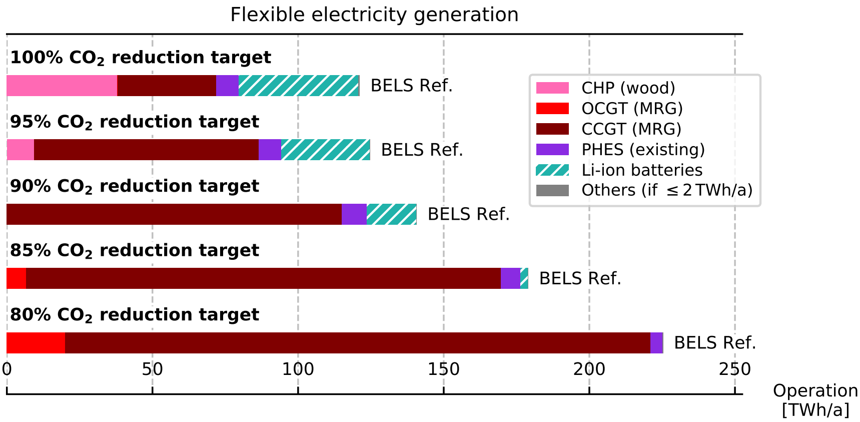

Figure B.4: Annual, flexible electricity consumption in the *BELS* reference scenario.

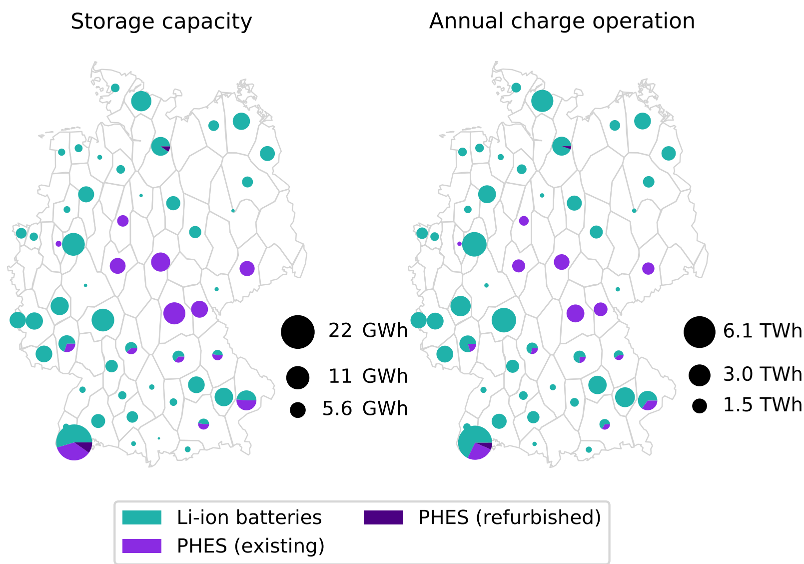

Figure B.5: Capacities and charging operation of electricity storage (*BELS*-100%).

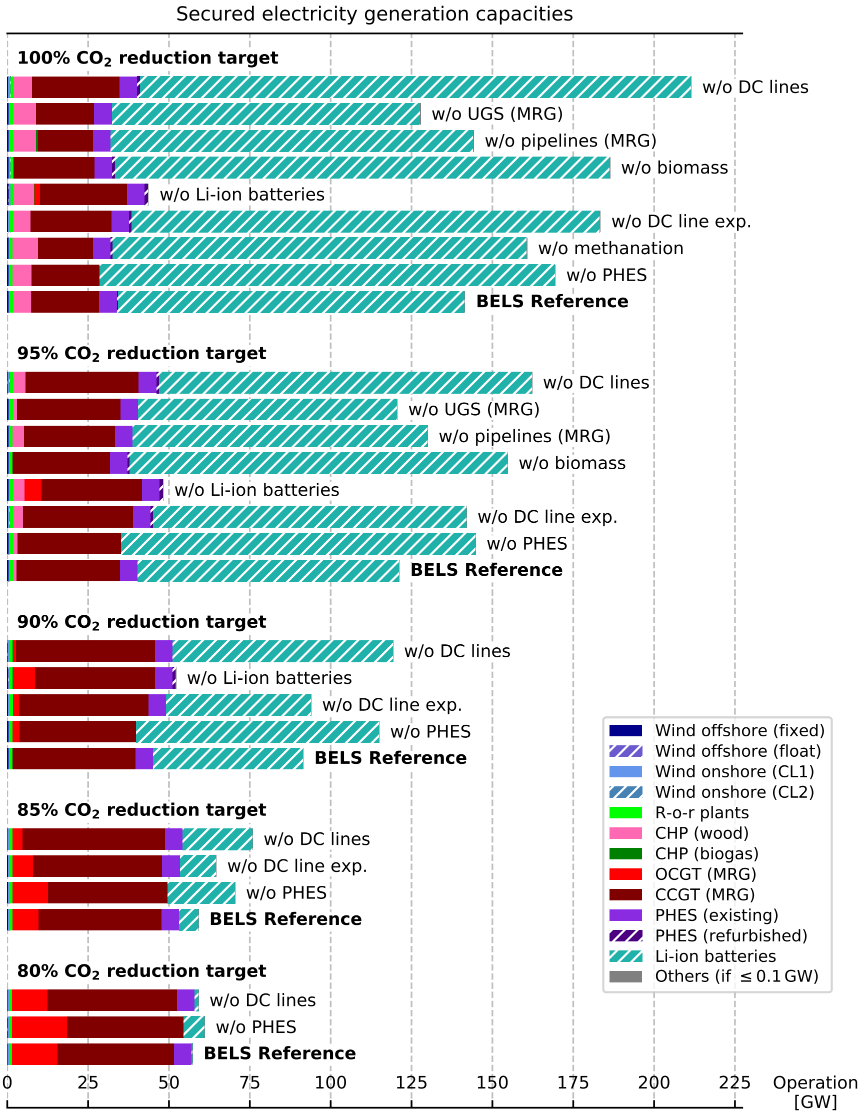

Figure B.6: Secured electricity generation capacities in the *BELS* scenario variations.

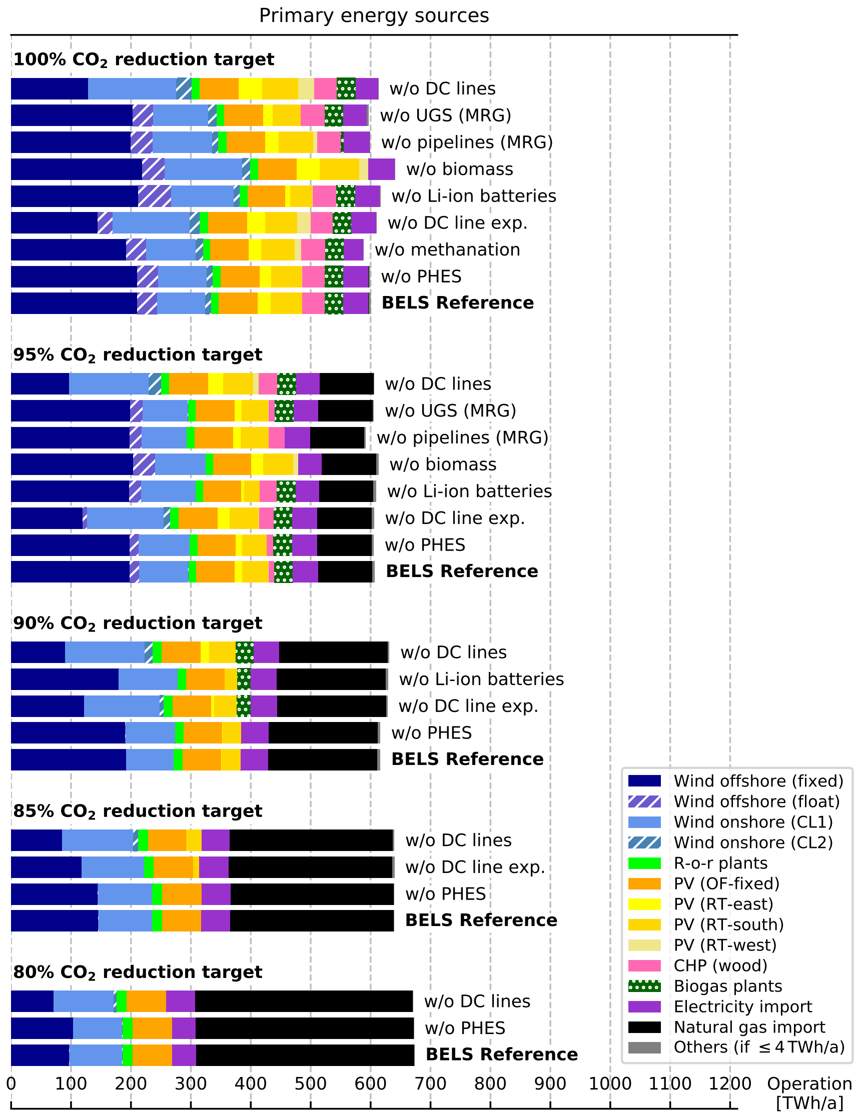

Figure B.7: Primary energy sources in the *BELS* scenario variations.

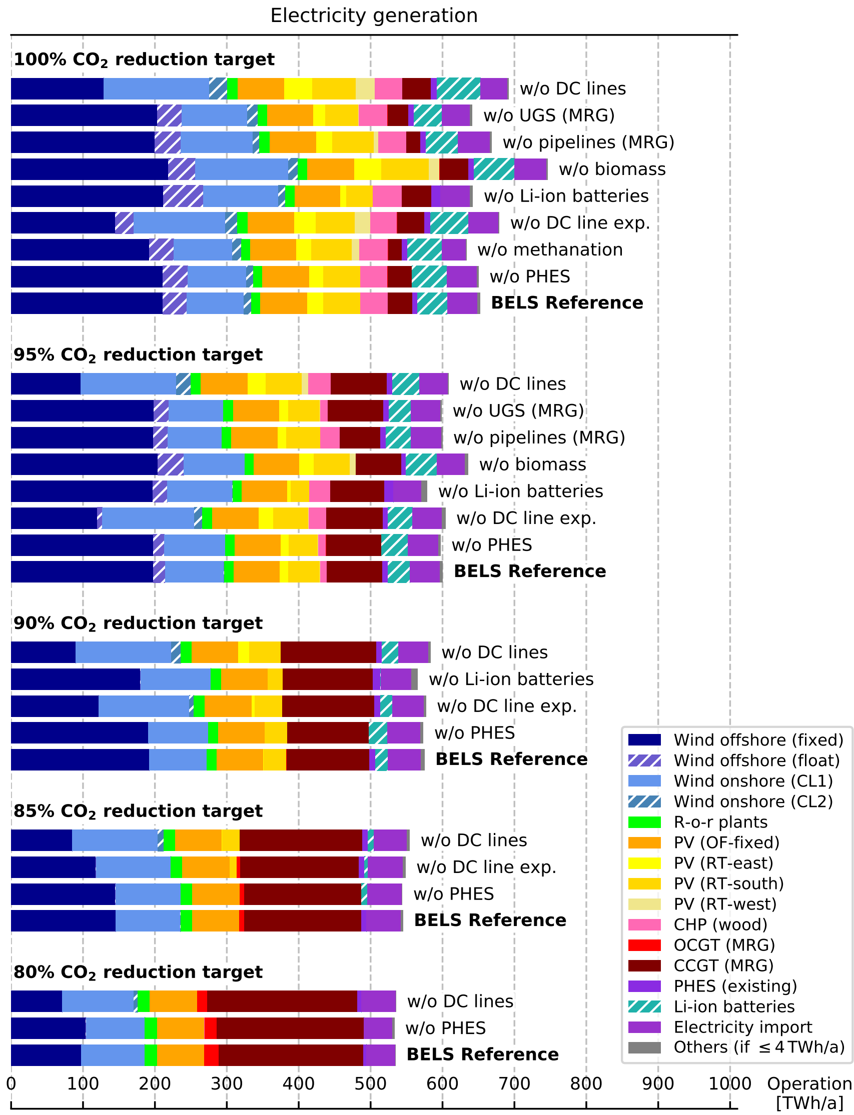

Figure B.8: Annual electricity generation in the *BELS* scenario variations.

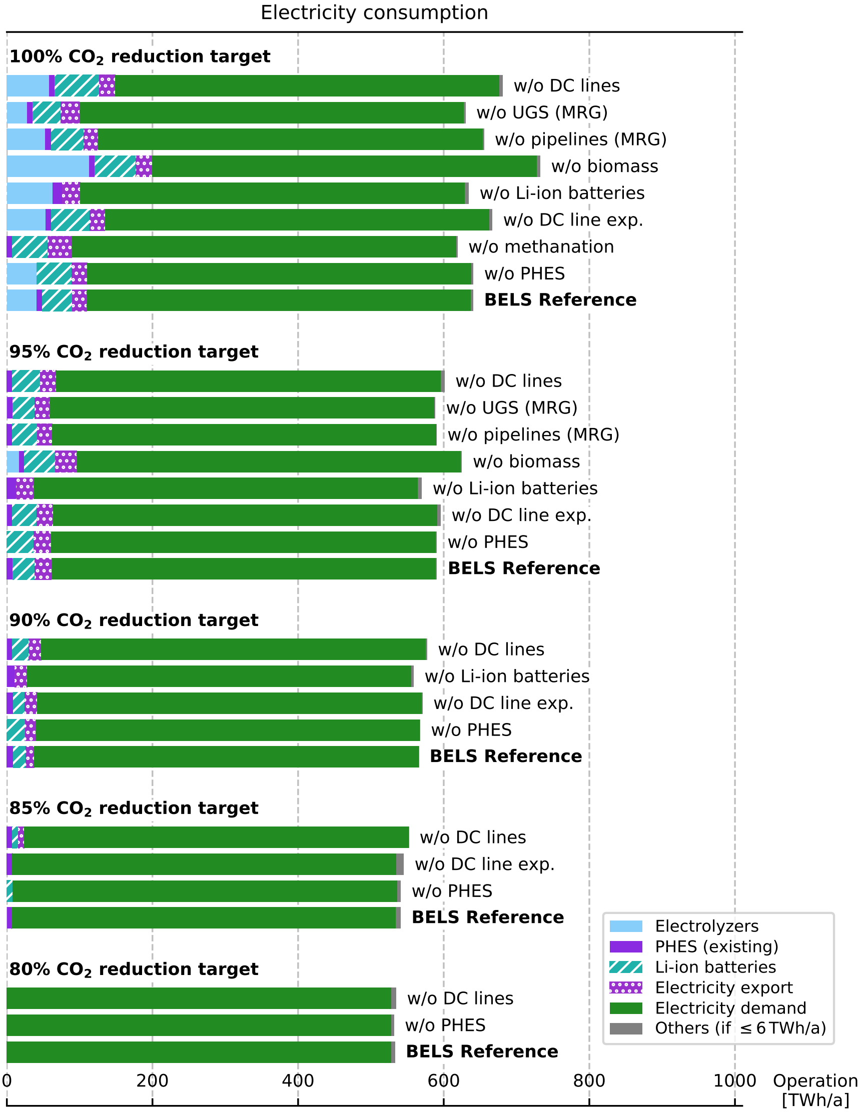

Figure B.9: Annual electricity consumption in the *BELS* scenario variations.

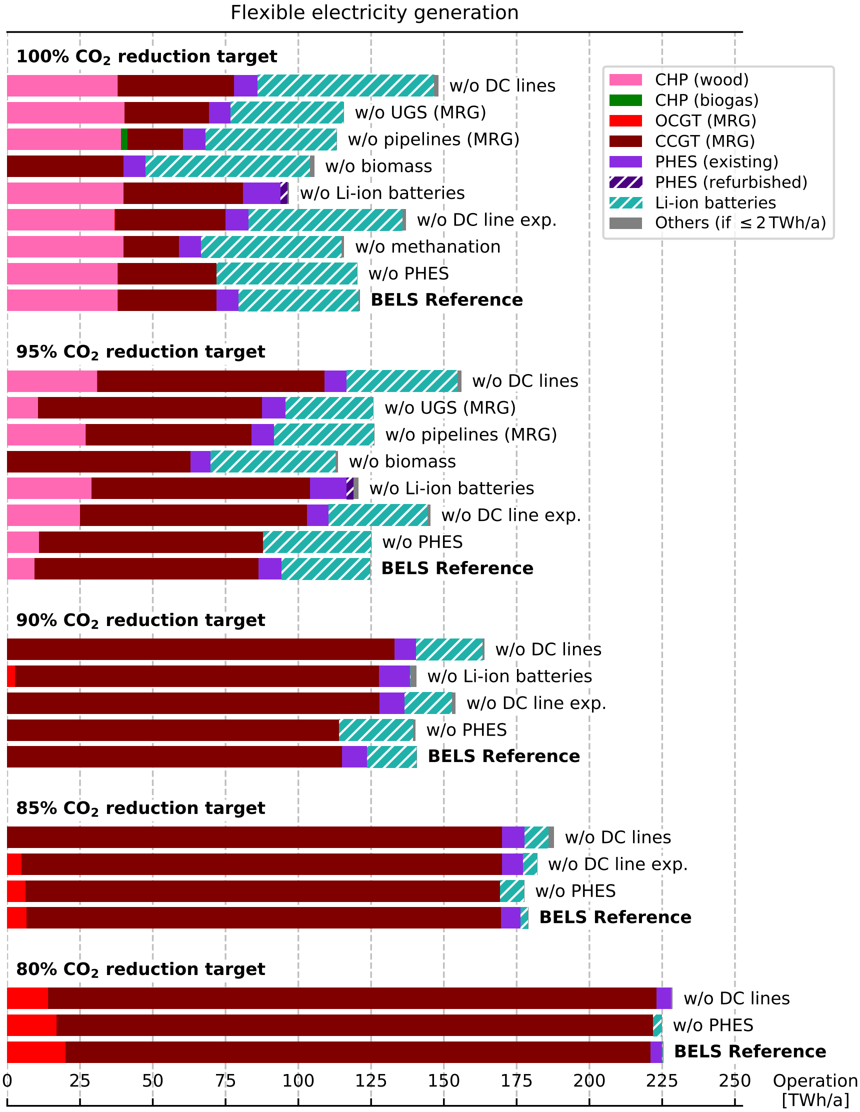

Figure B.10: Annual, flexible electricity generation in the *BELS* scenario variations.

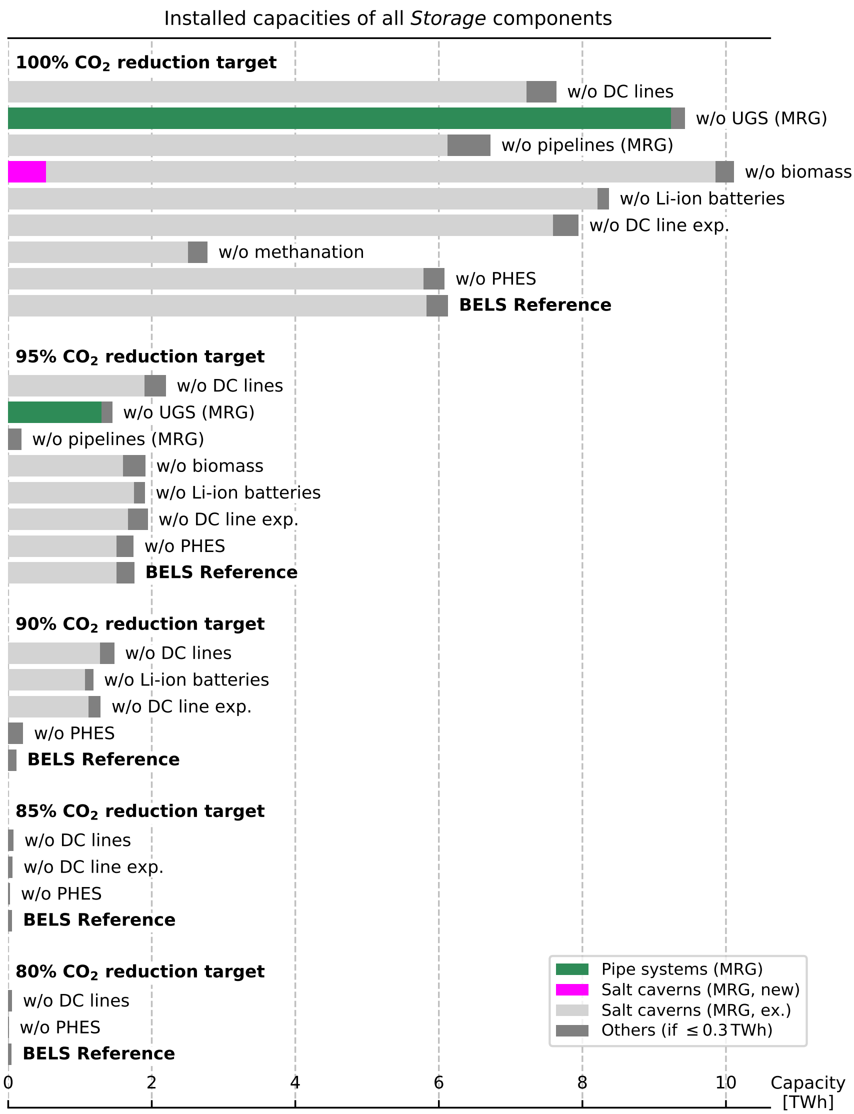

Figure B.11: Capacities of all *Storage* components in the *BELS* scenario variations (pore storage not visualized).

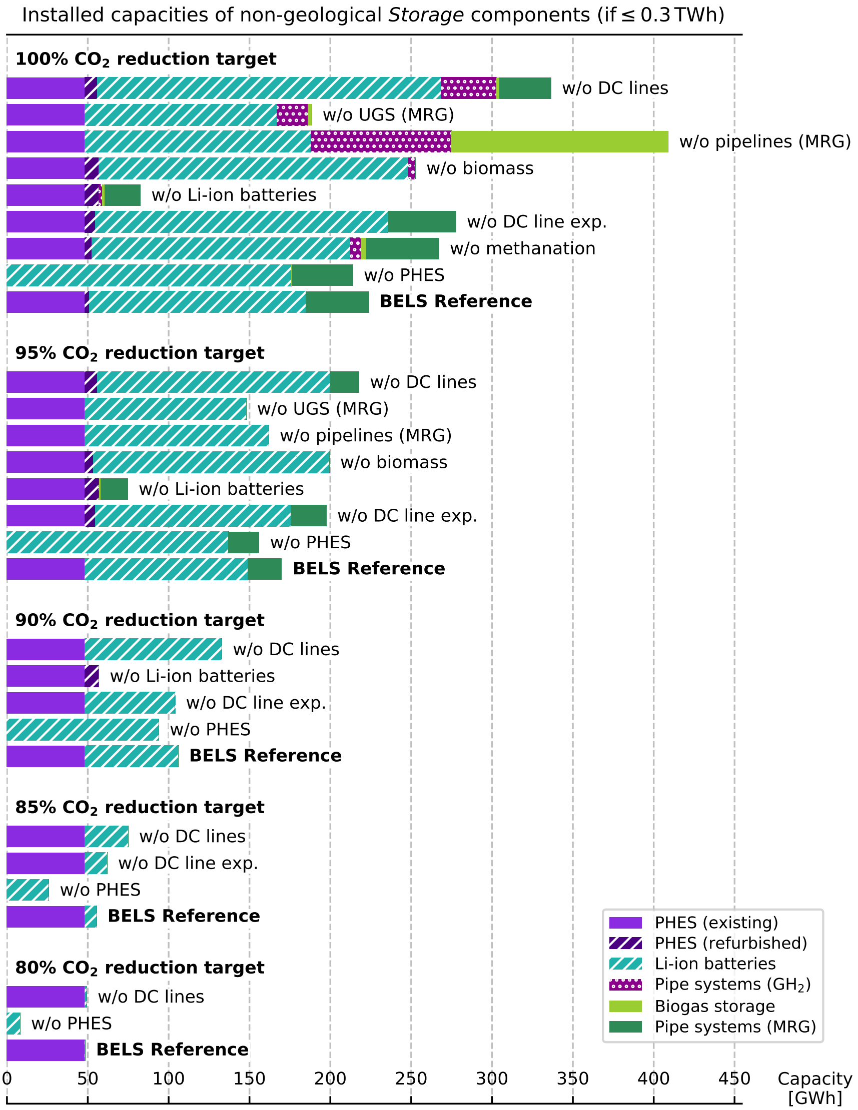

Figure B.12: Capacities of non-geological *Storage* components (when below 300 GWh) in the *BELS* scenario variations.

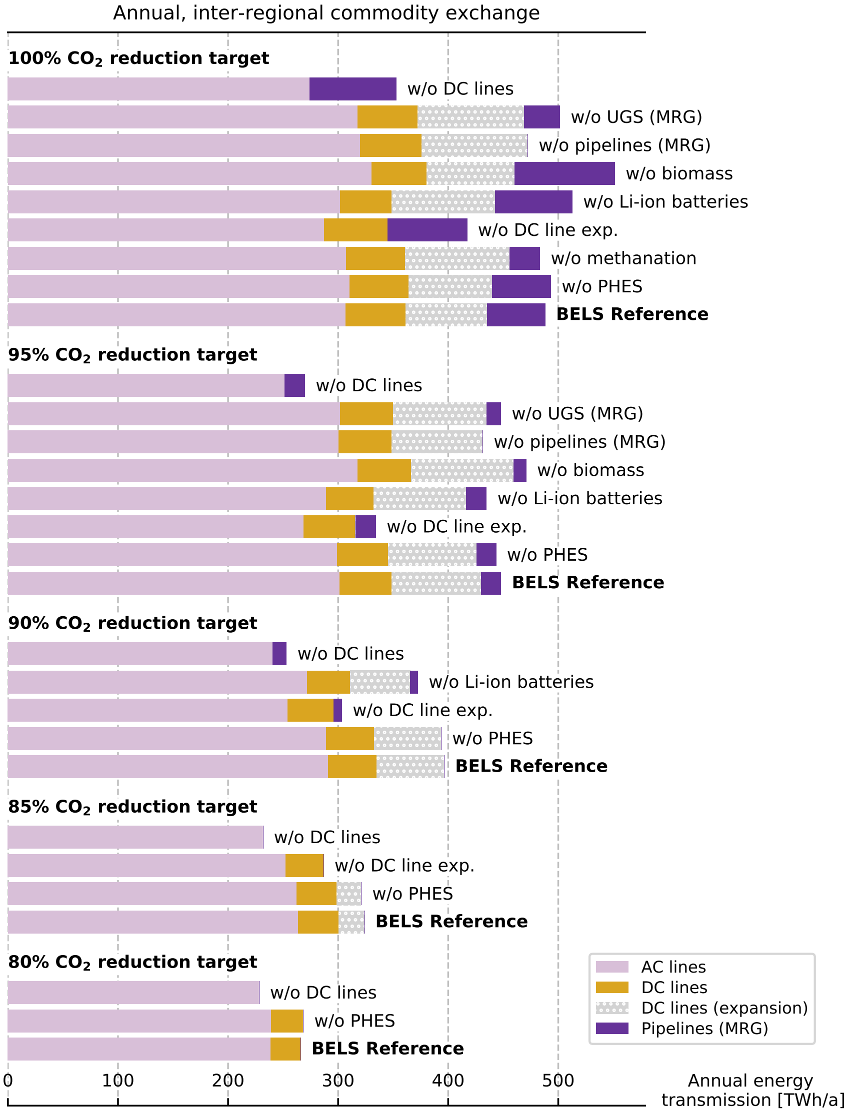

Figure B.13: Inter-regional commodity transmission in the *BELS* scenario variations.

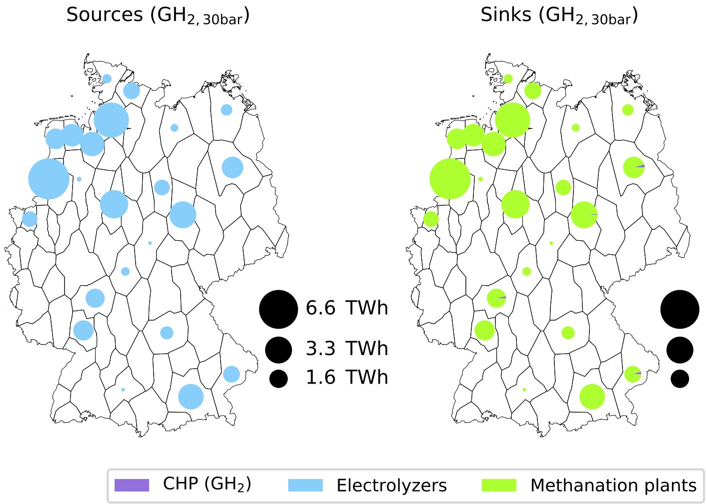

Figure B.14: Regional distribution of hydrogen sources and sinks (*BELS* - w/o MRG pipelines - 100%).

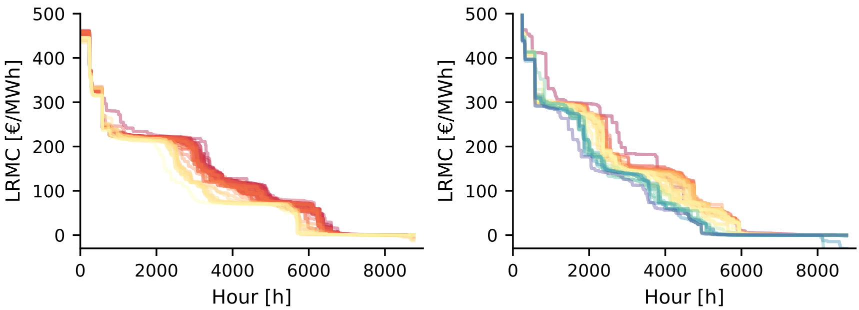

(a) *BELS*-100% Reference **(b)** *BELS*-100% w/o methanation

Figure B.15: Regional duration curves of the nodal, long-run marginal cost (*BELS*-100% Reference vs. *BELS*-100% w/o methanation).

B.2 *BELS⁺* Branch

In the following, additional figures generated in the *BELS⁺* scenario branch are displayed.

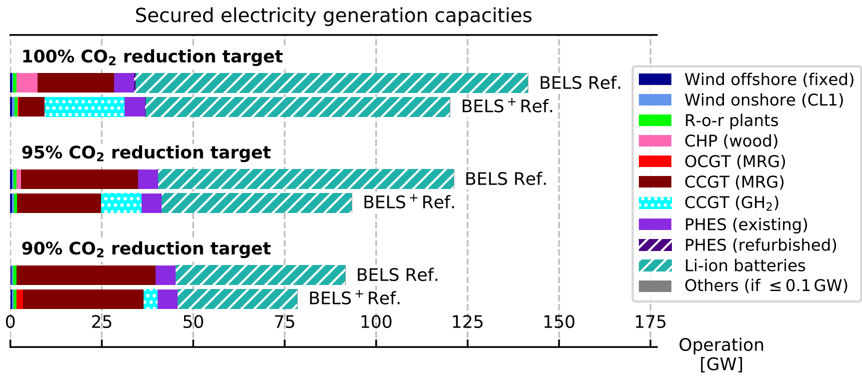

Figure B.16: Secured electricity generation supply capacities in the *BELS* and *BELS⁺* reference scenario.

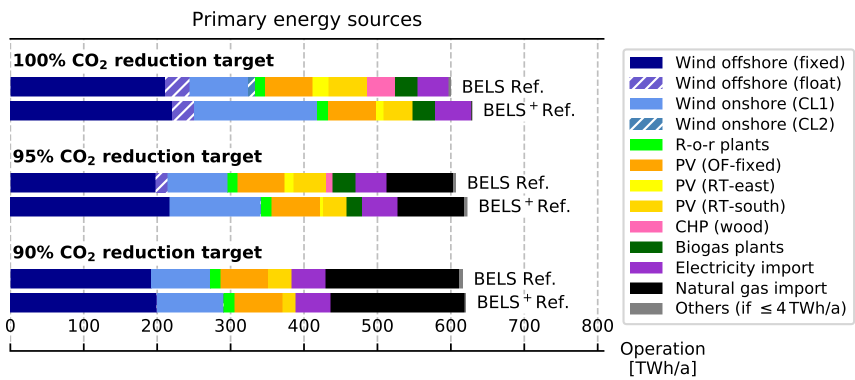

Figure B.17: Primary energy sources in the *BELS* and *BELS*$^+$ reference scenario.

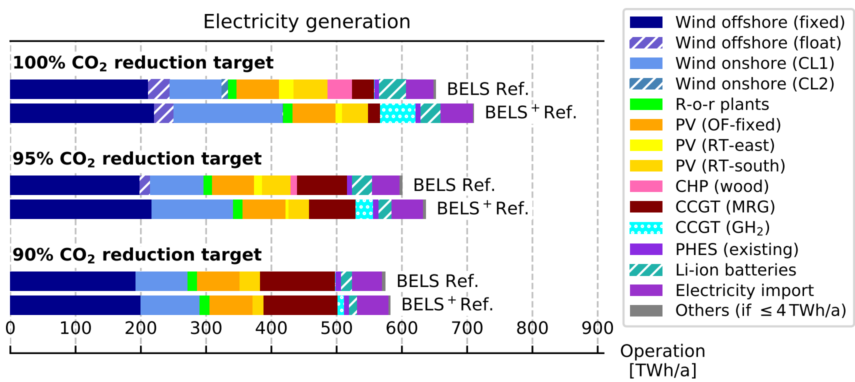

Figure B.18: Annual electricity generation in the *BELS* and *BELS*$^+$ reference scenario.

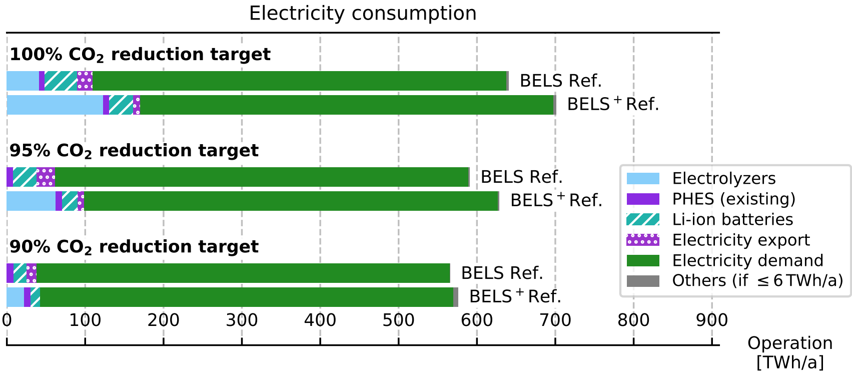

Figure B.19: Annual electricity consumption in the *BELS* and *BELS*$^+$ reference scenario.

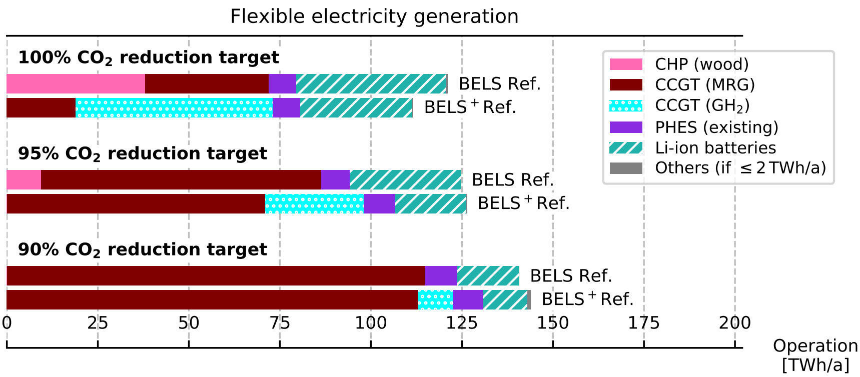

Figure B.20: Annual, flexible electricity generation in the *BELS* and *BELS*$^+$ reference scenario.

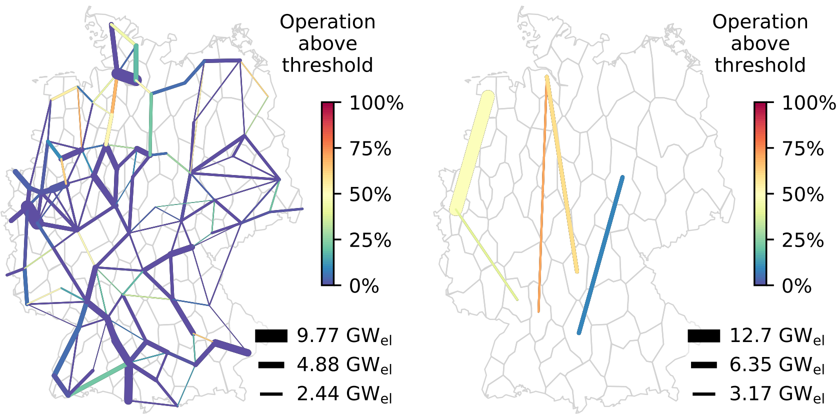

(a) AC lines

(b) DC lines (with expansion)

Figure B.21: Operation of AC/ DC lines above 80% of their capacity (*BELS*$^{+}$-100%).

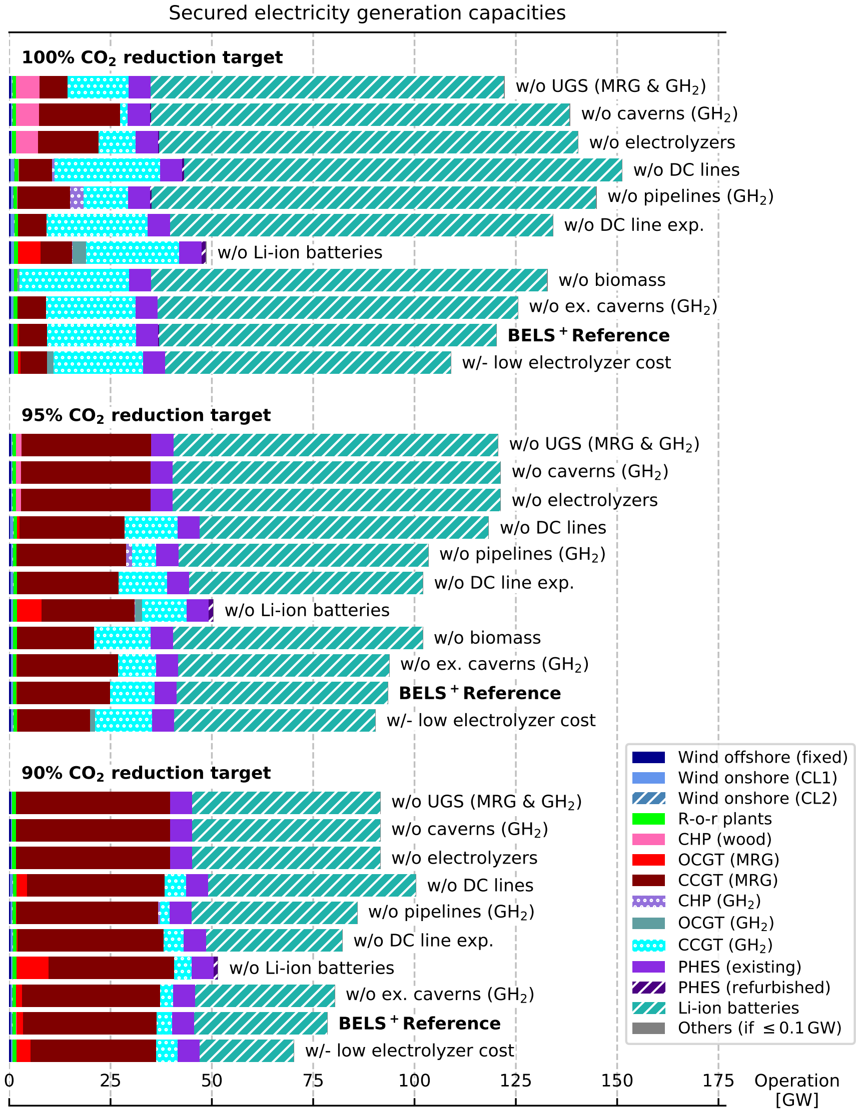

Figure B.22: Secured electricity generation capacities in the *BELS*⁺ scenario variations.

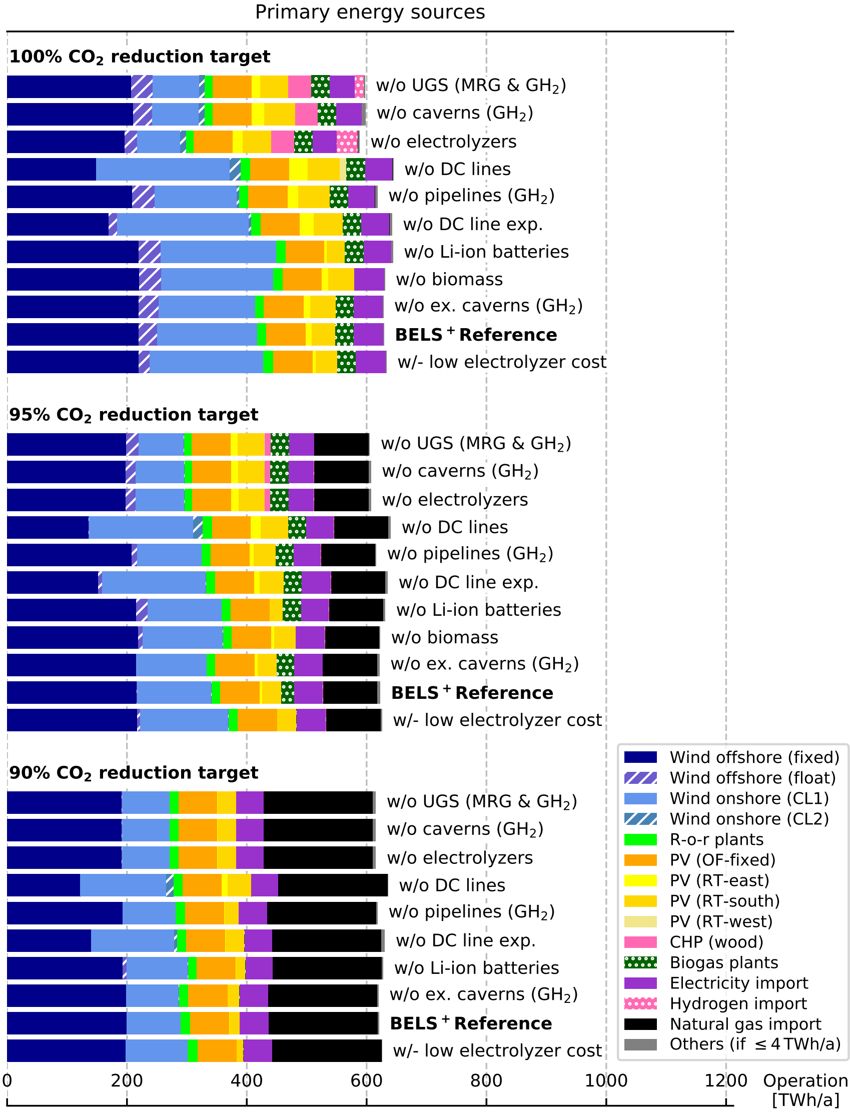

Figure B.23: Primary energy sources in the *BELS*$^+$ scenario variations.

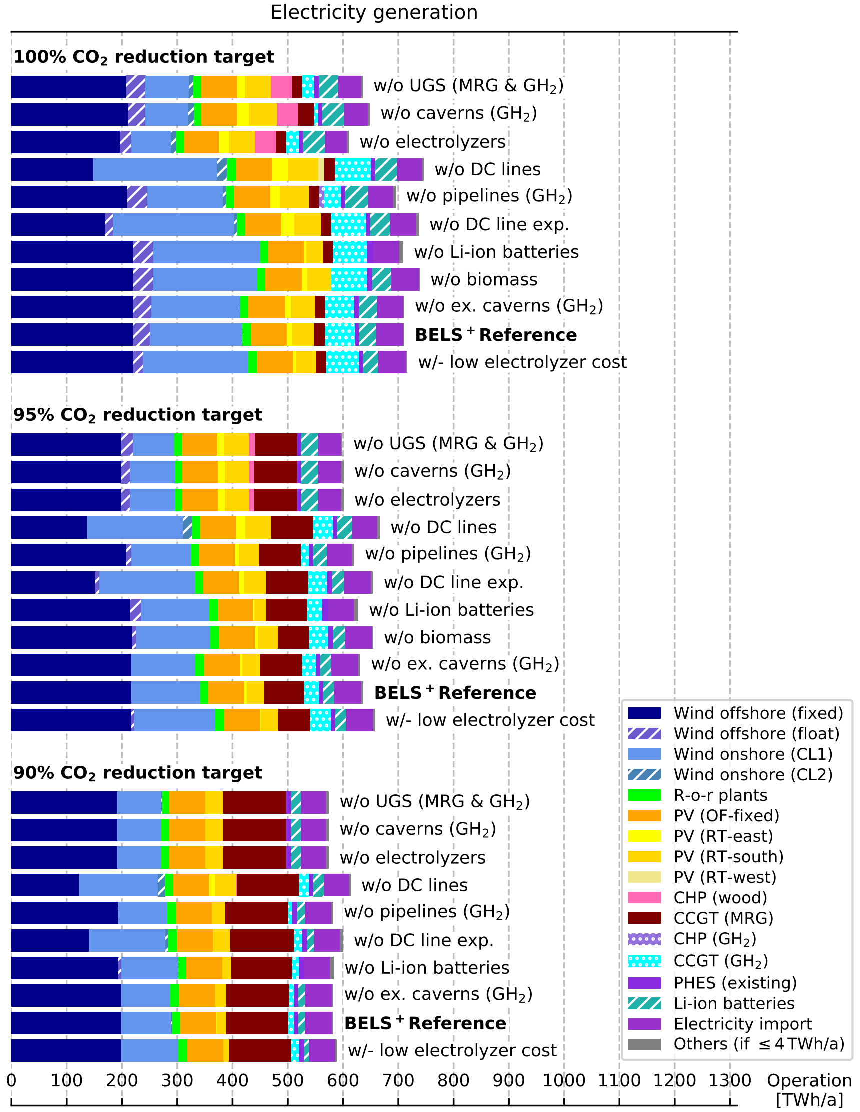

Figure B.24: Annual electricity generation in the *BELS*⁺ scenario variations.

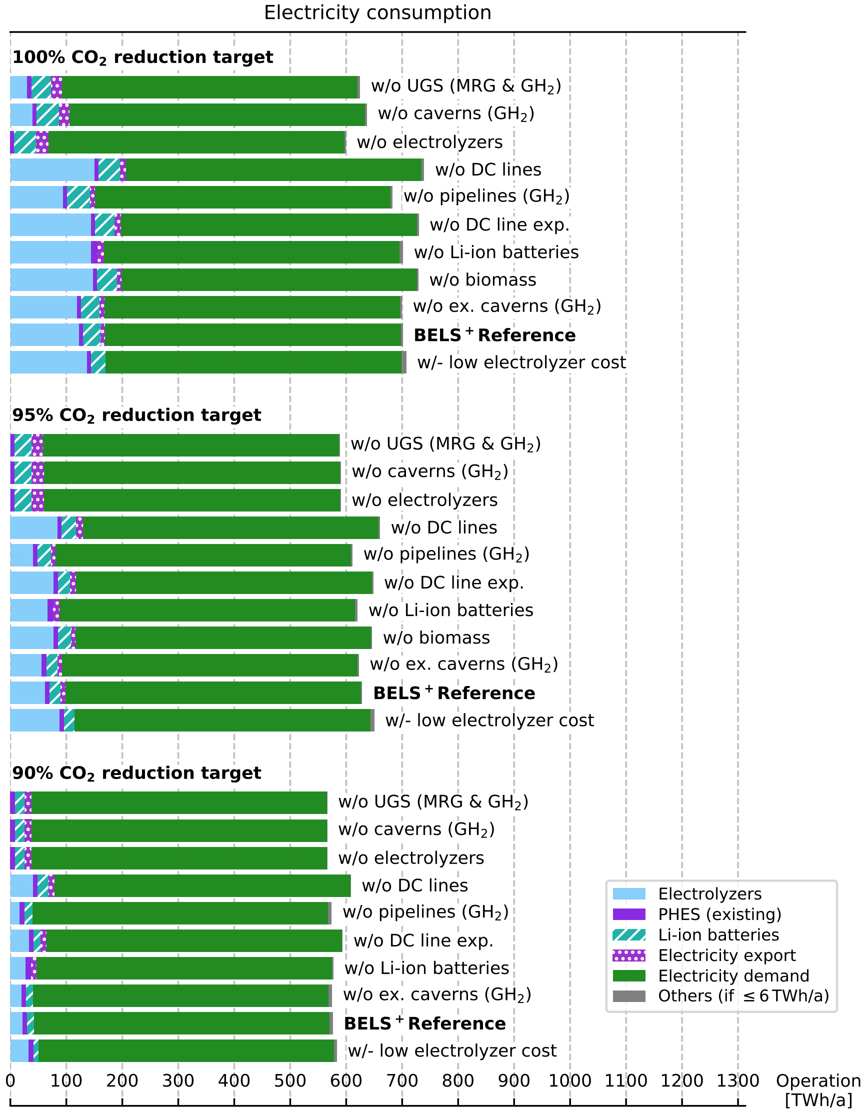

Figure B.25: Annual electricity consumption in the *BELS*$^+$ scenario variations.

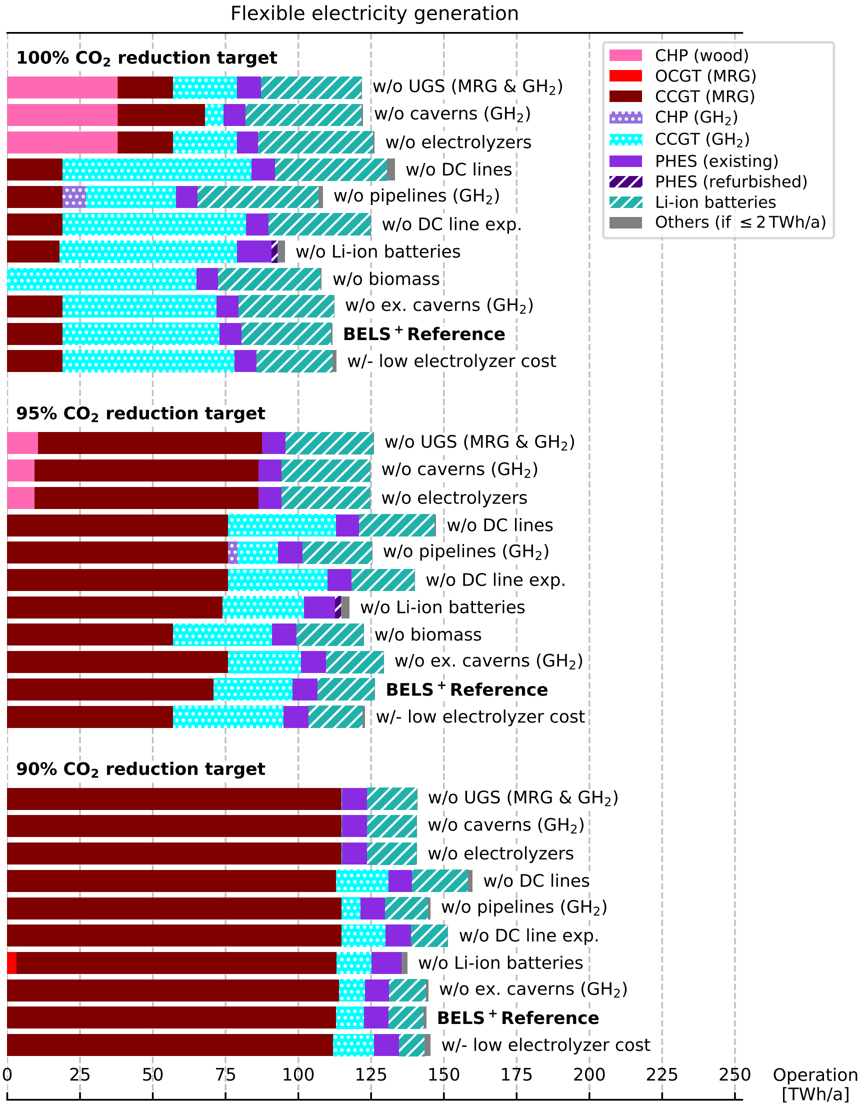

Figure B.26: Annual, flexible electricity generation in the *BELS+* scenario variations.

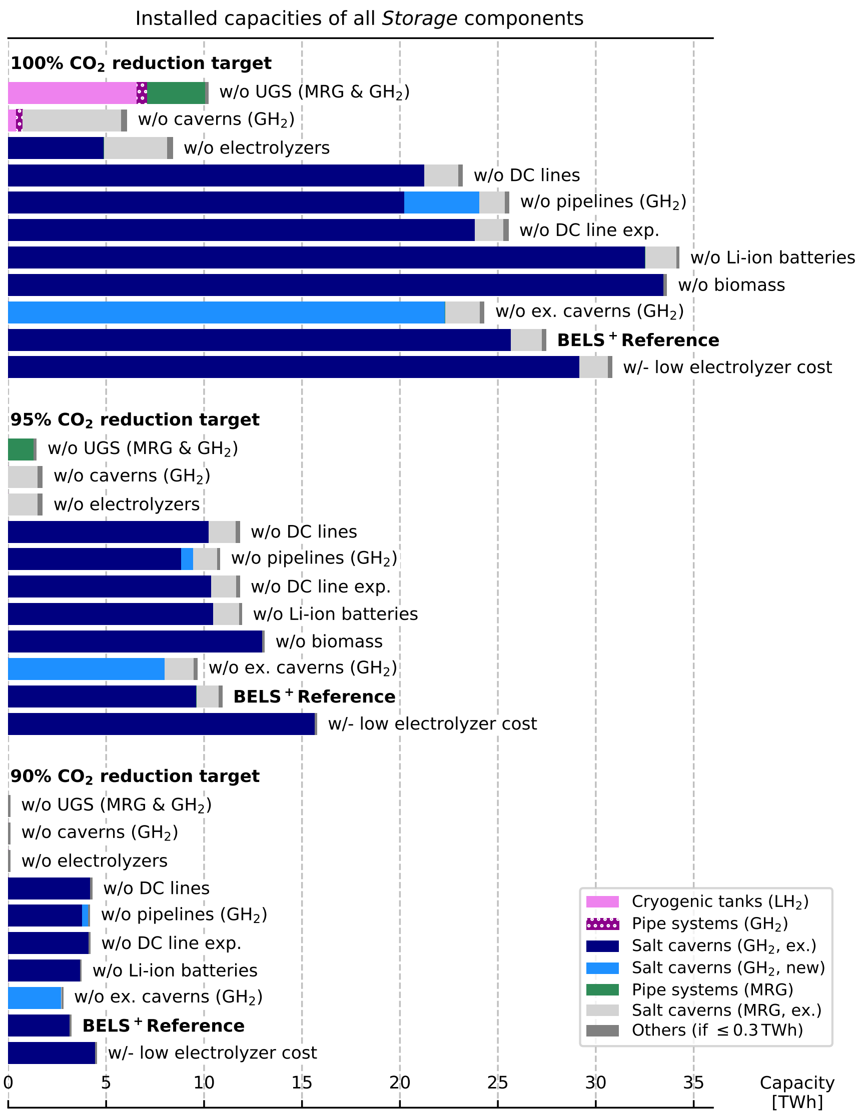

Figure B.27: Capacities of all *Storage* components in the *BELS*⁺ scenario variations (pore storage not visualized).

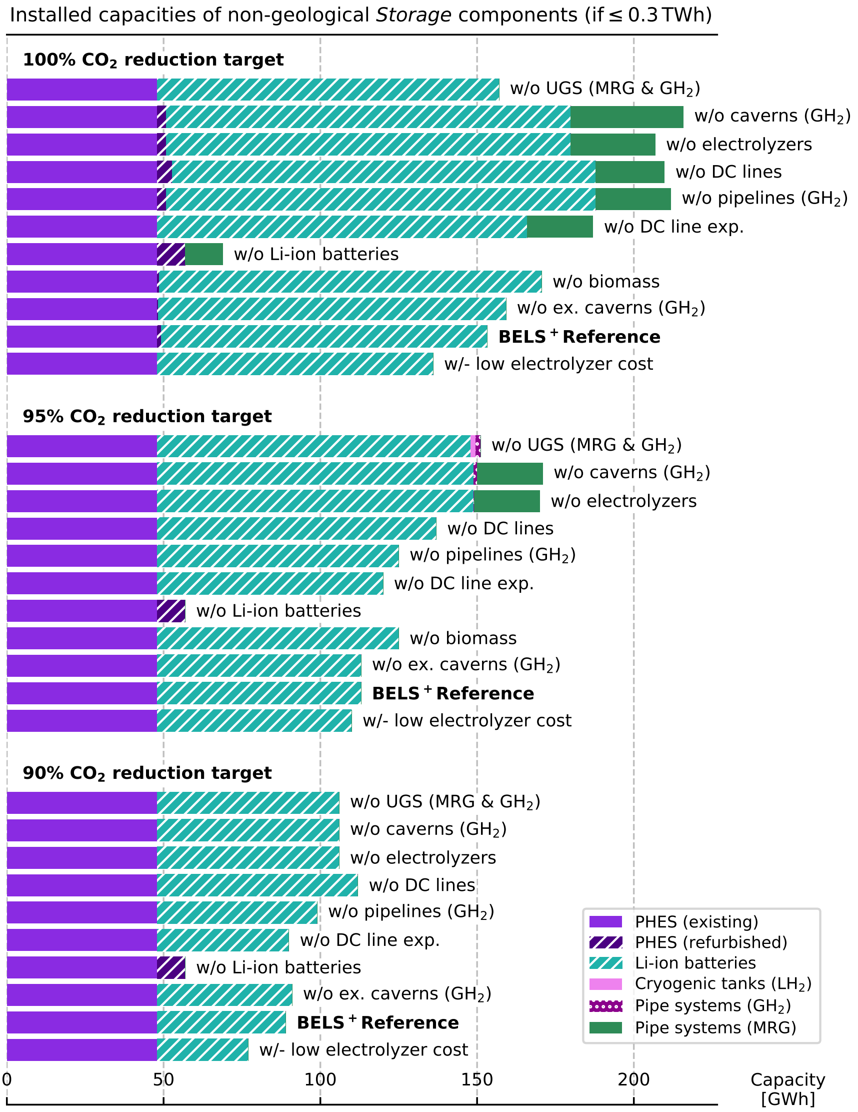

Figure B.28: Capacities of non-geological *Storage* components (when below 300 GWh) in the *BELS⁺* scenario variations.

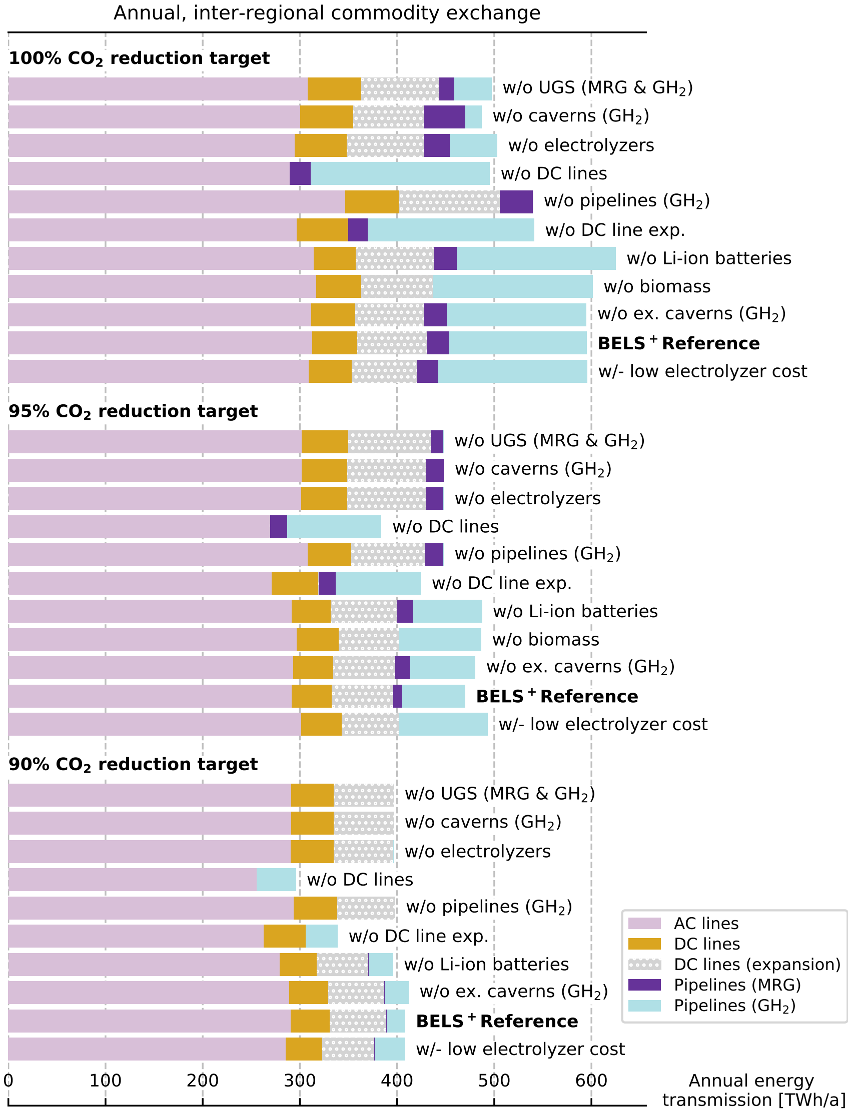

Figure B.29: Inter-regional commodity transmission in the *BELS*+ scenario variations.

B.3 *BLHYS* Branch

In the following, additional tables and figures generated in the *BLHYS* scenario branch are displayed.

Table B.1: Estimate of avoided CO_2 emissions in the different scenario configurations (in reference to the year 1990, estimated based on [177, 192]).

		Electricity generation	Cars	LDVs, HDVs & buses	Rail-ways	Ammonia production	Σ Mt_{CO_2}/a
80% target	*BELS*	293	0	0	0	0	293
	BELS⁺	293	0	0	0	0	293
	BLHYS (L-GH$_2$)	293	28	9.7	1.4	1.8	332
	BLHYS (M-GH$_2$)	293	56	19.3	2.2	3.6	370
	BLHYS (H-GH$_2$)	293	84	29	2.8	5.7	408
100% target	*BELS*	366	0	0	0	0	366
	BELS⁺	366	0	0	0	0	366
	BLHYS (L-GH$_2$)	366	28	9.7	1.4	1.8	405
	BLHYS (M-GH$_2$)	366	56	19.3	2.2	3.6	443
	BLHYS (H-GH$_2$)	366	84	29	2.8	5.7	481

Emissions electricity generation: [192]. Emissions transport sector: [177] (HDVs and buses aggregated in the database $\rightarrow$ penetration rate of HDVs considered). Industry sector: [177] (Only ammonia production; other process emissions, e.g. of methanol production, are either small or could not be identified and are thus neglected $\rightarrow$ emission budget underestimated).

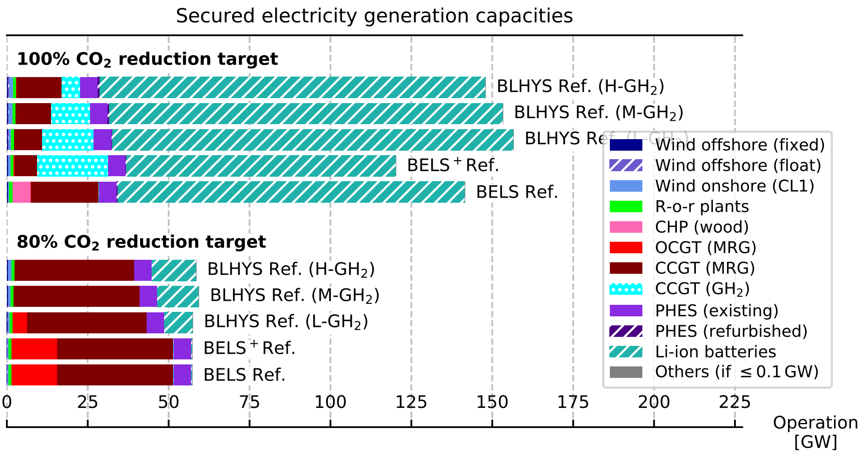

Figure B.30: Secured electricity generation supply capacities in the *BELS*, *BELS*$^+$ and *BLHYS* reference scenario.

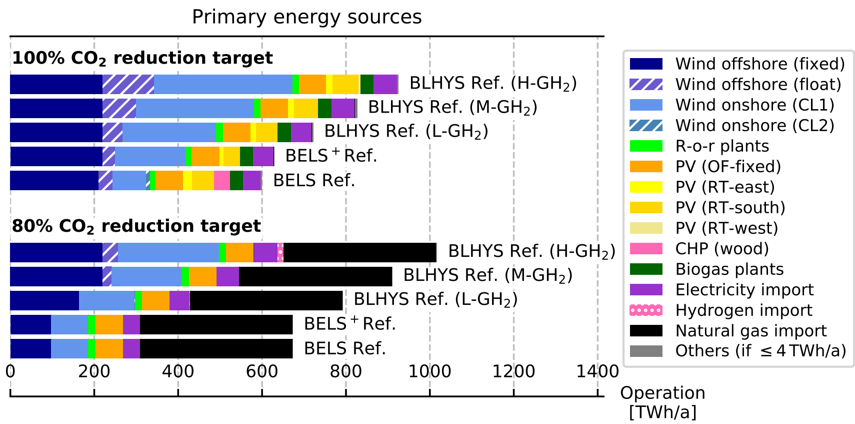

Figure B.31: Primary energy sources in the *BELS*, *BELS*$^+$ and *BLHYS* reference scenario.

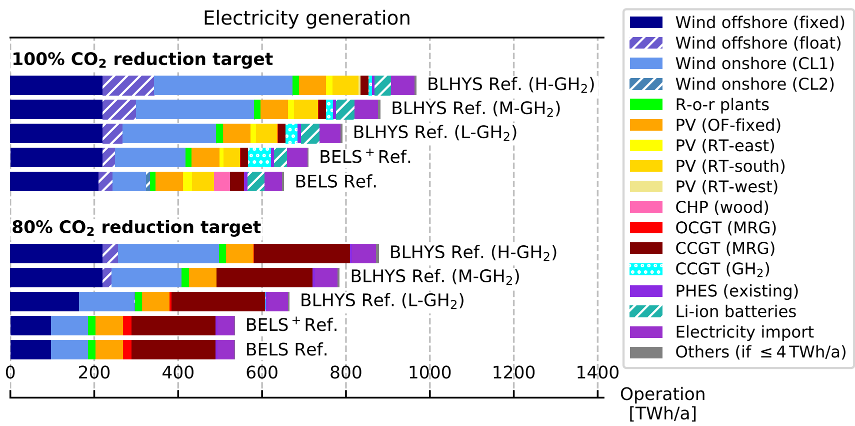

Figure B.32: Annual electricity generation in the *BELS*, *BELS*$^+$ and *BLHYS* reference scenario.

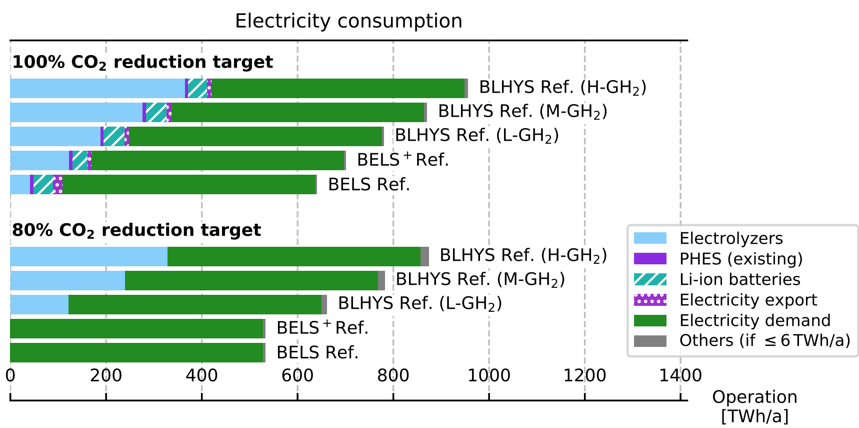

Figure B.33: Annual electricity consumption in the *BELS*, *BELS*$^+$ and *BLHYS* reference scenario.

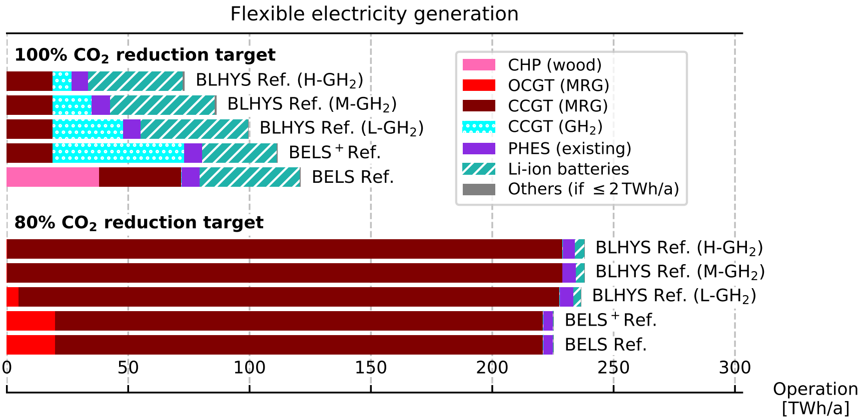

Figure B.34: Annual, flexible electricity generation in the *BELS*, *BELS*+ and *BLHYS* reference scenario.

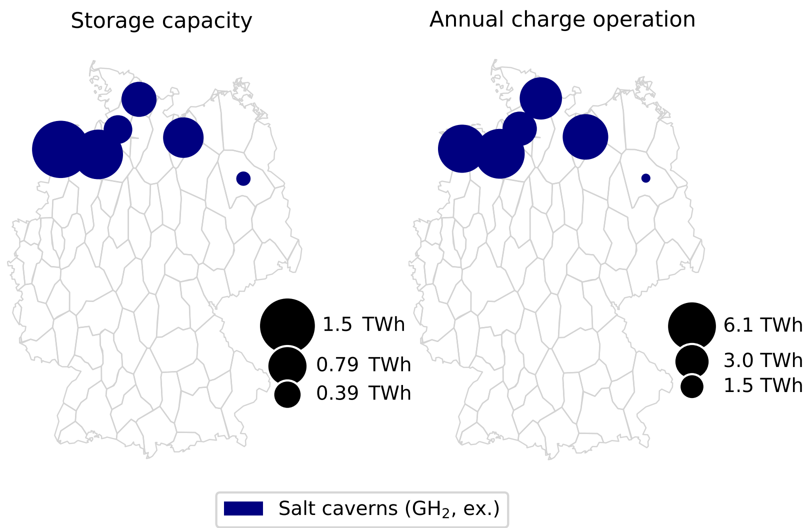

Figure B.35: Capacities and charging operation of hydrogen storage (*BLHYS*-80%-L-GH_2).

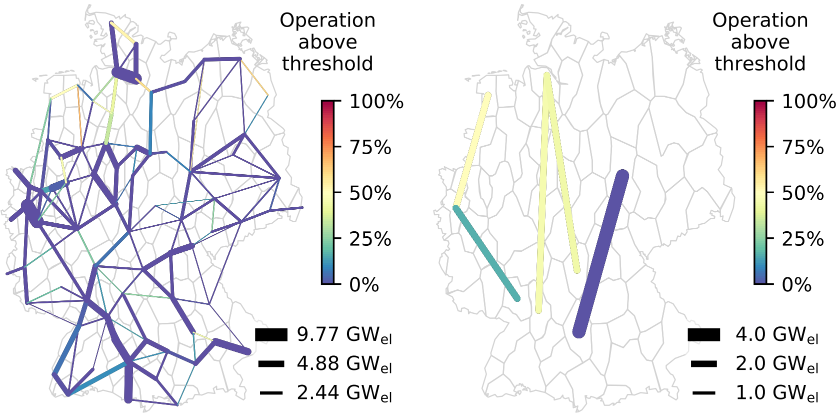

(a) AC lines **(b)** DC lines (with expansion)

Figure B.36: Operation of AC and DC lines above 80% of their capacity (*BLHYS*-80%-L-GH$_2$).

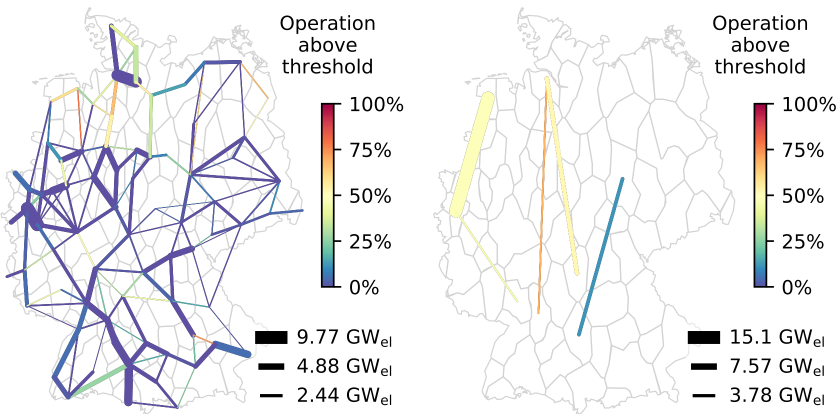

(a) AC lines **(b)** DC lines (with expansion)

Figure B.37: Operation of AC and DC lines above 80% of their capacity (*BLHYS*-100%-H-GH$_2$).

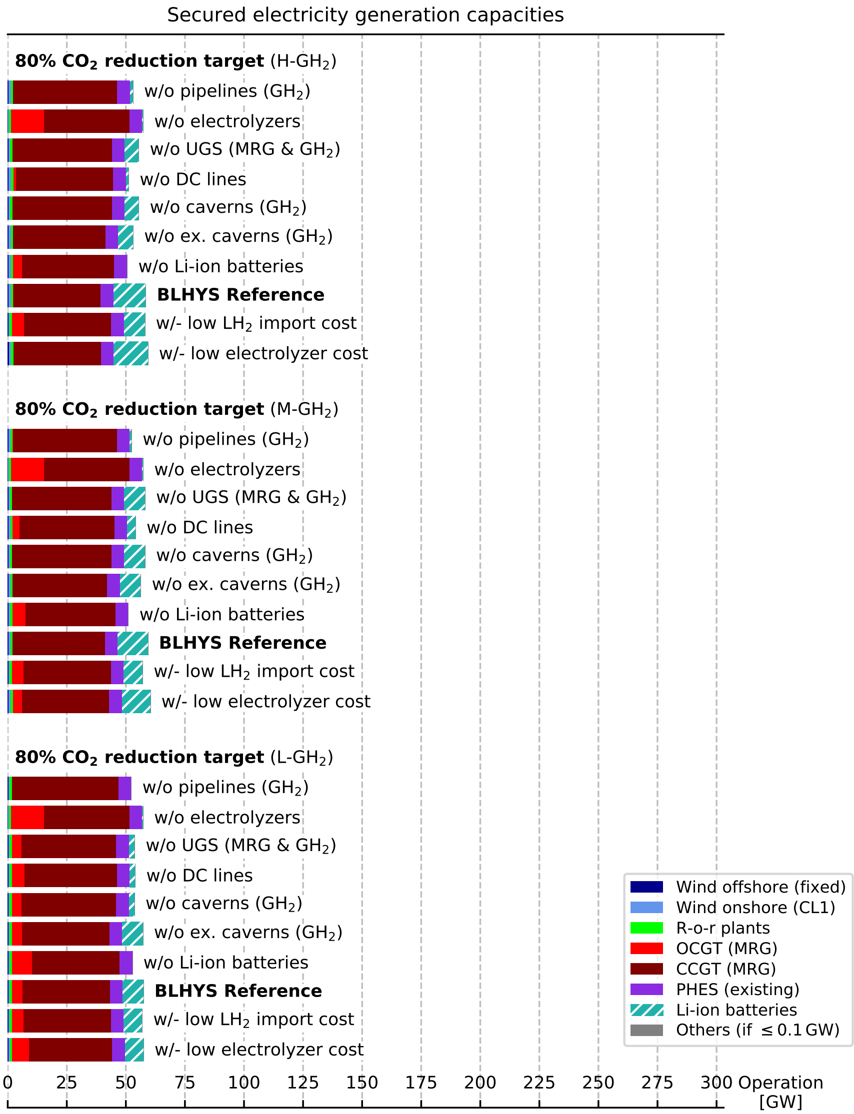

Figure B.38: Secured electricity generation capacities in the *BLHYS*-80% scenario variations.

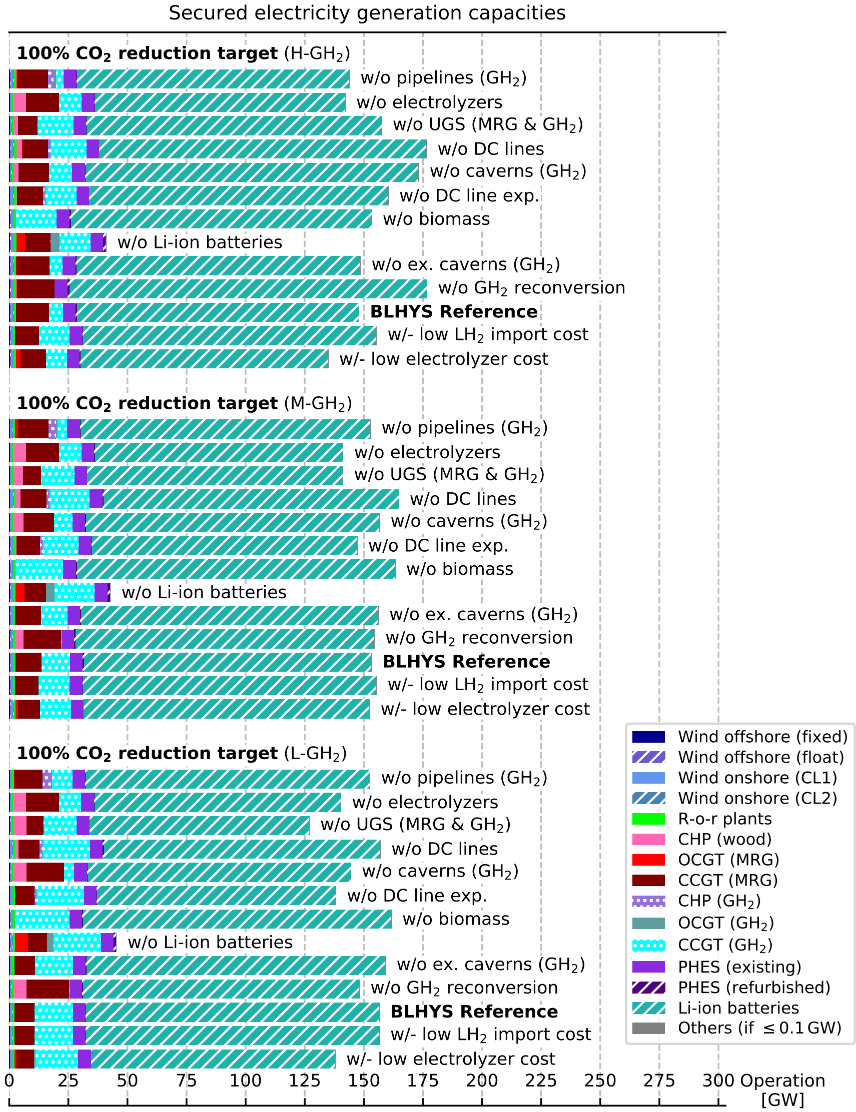

Figure B.39: Secured electricity generation capacities in the *BLHYS*-100% scenario variations.

Figure B.40: Primary energy sources in the *BLHYS*-80% scenario variations.

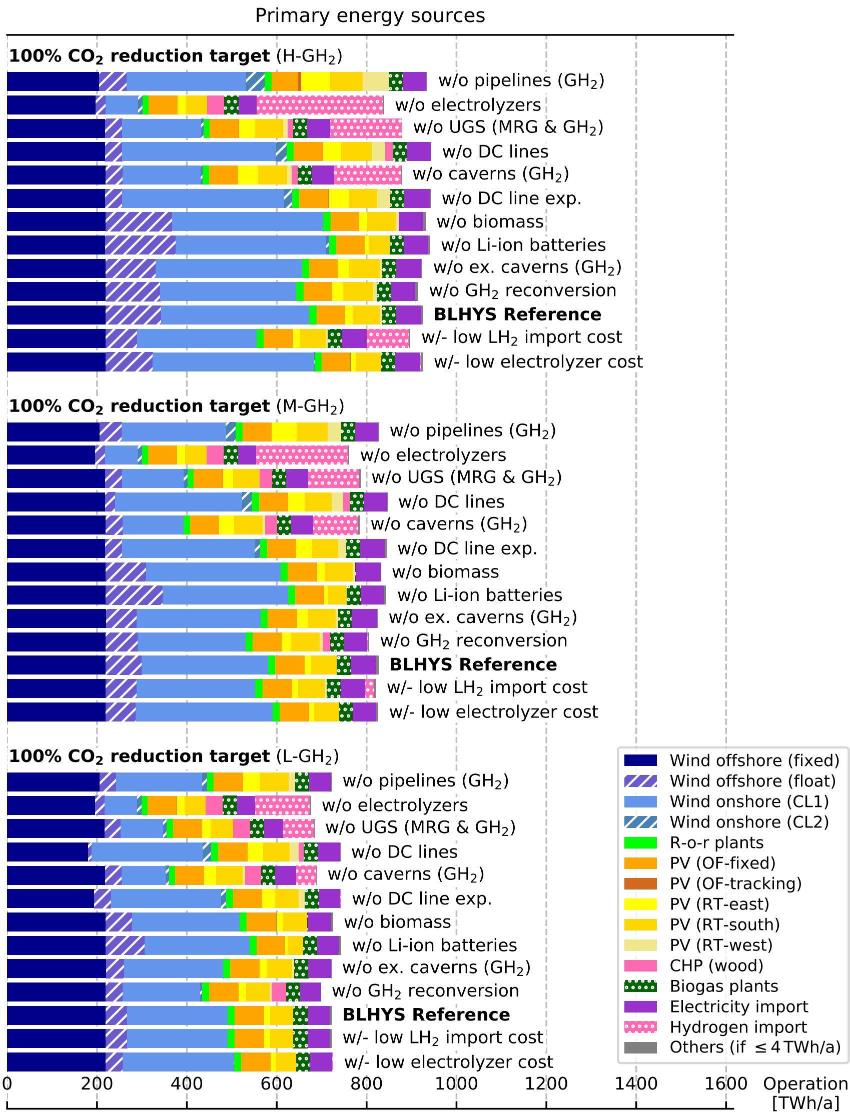

Figure B.41: Primary energy sources in the *BLHYS*-100% scenario variations.

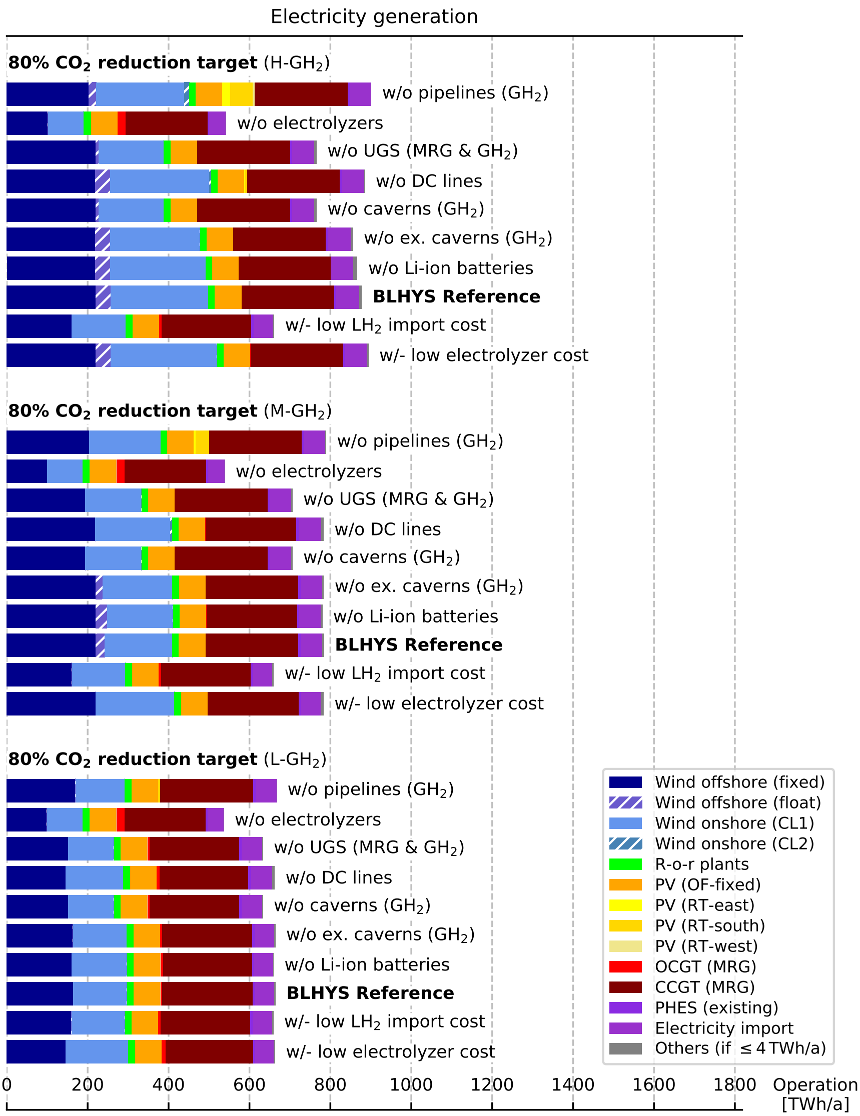

Figure B.42: Annual electricity generation in the *BLHYS*-80% scenario variations.

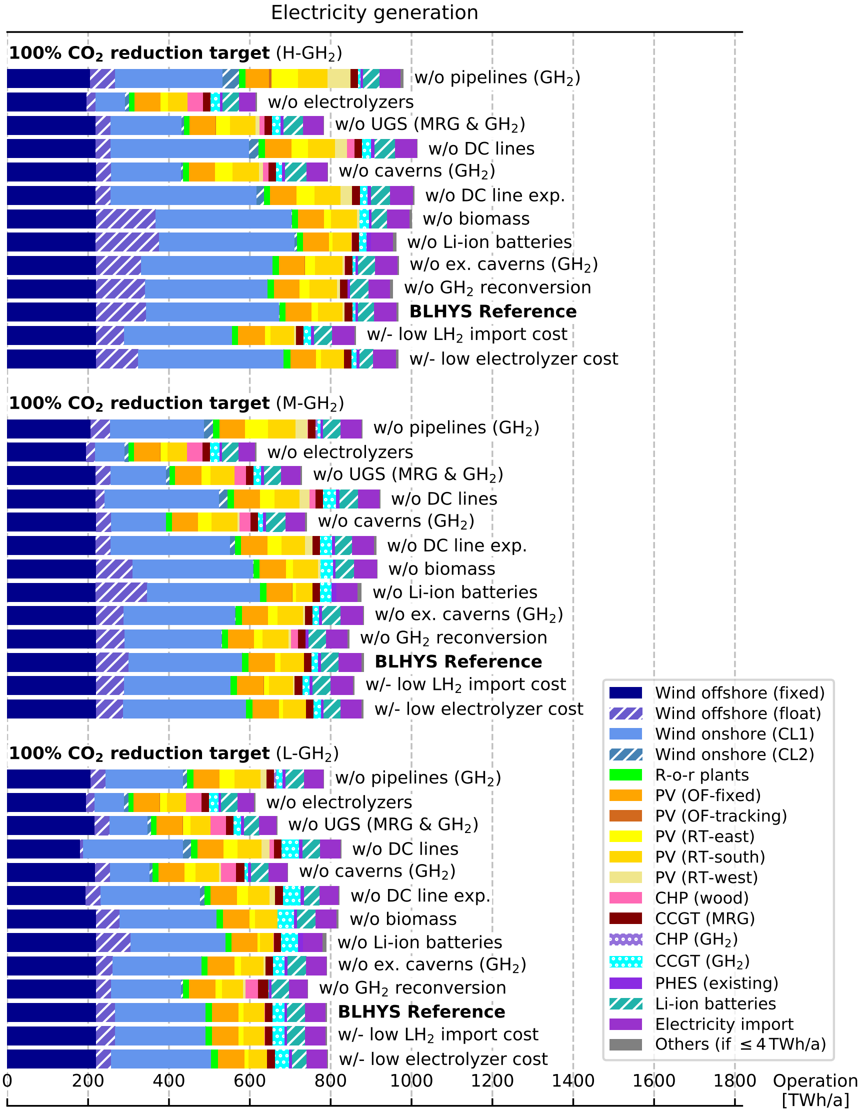

Figure B.43: Annual electricity generation in the *BLHYS*-100% scenario variations.

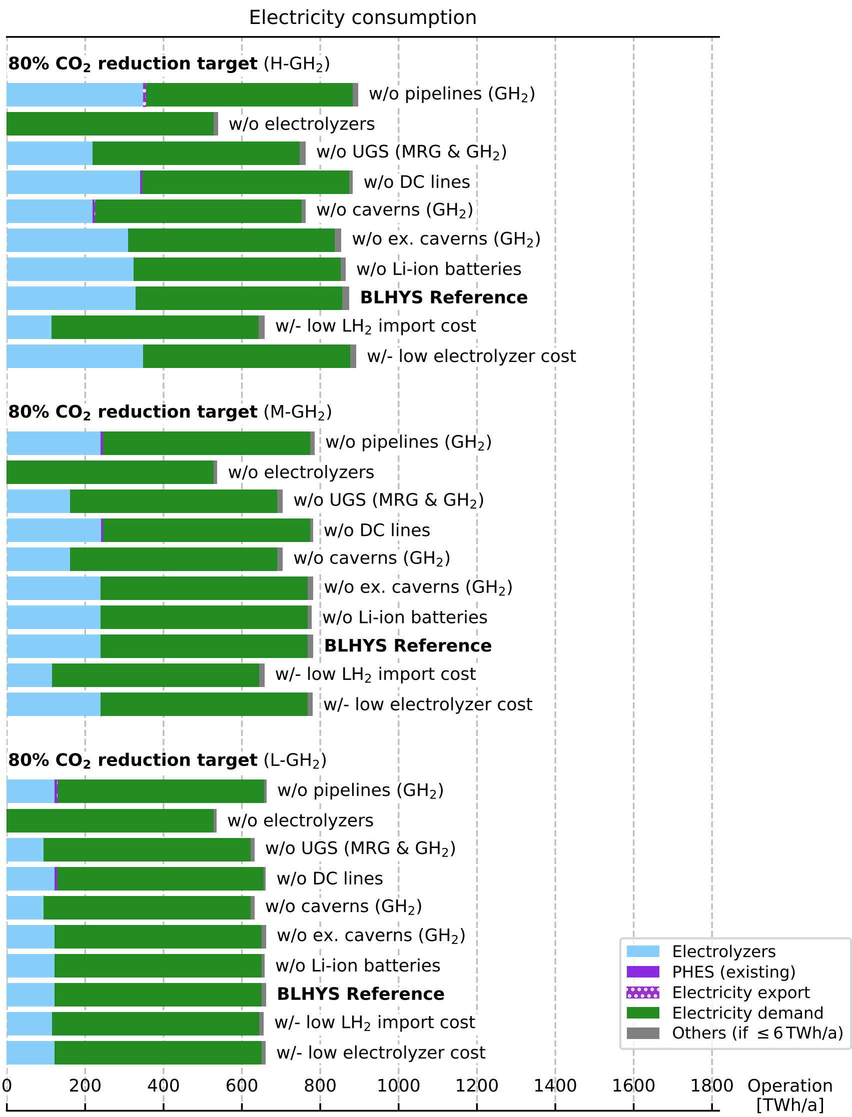

Figure B.44: Annual electricity consumption in the *BLHYS*-80% scenario variations.

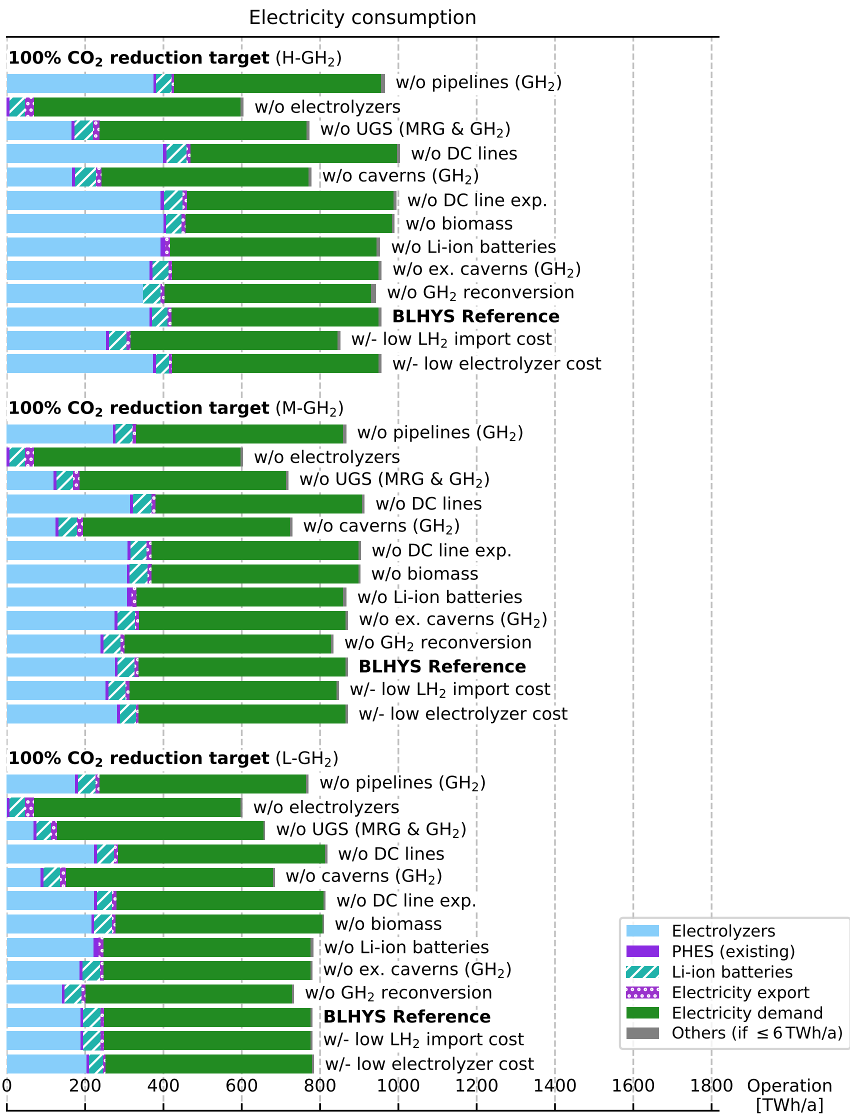

Figure B.45: Annual electricity consumption in the *BLHYS*-1000% scenario variations.

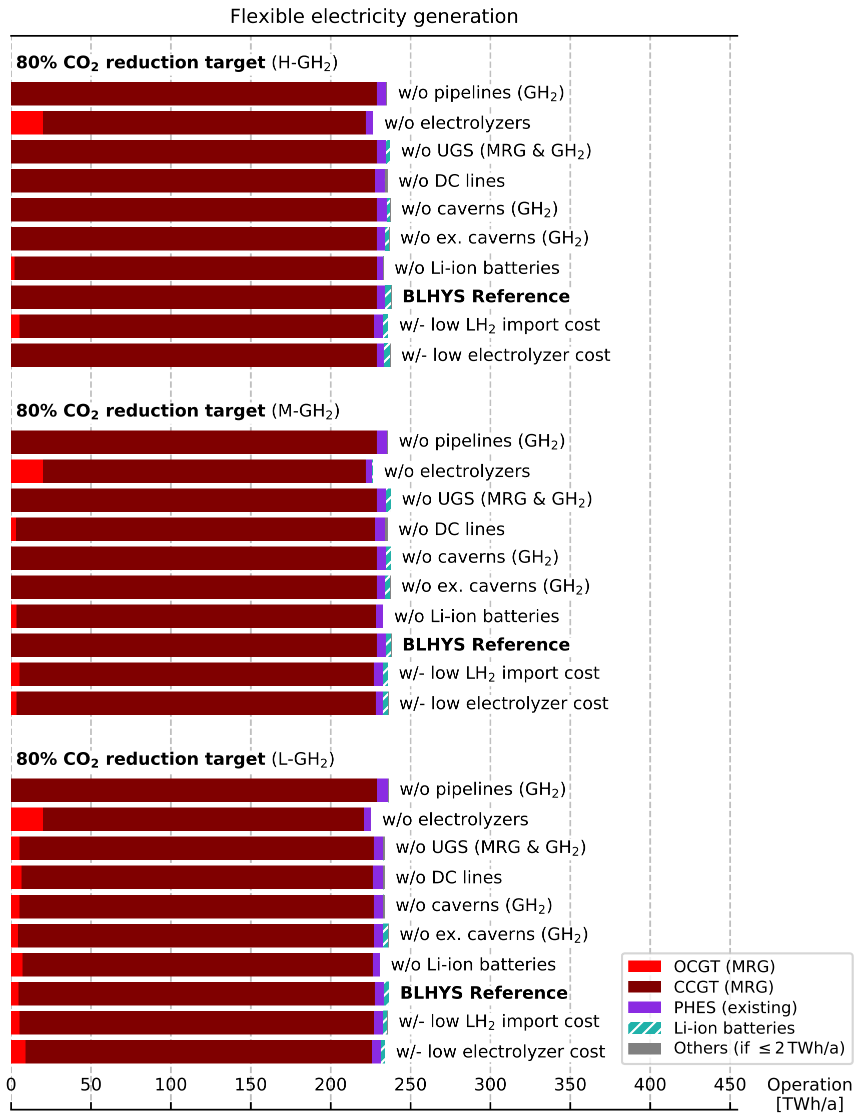

Figure B.46: Annual, flexible electricity generation in the *BLHYS*-80% scenario variations.

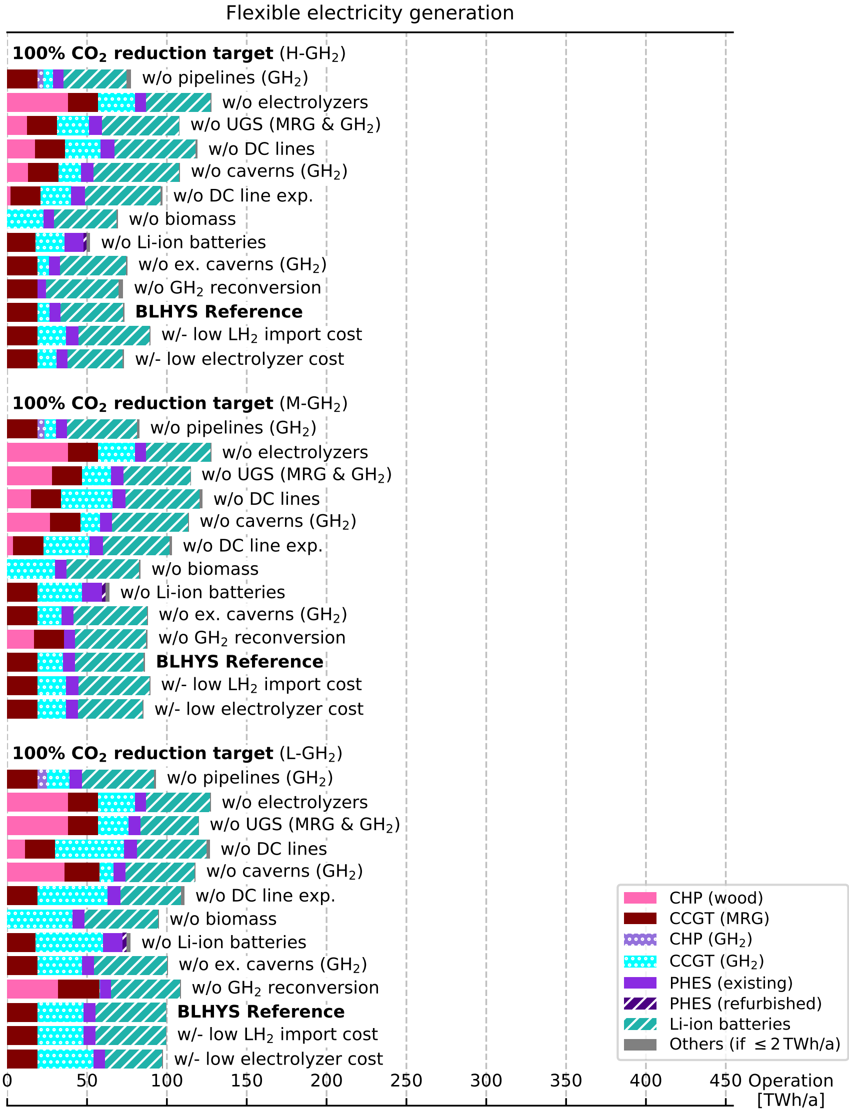

Figure B.47: Annual, flexible electricity generation in the *BLHYS*-100% scenario variations.

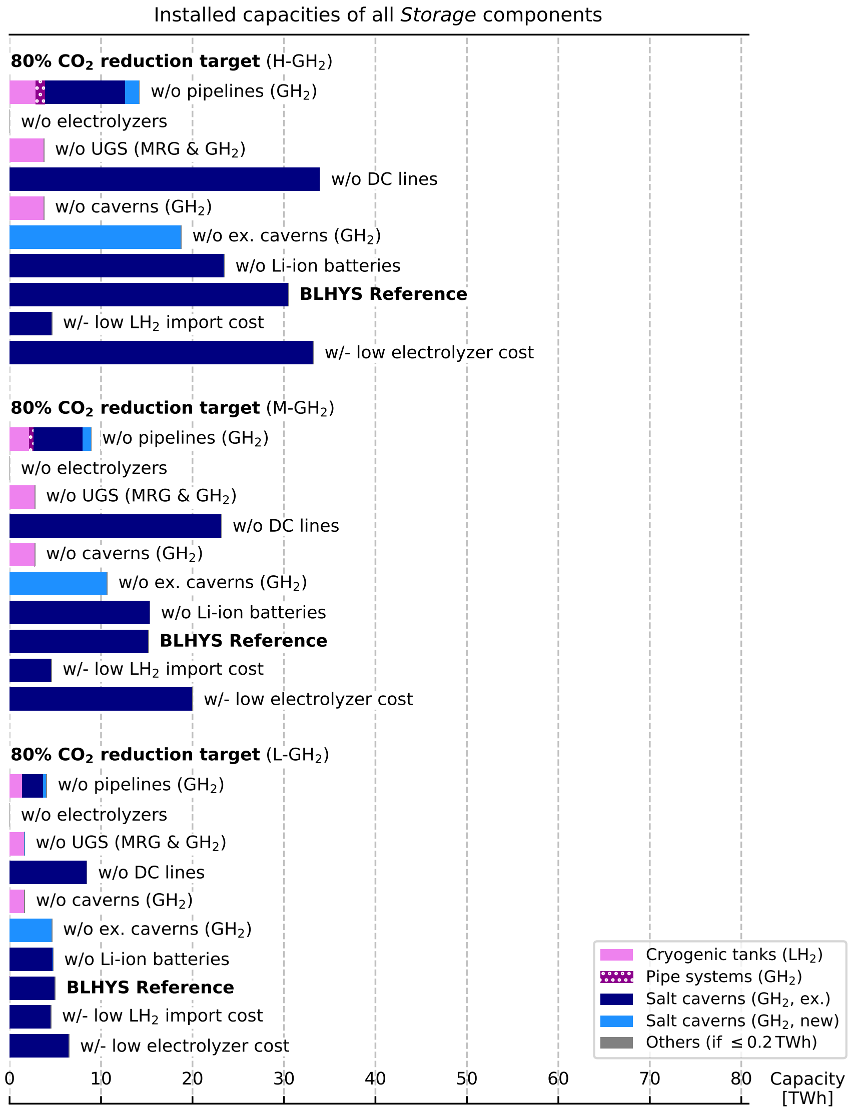

Figure B.48: Capacities of all *Storage* components in the *BLHYS*-80% scenario variations (pore storage not visualized).

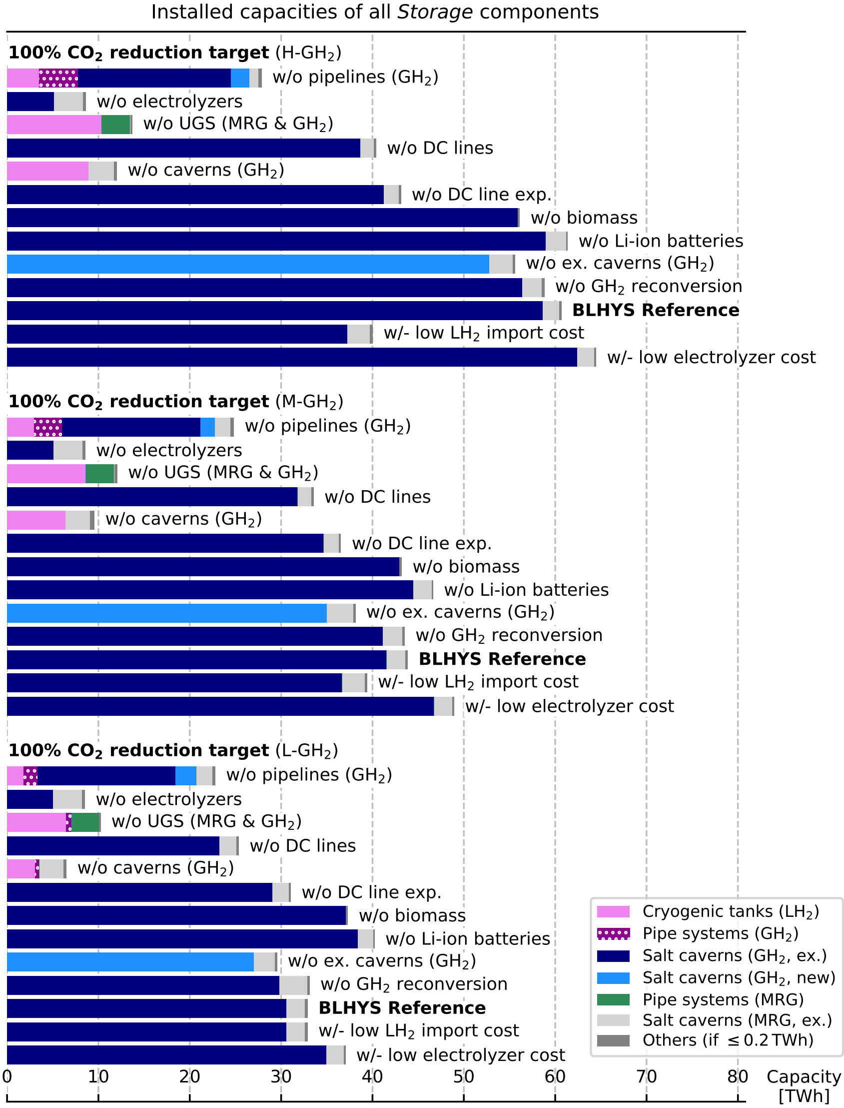

Figure B.49: Capacities of all *Storage* components in the *BLHYS*-100% scenario variations (pore storage not visualized).

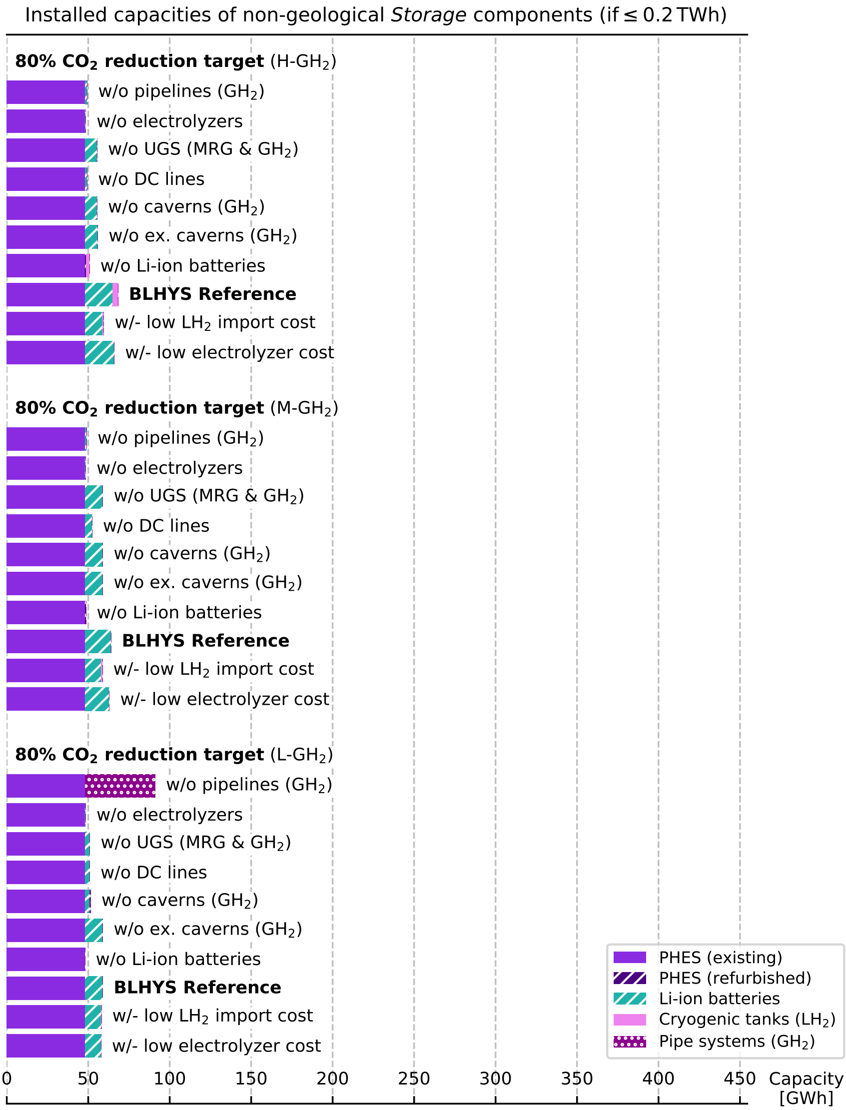

Figure B.50: Capacities of non-geological *Storage* components (when below 200 GWh) in the *BLHYS*-80% scenario variations.

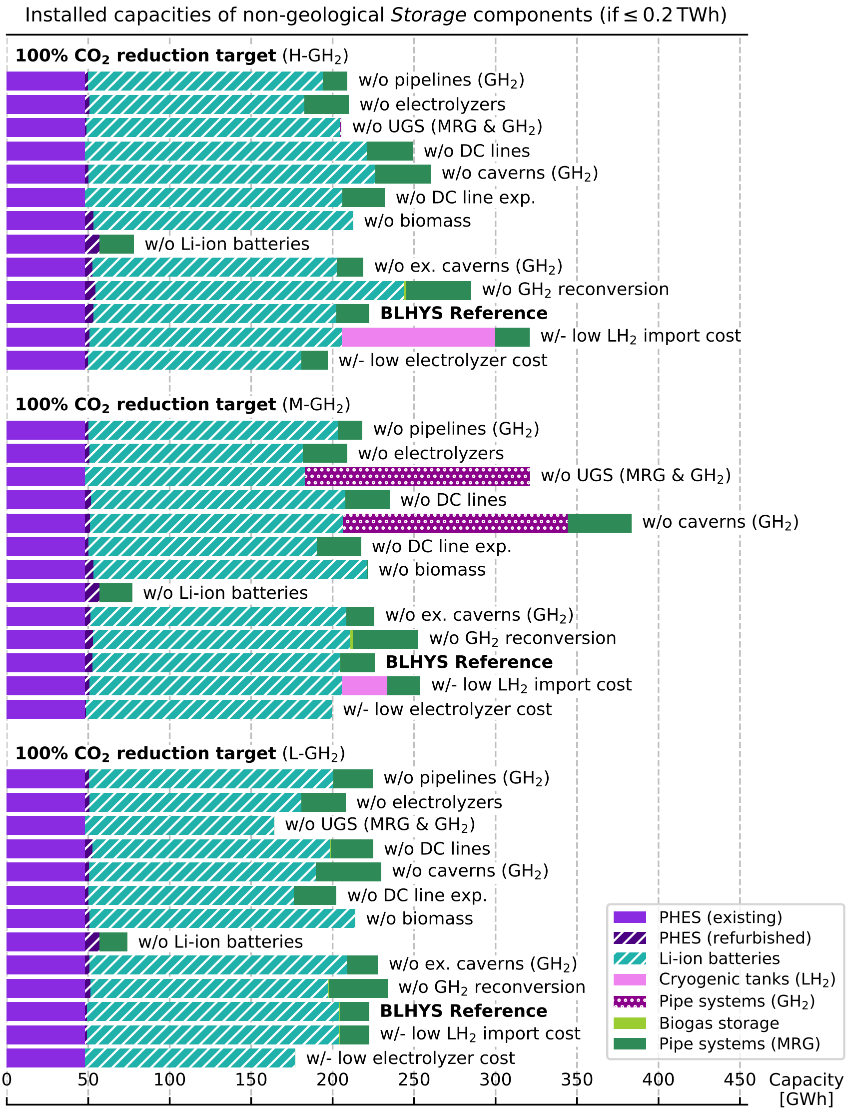

Figure B.51: Capacities of non-geological *Storage* components (when below 200 GWh) in the *BLHYS*-100% scenario variations.

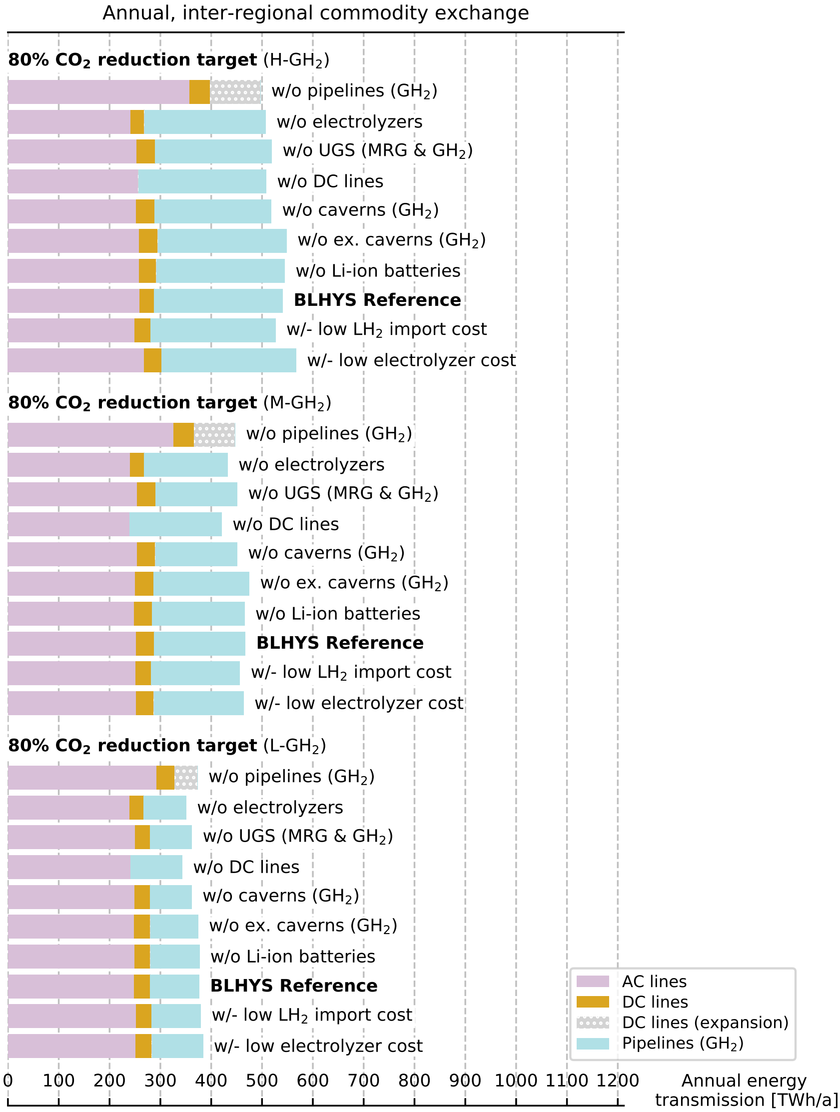

Figure B.52: Inter-regional commodity transmission in the *BLHYS*-80% scenario variations.

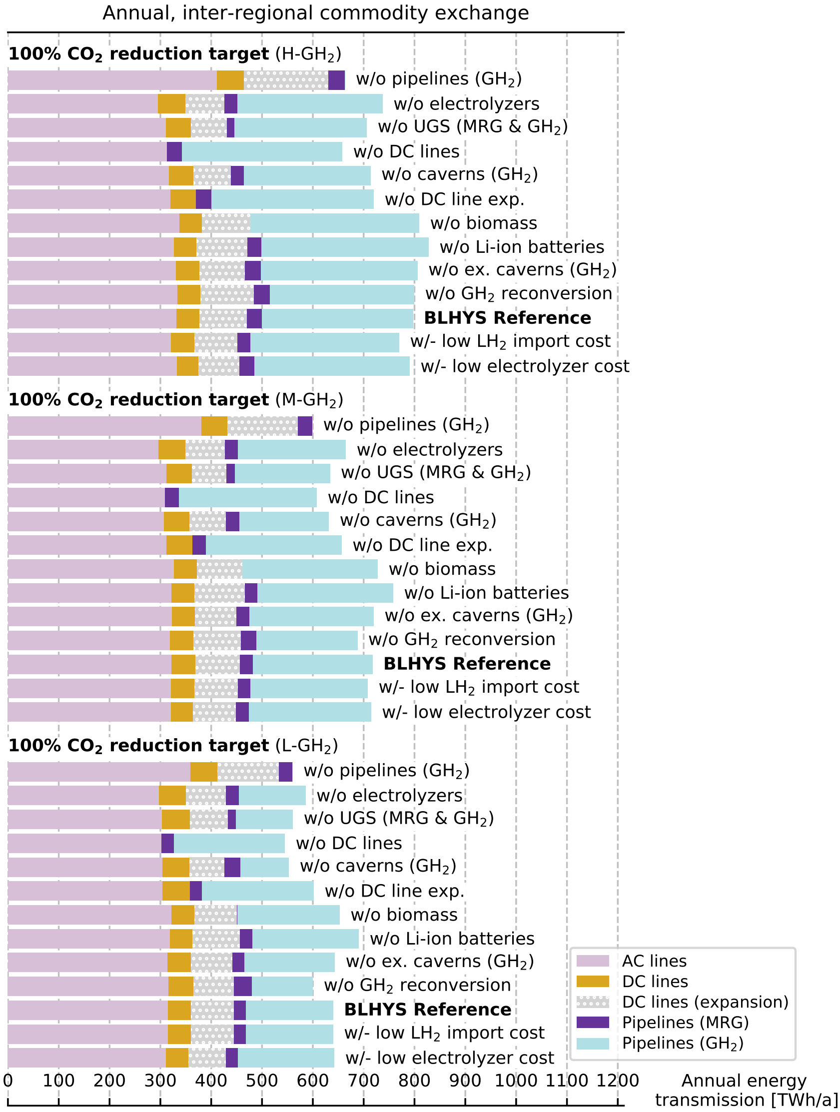

Figure B.53: Inter-regional commodity transmission in the *BLHYS*-100% scenario variations.

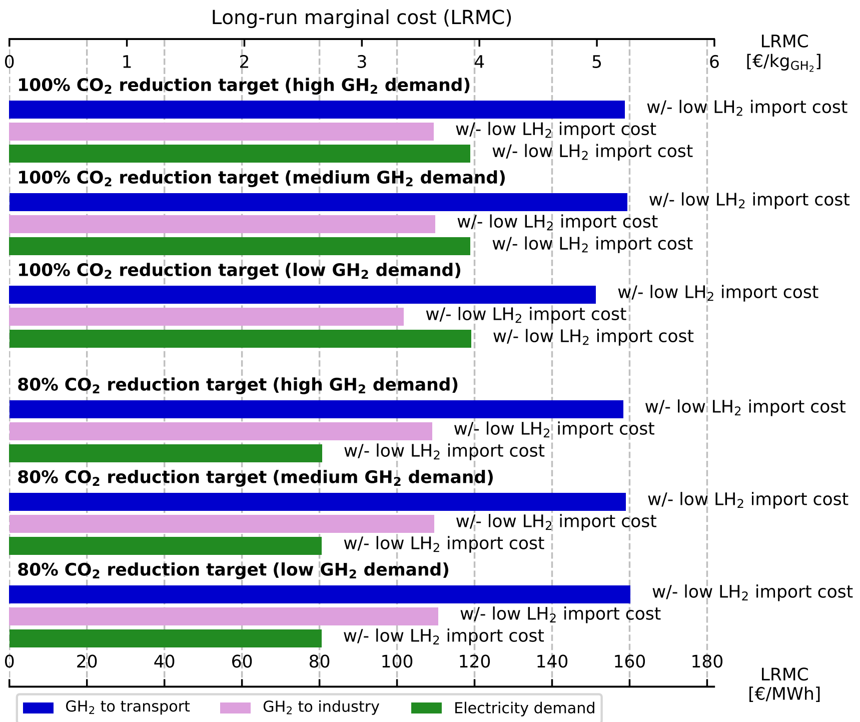

Figure B.54: Weighted long-run marginal cost in the *BLHYS-w/- low LH_2 import cost* scenario variation under varying carbon dioxide reduction targets.

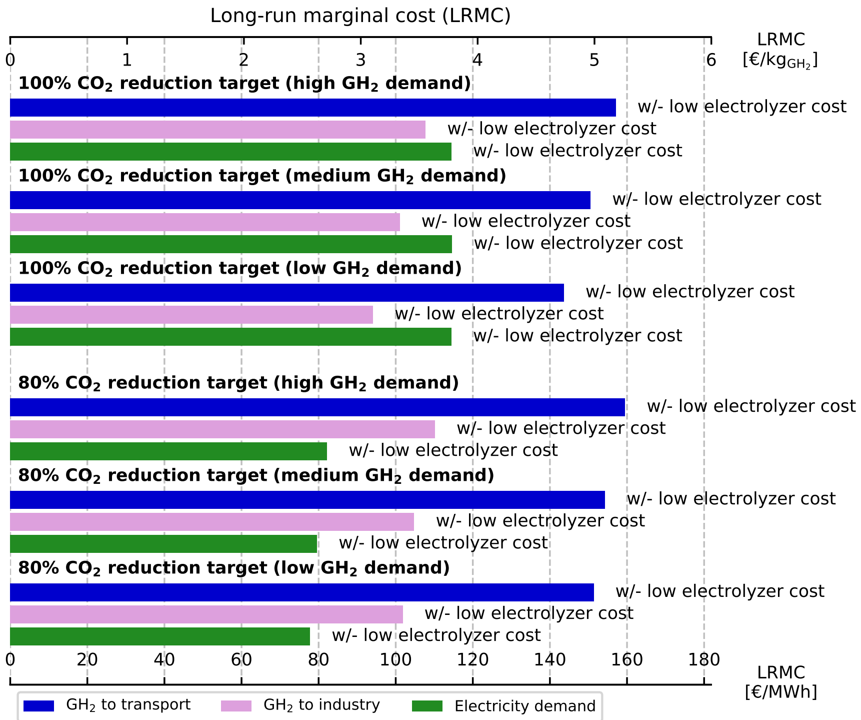

Figure B.55: Weighted long-run marginal cost in the *BLHYS-w/- low electrolyzer cost* scenario variation under varying carbon dioxide reduction targets.

Bibliography

[1] UNFCCC, "Adoption of the Paris agreement." https://unfccc.int/sites/default/files/english_paris_agreement.pdf, 2015. Accessed: 16.09.2019.

[2] L. Welder, D. S. Ryberg, L. Kotzur, T. Grube, M. Robinius, and D. Stolten, "Spatio-temporal optimization of a future energy system for power-to-hydrogen applications in Germany," *Energy*, 2018. 10.1016/j.energy.2018.05.059.

[3] S. Samsatli, I. Staffell, and N. J. Samsatli, "Optimal design and operation of integrated wind-hydrogen-electricity networks for decarbonising the domestic transport sector in Great Britain," *International Journal of Hydrogen Energy*, vol. 41, no. 1, pp. 447–475, 2016. 10.1016/j.ijhydene.2015.10.032.

[4] M. Robinius, A. Otto, P. Heuser, L. Welder, K. Syranidis, D. Ryberg, T. Grube, P. Markewitz, R. Peters, and D. Stolten, "Linking the power and transport sectors—Part 1: The principle of sector coupling," *Energies*, vol. 10, no. 7, p. 956, 2017.

[5] P. Lopion, P. Markewitz, M. Robinius, and D. Stolten, "A review of current challenges and trends in energy systems modeling," *Renewable and Sustainable Energy Reviews*, vol. 96, pp. 156–166, 2018.

[6] H.-K. Ringkjøb, P. M. Haugan, and I. M. Solbrekke, "A review of modelling tools for energy and electricity systems with large shares of variable renewables," *Renewable and Sustainable Energy Reviews*, vol. 96, pp. 440–459, 2018.

[7] M. Groissböck, "Are open source energy system optimization tools mature enough for serious use?," *Renewable and Sustainable Energy Reviews*, vol. 102, pp. 234–248, 2019.

[8] Bundesministerium für Umwelt, Naturschutz und nukleare Sicherheit, "Klimaschutzplan 2050–Klimaschutzpolitische Grundsätze und Ziele der

Bundesregierung." https://www.bmu.de/fileadmin/Daten_BMU/Download_PDF/Klimaschutz/klimaschutzplan_2050_bf.pdf, 2016. Accessed: 22.03.2019.

[9] M. Robinius, A. Otto, K. Syranidis, D. S. Ryberg, P. Heuser, L. Welder, T. Grube, P. Markewitz, V. Tietze, and D. Stolten, "Linking the power and transport sectors—Part 2: Modelling a sector coupling scenario for Germany," *Energies*, vol. 10, no. 7, p. 957, 2017.

[10] A. Bemporad and M. Morari, "Control of systems integrating logic, dynamics, and constraints," *Automatica*, vol. 35, no. 3, pp. 407–427, 1999.

[11] S. Hagspiel, C. Jägemann, D. Lindenberger, T. Brown, S. Cherevatskiy, and E. Tröster, "Cost-optimal power system extension under flow-based market coupling," *Energy*, vol. 66, pp. 654–666, 2014. https://doi.org/10.1016/j.energy.2014.01.025.

[12] F. Neumann and T. Brown, "Heuristics for Transmission Expansion Planning in Low-Carbon Energy System Models," *arXiv preprint arXiv:1907.10548*, 2019.

[13] K. Syranidis, M. Robinius, and D. Stolten, "Control techniques and the modeling of electrical power flow across transmission networks," *Renewable and Sustainable Energy Reviews*, vol. 82, pp. 3452–3467, 2018.

[14] M. Robinius, *Strom- und Gasmarktdesign zur Versorgung des deutschen Straßenverkehrs mit Wasserstoff*. Thesis, 2015.

[15] M. Reuß, L. Welder, J. Thürauf, J. Linßen, T. Grube, L. Schewe, M. Schmidt, D. Stolten, and M. Robinius, "Modeling hydrogen networks for future energy systems: A comparison of linear and nonlinear approaches," *International Journal of Hydrogen Energy*, 2019. https://doi.org/10.1016/j.ijhydene.2019.10.080.

[16] M. Koch, D. Bauknecht, C. Heinemann, D. Ritter, M. Vogel, and E. Tröster, "Modellgestützte Bewertung von Netzausbau im europäischen Netzverbund und Flexibilitätsoptionen im deutschen Stromsystem im Zeitraum 2020–2050," *Zeitschrift für Energiewirtschaft*, vol. 39, no. 1, pp. 1–17, 2015. 10.1007/s12398-015-0147-2.

[17] J. Egerer, "Open source electricity model for Germany (ELMOD-DE)." https://www.econstor.eu/handle/10419/129782, 2016. Accessed: 15.09.2019.

[18] J. Hörsch and T. Brown, "The role of spatial scale in joint optimisations of generation and transmission for European highly renewable scenarios," in *2017 14th International Conference on the European Energy Market (EEM)*, pp. 1–7, IEEE, 2017.

[19] J. Hörsch, F. Hofmann, D. Schlachtberger, and T. Brown, “PyPSA-Eur: An open optimisation model of the European transmission system,” *Energy strategy reviews*, vol. 22, pp. 207–215, 2018.

[20] S. Becker, R. A. Rodriguez, G. B. Andresen, S. Schramm, and M. Greiner, “Transmission grid extensions during the build-up of a fully renewable pan-European electricity supply,” *Energy*, vol. 64, pp. 404–418, 2014. https://doi.org/10.1016/j.energy.2013.10.010.

[21] D. Gunkel and D. Möst, “The German transmission grid expansion in long-term perspective —What is the impact of renewable integration?,” in *11th International Conference on the European Energy Market (EEM14)*, pp. 1–6, 2014.

[22] S. Babrowski, P. Jochem, and W. Fichtner, “Electricity storage systems in the future German energy sector: An optimization of the German electricity generation system until 2040 considering grid restrictions,” *Computers & Operations Research*, vol. 66, pp. 228–240, 2016. https://doi.org/10.1016/j.cor.2015.01.014.

[23] D. P. Schlachtberger, T. Brown, S. Schramm, and M. Greiner, “The benefits of cooperation in a highly renewable European electricity network,” *Energy*, vol. 134, pp. 469–481, 2017. https://doi.org/10.1016/j.energy.2017.06.004.

[24] M. Victoria, K. Zhu, T. Brown, G. B. Andresen, and M. Greiner, “The role of storage technologies throughout the decarbonisation of the sector-coupled European energy system,” *arXiv preprint arXiv:1906.06936*, 2019.

[25] T. Kannengießer, M. Hoffmann, L. Kotzur, P. Stenzel, F. Schuetz, K. Peters, S. Nykamp, D. Stolten, and M. Robinius, “Reducing Computational Load for Mixed Integer Linear Programming: An Example for a District and an Island Energy System,” *Energies*, vol. 12, no. 14, p. 2825, 2019.

[26] J. Deane, G. Drayton, and B. Ó. Gallachóir, “The impact of sub-hourly modelling in power systems with significant levels of renewable generation,” *Applied Energy*, vol. 113, pp. 152–158, 2014.

[27] R. J. Sánchez-García, M. Fennelly, S. Norris, N. Wright, G. Niblo, J. Brodzki, and J. W. Bialek, “Hierarchical spectral clustering of power grids,” *IEEE Transactions on Power Systems*, vol. 29, no. 5, pp. 2229–2237, 2014.

[28] S. Blumsack, P. Hines, M. Patel, C. Barrows, and E. C. Sanchez, “Defining power network zones from measures of electrical distance,” in *2009 IEEE Power & Energy Society General Meeting*, pp. 1–8, IEEE, 2009.

[29] C. Schaffner and R. Mihalic, “Economic evaluation of controllable devices in the Slovenian electric power system–a case study,” in *Proc. of 2005 Power Systems Computation Conference (PSCC'05), Liege, Belgium*, 2005.

[30] T. Anderski, Y. Surmann, S. Stemmer, N. Grisey, E. Momot, A.-C. Leger, B. Betraoui, and P. v. Roy, “HIGHWAY 2050 - Modular Development Plan of the Pan-European Transmission System 2050 - D 2.2 European cluster model of the Pan-European transmission grid.” `https://docs.entsoe.eu/baltic-conf/bites/www.e-highway2050.eu/fileadmin/documents/Results/D2_2_European_cluster_model_of_the_Pan-European_transmission_grid_20072015.pdf`, 2014. Accessed: 15.09.2019.

[31] Kotzur, Leander and Markewitz, Peter and Robinius, Martin and Stolten, Detlef, “Impact of different time series aggregation methods on optimal energy system design,” *Renewable Energy*, vol. 117, pp. 474–487, 2018.

[32] L. Kotzur, P. Markewitz, M. Robinius, and D. Stolten, “Time series aggregation for energy system design: Modeling seasonal storage,” *Applied Energy*, vol. 213, pp. 123–135, 2018.

[33] S. Samsatli and N. J. Samsatli, “A general spatio-temporal model of energy systems with a detailed account of transport and storage,” *Computers & Chemical Engineering*, vol. 80, pp. 155–176, 2015. `10.1016/j.compchemeng.2015.05.019`.

[34] B. Palmintier and M. Webster, “Impact of unit commitment constraints on generation expansion planning with renewables,” in *2011 IEEE power and energy society general meeting*, pp. 1–7, IEEE, 2011.

[35] S. Pfenninger and B. Pickering, “Calliope: a multi-scale energy systems modelling framework,” *J. Open Source Software*, vol. 3, no. 29, p. 825, 2018.

[36] S. Pfenninger, B. Pickering, T. Tröndle, M. Garchery, G. Hawker, and F. Lombardi, “Calliope - A multi-scale energy systems modelling framework.” `https://github.com/calliope-project/calliope`, 2019. Accessed: 15.09.2019.

[37] S. Hilpert, C. Kaldemeyer, U. Krien, S. Günther, C. Wingenbach, and G. Plessmann, “The Open Energy Modelling Framework (oemof) - A new approach to facilitate open science in energy system modelling,” *Energy Strategy Reviews*, vol. 22, pp. 16–25, 2018. `https://doi.org/10.1016/j.esr.2018.07.001`.

[38] oemof developer group, “oemof.” `https://github.com/oemof/oemof`, 2019. Accessed: 15.09.2019.

[39] M. Howells, H. Rogner, N. Strachan, C. Heaps, H. Huntington, S. Kypreos, A. Hughes, S. Silveira, J. DeCarolis, M. Bazillian, and A. Roehrl, "OSeMOSYS: The Open Source Energy Modeling System: An introduction to its ethos, structure and development," *Energy Policy*, vol. 39, no. 10, pp. 5850–5870, 2011. https://doi.org/10.1016/j.enpol.2011.06.033.

[40] OSeMOSYS developer group, "OSeMOSYS - Open Source Energy Modelling System." https://github.com/OSeMOSYS/OSeMOSYS_Pyomo, 2019. Accessed: 15.09.2019.

[41] L. Thurner, A. Scheidler, F. Schäfer, J.-H. Menke, J. Dollichon, F. Meier, S. Meinecke, and M. Braun, "Pandapower—An open-source python tool for convenient modeling, analysis, and optimization of electric power systems," *IEEE Transactions on Power Systems*, vol. 33, no. 6, pp. 6510–6521, 2018.

[42] L. Thurner, A. Scheidler, J. Dollichon, F. Schäfer, F. Meier, J.-H. Menke, S. Meinecke, R. Bolgaryn, J. K. Opara, W. Lorenzen, T. Deß, B. Junker, J. Kupka, L. Löwer, J. Ulffers, N. Bornhorst, J. Schütt, E. Drayer, D. Lohmeier, M. di Pierro, M. Braun, J.-C. Töbermann, and S. Gehler, "pandapower." https://github.com/e2nIEE/pandapower, 2019. Accessed: 15.09.2019.

[43] R. D. Zimmerman, C. E. Murillo-Sánchez, and R. J. Thomas, "MATPOWER: Steady-state operations, planning, and analysis tools for power systems research and education," *IEEE Transactions on power systems*, vol. 26, no. 1, pp. 12–19, 2010.

[44] R. Zimmerman, C. Murillo-Sanchez, S. Abhyankar, R. Bo, A. Borghetti, A. Flueck, D. Gan, R. Lincoln, D. Molzhan, and J. Thorp, "PYPOWER." https://github.com/rwl/PYPOWER, 2019. Accessed: 15.09.2019.

[45] T. Brown, J. Hörsch, and D. Schlachtberger, "PyPSA: Python for Power System Analysis," *Journal of Open Research Software*, vol. 6, no. 1, 2018. 10.5334/jors.188.

[46] T. Brown, J. Hörsch, and D. Schlachtberger, "PyPSA: Python for Power System Analysis." https://pypsa.org/, 2019. Accessed: 15.09.2019.

[47] Matthias Fripp and Rodrigo Henriquez and Patricia Hidalgo-Gonzalez and Josiah Johnston and Benjamin Maluenda and Ana Mileva and Mark Seaborn, "Switch." https://github.com/switch-model/switch, 2019. Accessed: 15.09.2019.

[48] TUM ENS, "urbs." https://github.com/tum-ens/urbs, 2019. Accessed: 15.09.2019.

[49] W. E. Hart, J.-P. Watson, and D. L. Woodruff, "Pyomo: modeling and solving mathematical programs in Python," *Mathematical Programming Computation*, vol. 3, no. 3, p. 219, 2011.

[50] W. E. Hart, C. D. Laird, J.-P. Watson, D. L. Woodruff, G. A. Hackebeil, B. L. Nicholson, and J. D. Siirola, *Pyomo-optimization modeling in python*, vol. 67. Springer, 2012.

[51] Gurobi, "Gurobi optimization." https://www.gurobi.com, 2019. Accessed: 15.09.2019.

[52] Gurobi, "Gurobi Guidelines for Numerical Issues." http://files.gurobi.com/Numerics.pdf, 2017. Accessed: 15.09.2019.

[53] Makhorin, Andrew, "GLPK (GNU Linear Programming Kit)." https://www.gnu.org/software/glpk/, 2019. Accessed: 15.09.2019.

[54] R. Loulou, G. Goldstein, and K. Noble, "Documentation for the MARKAL Family of Models." http://iea-etsap.org/MrklDoc-I_StdMARKAL.pdf, 2004. Accessed: 15.09.2019.

[55] IEA-ETSAP, "TIMES." https://iea-etsap.org/index.php/etsap-tools/model-generators/times, 2019. Accessed: 15.09.2019.

[56] W. McKinney, "Data structures for statistical computing in python," in *Proceedings of the 9th Python in Science Conference*, vol. 445, pp. 51–56, Austin, TX, 2010.

[57] GeoPandas developers, "GeoPandas." http://geopandas.org/, 2019. Accessed: 15.09.2019.

[58] D. S. Ryberg, J. Linßen, M. Robinius, and D. Stolten, "GeoKit - Geospatial toolkit for Python." https://github.com/FZJ-IEK3-VSA/geokit, 2019. Accessed: 15.09.2019.

[59] L. Kotzur, P. Markewitz, M. Robinius, and D. Stolten, "Time Series Aggregation Module." https://github.com/FZJ-IEK3-VSA/tsam, 2019. Accessed: 15.09.2019.

[60] F. U. Leuthold, H. Weigt, and C. von Hirschhausen, "A large-scale spatial optimization model of the European electricity market," *Networks and spatial economics*, vol. 12, no. 1, pp. 75–107, 2012.

[61] A. Schroeder, P.-Y. Oei, A. Sander, L. Hankel, and L. C. Laurisch, "The integration of renewable energies into the German transmission grid—A scenario comparison," *Energy Policy*, vol. 61, pp. 140–150, 2013. https://doi.org/10.1016/j.enpol.2013.06.006.

[62] K. Schaber, F. Steinke, and T. Hamacher, "Managing temporary oversupply from renewables efficiently: Electricity storage versus energy sector coupling in germany," in *International Energy Workshop, Paris*, 2013.

[63] K. Bruninx, D. Madzharov, E. Delarue, and W. D' Haeseleer, “Impact of the German nuclear phase-out on Europe's electricity generation—A comprehensive study,” *Energy Policy*, vol. 60, pp. 251–261, 2013. `https://doi.org/10.1016/j.enpol.2013.05.026`.

[64] S. Ludig, E. Schmid, M. Haller, and N. Bauer, “Assessment of transformation strategies for the German power sector under the uncertainty of demand development and technology availability,” *Renewable and Sustainable Energy Reviews*, vol. 46, pp. 143–156, 2015. `https://doi.org/10.1016/j.rser.2015.02.044`.

[65] C. Krüger, M. Buddeke, F. Merten, and A. Nebel, “Modelling the interdependencies of storage, DSM and grid-extension for Europe,” in *2015 12th International Conference on the European Energy Market (EEM)*, pp. 1–5, IEEE, 2015.

[66] C. Kemfert, F. Kunz, and J. Rosellón, “A welfare analysis of electricity transmission planning in Germany,” *Energy Policy*, vol. 94, pp. 446–452, 2016. `https://doi.org/10.1016/j.enpol.2016.04.011`.

[67] D. Heinemann, *Regenerative Stromversorgung & Speicherbedarf in 2050 (” RESTORE 2050”): Abschlussbericht des Verbund-Forschungsprojektes für den Verbundpartner Universität Oldenburg: Laufzeit: 01.11. 2012-30.06. 2016.* Carl von Ossietzky Universität Oldenburg, 2016.

[68] F. Cebulla, T. Naegler, and M. Pohl, “Electrical energy storage in highly renewable European energy systems: Capacity requirements, spatial distribution, and storage dispatch,” *Journal of Energy Storage*, vol. 14, pp. 211–223, 2017. `https://doi.org/10.1016/j.est.2017.10.004`.

[69] H. C. Gils, Y. Scholz, T. Pregger, D. Luca de Tena, and D. Heide, “Integrated modelling of variable renewable energy-based power supply in Europe,” *Energy*, vol. 123, pp. 173–188, 2017. `https://doi.org/10.1016/j.energy.2017.01.115`.

[70] M. Buddeke and F. Merten, “Nutzung von Wasserstoffspeichern im europäischen Stromsystem 2050,” 2017.

[71] P. Kluschke and F. Neumann, “Interaction of a Hydrogen Refueling Station Network for Heavy-Duty Vehicles and the Power System in Germany for 2050,” *arXiv preprint arXiv:1908.10119*, 2019.

[72] K. Bruhn, “Entwicklung der Brennstoffpreise von 2008 bis 2018,” *TFZ-Merkblatt 18WBr006*, 2018.

[73] H. C. Gils, “Economic potential for future demand response in Germany –Modeling approach and case study,” *Applied Energy*, vol. 162, pp. 401–415, 2016. `10.1016/j.apenergy.2015.10.083`.

[74] P. Seydel, *Entwicklung und Bewertung einer langfristigen regionalen Strategie zum Aufbau einer Wasserstoffinfrastruktur - aus Basis der Modellverknüpfung eines Geografischen Informationssystems und eines Energiesystemmodells.* Phd thesis, 2008.

[75] GermanHy, "Woher kommt der Wasserstoff in Deutschland bis 2050?." https://www.dena.de/fileadmin/dena/Dokumente/Pdf/9060_MOB_Studie_Woher_kommt_der_Wasserstoff_in_Deutschland_bis_2050__Abschlussbericht_.pdf, 2009. Accessed: 15.09.2019.

[76] S. Baufumé, F. Grüger, T. Grube, D. Krieg, J. Linssen, M. Weber, J.-F. Hake, and D. Stolten, "GIS-based scenario calculations for a nationwide German hydrogen pipeline infrastructure," *International journal of hydrogen energy*, vol. 38, no. 10, pp. 3813–3829, 2013.

[77] A. Almansoori and A. Betancourt-Torcat, "Design of optimization model for a hydrogen supply chain under emission constraints - A case study of Germany," *Energy*, vol. 111, pp. 414–429, 2016. https://doi.org/10.1016/j.energy.2016.05.123.

[78] A. Ochoa Bique and E. Zondervan, "An outlook towards hydrogen supply chain networks in 2050 —Design of novel fuel infrastructures in Germany," *Chemical Engineering Research and Design*, vol. 134, pp. 90–103, 2018. https://doi.org/10.1016/j.cherd.2018.03.037.

[79] A. C. Weber and L. G. Papageorgiou, "Design of hydrogen transmission pipeline networks with hydraulics," *Chemical Engineering Research and Design*, vol. 131, pp. 266–278, 2018. https://doi.org/10.1016/j.cherd.2018.01.022.

[80] M. Reuß, T. Grube, M. Robinius, and D. Stolten, "A hydrogen supply chain with spatial resolution: Comparative analysis of infrastructure technologies in Germany," *Applied Energy*, vol. 247, pp. 438–453, 2019.

[81] S. Cerniauskas, T. Grube, A. Praktiknjo, D. Stolten, and M. Robinius, "Future Hydrogen Markets for Transport and Industry-The Impact of CO2 Taxes," 2019.

[82] D. Caglayan, H. Heinrichs, J. Linßen, M. Robinius, and D. Stolten, "Impact of Different Weather Years on the Design of Hydrogen Supply Pathways for Transport Needs," *Preprints*, 2019. 10.20944/preprints201906.0056.v1.

[83] M. Robinius, L. Schewe, M. Schmidt, D. Stolten, J. Thürauf, and L. Welder, "Robust optimal discrete arc sizing for tree-shaped potential networks," *Computational Optimization and Applications*, 2019. 10.1007/s10589-019-00085-x.

[84] Arbeitsgemeinschaft Energiebilanzen e.V. , "Energieverbrauch in Deutschland im Jahr 2013." www.ag-energiebilanzen.de/index.php?article_id=29&fileName=ageb_jahresbericht2013_20140317.pdf, 2014. Accessed: 20.03.2015.

[85] S. Cerniauskas, A. J. Chavez Junco, T. Grube, M. Robinius, and D. Stolten, "Reassignment Options of Natural Gas Transmission Grid for Hydrogen Transport: the Case of Germany," 2019.

[86] J. Stenglein, S. Achner, S. Brühl, B. Milatz, L. Schuffelen, N. Krzikalla, H. Wolter, R. Werner, M. Sandrock, and S. Häseler, "Klimaschutz: Der Plan Energiekonzept für Deutschland." https://www.greenpeace.de/sites/www.greenpeace.de/files/publications/klimaschutz-der-plan-greenpeace-20151117.pdf, 2015. Accessed: 15.09.2019.

[87] H.-M. Henning and A. Palzer, "Was kostet die Energiewende? Wege zur Transformation des deutschen Energiesystems bis 2050." https://www.fraunhofer.de/content/dam/zv/de/Forschungsfelder/Energie-Rohstoffe/Fraunhofer-ISE_Transformation-Energiesystem-Deutschland_final_19_11%20(1).pdf, 2015. Accessed: 15.09.2019.

[88] J. Nitsch, "Erfolgreiche Energiewende nur mit verbesserter Energieeffizienz und einem klimagerechten Energiemarkt –Aktuelle Szenarien 2017 der deutschen Energieversorgung." https://www.bee-ev.de/home/presse/mitteilungen/detailansicht/energieszenarien-2017-erfolgreiche-energiewende-nur-mit-verbesserter-energieeffizienz/, 2017. Accessed: 15.09.2019.

[89] J. Repenning, F. C. Matthes, R. Blanck, L. Emele, U. Döring, H. Förster, M. Haller, R. Harthan, K. Henneberg, H. Hermann, W. Jörß, P. Kasten, S. Ludig, C. Loreck, M. Scheffler, K. Schumacher, W. Eichhammer, S. Braungardt, R. Elsland, T. Fleiter, J. Hartwig, J. Kockat, B. Pfluger, W. Schade, B. Schlomann, F. Sensfuß, U. Athmann, and H.-J. Ziesing, "Klimaschutzszenario 2050 1. Modellierungsrunde." https://www.isi.fraunhofer.de/content/dam/isi/dokumente/ccx/2014/Bericht_Runde_1.pdf, 2014. Accessed: 15.09.2019.

[90] J. Repenning, L. Emele, R. Blanck, H. Böttcher, G. Dehoust, H. Förster, B. Greiner, R. Harthan, K. Henneberg, H. Hermann, W. Jörß, C. Loreck, S. Ludig, M. Scheffler, K. Schumacher, K. Wiegmann, C. Zell-Ziegler, S. Braungardt, W. Eichhammer, R. Elsland, T. Fleiter, J. Hartwig, J. Kockat, B. Pfluger, W. Schade, B. Schlomann, F. Sensfuß, and H.-J. Ziesing, "Klimaschutzszenario 2050 2. Endbericht." https://www.isi.fraunhofer.de/content/dam/isi/dokumente/ccx/2015/Bericht_Runde_2.pdf, 2015. Accessed: 15.09.2019.

[91] M. Schlesinger, D. Lindenberger, and C. Lutz, “Entwicklung der Energiemärkte - Energiereferenzprognose.” https://www.bmwi.de/Redaktion/DE/Publikationen/Studien/entwicklung-der-energiemaerkte-energiereferenzprognose-endbericht.pdf?__blob=publicationFile&v=7, 2014. Accessed: 15.09.2019.

[92] J. Nitsch, “Die Energiewende nach COP 21 –Aktuelle Szenarien der deutschen Energieversorgung.” https://www.bee-ev.de/fileadmin/Publikationen/Studien/Joachim_Nitsch_Energiewende_nach_COP21.pdf, 2016. Accessed: 15.09.2019.

[93] J. Nitsch, T. Pregger, T. Naegler, D. Heide, D. L. d. Tena, F. Trieb, Y. Scholz, K. Nienhaus, N. Gerhardt, M. Sterner, T. Trost, A. v. Oehsen, R. Schwinn, C. Pape, H. Hahn, M. Wickert, and B. Wenzel, “Langfristszenarien und Strategien für den Ausbau der erneuerbaren Energien in Deutschland bei Berücksichtigung der Entwicklung in Europa und global - Schlussbericht.” https://www.dlr.de/dlr/Portaldata/1/Resources/bilder/portal/portal_2012_1/leitstudie2011_bf.pdf, 2012. Accessed: 15.09.2019.

[94] B. Pfluger, T. Fleiter, L. Kranzl, M. Hartner, W. Schade, A. Hennecke, H. Fehrenbach, L. Brischke, B. Tersteegen, F. Sensfuß, and J. Steinbach, “Langfristszenarien für die Transformation des Energiesystems in Deutschland Modul 10.a: Reduktion der Treibhausgasemissionen Deutschlands um 95 % bis 2050 (Kurzfassung) Studie im Auftrag des Bundesministeriums für Wirtschaft und Energie.” https://www.bmwi.de/Redaktion/DE/Downloads/B/berichtsmodul-10-a-bericht-reduktion-der-treibhausgasemissionen-deutschlands-langfassung.pdf?__blob=publicationFile&v=4, 2017. Accessed: 15.09.2019.

[95] H. Hecking, J. Kruse, O. Hennes, T. Wildgrube, W. Autoren, D. Lencz, M. Hintermayer, M. Gierkink, J. Peter, S. Lorenczik, C. Rehtanz, M. Greve, U. Häger, S. Kippelt, J. F. Rettberg, C. Wagner, M. Tretschock, A. H. Holm, F. Kagerer, B. Oschatz, B. Winiewska, B. Mailach, and P. Radgen, “Leitstudie Integrierte Energiewende.” https://www.dena.de/integrierte-energiewende/, 2018. Accessed: 15.09.2019.

[96] A. P. Hans-Martin Henning, “Energiesystem Deutschland 2050.” https://www.ise.fraunhofer.de/content/dam/ise/de/documents/publications/studies/Fraunhofer-ISE_Energiesystem-Deutschland-2050.pdf, 2013. Accessed: 15.09.2019.

[97] K. Hillebrandt, S. Samadi, and M. Fischedick, “Pathways to deep decarbonization in Germany.” https://wupperinst.org/uploads/tx_wupperinst/DDPP_DE_summary_en.pdf, 2015. Accessed: 15.09.2019.

[98] M. Robinius, P. Markewitz, P. Lopion, F. Kullmann, P.-M. Heuser, K. Syranidis, S. Cerniauskas, M. Reuß, S. Ryberg, L. Kotzur, D. Caglayan, L. Welder, J. Linßen, T. Grube, H. Heinrichs, and P. S. D. Stolten, "Kosteneffiziente und klimagerechte Transformationsstrategien für das deutsche Energiesystem bis zum Jahr 2050 (Kurzfassung)," tech. rep., 2019.

[99] L. Welder, P. Stenzel, N. Ebersbach, P. Markewitz, M. Robinius, B. Emonts, and D. Stolten, "Design and evaluation of hydrogen electricity reconversion pathways in national energy systems using spatially and temporally resolved energy system optimization," *International Journal of Hydrogen Energy*, vol. 44, no. 19, pp. 9594–9607, 2019.

[100] Übertragungsnetzbetreiber, "Bericht der deutschen Übertragungsnetzbetreiber zur Leistungsbilanz 2016." `http://www.netztransparenz.de/portals/1/Content/Ver%C3%B6ffentlichungen/Bericht_zur_Leistungsbilanz_2016.pdf`, 2016. Accessed: 15.09.2019.

[101] Bundesnetzagentur and Bundeskartellamt, "Bericht Monitoringbericht 2018," tech. rep., Bundesnetzagentur, Bundeskartellamt, 8 Feb. 2019 2019.

[102] D. S. Ryberg, D. G. Caglayan, S. Schmitt, J. Linßen, D. Stolten, and M. Robinius, "The Future of European Onshore Wind Energy Potential: Detailed Distribution and Simulation of Advanced Turbine Designs," *Preprint*, 2018. `10.20944/preprints201812.0196.v1`.

[103] I. Staffell and S. Pfenninger, "Using bias-corrected reanalysis to simulate current and future wind power output," *Energy*, vol. 114, pp. 1224–1239, 2016.

[104] D. Ryberg, M. Robinius, and D. Stolten, "Evaluating Land Eligibility Constraints of Renewable Energy Sources in Europe," *Energies*, vol. 11, no. 5, p. 1246, 2018.

[105] D. G. Caglayan, S. Ryberg, H. Heinrichs, J. Linßen, D. Stolten, and M. Robinius, "The Techno-Economic Potential of Offshore Wind Energy with Optimized Future Turbine Designs in Europe," *Preprint*, 2019. `10.20944/preprints201902.0121.v1`.

[106] M. Robinius, J. Linßen, T. Grube, M. Reuß, P. Stenzel, K. Syranidis, P. Kuckertz, and D. Stolten, "Comparative Analysis of Infrastructures: Hydrogen Fueling and Electric Charging of Vehicles," *Forschungszentrum Jülich. Jülich (Schriften des Forschungszentrums Jülich, Reihe Energie und Umwelt, 408)*, 2018.

[107] Übertragungsnetzbetreiber, "Anhang zum Netzentwicklungsplan Strom 2025, Version 2015, 1. Entwurf." `https://www.netzentwicklungsplan.`

de/sites/default/files/paragraphsfiles/NEP_2025_1_Entwurf_Teil2.pdf, 2015. Accessed: 18.07.2017.

[108] Bundesnetzagentur, "MaStR Marktstammdatenregister - Öffentliche Einheitenübersicht - Stromerzeugungseinheiten." https://www.marktstammdatenregister.de/MaStR/Einheit/Einheiten/OeffentlicheEinheitenuebersicht, 2019. Accessed: 14.07.2019.

[109] S. Pfenninger and I. Staffell, "Long-term patterns of European PV output using 30 years of validated hourly reanalysis and satellite data," *Energy*, vol. 114, pp. 1251–1265, 2016.

[110] D. S. Ryberg, *Generation Lulls from the Future Potential of Wind and Solar Energy in Europe*. Thesis, 2019.

[111] European Commission, "ETRI 2014–Energy Technology Reference Indicator Projections for 2010–2050." http://publications.jrc.ec.europa.eu/repository/bitstream/JRC92496/ldna26950enn.pdf, 2014. Accessed: 15.09.2019.

[112] Bundesministerium für Wirtschaft und Energie, "Zeitreihen zur Entwicklung der erneuerbaren Energien in Deutschland." https://www.erneuerbare-energien.de/EE/Redaktion/DE/Downloads/zeitreihen-zur-entwicklung-der-erneuerbaren-energien-in-deutschland-1990-2018-excel.xlsx?__blob=publicationFile&v=19, 2019. Accessed: 02.05.2019.

[113] ENTSO-E, "Yearly Statistics and Adequacy Retrospect - 2015 Background Data." https://docstore.entsoe.eu/Documents/Publications/Statistics/YSAR/YS_AR2015_data.zip, 2015. Accessed: 02.05.2019.

[114] K. Syranidis, *Investigation of the Integration of Renewable Energy Sources into the Future European Power System Using a Verified Dispatch Model with High Spatiotemporal Resolution*. Thesis, 2019.

[115] B. Pieprzyk, P. Rojas, C. Kunz, and A. Knebel, "Metaanalyse über Perspektiven fester, flüssiger und gasförmiger Bioenergieträger." http://www.forschungsradar.de/fileadmin/content/bilder/Vergleichsgrafiken/meta_Perspektiven_Bioenergietraeger_16/AEE_Metaanalyse_Bioenergie_Nov16.pdf, 2016. Accessed: 15.09.2019.

[116] D. Thrän, K. Bunzel, U. Seyfert, V. Zeller, M. Buchhorn, K. Müller, B. Matzdorf, N. Gaasch, and K. Klöckner, "Final Report Global and Regional Spatial Distribution of Biomass Potentials: Status quo and options for specification." https://www.dbfz.de/fileadmin/user_upload/Referenzen/DBFZ_Reports/DBFZ_Report_7.pdf, 2015. Accessed: 15.09.2019.

[117] M. Bossard, J. Feranec, and J. Otahel, “CORINE land cover technical guide: Addendum 2000,” tech. rep., 2000.

[118] Copernicus, “Corine Land Cover (CLC) 2012, Version 18.5.1 [dataset].” https://land.copernicus.eu/pan-european/corine-land-cover, 2012. Accessed: 01.04.2017.

[119] D. S. Ryberg, J. Linßen, M. Robinius, and D. Stolten, “Geospatial Land Availability for Energy Systems (GLAES).” https://github.com/FZJ-IEK3-VSA/glaes, 2019. Accessed: 15.09.2019.

[120] Danish Energy Agency, “Technology Data for Energy Plants for Electricity and District heating generation.” https://ens.dk/sites/ens.dk/files/Analyser/technology_data_catalogue_for_el_and_dh_-_aug_2016_upd_dec18.pdf, 2016. Accessed: 15.09.2019.

[121] Fachagentur Nachwachsende Rohstoffe, “Biogas: Faustzahlen.” https://biogas.fnr.de/daten-und-fakten/faustzahlen/, 2019. Accessed: 17.01.2019.

[122] D. B. gemeinnützige GmbH (DBFZ), “Leitfaden Biogas - Von der Gewinnung zur Nutzung.” http://www.fnr.de/fileadmin/allgemein/pdf/broschueren/Leitfaden_Biogas_web_V01.pdf, 2016. Accessed: 15.09.2019.

[123] WIND-WASSERSTOFF-projekt GmbH & Co. KG, “Das Projekt RH2-WKA.” https://www.rh2-wka.de/projekt.html, 2017. Accessed: 10.05.2019.

[124] IWR Online, “Erste KWK-Anlage nutzt regenerativen Wasserstoff im Alltagsbetrieb.” https://www.iwr.de/news.php?id=35473, 2018. Accessed: 15.09.2019.

[125] Bundesregierung, “Gesetz über die friedliche Verwendung der Kernenergie und den Schutz gegen ihre Gefahren (Atomgesetz). AtG. Ausfertigungsdatum: 23.12. 1959. Vollzitat:”Atomgesetz in der Fassung der Bekanntmachung vom 15. Juli 1985 (BGBl. I S. 1565), das zuletzt durch Artikel 1 des Gesetzes vom 10. Juli 2018 (BGBl. I S. 1122, 1124) geändert worden ist”,” tech. rep., 2018.

[126] Bundesministerium für Wirtschaft und Energie, “Kommission ,,Wachstum, Strukturwandel und Beschäftigung“- Abschlussbericht,” tech. rep., 2019.

[127] P. Markewitz, “Lebensdaueranalyse fossil gefeuerter Kraftwerke,” *Zeitschrift für Energiewirtschaft*, vol. 40, no. 3, pp. 171–177, 2016.

[128] P. Markewitz, M. Robinius, and D. Stolten, “The future of fossil fired power plants in Germany—A lifetime analysis,” *Energies*, vol. 11, no. 6, p. 1616, 2018.

[129] S. Pasini, "Fusina: Achieving low NOx from hydrogen combined-cycle power." http://www.powerengineeringint.com/articles/print/volume-18/issue-9/features/fusina-achieving-low-nox-from-hydrogen-combined-cycle-power.html, 2010. Accessed: 13.10.2016.

[130] Open Power System Data, "Conventional power plants." https://data.open-power-system-data.org/conventional_power_plants/2018-12-20, 2018. Accessed: 15.09.2019.

[131] P. Stenzel, W. Hennings, and J. Linssen, "Energiespeicher," *BWK*, vol. 69, no. 5, 2017.

[132] P. Stenzel, J. Linssen, M. Robinius, D. Stolten, V. Gottke, H. Teschner, A. Velten, and F. Schäfer, "Energiespeicher," *BWK*, 2019.

[133] P. Elsner and D. U. Sauer, *Energiespeicher - Technologiesteckbrief zur Analyse ,,Flexibilitätskonzepte für die Stromversorgung 2050"*. Schriftenreihe Energiesysteme der Zukunft, München: acatech –Deutsche Akademie der Technikwissenschaften e. V., 2015.

[134] G. Fuchs, B. Lunz, M. Leuthold, and D. U. Sauer, "Technology Overview on Electricity Storage." http://www.sefep.eu/activities/projects-studies/120628_Technology_Overview_Electricity_Storage_SEFEP_ISEA.pdf, 2012. Accessed: 15.09.2019.

[135] C. Pape, N. Gerhardt, P. Härtel, A. Scholz, R. Schwinn, T. Drees, A. Maaz, J. Sprey, C. Breuer, A. Moser, F. Sailer, S. Reuter, and T. Müller, "ROADMAP SPEICHER SPEICHERBEDARF FÜR ERNEUERBARE ENERGIEN –SPEICHERALTERNATIVEN –SPEICHERANREIZ –ÜBERWINDUNG RECHTLICHER HEMMNISSE Endbericht." http://www.fvee.de/fileadmin/publikationen/Politische_Papiere_FVEE/14.IWES_Roadmap-Speicher/14_IWES-etal_Roadmap_Speicher_Langfassung.pdf, 2014. Accessed: 15.09.2019.

[136] P. Stenzel, J. Linssen, S. Stemmer, M. Robinius, D. Stolten, V. Gottke, and H. Teschner, "Energiespeicher," *BKW*, vol. 70, no. 5, pp. 35–46, 2018.

[137] Bundesnetzagentur, "Quartalsbericht zu Netz- und Systemsicherheitsmaßnahmen Zweites bis Drittes Quartal 2017," 2018.

[138] Bundesnetzagentur, "Quartalsbericht zu Netz- und Systemsicherheitsmaßnahmen Zweites bis Drittes Quartal 2018," 2019.

[139] Übertragungsnetzbetreiber, "Anhang zum Netzentwicklungsplan Strom 2030, Version 2017, 2. Entwurf." https://www.netzentwicklungsplan.de/sites/default/files/paragraphs-files/NEP_2030_2_Entwurf_Teil2.pdf, 2017. Accessed: 15.09.2019.

[140] Übertragungsnetzbetreiber, “Anhang zum Netzentwicklungsplan Strom 2030, Version 2019, 2. Entwurf.” https://www.netzentwicklungsplan.de/sites/default/files/paragraphs-files/NEP_2030_V2019_2_Entwurf_Teil2.pdf, 2019. Accessed: 15.09.2019.

[141] K. Van den Bergh, E. Delarue, and W. D'haeseleer, “DC power flow in unit commitment models,” *TMF Working Paper-Energy and Environment, Tech. Rep.*, 2014.

[142] E. Jones, T. Oliphant, and P. Peterson, “SciPy: Open source scientific tools for Python.” http://www.scipy.org/, 2001. Accessed: 15.09.2019.

[143] T. E. Oliphant, “Python for scientific computing,” *Computing in Science & Engineering*, vol. 9, no. 3, pp. 10–20, 2007.

[144] F. Boing, A. Murmann, and A. Guminski, “Electrification and coal phase-out in Germany: A scenario analysis,” in *2018 15th International Conference on the European Energy Market (EEM)*, pp. 1–6, IEEE, 2018.

[145] P3 energy and storage GmbH and Institut für Hochspannungstechnik der RWTH Aachen, “Szenarien für eine langfristige Netzentwicklung - Schlussbericht –Aachen, 02.11.2012 - Studie im Auftrag des Bundesministeriums für Wirtschaft und Technologie.” https://publications.rwth-aachen.de/record/47989, 2012. Accessed: 15.09.2019.

[146] Übertragungsnetzbetreiber, “Kostenschätzung (NEP 2030 (2019), 2. Entwurf).” https://www.netzentwicklungsplan.de/sites/default/files/paragraphs-files/NEP_2030_2019_2_Entwurf_Kostenschaetzungen.pdf, 2019. Accessed: 15.09.2019.

[147] Energie-Forschungszentrum Niedersachsen and OECOS GmbH, “Ökologische Auswirkungen von 380-kV-Erdleitungen und HGÜ-Erdleitungen.” http://www.gbv.de/dms/clausthal/E_BOOKS/2012/2012EB137.pdf, 2012. Accessed: 05.09.2017.

[148] E-Highway 2050, “Highway database per country.” https://docs.entsoe.eu/baltic-conf/bites/www.e-highway2050.eu/fileadmin/documents/Results/e-Highway_database_per_country-08022016.xlsx, 2016. Accessed: 15.09.2019.

[149] King & Spalding, “LNG in Europe 2018 - An Overview of LNG Import Terminals in Europe.” https://www.kslaw.com/attachments/000/006/010/original/LNG_in_Europe_2018_-_An_Overview_of_LNG_Import_Terminals_in_Europe.pdf?1530031152, 2018. Accessed: 06.05.2019.

[150] P.-M. Heuser, D. S. Ryberg, T. Grube, M. Robinius, and D. Stolten, "Techno-economic analysis of a potential energy trading link between Patagonia and Japan based on CO2 free hydrogen," *International Journal of Hydrogen Energy*, 2019.

[151] K. Stratmann, "LNG-Terminal in Sicht - Bewerber Brunsbüttel findet neuen Kunden." https://www.handelsblatt.com/politik/deutschland/gasversorgung-lng-terminal-in-sicht-bewerber-brunsbuettel-findet-neuen-kunden/23973108.html?ticket=ST-468515-zoC4ZUCDVUzg44jL7Q0L-ap3, 2019. Accessed: 11.02.2019.

[152] FNB Gas, "Entwurf Netzentwicklungsplan Gas 2018-2028." https://www.fnb-gas.de/files/2018_03_29_entwurf_nep-gas-2018-2028_1.pdf, 2018. Accessed: 15.09.2019.

[153] M. Reuß, *Techno-ökonomische Analyse alternativer Wasserstoffinfrastruktur*. Thesis, 2019.

[154] M. Reuß, T. Grube, M. Robinius, P. Preuster, P. Wasserscheid, and D. Stolten, "Seasonal storage and alternative carriers: A flexible hydrogen supply chain model," *Applied energy*, vol. 200, pp. 290–302, 2017.

[155] K. Stolzenburg and R. Mubbala, "Hydrogen Liquefaction Report." https://www.idealhy.eu/uploads/documents/IDEALHY_D3-16_Liquefaction_Report_web.pdf, 2013. Accessed: 15.09.2019.

[156] C. Wulf, J. Linßen, and P. Zapp, "Review of power-to-gas projects in Europe," *Energy Procedia*, vol. 155, pp. 367–378, 2018.

[157] DVGW, "Wo aus Wind und Sonne grünes Gas wird ... Eine Übersicht der Power-to-Gas-Projekte in Deutschland." https://www.dvgw.de/themen/gas-und-energiewende/power-to-gas/, 2019. Accessed: 29.04.2019.

[158] A. Buttler and H. Spliethoff, "Current status of water electrolysis for energy storage, grid balancing and sector coupling via power-to-gas and power-to-liquids: A review," *Renewable and Sustainable Energy Reviews*, vol. 82, pp. 2440–2454, 2018.

[159] O. Schmidt, A. Gambhir, I. Staffell, A. Hawkes, J. Nelson, and S. Few, "Future cost and performance of water electrolysis: An expert elicitation study," *International Journal of Hydrogen Energy*, vol. 42, no. 52, pp. 30470–30492, 2017. https://doi.org/10.1016/j.ijhydene.2017.10.045.

[160] T. Smolinka, N. Wiebe, P. Sterchele, A. Palzer, F. Lehner, M. Jansen, S. Kiemel, R. Miehe, S. Wahren, and F. Zimmermann, "Studie IndWEDe - Industrialisierung der Wasserelektrolyse in Deutschland: Chancen und Herausforderungen für nachhaltigen Wasserstoff für Verkehr, Strom und

Wärme.” https://www.now-gmbh.de/content/service/3-publikationen/1-nip-wasserstoff-und-brennstoffzellentechnologie/indwede-studie_v04.1.pdf, 2018. Accessed: 15.09.2019.

[161] S. M. Saba, M. Müller, M. Robinius, and D. Stolten, “The investment costs of electrolysis–a comparison of cost studies from the past 30 years,” *International Journal of Hydrogen Energy*, vol. 43, no. 3, pp. 1209–1223, 2018.

[162] G. Glenk and S. Reichelstein, “Economics of converting renewable power to hydrogen,” *Nature Energy*, vol. 4, no. 3, pp. 216–222, 2019. 10.1038/s41560-019-0326-1.

[163] Nexant and Air Liquide and Argonne National Laboratory and Chevron Technology Venture Gas Technology Institute and National Renewable Energy Laboratory and Pacific Northwest National Laboratory and LLC, TIAX, “H2A Hydrogen Delivery Infrastructure Analysis Models and Conventional Pathway Options Analysis Results,” 2008.

[164] Roads2HyCom, “Large Hydrogen Underground Storage.” http://refman.energytransitionmodel.com/publications/1793, 2013. Accessed: 30.01.2017.

[165] K. Stolzenburg, R. Hamelmann, M. Wietschel, F. Genoese, J. Michaelis, J. Lehmann, A. Miege, S. Krause, C. Sponholz, S. Donadei, F. Corotogino, A. Acht, and P.-L. Horvath, “Integration von Wind-Wasserstoff-Systemen in das Energiesystem - Abschlussbericht.” https://www.now-gmbh.de/content/1-aktuelles/1-presse/20140402-abschlussbericht-zur-integration-von-wind-wasserstoff-systemen-in-das-energiesystem-ist-veroeffentlicht/abschlussbericht_integration_von_wind-wasserstoff-systemen_in_das_energiesystem.pdf, 31.03.2014 2014. Accessed: 15.09.2019.

[166] O. Kruck, F. Crotogino, R. Prelicz, and T. Rudolph, “Assessment of the potential, the actors and relevant business cases for large scale and seasonal storage of renewable electricity by hydrogen underground storage in Europe. Overview on all Known Underground Storage Technologies for Hydrogen.” http://www.fch.europa.eu/project/assessment-potential-actors-and-relevant-business-cases-large-scale-and-seasonal-storage-ren, 2013. Accessed: 05.09.2017.

[167] C. Noack, F. Burggraf, S. S. Hosseiny, P. Lettenmeier, S. Kolb, S. Belz, J. Kallo, K. Friedrich, T. Pregger, and K. Cao, “Studie über die Planung einer Demonstrationsanlage zur Wasserstoff-Kraftstoffgewinnung durch Elektrolyse mit Zwischenspeicherung in Salzkavernen unter Druck.” https:

//elib.dlr.de/94979/1/2014_DLR_ISE_KBB_LBST_PlanDelyKaD.pdf, 2015. Accessed: 15.09.2019.

[168] Sedlacek, R., *Untertage-Erdgasspeicherung in Deutschland*, vol. 118. 2002.

[169] L. Welder, J. Linßen, M. Robinius, and D. Stolten, "FINE - Framework for Integrated Energy System Assessment." https://github.com/FZJ-IEK3-VSA/FINE, 2019. Accessed: 01.04.2019.

[170] EID Energie Informationsdienst GmbH, *Untertage-Gasspeicherung in Deutschland*, vol. 133. 2017.

[171] J. Mischner, H. Fasold, and J. Heymer, *Systemplanerische Grundlagen der Gasversorgung*. Deutscher Industrieverlag, 2015.

[172] F. Fuoli, "Für 21 Millionen entsteht ein riesiger Erdgasspeicher." https://www.limmattalerzeitung.ch/limmattal/region-limmattal/fuer-21-millionen-entsteht-ein-riesiger-erdgasspeicher-125016057, 2012. Accessed: 15.09.2019.

[173] HyARC, "Hydrogen Pipelines." https://h2tools.org/hyarc/hydrogen-data/hydrogen-pipelines, 2016. Accessed: 13.05.2019.

[174] D. Krieg, *Konzept und Kosten eines Pipelinesystems zur Versorgung des deutschen Straßenverkehrs mit Wasserstoff*. Thesis, 2012.

[175] C. Yang and J. Ogden, "Determining the lowest-cost hydrogen delivery mode," *International Journal of Hydrogen Energy*, vol. 32, no. 2, pp. 268–286, 2007.

[176] I. H. Bell, J. Wronski, S. Quoilin, and V. Lemort, "Pure and Pseudo-pure Fluid Thermophysical Property Evaluation and the Open-Source Thermophysical Property Library CoolProp," *Industrial & Engineering Chemistry Research*, vol. 53, no. 6, pp. 2498–2508, 2014. 10.1021/ie4033999.

[177] United Nations Climate Change, "National Inventory Submissions - DEU_2018_2013." https://unfccc.int/process-and-meetings/transparency-and-reporting/reporting-and-review-under-the-convention/greenhouse-gas-inventories-annex-i-parties/national-inventory-submissions-2018, 2018. Accessed: 15.09.2019.

[178] P. Krause, R. Oetjen-Dehne, I. Dehne, D. Dehnen, and H. Erchinger, "Verpflichtende Umsetzung der Getrenntsammlung von Bioabfällen." https://www.umweltbundesamt.de/sites/default/files/medien/378/publikationen/texte_84_2014_verpflichtende_umsetzung_der_getrenntsammlung_von_bioabfaellen.pdf, 2014. Accessed: 15.09.2019.

[179] S. Jacobs, "Biotonnen-Pflicht in ganz Berlin ab 2019." https://www.tagesspiegel.de/berlin/bsr-plant-neues-tarifmodell-biotonnen-pflicht-in-ganz-berlin-ab-2019/21239350.html, 2018. Accessed: 15.09.2019.

[180] S. Klinski, F. Hofmann, A. Plättner, S. Lulies, F. Scholwin, K. Diesel, W. Urban, and F. Burmeister, "Einspeisung von Biogas in das Erdgasnetz." https://www.infothek-biomasse.ch/images/2006_FNR_Einspeisung_biogas.pdf, 2006. Accessed: 15.09.2019.

[181] Statistische Ämter des Bundes und der Länder, "Aufkommen an Haushaltsabfällen." https://www.statistikportal.de/de/aufkommen-haushaltsabfaellen, 2019. Accessed: 23.05.2019.

[182] European Commission, Joint Research Centre (JRC) and Columbia University, Center for International Earth Science Information Network, "GHS population grid, derived from GPW4, multitemporal (1975, 1990, 2000, 2015)." http://data.europa.eu/89h/jrc-ghsl-ghs_pop_gpw4_globe_r2015a, 2015. Accessed: 15.09.2019.

[183] Danish Energy Agency, "Technology Data for Renewable Fuels June 2017." https://ens.dk/sites/ens.dk/files/Analyser/technology_data_catalogue_for_el_and_dh_-_aug_2016_upd_dec18.pdf, 2018. Accessed: 15.09.2019.

[184] Agora Energiewende and Frontier Economics, "Die zukünftigen Kosten strombasierter synthetischer Brennstoffe." https://www.agora-energiewende.de/fileadmin2/Projekte/2017/SynKost_2050/Agora_SynCost-Studie_WEB.pdf, 2018. Accessed: 15.09.2019.

[185] P. R. Schmidt, W. Zittel, W. Weindorf, and T. Raksha, "Renewables in Transport 2050 Empowering a sustainable mobility future with zero emission fuels from renewable electricity." http://www.lbst.de/news/2016_docs/FVV_H1086_Renewables-in-Transport-2050-Kraftstoffstudie_II.pdf, 2016. Accessed: 15.09.2019.

[186] T. Barchmann, E. Mauky, M. Dotzauer, M. Stur, S. Weinrich, H. F. Jacobi, J. Liebetrau, and M. Nelles, "Expanding the flexibility of biogas plants –substrate management, schedule synthesis and economic assessment," *Landtechnik Agricultural Engineering*, vol. 71, no. 6, pp. 233–251, 2016. DOI:10.15150/lt.2016.3146.

[187] P. Hauser, S. Heidari, C. Weber, and D. Möst, "Does Increasing Natural Gas Demand in the Power Sector Pose a Threat of Congestion to the German Gas Grid? A Model-Coupling Approach," *Energies*, vol. 12, no. 11, p. 2159, 2019.

[188] FNB Gas, “Zahlen und Fakten.” https://www.fnb-gas.de/de/fernleitungsnetze-/zahlen-und-fakten/zahlen-und-fakten.html, 2019. Accessed: 25.07.2019.

[189] K. Görner and D. U. Sauer, “Konventionelle Kraftwerke - Technologiesteckbrief zur Analyse ,,Flexibilitätskonzepte für die Stromversorgung 2050“.” https://epub.wupperinst.org/frontdoor/deliver/index/docId/6342/file/6342_Flexibilitaetskonzepte.pdf, 2016. Accessed: 15.09.2019.

[190] J. Nitsch, T. Pregger, Y. Scholz, T. Naegler, M. Sterner, N. Gerhardt, A. von Oehsen, C. Pape, Y.-M. Saint-Drenan, and B. Wenzel, “Langfristszenarien und Strategien für den Ausbau der erneuerbaren Energien in Deutschland bei Berücksichtigung der Entwicklung in Europa und global.” http://www.dlr.de/dlr/Portaldata/1/Resources/documents/leitstudie2010.pdf, 2010. Accessed: 15.09.2019.

[191] F. Sandau, A. Scholz, H. Henning, P. Schumacher, C. Sager, F. Bergk, C. Kämper, W. Knörr, J. Kräck, U. Lambrecht, O. Antoni, J. Hilpert, K. Merkel, and T. Müller, “Interaktion EE-Strom, Wärme und Verkehr.” https://www.iee.fraunhofer.de/content/dam/iee/energiesystemtechnik/de/Dokumente/Veroeffentlichungen/2015/Interaktion_EEStrom_Waerme_Verkehr_Endbericht.pdf, 2015. Accessed: 15.09.2019.

[192] P. Icha and G. Kuhs, “Entwicklung der spezifischen Kohlendioxid-Emissionen des deutschen Strommix in den Jahren 1990–2017.” https://www.umweltbundesamt.de/sites/default/files/medien/1410/publikationen/2018-05-04_climate-change_11-2018_strommix-2018_0.pdf, 2018. Accessed: 15.09.2019.

Band / Volume 581
Schlussbericht
Accelerating Low- carbon Industrial Growth through
CCUS (ALIGN-CCUS)
S. Weiske, S. Schemme, R. C. Samsun, R. Peters, S. Troy, S. Morgenthaler, D. Schumann, P. Zapp (2022), 216 pp
ISBN: 978-3-95806-632-8

Band / Volume 582
Closed Carbon Cycle Mobility –
Klimaneutrale Kraftstoffe für den Verkehr der Zukunft
F. Schorn, J. Häusler, J. L. Breuer, S. Weiske, J. Pasel, R. C. Samsun, R. Peters (2022), 220 pp
ISBN: 978-3-95806-636-6

Band / Volume 583
Machine learning for monitoring groundwater resources over Europe
Y. Ma (2022), viii, 125 pp
ISBN: 978-3-95806-638-0

Band / Volume 584
Mechanical properties of single and dual phase proton conducting membranes
W. Zhou (2022), IV, VI, 133 pp
ISBN: 978-3-95806-645-8

Band / Volume 585
Improvements to gravity wave physics from an observational perspective
M. Geldenhuys (2022), vii, 136 pp
ISBN: 978-3-95806-647-2

Band / Volume 586
Impact of severe convection on the water vapor mixing ratio in the extra-tropical stratosphere
D. Khordakova (2022), ii, 136 pp
ISBN: 978-3-95806-648-9

Band / Volume 587
Effects of salt precipitation during evaporation on porosity and permeability of porous media
J. Piotrowski (2022), xxvii, 139 pp
ISBN: 978-3-95806-650-2

Band / Volume 588
IEK-14 Report 2022
Forschung für die Energiewende und den Wandel im Rheinischen Revier
B. Emonts (Hrsg.) (2022)
ISBN: 978-3-95806-652-6

Band / Volume 589
Oxidation of monoterpenes studied in atmospheric simulation chambers
L. L. Hantschke (2022), 188 pp
ISBN: 978-3-95806-653-3

Band / Volume 590
NiFe Layered Double Hydroxide Catalysts for Oxygen Evolution Reaction in Alkaline Water Electrolysis
W. Jiang (2022), 165 pp
ISBN: 978-3-95806-658-8

Band / Volume 591
Optimizing Cross-linked Infrastructure for Future Energy Systems
L. Welder (2022), xxiii, 360 pp
ISBN: 978-3-95806-659-5

Weitere ***Schriften des Verlags im Forschungszentrum Jülich*** unter
http://wwwzb1.fz-juelich.de/verlagextern1/index.asp

Energie & Umwelt / Energy & Environment
Band / Volume 591
ISBN 978-3-95806-659-5

JÜLICH
Forschungszentrum